BOARD OF DIRECTORS, 1955
J. D. Ryder, *President*
Franz Tank, *Vice-President*
W. R. G. Baker, *Treasurer*
Haradan Pratt, *Secretary*
John R. Pierce, *Editor*
J. W. McRae, *Senior Past President*
W. R. Hewlett, *Junior Past President*

1955
S. L. Bailey
A. N. Goldsmith
A. V. Loughren
C. J. Marshall (R5)
L. E. Packard (R1)
J. M. Pettit (R7)
B. E. Shackelford
C. H. Vollum
H. W. Wells (R3)

1955–1956
E. M. Boone (R4)
J. N. Dyer (R2)
J. T. Henderson (R8)
A. G. Jensen
George Rappaport
D. J. Tucker (R6)

1955–1957
J. F. Byrne
Ernst Weber

George W. Bailey, *Executive Secretary*

John B. Buckley, *Chief Accountant*
Laurence G. Cumming, *Technical Secretary*
Evelyn Davis, *Assistant to the Executive Secretary*
Emily Sirjane, *Office Manager*

EDITORIAL DEPARTMENT
Alfred N. Goldsmith, *Editor Emeritus*
John R. Pierce, *Editor*
E. K. Gannett, *Managing Editor*
Marita D. Sands, *Production Manager*

ADVERTISING DEPARTMENT
William C. Copp, *Advertising Manager*
Lillian Petranek, *Assistant Advertising Manager*

EDITORIAL BOARD
John R. Pierce, *Chairman*
D. G. Fink
E. K. Gannett
T. A. Hunter
W. R. Hewlett
J. A. Stratton
W. N. Tuttle

Responsibility for the contents of papers published in the PROCEEDINGS of the IRE rests upon the authors. Statements made in papers are not binding on the IRE or its members.

Change of address (with 15 days advance notice) and letters regarding subscriptions and payments should be mailed to the Secretary of the IRE, 1 East 79 Street, New York 21, N. Y.

All rights of publication, including foreign language translations are reserved by the IRE. Abstracts of papers with mention of their source may be printed. Requests for republication should be addressed to The Institute of Radio Engineers.

PROCEEDINGS OF THE IRE

Published Monthly by

The Institute of Radio Engineers, Inc.

VOLUME 43 *November, 1955* NUMBER 11, PT. I

CONTENTS

Theodore A. Hunter, Director, 1955 1572
The IRE Student Quarterly ..... *The Editor* 1573
5543. The ABC's of Color Television ..... *J. M. Barstow* 1574
Correction to "The Design of Stagger-Tuned Double-Tuned Amplifiers for Arbitrarily Large Bandwidth," by *M. M. McWhorter* and *T. M. Pettit* 1579
5544. Electronically-Controlled Audio Filters ..... *L. O. Dolanský* 1580
5545. Magnetic Fields in Small Ferrite Bodies with Applications to Microwave Cavities Containing Such Bodies ..... *A. D. Berk and B. A. Lengyel* 1587
5546. On the Principle and Design of a Trigger Circuit of a Signal-Seeking Radio Using "Difference-Voltage" ..... *Chih Chi Hsu* 1591
5547. IRE Standards, Graphical and Letter Symbols: Feedback Control Systems, 1955 1608
5548. IRE Standards on Pulses: Methods of Measurement of Pulse Quantities, 1955 1610
5549. The Cascade Backward-Wave Amplifier: A High-Gain Voltage-Tuned Filter for Microwaves ..... *M. R. Currie and J. R. Whinnery* 1617
5550. Junction Transistor Blocking Oscillators ..... *J. G. Linvill and R. H. Mattson* 1632
5551. Theory of Shot Noise in Junction Diodes, Junction Transistors ..... *A. van der Ziel* 1639
5552. Multiple Frequency Shift Teletype Systems ..... *D. B. Jordan, H. Greenberg, E. E. Eldredge, and W. Serniuk* 1647
5553. The Use of a Ring Array as a Skip Range Antenna ..... *J. D. Tillman, W. T. Patton, C. E. Blakely, and F. V. Schultz* 1655
5554. Microwave High-Speed Continuous Phase Shifter ..... *W. Sichak and D. J. Levine* 1661
5555. A Comparison of Two Radiometer Circuits ..... *S. J. Goldstein* 1663
Correspondence:
5556. Optimizing the Design Characteristics of Triodes for Maximum Gain into a Fixed Load Impedance ..... *M. Bareiss* 1667
5557. Influence of the Order of Overtone on the Temperature Coefficient of Frequency of AT-Type Quartz Resonators ..... *R. Bechmann* 1667
5558. Optimum Tube Utilization in Cascaded Distributed Amplifiers ..... *A. I. Talkin and J. V. Cuneo* 1668
5559. Self-Bias Cutoff Effect in Power Transistors ..... *N. H. Fletcher* 1669
5560. A Note on the Transfer Voltage Ratio of Resistive Networks with Positive Elements ..... *R. J. Schwarz* 1670
5561. Two Problems in Geometrical Optics and Application of the Results in Electron Trajectory Calculations ..... *S. V. Yadavalli* 1670
Contributors 1672
IRE News and Radio Notes:
IRE Presents 1956 Awards 1675
Professional Group News 1676
Technical Committee Notes 1677
5562–5569. Books 1677
Professional Groups 1680
Sections 1680
5570. Abstracts of IRE Transactions 1683
5571. Abstracts and References 1684
Meetings with Exhibits 6A
News and New Products 34A
Industrial Engineering Notes 38A
Membership 53A
IRE People 70A
Section Meetings 85A
Positions Wanted 152A
Positions Open 175A

Cover—A newly developed miniature transmitter comprised of two units, each no larger than a package of cigarettes, demonstrates its use in one of several fields, medical electronics. Diagnostic tests such as the simultaneous transmission of heart sounds and electrocardiograph voltages may be performed on ambulatory subjects. It is now possible to make cardiac examinations while a patient performs normal activities. Numerous other applications to medical electronics are possible, such as blood pressure, respiratory, and brain wave measurements.

Photo—Jansky and Bailey, Inc. Washington, D.C.

Copyright, 1955, by the Institute of Radio Engineers, Inc.

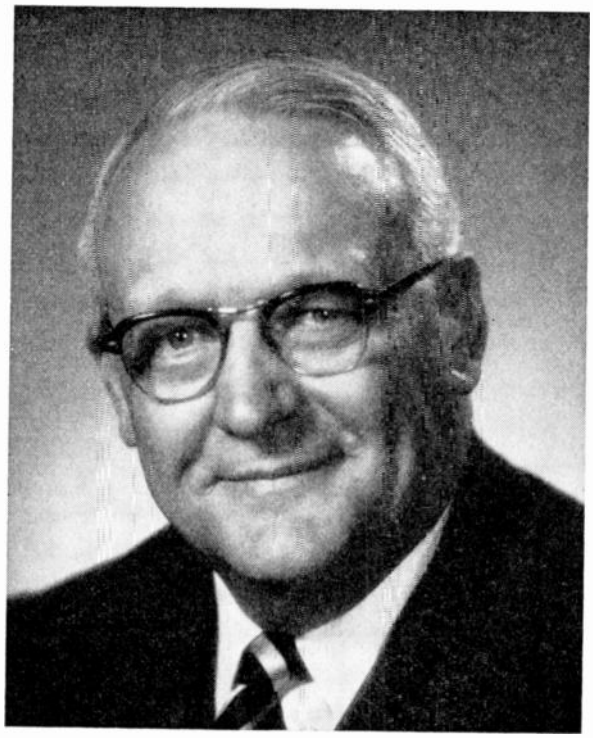

Theodore A. Hunter

DIRECTOR, 1955

Theodore A. Hunter was born December 5, 1900, in Dike, Iowa. He received the B.S. degree in electrical engineering from the State University of Iowa in 1922. In 1923, the university awarded him the M.S. in physics and in 1933, the E.E.

Mr. Hunter joined the North West Bell Telephone Company as a transmission line inspector. Following that, he was an instructor in physics at the University of Pittsburgh. He then joined Crosley Radio Corporation as supervisor of loud speaker development. From 1931, he served as a physics instructor at Rose Polytechnic Institute. In 1940, Mr. Hunter became associated with Collins Radio Company as director of oscillator development. The Collins 32V-1, Collins Oscillator Series 70E-1 to 9, and the 310-B exciter unit were developed by Mr. Hunter. At present, he is Professor of Research in the Psychology Department at the State University of Iowa as well as President of the Hunter Manufacturing Company.

Mr. Hunter organized the Cedar Rapids Engineering Club and has served as President and Program Chairman of the group. He also has been President and Program Chairman of the Collins Radio Technical Society, another group which he organized. He is a member of the Iowa Engineering Society and Sigma Xi.

Mr. Hunter was a Charter Member of the Cincinnati Section and co-organizer of the Cedar Rapids Section. He was General Chairman of the first Cedar Rapids Communication Conference and has been on the Executive Committee of the Cedar Rapids Section for eight years. Mr. Hunter was the first Regional Director for Region Five. He has served on many committees, including Sections, Papers, Policy Advisory, and Nominations, of which he was chairman from 1949 to 1951.

Mr. Hunter joined the IRE as an Associate in 1928; he became a Member in 1941, Senior Member in 1943, and a Fellow in 1947. He is now serving on the Education Committee and devotes himself to editing the newly created *Student Quarterly*.

The IRE Student Quarterly

The IRE has a student quarterly publication because Ted Hunter realized that the students needed one, and that it was in the interests of the IRE to supply it. In 1953, with the help of friends and students, he got out a sample issue himself. He sold the idea to the IRE. Starting September of last year, every Student Member has received a free copy of each issue.

The IRE has a good student quarterly because Ted Hunter understands students. Having true understanding, he questions it and refreshes it himself. He is advised and supported by an excellent Student Quarterly Committee, which includes students among its members. In January and February 1955 he made a three-week tour, during which he visited eleven Student Branches to see what students and faculty members thought of *The Quarterly*. Ted also understands the professional world students enter after leaving college, and he understands the IRE. He likes them all.

The Student Quarterly tells and reassures the students about the experiences in a first engineering job in words they can understand—the words of men a few months out of college. It tells students about the opportunities in various fields of engineering. It tells the students about the various Professional Groups (a Student Member may belong to one Professional Group for a dollar a year). It contains understandable technical articles which members of the faculty can assign as course work if the students fail to read them voluntarily (is this treason?). It contains real humor with a real point, in the characters, actions, and appearances of Professor Floop, who, when at the board, erases notes faster than the students can copy them; A. G. Goodfellow, whom we all revere; and Beamie (see PROC. IRE, vol. 43, p. 380; March, 1955), who is always on the student's side.

Although *The Student Quarterly* is designed primarily for students, I myself enjoy reading it a lot, and I think that other IRE members would, too. They can subscribe for two dollars a year. A paper reprinted in this issue of the PROCEEDINGS, "The ABC's of Color Television" by J. M. Barstow, is a sample of just one sort of thing to be found in *The Student Quarterly*. The contents are varied, sound, sensible, and never stuffy. There is no nonsense about Ted Hunter. When he speaks, he talks about real problems. His humor is never old, inappropriate jokes dragged in by the heels for the sake of a laugh. He tries to make his authors live up to these principles, and he succeeds pretty well in doing so.

Publications take work. *The Student Quarterly* takes a lot of work. IRE members are used to writing learned papers for the PROCEEDINGS, but they aren't yet accustomed to writing for *The Student Quarterly*. Ted Hunter needs the help of the membership in getting good articles. He wants good technical articles by students. He wants good articles by students who have gone into industry recently, telling what they have learned out of college and what they wish they had learned before leaving. But he needs articles by more mature and experienced engineers as well. Do you have something to say about your particular field of work, something you think would interest and help students? Do you have some reflections about professional life which are really wisdom and not prejudice? Do you know about some fresh technical matter which you think would interest students and help them to understand something important? Get in touch with Ted Hunter, 1164 East Court Street, Iowa City, Iowa. Student Member or Fellow, you will find him appreciative, helpful, and a severe and honest critic. If you write an article acceptable to him, you can be pretty sure that you will be helping the students or at least making them think. If he finds what you have written unacceptable, whether you are a Student Member or a Fellow you can be pretty sure that it is because someone else had something more suitable to say, or has said it better.

—*The Editor*

The ABC's of Color Television*

J. M. BARSTOW†, SENIOR MEMBER, IRE

TELEVISION PROGRAMS in color are now being produced regularly by major broadcasting companies, and the corresponding signals are being transmitted over both the local and intercity facilities of the Bell System to color TV transmitters. Although much publicity has been given to the advent of this rather astonishing new development, most of the articles have been either highly technical or intended for the newspapers. They have not provided an understanding of the system for intelligent engineers who are not able to devote sufficient time to the subject to master the more obscure technical details. This article is intended to fill a need felt in many quarters to answer a number of questions which have arisen concerning the generation of the signals and the manner in which they are used to produce a color picture.

It will be assumed that the reader has some knowledge of how a black-and-white TV picture signal is generated and displayed; *i.e.*, the picture is "painted" on the TV tube by the modulated intensity of a spot which is swept repeatedly across the face of the tube from left to right, each sweep taking about 1/15,750 second, the spot descending gradually from top to bottom of the tube in about 1/60 of a second. This cycle of events occurs over and over again, giving rise to the illusion of continuous motion in any televised scene.

With this background in mind, curious engineers generally have several simple questions in mind when they are told that by a modified, but compatible, system, a color picture can be painted on the tube face. Some of these questions are: (1) how does the system work in simple terms? (2) how is color (hue) produced on the picture tube of a color receiver? (3) how can color TV signals and monochrome TV signals be "compatible"; *i.e.*, what does a monochrome receiver do with the color information signals (which it does not need and cannot use), and how can a color receiver do without color information? In an attempt to answer these questions in easily understandable terms, a description will be given in the following paragraphs and associated figures of the general plan employed, without going into details as to how the plan is carried out.

Colorimetry and the Color Picture Tube

A few rudimentary principles of colorimetry must first be understood; *i.e.*, those having to do with the reaction of human vision to lights of differing color. The necessary principles may best be understood by describing an experiment with colored lights. Suppose, for example, in a darkened room, a white reflecting surface is illuminated in three different spots with light from three different projection lanterns. In the path of the light from one lantern, a filter will be placed which will allow green light to pass through, but no other color. Similarly, in the paths of the beams from the other lanterns, red and blue filters will be placed respectively, so that to an observer with good color vision, the spots will appear to be green, red, and blue. Now suppose the projection lanterns are oriented so that the three spots partially merge. The area on which all three lights fall simultaneously will appear white. The area on which green and red light falls will appear yellow; the area on which red and blue light falls will appear as lavender or magenta, and the area on which the blue and green light falls will appear blue-green or cyan. These results are shown on Fig. 1 (see color insert following p. 1578) and the results of the experiment illustrate the additive properties of colors (not to be confused with the subtractive properties of color when different color pigments are mixed).

The additive properties of colored lights are employed in color television. When the eye can see separate areas (*i.e.*, areas large enough to be resolved by human vision) illuminated by different colored lights, it will recognize the different colors, but when the colors merge, or the areas become so small and so close together that the eye sees them as if they were in the same place, the individual colors no longer are recognized. In the experiment described above, if the dots were each reduced in size to about that of a pinhead, and then so located on the white surface that they did not merge but were tangent to each other, the area which they effectively cover would appear white from a distance of about 15 feet. At a distance of a few inches, the three separate colors would be recognized.

The structure of a color television picture tube is shown in Fig. 2 (opposite). Phosphor plate of tube is a glass screen covered with about 1,070,000 phosphor dots (21″ tube), one-third of which will glow green under the influence of a beam of electrons, one-third, red and one-third, blue. The dots are placed on the phosphor plate of the tube in clusters of three: one green, one red, and one blue, so that there are about 350,000 clusters of three dots each, uniformly distributed over the active area of the tube. The neck of the tube contains three electron guns, the first, for emitting a beam intended for the green glowing dots, the second, for emitting a beam for the red glowing dots, and the third, a beam for the blue glowing dots. Between the electron guns and the phosphor plate, but only about one-half inch from the phosphor, is a masking plate which has 350,000 small holes in it, each hole being placed approximately over the center of a cluster of three phosphor dots. Under the influence of focusing coils and magnets,

* Original manuscript received by the IRE July 9, 1955.
† Bell Telephone Labs., New York, N. Y.

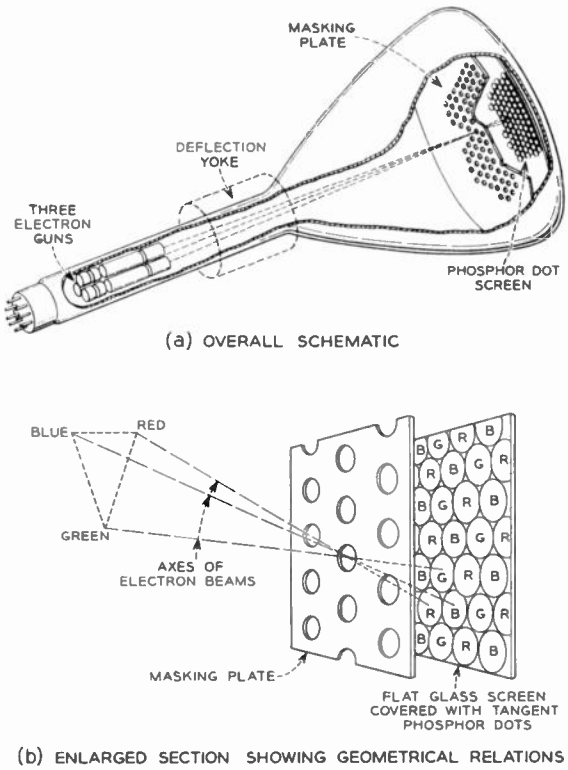

Fig. 2—Structure of tri-colored television tube: (a) over-all schematic; (b) enlarged section showing geometrical arrangement. (Courtesy of RCA.)

the three beams from the three guns are made to converge at the masking plate, and hence, they diverge slightly beyond the masking plate. This slight divergence is sufficient so that the beam from the green gun strikes only the green glowing dots and similarly, the beams from the red and blue guns strike only the red and blue glowing dots, respectively. A cluster of three phosphor dots is so small that one dot cannot be resolved from another at distances greater than a few feet. Therefore, at distances of four times picture height or greater, a wide range of colors can be produced (including white) by controlling the magnitudes of the beams from the three guns. The apparent sharpness of the picture is reduced very little. When the beams from the three guns are strong, and correctly proportioned in magnitude, white is produced. If they remain in the same proportions, but are gradually reduced in magnitude to near zero, the white is correspondingly reduced in intensity through shades of gray to black. If the beam from the green gun is strong and the others near zero, the color produced is green (the red and blue glowing dots do not glow). Similarly, any color can be produced that is within the range of colors that can be synthesized from green, red and blue. This range embraces nearly all those seen in nature or employed by human beings for decorative purposes.

As the tube is scanned from left to right and from top to bottom by the three beams in unison, the convergence of the beams at the masking plate is maintained within close limits.

The remaining features of the system are concerned with the production and transmission over one 4.2-mc circuit of the signals applied to the three guns of the picture tube.

Color Signal Generation

Color signals are generated in a manner shown in Fig. 3 below. Three cameras are used effectively with light filters so that the ouptut of one camera is due to the green light obtained from the object being televised,

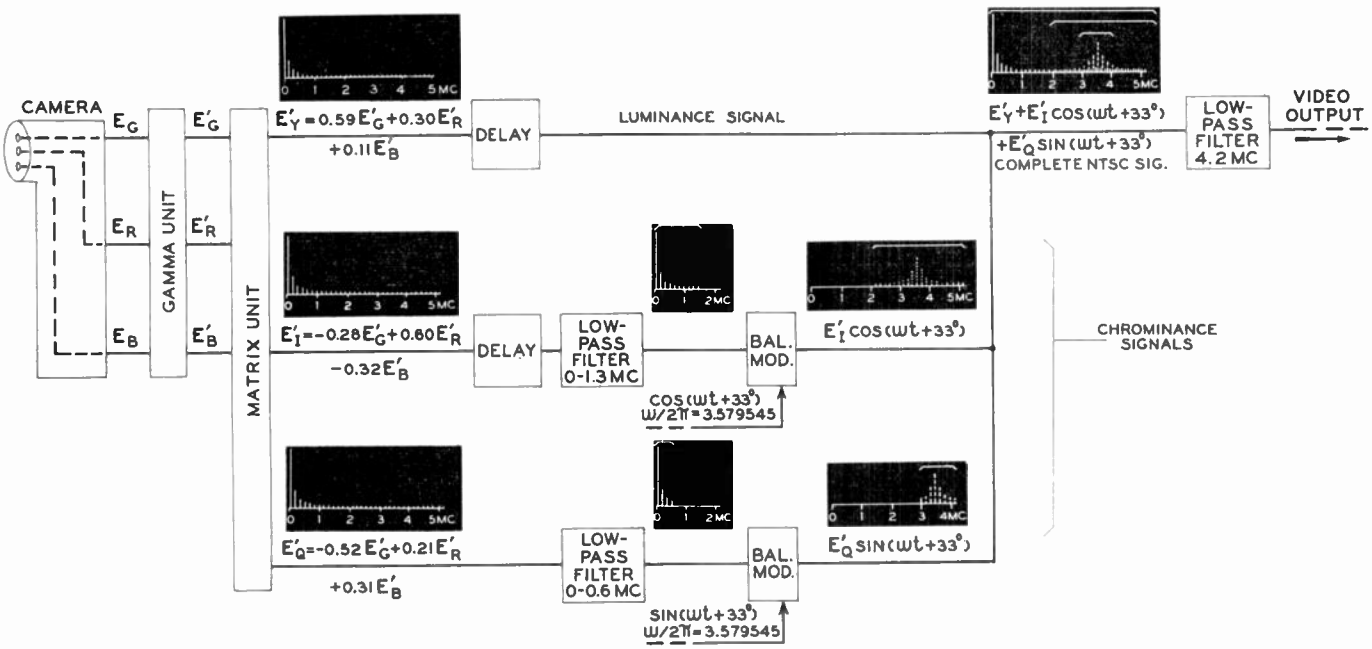

Fig. 3—Schematic of equipment component functions for generating NTSC color video signals.

the output of the second, due to red light, and that of the third, due to blue light. The horizontal and vertical sweep voltages and associated pulses are provided by the camera equipment which converts the light signal to electrical potentials E_{Red}, E_{Green} and E_{Blue}. The gamma unit contains a set of nonlinear amplifiers through which the electrical signals are passed. The unit is used at the early stage of signal generation to anticipate and correct for a characteristic of picture tubes used in receiving sets. The light output of a phosphor in a picture tube is directly proportional to the beam current striking it, but the beam current is proportional to about the 2.2 power of the voltage applied to the picture tube grid. Hence, in the gamma unit, the nonlinear amplifiers whose outputs are proportional to approximately the 1/2.2 power of the inputs, are correct for the opposite kind of nonlinearity in the picture tube. Between the outputs of the gamma unit and the picture tube grids, the system is intended to be linear.

The three outputs of the gamma unit are usually adjusted to be equal when a white area is being televised. They are then fed into a matrix unit which derives three signals: one to be used as a brightness or luminance signal similar in every respect to a monochrome signal, and the other two to be used as color information signals. In Fig. 3, the brightness signal is labeled E_y', and is formed by adding .59 of the green signal, .3 of the red signal, and .11 of the blue signal. These fractions of the individual color signals are combined because it has been determined subjectively that the three colors contribute to the total brightness of a scene in these proportions. The brightness of a given area in a televised scene corresponds to the "lightness" of the area, or the inverse of the "darkness" of the area, irrespective of "hue."

The two color information signals are formed as indicated on the figure. These signals are going to be used to modulate two single frequencies (color subcarriers) which are identical except for a 90 degree phase difference. Therefore, the proportions of each color output used are selected so that, if the different hues are considered as located along a circle, as indicated in Fig. 4, (see color insert following p. 1578) their projections on E'_i and E'_Q axes will result in the correct magnitudes of modulating voltages. Before projecting the primary color voltages onto the E'_i (in phase) and E'_Q (quadrature phase) axes, two other magnitude adjustments are made. One governs the relative magnitude of chrominance and luminance signals, and the other adjusts the three primary color magnitudes so that when a white or gray area is televised (corresponding to equal gamma corrected color voltage outputs in each of the three colors), the color voltages projected onto the E'_i and E'_Q axes will sum to zero. Hence, the modulators will have zero output. These two adjustments in the color signal voltage magnitudes produce levels of $E'_G = .593$, $E'_R = .632$, and $E'_B = .447$ before projection on the E'_i and E'_Q axes. When these color voltages are projected onto the E'_i and E'_Q axes, the results are as shown on Fig. 3. It will be noticed in this figure that the coefficients of the color voltages sum algebraically to zero, indicating that when the original gamma corrected output color voltages are equal, both the E'_i and E'_Q modulating voltages reduce to zero. It is obvious from the signs of the coefficients of the color signals emerging from the matrix unit that this unit must contain phase inverters as well as attenuators, amplifiers, and mixing circuits.

Fig. 4 shows the magnitudes and the angles of both the primary colors-red, blue and green, and the complementary colors-yellow, cyan, and magenta. The magnitudes and angles of the complementary colors are the vector resultants of the adjacent primary colors; *i.e.*, yellow .447 at 167 degrees is the vector resultant of red and green; similarly, cyan is the resultant of green and blue, and magenta resultant of blue and red.

The two modulated subcarrier outputs are combined as indicated in Fig. 3. Since each output consists of an amplitude-modulated color subcarrier, the combination will also be an amplitude-modulated color subcarrier. Since the two components differ in phase by 90 degrees, their vector sum will have an angle which is determined by the relative magnitudes of each component and thus will be phase modulated also. It should be noted that each component output may have reversed phase, (*i.e.*, 180 degrees from normal), as when the modulating voltage changes sign from positive to negative. The arrangement, therefore, provides that the color information is contained in an amplitude-modulated subcarrier whose angle, referred to an arbitrary reference, may have any value from 0 to 360 degrees.

The color signal is then combined with the luminance signal as shown schematically in Fig. 3. Since the color subcarrier has been chosen to be an odd multiple of half-line frequency (455×half-line frequency), the color signal interleaves with the luminance signal as shown in the small bandwidth illustration near the line schematically representing the output signal. This is the video signal which is transmitted. A somewhat more-detailed illustration is given in Fig. 5. The solid vertical

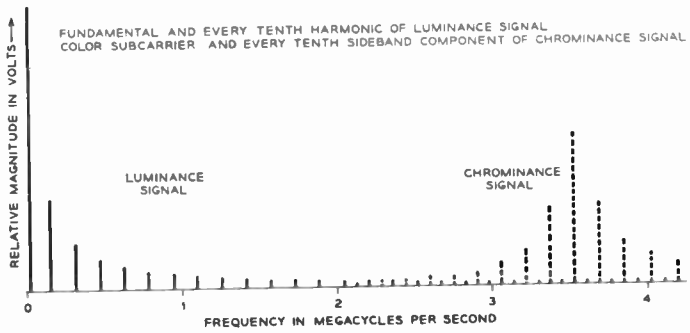

Fig. 5—Frequency composition of typical NTSC color TV signal.

lines indicating frequency components comprise the luminance signal, and the dotted lines, the chrominance signal. Only one-tenth of the number of components

are plotted for clarity of illustration. In this signal, the components of the luminance signal are separated by line frequency, (approximately 15.75 kc), as are those of the chrominance signal. It should be remembered that the luminance signals are present at all times during the transmission of a picture, although the levels of the higher frequency components vary considerably, depending on picture content. On the other hand, the chrominance components will disappear entirely when black and white objects are being televised.

Fig. 6(a) (see color insert following p. 1578) shows a color bar pattern as it would appear on the screen of a color television set and Fig. 6(b) shows the corresponding video signal waveform in one-line interval. The scale at the left of Fig. 6(b) may be considered as a video voltage scale in one-hundredth volt units. The first negative pulse is the line-synchronizing pulse which is used to send the three converging color beams back to the left side of the raster. The next short burst, at a low-voltage level corresponding to black, or at least a dark level, is the color subcarrier synchronizing burst, and is used to control the frequency and phase of the demodulating oscillator in the receiver. The phase of this burst is always 180 degrees away from reference phase, as indicated on Fig. 4. The next burst of frequencies corresponds to fully saturated green, having a peak-to-peak amplitude of $2\times.593=1.186$ and an axis level equal to green brightness or .59 (brightness indicated by light dotted lines). The next burst corresponds to saturated yellow and has a peak-to-peak amplitude of twice the resultant of maximum red and green (see Fig. 4), or $2\times.447=.894$ with an axis level equal to yellow brightness (green brightness plus red brightness), or $.59+.30=.89$. The next burst corresponds to saturated red with an amplitude of $2\times.632$ or 1.264, with an axis level at red brightness or .30. The other bursts and the corresponding colors can be seen and the amplitudes and levels of axes computed in a like manner. The factor of 2 in all these computations is used to obtain the peak-to-peak magnitudes from zero-to-peak magnitudes commonly used in electrical engineering as an expression for the maximum amplitude of a sinusoidal wave form.

The phases of the different groups of waves correspond to those shown in Fig. 4, although this cannot be well illustrated in the figure.

In review of what is shown on Fig. 6, three principles should be stated:

1. Level of zero axis of a group of waves representing a single color represents brightness of the color. [*E.g.*, yellow and cyan have highest and next-highest brightnesses in Fig. 6(b) and are brightest of the six portrayed on color bar pattern, Fig. 6(a)].

2. At any brightness level, the amplitude of a group of waves representing a color corresponds to the saturation of the color. The word "purity" has been applied to this characteristic and it indicates the extent to which the color approaches that of light of a single wavelength. Low purity (amplitude) would indicate dilution with other colors, tending to make the resultant move toward some shade between black and white.

3. The phase of the group of waves representing a single color determines the hue of the color.

Fig. 6 also shows the signal corresponding to black-and-white. When the spot formed by the three converging beams passes over the lower half of the image (corresponding to the black-and-white portion of the subject material), the gamma corrected color outputs are equal; they are equal to approximately zero for the left part of the lower half of the picture. They remain equal, but assume high values (unity) for the white area shown at the lower right. The video waveform signal corresponding to this lower picture area is indicated by the heavy solid line at the zero potential level and at the 100 level.

Signal Reception

Once the general scheme for producing the signal is understood, the method of demodulating it to provide signals for each of the three guns in the color tube is rather easily followed. The method is indicated schematically in Fig. 7 on the following page.

There is no attempt made to separate out the chrominance signal from the luminance signal by toothed, or comb, filters. The complete signal is used for a luminance signal as indicated, although the chrominance information in it is unwanted. This unwanted signal, however, has such a frequency composition as to greatly reduce its visibility in the picture. This is because the error it produces in the picture effectively phases out in the succession of lines and fields by means of which the picture is presented. Specifically, if the chrominance signals produce a brightness error at one spot on the picture, as this spot is traversed by the resultant beam from the three guns, an error of opposite sign will be produced at this location in the horizontal motion of the spot on the next line in that field. That is, if the error due to chrominance is too bright a spot in the first line referred to above, the corresponding spot will be too dark on the next traverse of the beam across the picture. These errors are therefore close together on the picture; they are of opposite sign and occur rapidly. These three factors tend to reduce their visibility. Also, when the subject material is black-and-white (or any shade of gray in between), the error disappears altogether because the color subcarrier disappears. As a further safeguard against brightness error due to chrominance signal, manufacturers of color sets are using a low-pass filter to cut off the luminance signal at about 3 mc, cutting off also the chrominance signal, which is an error signal so far as luminance is concerned. The philosophy is that a 3 mc luminance signal *without* the chrominance error signal is better than a 4.2 mc luminance signal *with* the chrominance error signal. This is indicated in Fig. 7 by the chrominance signal elimination filter characteristic applied to the luminance signal.

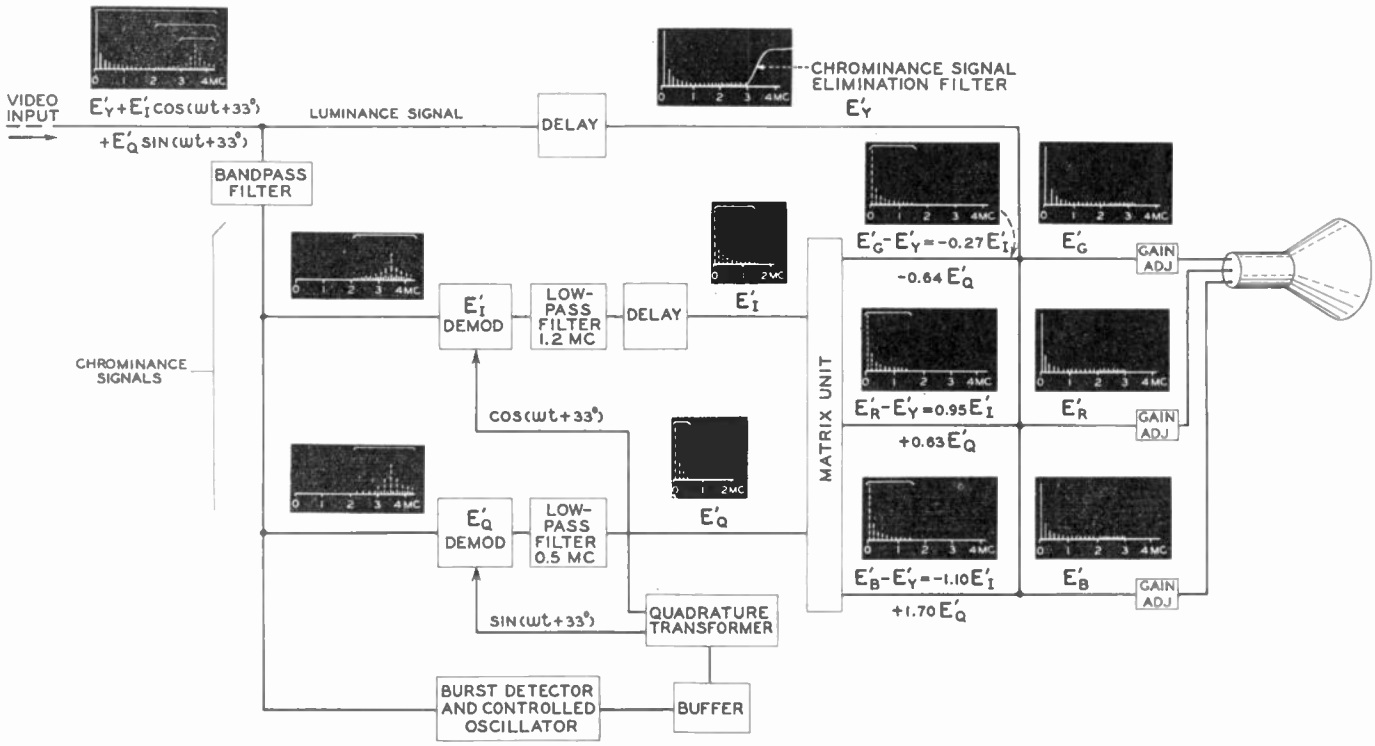

Fig. 7—Schematic of equipment component functions for receiving NTSC color video signals.

As indicated in Fig. 7, a band pass filter is used in the chrominance branch to remove the low frequency luminance signal. The chrominance signals are demodulated with a synchronous demodulator and the E'_i and E'_Q components are derived. The error in the chrominance signal due to the high frequency luminance signal is small because (1) the error signal components are small; (2) synchronous detection plus low-pass filtering are used so that the high frequency positive and negative errors are effectively eliminated.

It is more convenient at the receiver to derive the "color difference" signals first from the chrominance signals. This can be done by combining different fractions of the E'_i and E'_q as follows:

$$E'_G - E'_y = -0.27E'_i - 0.64E'_q$$
$$E'_R - E'_y = 0.95E'_i + 0.63E'_q$$
$$E'_B - E'_y = -1.10E'_i + 1.70E'_q$$

These equations follow directly from the equations shown on Fig. 3.

The luminance signal is then added to each of the three color difference signals, thus forming the three primary color signals.

$$(E'_G - E'_y) + E'_y = E'_G$$
$$(E'_R - E'_y) + E'_y = E'_R$$
$$(E'_B - E'_y) + E'_y = E'_B$$

These three signals correspond exactly (except for the errors discussed above) to the gamma corrected color signals put out by the camera, and are applied through separate gain-adjusting networks to the three guns of the color tube. The gain adjustments are for the purpose of proportioning the beam currents to produce radiations from the phosphors which will produce white (or shades of gray to black) when equal voltages are applied to inputs of gain adjusting networks. The manner in which color tube uses these signals has been explained.

Transmission of the Color Signal

The color signal which must be transmitted has been described here in two ways: (1) amplitude vs frequency (Fig. 5), and (2) amplitude vs time (Fig. 6(b)). It will be apparent from Fig. 5 that since the color is carried by a frequency of 3.58 mc and sidebands, it is important that this frequency region be transmitted with high fidelity. Subjective tests indicate that a 1 db change in the response of the circuit at 3.58 mc can be easily detected, and a loss of 3 db in this region, compared to the transmission at low frequencies (luminance transmission) begins to be objectionable. In other words, transmission at 3.58 mc is as important for chrominance as is transmission at low frequencies (below 1 mc) for luminance. This added requirement for color signal transmission necessitates more exacting maintenance of circuit response.

The second requirement which makes color TV transmission more difficult is the delay requirements. In this case, the delay characteristic of most importance is the differential delay characteristic at the color subcarrier frequency; *i.e.*, variation in delay with the various voltage positions the subcarrier may occupy in transmission, rather than the delay characteristic most frequently referred to in wide-band transmission, which is delay vs frequency. This latter delay must also be

FIG. 1 PRIMARY COLORS OF THE ADDITIVE SYSTEM

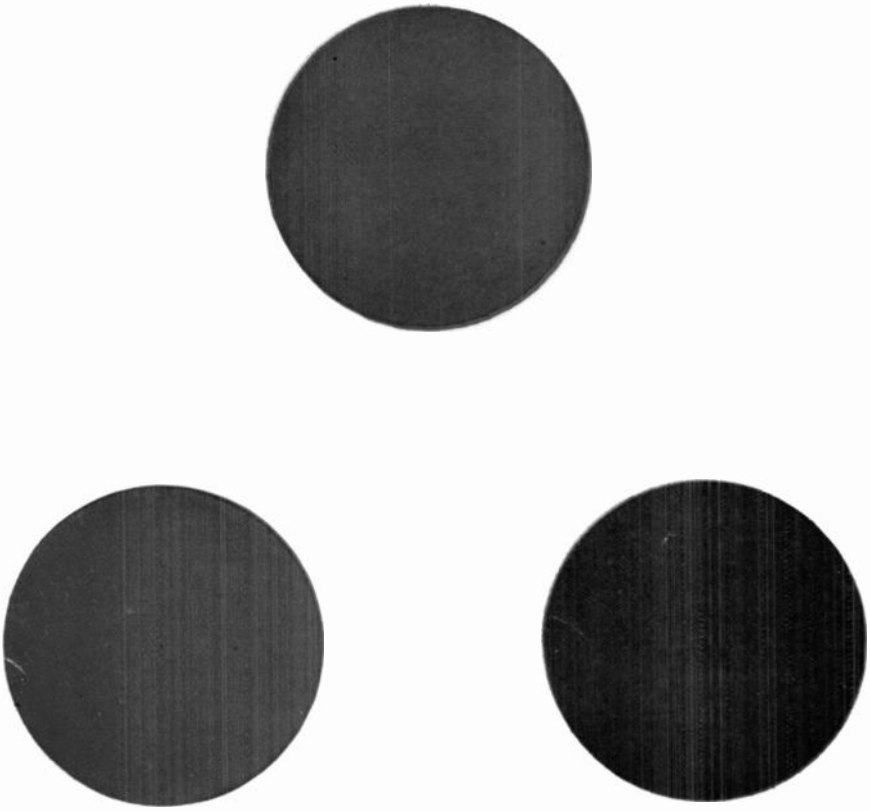

a. Shown separately

b. Shown partially merged

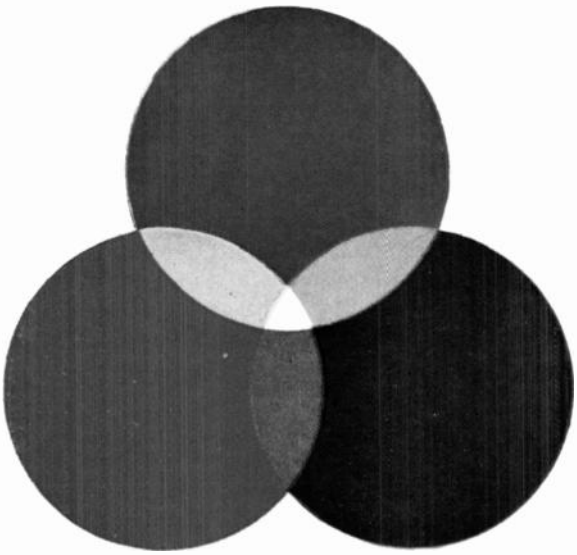

FIG. 4 COLOR CIRCLE DIAGRAM

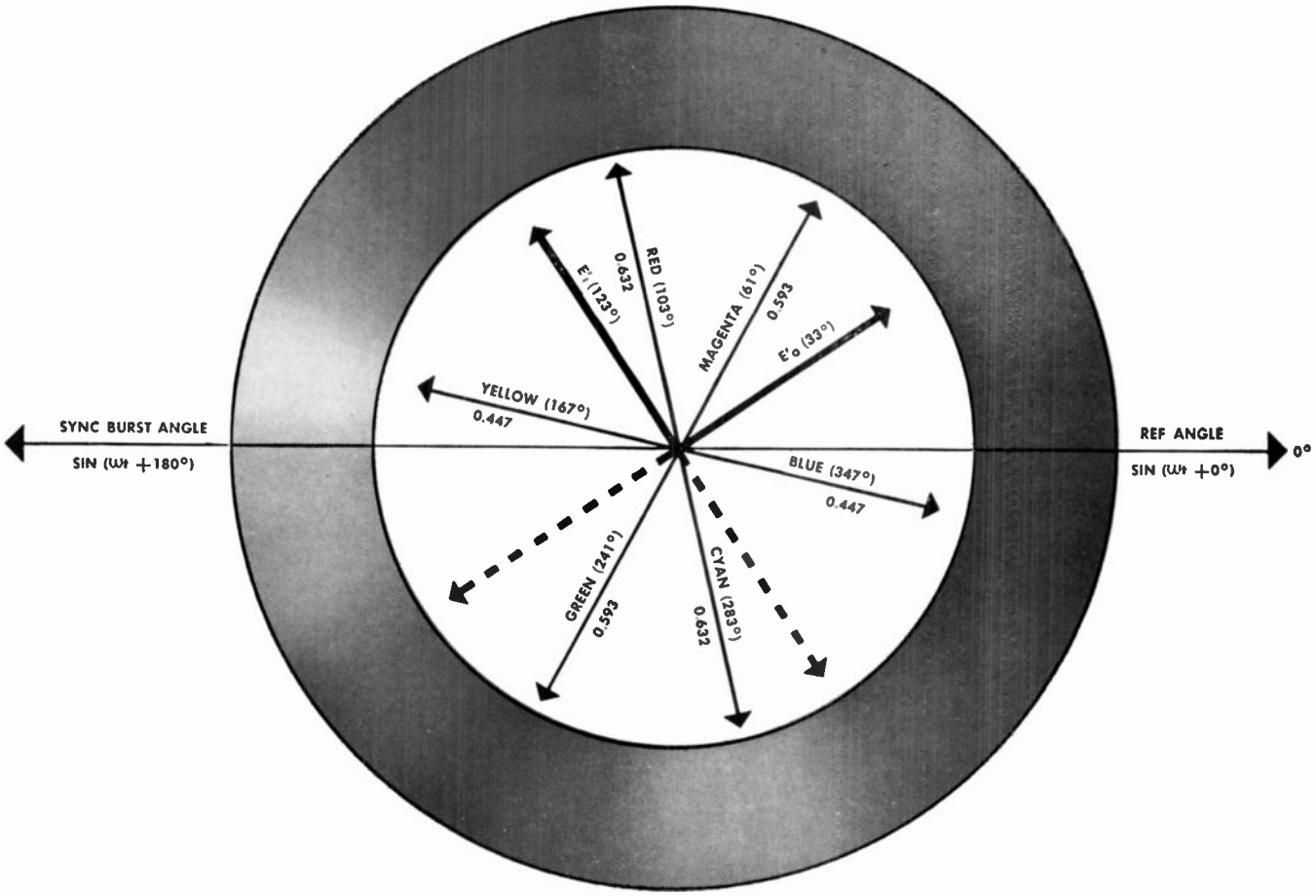

FIG. 6 COLOR BAR PATTERN AND CORRESPONDING COLOR VIDEO SIGNAL

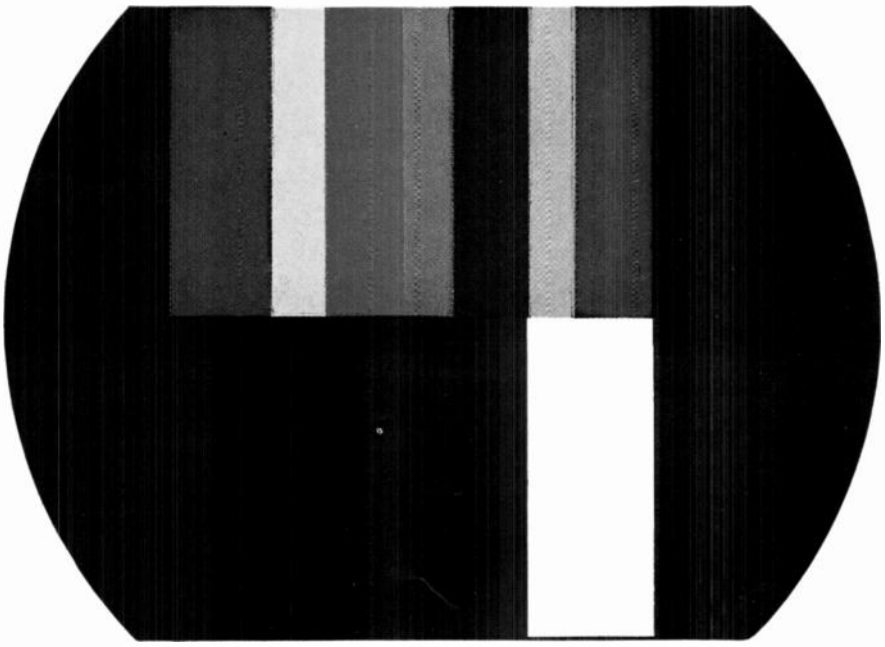

a. Color bar pattern

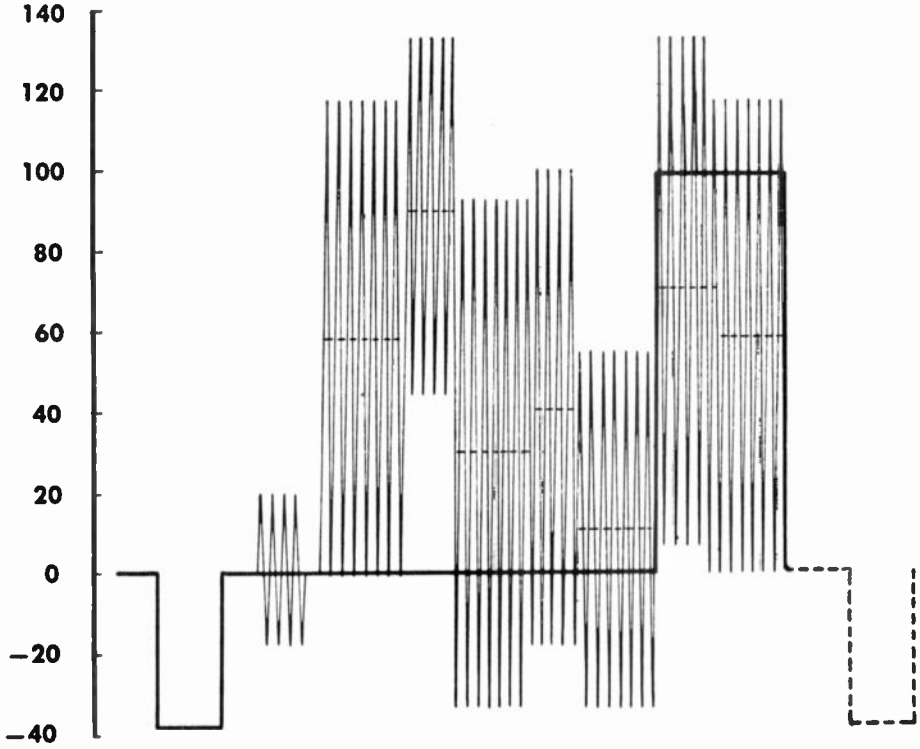

b. Color video signal

maintained constant over the whole frequency band within rather narrow tolerances.

Fig. 6 shows that different colors are transmitted at different potential levels through the transmission systems. For example, the axis of the synchronizing burst is at a zero level in the figure, while that of the group of waves transmitting the yellow signal is at a level of 0.89. Since, in the receiving set, the hue of the color is determined by the relationship of the phase of the synchronizing burst and that of the group of waves carrying the color information, it is necessary that the relationship between the phases of these groups of waves be preserved with great fidelity from the point of signal generation to the point where the signal is used. In the example cited, if the group of waves carrying the yellow color information is shifted in phase by as much as 5 degrees with respect to the phase of the waves in the synchronizing burst, a change in hue will be noticed in the picture. If the phase of the yellow color-carrying group of waves is advanced, the yellow color in the picture will become slightly greenish; if the phase is retarded, it will move slightly towards the orange (see Fig. 4). Hence, a differential phase requirement is born, which was not given serious consideration before the advent of color TV. It was considered necessary in overall transmission to maintain differential phase shift within about $\pm 5°$ limits at color subcarrier frequency.

In regard to compatibility, when a monochrome receiver is fed color signals, only the luminance signal is required. Referring to Fig. 7, the circuitry for selecting the high frequency chrominance components and demodulating them into color difference signals is not present, and the one gun in the monochrome tube is supplied with the luminance signal, plus the interleaved chrominance signal. As was explained above, the frequency composition of the chrominance signal, which is an error signal so far as luminance is concerned, is of such a nature that its visibility is reduced. In a given small area in a picture, plus- and minus-errors will occur in rapid succession and human vision tends to average them out. Hence, it may be said that the signal is so designed that when received by a monochrome receiver, the visibility of the chrominance portion of the signal in the picture area is materially reduced.

When a color receiver is fed a monochrome signal, the outputs of the synchronous demodulators equal zero; the color difference signals are zero; and therefore, the signal supplied to the gain-adjusting network associated with each gun is the same, namely, the E'_y signal. With equal inputs at these points the beams are of the proper relative strength to produce black-and-white.

Conclusion

It is beyond the scope of this article to go into further detail in regard to how the severe requirements of television transmission are met. It will be sufficient to say that in spite of bandwidths about one thousand times as great as those used for single telephone channels, more severe transmission requirements than those used for telephone transmission are necessary for monochrome TV transmission. More severe requirements must be applied for color television signals, primarily due to the necessity for maintaining amplitude responses constant over the whole 4 mc band, and to the differential delay requirement. Steps are being taken to satisfy these needs, and it is expected that in the reasonably near future, regular color transmissions will be achieved with only moderately-increased difficulty over that encountered in the past for monochrome transmissions.

Information on the formation of color TV signals was obtained largely from the reports of Panels 12 and 13 of the National Television Systems Committee. A short bibliography of particular articles of interest is given for the benefit of readers who would like to learn more of the details of the NTSC color system.

Bibliography

1. Report of Panel 12. National Television Systems Committee; cf. NTSC Monograph No. 4A.
2. Report of Panel 13. National Television Systems Committee; cf. "Recommendations," Chairman's Report.
3. Mc Ilwain, K., and Dean, C. E., "Principles of Color Television," Reports of Hazeltine Corporation. To be published as a book by John Wiley and Sons, New York, N. Y.
4. Petition of the National Television System Committee for Adoption of Transmission Standards for Color Television, July 21, 1953.
5. Fink, D. G., "NTSC Color Television Standards." *Electronics*, Vol. 26, No. 12 (December, 1953), pp. 138–150.
6. Law, H. B., "A Three-Gun Shadow Mask Color Kinescope." Proceedings of the IRE, Vol. 39, No. 10 (October, 1951), pp. 1186–1194.

Correction

M. M. McWhorter and J. M. Pettit, authors of the paper, "The Design of Stagger-Tuned Double-Tuned Amplifiers for Arbitrarily Large Bandwidth," which appeared on pages 923–931 of the August, 1955 issue of the Proceedings of the IRE, have brought the following corrections to the attention of the editors.

1. In discussion of Fig. 4, three lines below Fig. 5, the equation in text should read

$$\gamma = \omega_u/\omega_l$$

2. Subscript e in Fig. 7 should be l.
3. In Fig. 20, the axes should be $j\Omega$ and Σ.
4. Five lines below Eq. (12) should read poles a and f, b and e, c and d.

Electronically-Controlled Audio Filters*

L. O. DOLANSKÝ†, SENIOR MEMBER, IRE

Summary—**The use of filters whose cutoff characteristics are controllable by electronic means is often desirable in problems dealing with audio signals. Based on the recent work on fixed RC active filters by J. G. Linvill, variable active low-pass and high-pass filters have been developed using transistor negative-impedance converters.**

The design theory of such filters is summarized, and measured characteristics and other experimental results are presented. An application, in which the cutoff characteristics are controlled by the incoming audio signal for use in formant tracking, is described, and experimental results are given.

Introduction

IN CERTAIN problems dealing with audio signals[1] it is desirable to use filters whose cutoff characteristics are continuously variable in accordance with an applied voltage or current signal, preferably with a minimum of delay. The requirement of variable cutoff characteristics implies (a) that some of the filter components can be varied almost instantaneously by means of a suitable control signal and (b) that such a control signal can be obtained. The control signal may either be related to some property of the incoming audio signal, or it may be generated by independent means.

In the application considered, a low-pass and high-pass filter were required, both having cutoff frequencies continuously variable between 200 and 1,000 cps.

Theoretical Considerations

The filter design adopted was based on the recent work on fixed RC active filters by J. G. Linvill.[1] In this design a negative-impedance converter is used in addition to passive elements; however, the magnitude of the reactive filter elements used here can be varied by electronic means so that electronically variable filter cutoff frequencies are obtained.

The negative-impedance converter transforms the impedance of a two-terminal network by changing the sign of the impedance value. While the need for electronically-controllable elements is thereby not eliminated, the availability of negative impedances results in a greater flexibility of the filter design. For example, a positive resistance present in a physical inductor can be reduced or canceled by connecting a negative resistance $-R$ in series with the inductor. The negative resistance $-R$ can be made to appear between the input terminals of a negative-impedance converter by connecting $+R$ across its output terminals.

* Original manuscript received by the IRE, March 2, 1955; revised manuscript received June 24, 1955. This paper was presented at the National Convention of the IRE, New York, N. Y., March 22, 1955. The work in this paper was performed under Contract AF19 (604)-1039 with the Air Force Cambridge Research Center of the Air Research and Development Command.

† Electronic Research Project, Northeastern University, Boston, Mass.

[1] E.g., formant tracking in speech analysis.

The block diagram of either the low-pass or the high-pass filter constructed is shown in Fig. 1. The transfer function of the entire filter in terms of the open circuit driving-point and transfer impedances of the individual networks can be shown to be equal to

$$H(s) = Z_{21}\Big|_{I_2=0} = \frac{E_2}{I_1}\Big|_{I_2=0}$$
$$= \left[\frac{-1}{(z_{12})_a}\cdot\frac{(z_{11})_b}{(z_{12})_b} + \frac{(z_{22})_a}{(z_{12})_a}\cdot\frac{1}{(z_{12})_b}\right]^{-1}$$
$$= \frac{(z_{12})_a(z_{12})_b}{(z_{22})_a - (z_{11})_b}. \tag{1}$$

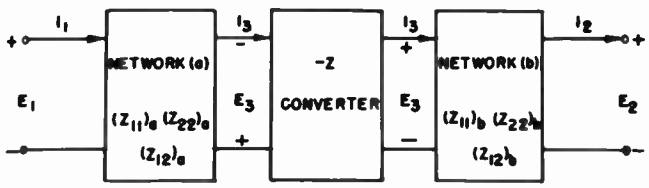

Fig. 1—Block diagram of HP or LP filter.

$H(s)$ will be a ratio of two polynomials and can be written

$$H(s) = \frac{N(s)}{D(s)}. \tag{2}$$

In order to synthesize $H(s)$ by means of RC and RL networks only, it is convenient to divide both $N(s)$ and $D(s)$ by

$$M(s) = (s = \sigma_1)(s - \sigma_2)\cdots(s - \sigma_n) \tag{3}$$

where $\sigma_1, \sigma_2 \cdots \sigma_n$ represent the poles of $(z_{22})_a$ and $(z_{11})_b$. The denominator of $H(s)$ becomes

$$D'(s) = \frac{D(s)}{\prod_{i=1}^{n}(s - \sigma_i)}$$
$$= k_0 + \sum_{i=1}^{n}\frac{k_i}{s - \sigma_i} = (z_{22})_a - (z_{11})_b, \tag{4}$$

while the numerator is equal to

$$N'(s) = \frac{N(s)}{\prod_{i=1}^{n}(s - \sigma_i)} = (z_{12})_a(z_{12})_b. \tag{5}$$

If, in (4), the positive k's are associated with $(z_{22})_a$ and the negative ones with $(z_{11})_b$, the networks a and b can be synthesized; e.g., by Cauer's continued fraction expansion. The negative sign before $(z_{11})_b$ is supplied by the negative-impedance converter.

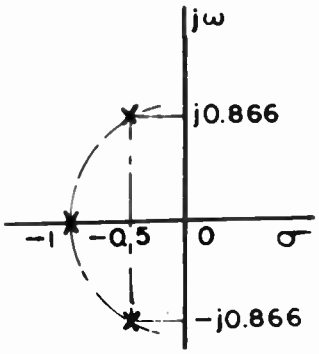

Fig. 2—Pole pattern for Butterworth LP filter.

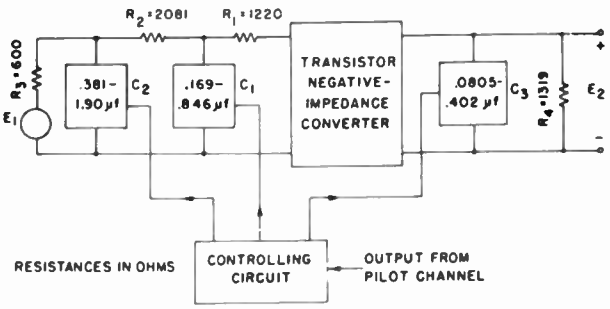

Fig. 3—Simplified circuit diagram of electronically-controllable LP filter.

Low-Pass Filter

The desired low-pass filter characteristic is of the Butterworth type ($n=3$), so that, in normalized form,

$$H(s) = \frac{k}{(s+1)(s^2+s+1)} \tag{6}$$

The distribution of the poles of $H(s)$ is shown in Fig. 2. A considerable freedom of choice exists about the location of the σ_i's. In the present design, $\sigma_1 = -0.3$, $\sigma_2 = -1.05$ and $\sigma_3 = -1.5$ have been chosen. The circuit element values, after scaling to a suitable frequency and impedance level, are given in Fig. 3. As indicated in the diagram, three electronically controllable capacitors are used in the filter. The negative-impedance converter[2] simulates at its input terminals the negative of the physical impedance connected across its output terminals, which in this case is composed of a 1,319-ohm resistor and a capacitor whose value varies between 0.0805 and 0.402 μf.

Negative-Impedance Converter

The requirements which the negative-impedance converter must meet exceed the possibilities of a combination of passive elements alone. The converter must therefore contain active elements as well. As indicated by Fig. 4, two transistors are included in the negative-impedance-converter circuit. When Z_L is connected to the output terminals, the apparent input impedance Z_{in} is approximately equal to $-Z_L$. Since this circuit differs only in minor details from the original design described by J. G. Linvill,[1] a detailed description of its operation will be omitted here. Fig. 5 represents the

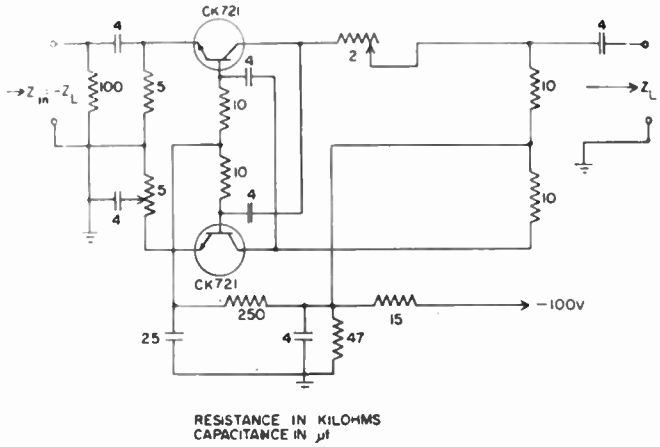

Fig. 4—Transistor negative-impedance converter.

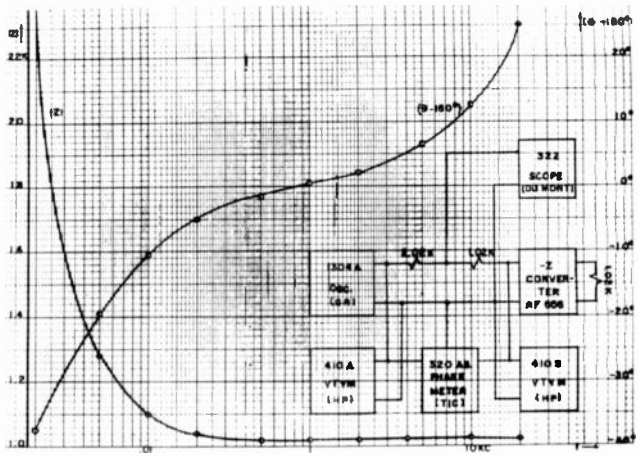

Fig. 5—Values of $|Z|$ and (θ-180 degrees) vs frequency.

values of the input impedance magnitude $|Z|$ and phase angle θ for a purely resistive $Z_L = 1.02$ kohm. It is seen that $|Z|$ is substantially constant for 200 cps $< f <$ 20 kc, and increases rapidly for frequencies lower than 200 cps. The phase varies from -10.5 degrees to $+12.5$ degrees for 100 cps $< f <$ 10 kc.

Variable C Circuit

In the electronically-controllable low-pass filter three electronically-controllable capacitors are required. A three-tube circuit, whose apparent input capacitance can be varied by means of a varying dc voltage, has been designed. The operation, which is based on the so-called Miller effect, can be explained by means of the simplified circuit shown in Fig. 6 (next page).

Assuming that the loading of the plate circuit by C_2 is negligible, the input current

$$I = [j\omega C_1 + j\omega C_2(1+A)]E, \tag{7}$$

where

$$A = \text{stage amplification.}$$

Thus the input admittance

$$Y = I/E = j\omega[C_1 + C_2(1+A)]$$
$$= j\omega C_{eq}, \tag{8}$$

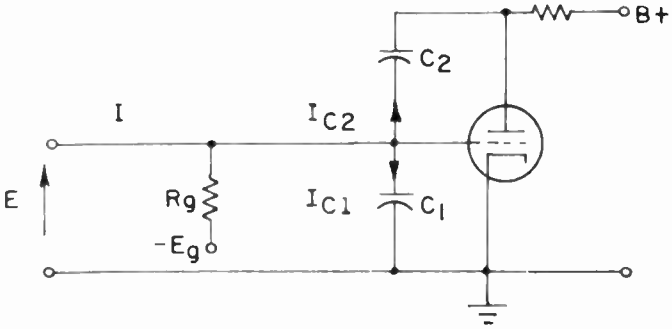

Fig. 6—Principle of operation of electronically variable capacitor.

if A is a real number.

The equivalent input capacitance

$$C_{eq} = C_1 + C_2(1 + A) \tag{9}$$

can be varied if the stage gain is varied, for example by varying the g_m of the tube.

In the present application, fairly large values of C_{eq} are required, which means that large grid-to-plate capacitors must be used. This causes the stage gain to become complex, so that the input impedance has a resistive component as well. The loading of the plate circuit by C_2 is not negligible. To remove this excessive loading of the plate circuit, a cathode follower has been inserted between the plate load resistor and C_2.

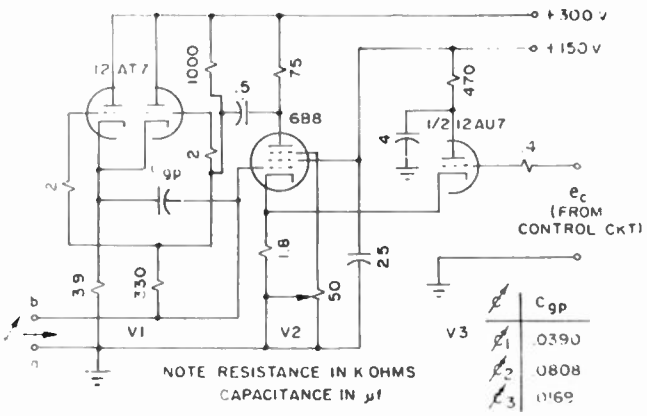

Fig. 7—Circuit diagram of electronically controllable capacitors.

The complete variable-capacitor circuit is shown in Fig. 7. The heart of the circuit is a type 6B8 variable-g_m tube (V_2). The gain of this stage varies according to the variations in the grid-to-cathode voltage. These variations are achieved by controlling the dc input to V_3. The first stage (V_1) represents the isolation cathode follower mentioned before. The variable capacitor $\hat{C}$ appears between the terminals a and b. For each of the three variable capacitors used in the low-pass filter a different value of C_{gq} must be used, as indicated in the table of Fig. 7. Otherwise the three circuits are identical.

Tracking of the Electronically Controllable Capacitors

Each of the controllable capacitors should be capable of a 5:1 variation in apparent capacitance, corresponding to the 5:1 variation in filter cutoff frequency. Moreover, the same increment in control voltage e_c should vary the capacitance values by the same ratio for all three capacitors. The measured values of apparent input capacitances $\hat{C}_1$, $\hat{C}_2$, $\hat{C}_3$ are shown in Fig. 8. The ratios of the capacitance values vary over the following ranges as shown in Table I:

TABLE I

Ratio	Desired Value (for 200 cps $< f <$ 1,000 cps)	Measured Value
$\hat{C}_1/\hat{C}_2$	0.445	0.443–0.516
$\hat{C}_2/\hat{C}_3$	4.73	4.40 –4.70
$\hat{C}_1/\hat{C}_3$	2.11	2.00 –2.42

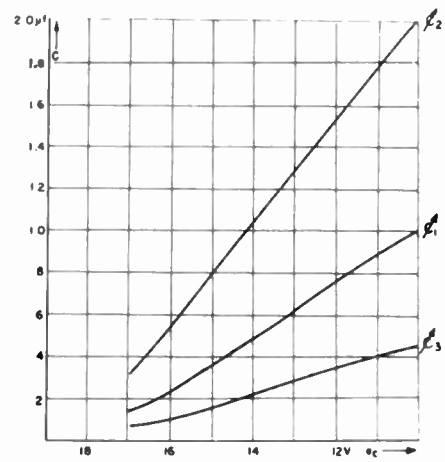

Fig. 8—Variation of $\hat{C}_1$, $\hat{C}_2$ and $\hat{C}_3$ vs control voltage e_c.

Experimental Circuit

A circuit diagram of the entire electronically-controllable low-pass filter is presented in Fig. 9. A cathode-follower circuit (V_1) is included to provide the proper impedance for the low-impedance input of the filter; it also prevents any disturbing loading of the preceding 850-cps LP filter. Tubes V_2 through V_{10} represent the three controllable capacitors while the filter resistors are shown before and after the negative-impedance converter.

High-Pass Filters

Low-pass-High-pass Transformation

If in the original low-pass filter expressions (see (6)) s is replaced by $1/s$, a high-pass filter with the same cutoff frequency is obtained. The impedances which replace the variable capacitors must vary in proportion to s instead of $1/s$ as was required in the low-pass case. Thus an electronically controllable inductor[2] is needed in the high-pass filter.

Driving Circuit for "Increductor"

The "Increductor" is a saturable inductor and its inductance depends upon the degree of magnetic saturation of the core which in turn depends upon the mag-

[2] A suitable unit has recently been manufactured by CGS Laboratories under the name "Increductor."

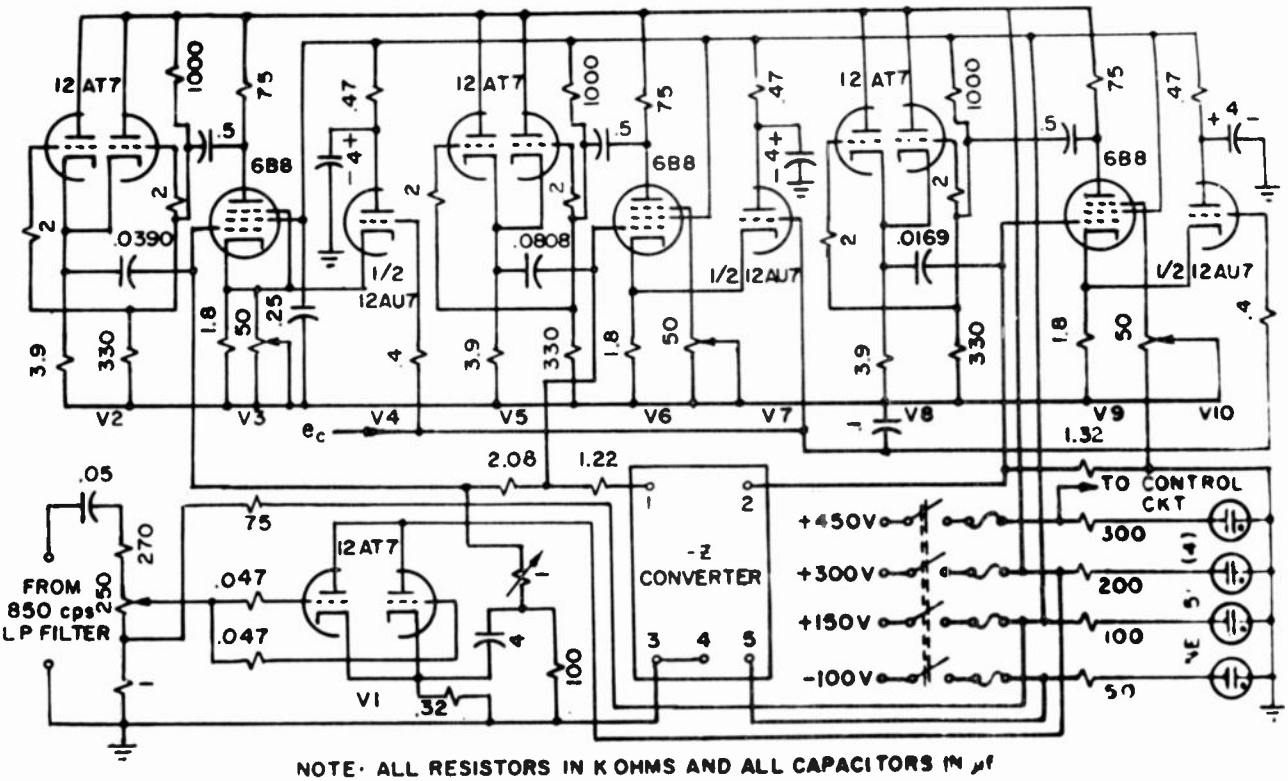

Fig. 9—Electronically controlled LP filter.

nitudes of the currents in two available control windings. While a control voltage source was necessary to achieve the desired variations of the capacitors in the low-pass case a suitable current source had to be designed to vary the variable inductors over the desired range in the high-pass case. It was desired, however, to start with the same original control signal for both filters. Hence, a circuit for transforming variations of voltage into variations of a current source has been designed, as shown in Fig. 10. The control voltage in this circuit is fed into the 6AG7 pentode which represents an approximate current source.

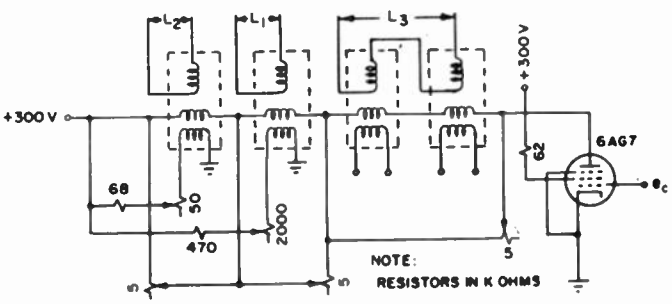

Fig. 10—Control circuit for electronically controlled HP filter.

Tracking of the Electronically Controllable Inductors

As in the case of the electronically-controllable capacitors, the inductors should change by the same ratio for a given change in control signal. This is achieved by connecting all the main control windings of all Increductors in series and bypassing each of them by a suitable resistor so that only the desired fraction of the total varying control current passes through the winding. A constant difference in magnetization between any two Increductors can be achieved by means of the second control winding, usually called "bias" winding, which is connected to +300v through a suitable resistor.

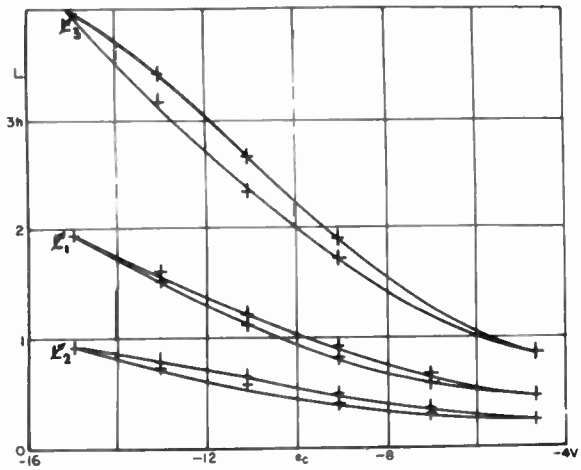

Fig. 11—Variation of L_1, L_2 and L_3 vs control voltage e_c.

The measured variation of the electronically controllable inductors is given in Fig. 11. Because of the large control-winding inductance and comparatively small parallel resistance, the time constant of the control circuit is somewhat excessive. It is believed that this drawback can be minimized by using a separate control pentode for each Increductor, and by reducing the total control current, rather than by passing a part of it through the parallel resistor. Another difficulty en-

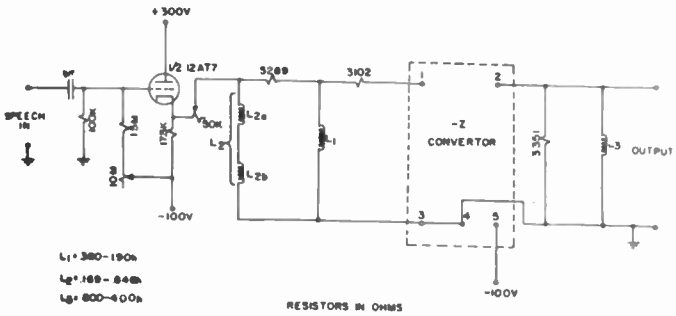

Fig. 12—Electronically controlled HP filter.

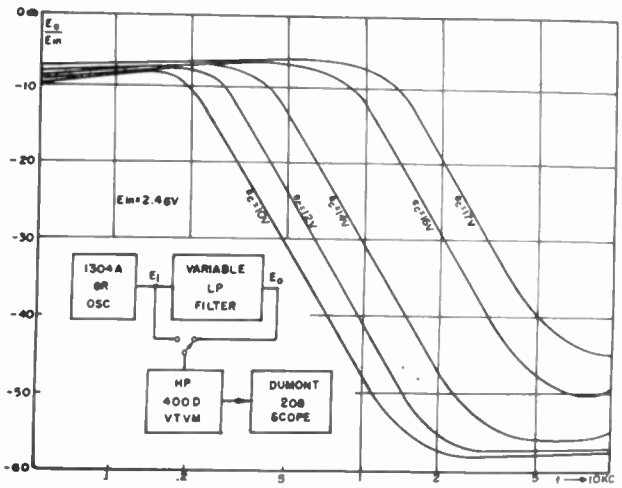

Fig. 13—Response of electronically controlled LP filter for various values of control voltage e_c.

countered with the use of Increductors is a certain amount of hysteresis. Both these effects will be demonstrated presently by means of dynamic-behavior oscillograms, representing the output signals of the filters.

Experimental Circuit

Fig. 12 represents the electronically controllable high-pass filter, without the control circuit which has already been shown in Fig. 10. As in the case of the low-pass filter, two of the variable reactances are before, one behind, the negative-impedance converter. In order to secure more favorable conditions with respect to hysteresis and Q, L_2 is composed of two Increductors L_{2a} and L_{2b}. In this way it is possible to operate all Increductors nearer to their optimum ranges.

Experimental Results

Low-Pass Filter

A family of curves representing the sinusoidal steady-state response of the low-pass filter for various values of the control voltage e_c is given in Fig. 13.

The attenuation in the stop-band is at a rate of about 17 db per octave. The theoretically expected value is 18 db per octave. Once the attenuation of 35 db is reached, the response remains below this value for all higher frequencies. The residual output at these higher frequencies seems to be mostly due to high-frequency noise

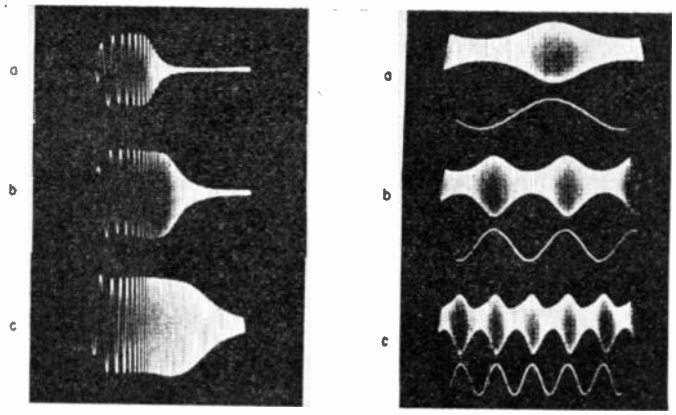

Fig. 14—Filter output for varying input signal frequency and control voltage. (Left: $f_s=100$–$1{,}500$ cps, e_c adjusted for $f_c=200$ cps (a), 500 cps (b), 1,000 cps (c).) (Right: $f_s=500$ cps, sinusoidal control voltage, $f_{cv}=5$ cps (a), 10 cps (b), 20 cps (c).)

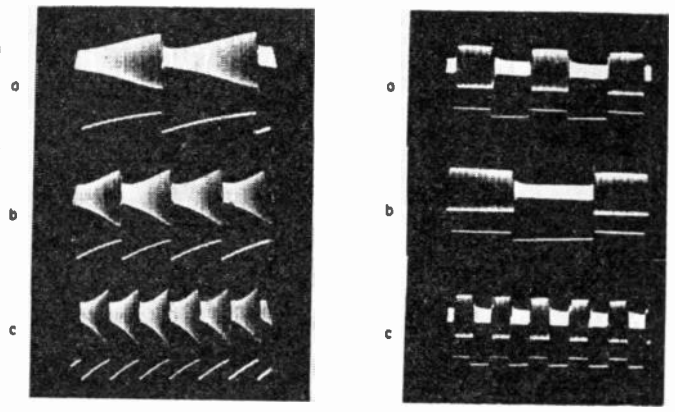

Fig. 15—Filter output for fixed input signal frequency and varying control voltage. (Left: $f_s=500$ cps, saw-tooth control voltage, $f_{cv}=5$ cps (a), 10 cps (b), 17 cps (c).) (Right: $f_s=500$ cps, square-wave control voltage, $f_{cv}=10$ cps (a), 5 cps (b), 20 cps (c).)

generated by the transistor-negative-impedance circuit, with a smaller component due to 60 cps hum. A larger input signal will increase the difference between the pass-band and stop-band response, but at the same time a distortion of the sinusoidal output is observed.

Fig. 14(a) represents the output of the low-pass filter for three values of the control voltage, corresponding to three cutoff frequencies—200 cps, 500 cps and 1,000 cps—when the frequency of a constant-magnitude signal sweeps between 100 and 1,500 cps. In Fig. 14(b) the input-signal frequency is fixed but the control voltage varies sinusoidally at various rates. In Figs. 15(a) and 15(b) the control signal varies in a saw-tooth and square-wave fashion, respectively, the remaining conditions being the same as in the preceding figure.

Sudden changes in the control signal cause transients in the output signal, as indicated in Fig. 15. This is due to the fact that the desired change in g_m of the variable-g_m tube V_2 (see Fig. 7) is accompanied by dc level transients in various parts of the variable-capacitor circuit. Since in the present application this effect appears to cause little error in the final result, no effort has been made to eliminate these formants. If necessary, however, an attempt could be made to balance the dc step at the plate of V_2 by another step of equal magnitude

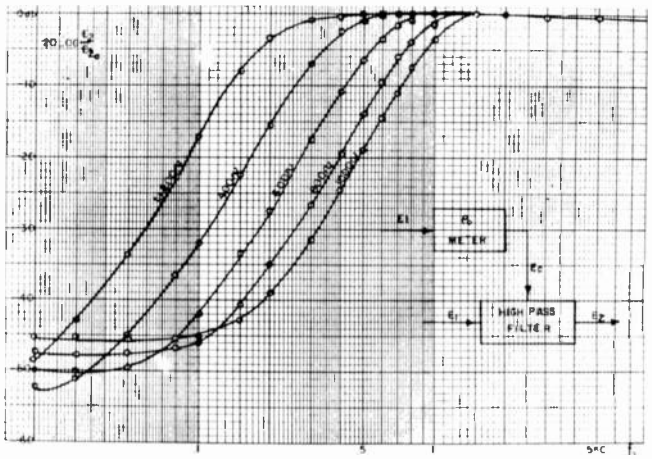

Fig. 16—Response curves of electronically controlled HP filter for various values of input frequency.

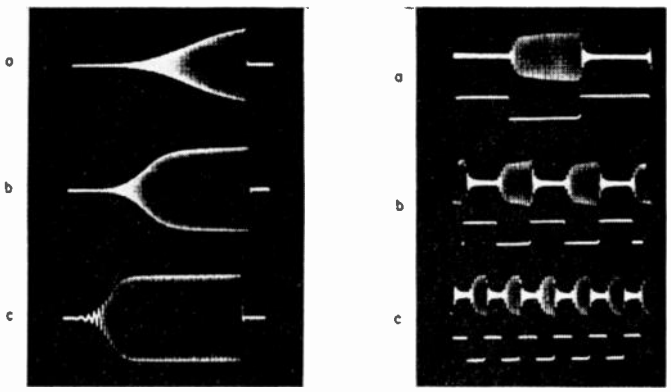

Fig. 17—Dynamic response characteristics of electronically controllable high-pass filter. (Left: sinusoidal sweep 0–1,500 cps, $e_s=2$v rms, $f_i=1{,}000$ cps (a), 500 cps (b), 200 cps (c).) (Right: $f_s=300$ cps, $e_s=2$v rms, $e_c=8.8$v dc plus square wave 10v peak-to-peak, $f_c=5$ cps (a), 10 cps (b), 20 cps (c).)

and opposite polarity, so that the dc level at the plate of V_2 would remain undisturbed.

High-pass Filter

A family of measured response curves of the electronically-controllable high-pass filter is given in Fig. 16. It is seen that desired 5:1 variation in cutoff frequency can be achieved, and filter attenuates at about 16 db per octave with a stop-band attenuation of 45 db or more.

The response for a constant-magnitude sweeping-frequency input signal is demonstrated by Fig. 17(a), three fixed values of the control signal corresponding again to three cutoff frequencies. The response of the filter in the case of a constant sinusoidal signal, with the control voltage varying in a square-wave fashion, is shown in Fig. 17(b). Although the control voltage assumes the new value almost instantaneously, the output reaches the new steady-state response only after considerable delay.

Fig. 18 represents the output of the filter when the control voltage is varied very slowly in a triangular fashion, so that the sluggishness of the control circuit is minimized. This oscillogram is indicative of the effect

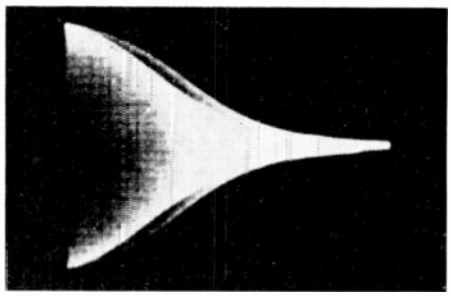

Fig. 18—Hysteresis display, sweep rate 0.33 cps, triangular variation of e_c between 3.6v and 16v.

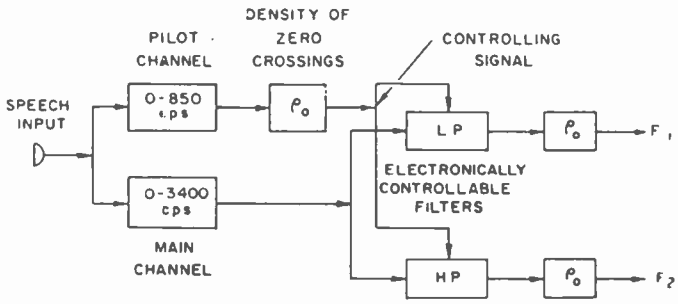

Fig. 19—A scheme for formant tracking.

of hysteresis upon the filter response. Variations of up to about 10 per cent of the total inductance value have been observed when the Increductor is subjected to the maximum control-current variation, which is required for the 5:1 change in inductance.

Application to Formant Tracking

The short-time power spectrum of most speech sounds has several broad peaks along the frequency axis; these concentrations of sound energy are sometimes called formants. The formant frequency indicates their approximate location on the frequency axis. When time and frequency are represented on the horizontal and vertical axes, respectively, while the presence of relatively large amounts of sound energy is represented by dark areas, the so-called "visible speech" pattern is obtained. An example of such a record is shown in Fig. 20, where the formants are represented by the dark bars.

Since the formants are significantly different for different sounds, it is often desirable to obtain automatically an approximate continuous indication of the varying values of the formant frequencies. The block diagram of Fig. 19 represents a scheme for the separation of the formants.[3],[4] An 850 cps LP filter eliminates that part of the power spectrum which, as a rule, does not contain the first formant. The density of zero-crossings of the remaining signal is converted into a voltage signal which controls the cutoff frequencies of a low-pass and a high-pass filter. The output of the low-pass filter should contain essentially only the first formant and a voltage proportional to the first formant frequency should appear at F_1. Similarly, the output of the high-pass filter should contain the second and possibly higher formants.

As an example of the performance of the electroni-

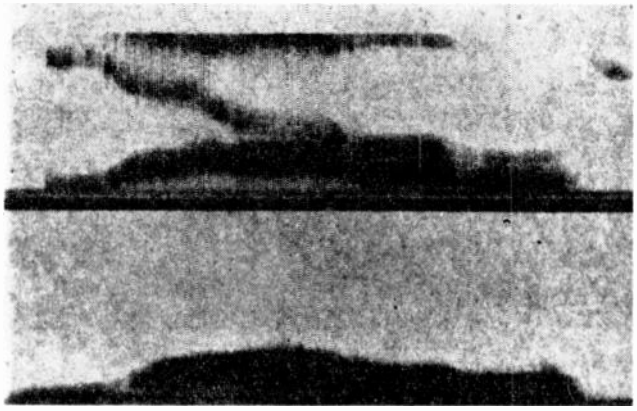

Fig. 20—Spectrograms for *i-ε-a-o-u*. (a) wide band, no filter; (b) wide band, variable LP filter. Note: the sonagraph was set on HS (high shaping).

cally-controllable low-pass filter, sound spectrograms of the sound sequence *i-ε-a-o-u* are shown in Fig. 20.

In these spectrograms, the formants are represented as dark bars whose vertical position, corresponding to frequency, varies with time. Fig. 20(a) represents the sound before filtering, while Fig. 20(b) shows the spectrogram after the sound sequence has been filtered through the electronically-controllable low-pass filter. It is seen that the separation of the first formant is accomplished reasonably well even if the second formant is very close to the first formant, as, for example, for *o* and *u*.

In Fig. 21, the behavior of the electronically-controllable high-pass filter is indicated by means of the oscillograms of the filtered and unfiltered sound *i*. It is seen that the lower frequency components have been attenuated considerably, although for the given purpose more attenuation would be desirable.

Conclusions and Limitations

In view of the investigations which have been reported in this paper, the following conclusions can be made:

1. The performance of the constructed electronically-controllable low-pass and high-pass filters have been found to be close to the expected behavior in the pass-band and in the cutoff region.
2. A suitable voltage source is needed for the control of the cutoff frequency of the low-pass filter.
3. A current source is needed for the control of the cutoff frequency of the high-pass filter.
4. The 5:1 range of the cutoff frequency is close to the maximum value which can be achieved with the present low-pass filter.
5. In the case of the high-pass filter, the range of the cutoff frequency is presently limited by the maximum current of the controlling pentode. However, if a larger current source were used, a deterioration of the slope in the cutoff region is to be expected because of the lower Q of the Increductors under such conditions.
6. In the stop-band the response is at least 35 db below the maximum response for the low-pass filter, and about 45 db for the high-pass filter. A larger attenuation would be desirable, particularly in the low-pass case. The residual signal seems to be predominantly high-frequency noise, with a smaller hum component.
7. At present, the transistor-negative-impedance converter is the limiting factor for maximum signal size without distortion. However, the limitations imposed by the variable reactance elements are only slightly above the limitations of the transistor circuit.
8. Hysteresis causes the apparent inductance of the saturable inductors to vary by about 10 per cent, for the same value of the control current.

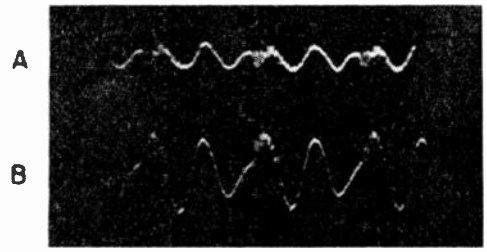

Fig. 21—Filtered (a) and unfiltered (b) samples of the sound *i*.

Acknowledgment

The author wishes to express his gratitude to the members of the Speech Project at Northeastern University, particularly to Professor M. W. Essigmann for his encouragement, to Dr. S. H. Chang for suggestions and criticism, to Dr. H. L. Stubbs for his suggestions during the preparation of this paper, and to Mr. C. Howard for his cooperation on details of circuitry and testing; the help extended to the author by Mrs. M. D. Reynolds and Mr. W. F. Geddard during the preparation of the manuscript is also very much appreciated.

Bibliography

(1) Linvill, J. G., "RC Active Filters." Proceedings of the IRE, Vol. 42, (March, 1954), pp. 555–564.
(2) Linvill, J. G., "Transistor Negative Impedance Converters." Proceedings of the IRE, Vol. 41, No. 6 (June, 1953), pp. 725–729.
(3) Interim Technical Report No. 1, Contract No. AF19(604)-1039, Item I, March 1, 1954 through August 31, 1954, Visual Message Presentation (Northeastern University).
(4) Scientific Report No. 2, Contract No. AF19(604)-1039, Item I, September 1, 1954 through February 28, 1955, Visual Message Presentation (Northeastern University).
(5) Peterson, G. E., and Barney, H. L., "Control Methods Used in a Study of the Vowels." *Journal of the Acoustical Society of America*, Vol. 24 (March, 1952), pp. 175–184.

Magnetic Fields in Small Ferrite Bodies with Applications to Microwave Cavities Containing Such Bodies*

A. D. BERK† AND B. A. LENGYEL†, SENIOR MEMBER, IRE

Summary—**The microwave magnetic field in a small ferrite sphere and thin circular cylinder is found in first approximation. In a circularly polarized exciting field the internal field is again circularly polarized. The ratio of the internal field to the exciting field is $3(\mu \pm \alpha + 2)^{-1}$ for the sphere and $2(\mu \pm \alpha + 1)^{-1}$ for the cylinder. When the exciting field is linearly polarized the internal field is elliptically polarized. The expressions derived are applied to the calculation of the detuning and change of Q of microwave resonators containing ferrite spheres, cylinders and discs. Conversely they provide a means for the calculation of the elements of the permeability tensor from the experimentally observable change in cavity characteristics. The ferromagnetic resonant frequencies calculated from the present formulas are in agreement with those obtained by Kittel by the use of demagnetizing factors.**

Introduction

MICROWAVE propagation in ferrites placed in an orienting steady magnetic field has been the subject of many recent investigations. The distinctive macroscopic property of ferrites is the tensor character of their permeability. When orienting field is in z direction, and of sufficient magnitude for saturation, intrinsic permeability is described by tensor:

$$\mathbf{\mu} = \mu_0 \begin{pmatrix} \mu & -j\alpha & 0 \\ j\alpha & \mu & 0 \\ 0 & 0 & 1 \end{pmatrix}, \tag{1}$$

where μ_0 is the permeability of free space, μ and α are functions of the frequency and of the orienting field.[1] Quantities μ and α are complex, but for frequencies sufficiently far removed from ferromagnetic resonance, their imaginary parts are small. Dielectric constant of a ferrite is a scalar, $\epsilon = \epsilon_0 \kappa$. Values of κ of about 10 are common.

Experimental work aimed at the determination of the magnetic properties of ferrites usually consist of the observation of changes in the characteristics of a resonant cavity induced by a small test piece of ferrite placed in the cavity. The object of most investigations utilizing this technique has been the study of ferromagnetic resonance.[2–4] In this paper, however, the emphasis is on the actual computation of the material constants μ and α from observational data.

This problem has interested a number of investigators. Lax and Berk[5] presented formulas for both the real and the imaginary parts of the permeability tensor in terms of the shift in frequency and change in Q of a degenerate cylindrical cavity containing a small sphere of ferrite. An experimental procedure was described by Artman and Tannenwald[6] for the application of these formulas. However, the permeability tensor utilized in both references[5,6] is an "effective" quantity different from the intrinsic permeability tensor of (1). Van Trier[7] developed a method for the measurement of the intrinsic permeability tensor. It utilizes a coaxial cavity with a long thin ferrite cylinder. In order to yield accurate results, this method requires the use of very thin uniform cylinders which are not easy to come by.

Rowen and von Aulock[8] proposed, recently, using thin disks rather than small spheres for samples in a cavity. While their initial results are encouraging, they have overestimated some of the difficulties associated with spherical samples and underestimated some of the difficulties associated with thin disks of large diameter.

In order to explore the relative merits of different configurations and to provide a source of reference for the evaluation of experimental data, we have calculated the shift in resonant frequency and the change of Q of cavities containing ferrites of spherical, cylindrical and disk shapes, in terms of the intrinsic permeability tensor.

An essential step in deriving such expressions, consists of the determination of the rf field within each sample. We shall obtain these internal fields by direct use of field theory—solving a quasi-static equation subject to boundary conditions. Our results agree with those implied in Polder's equations[1] formulated on the basis of demagnetizing factors.

Field in a Sphere

The simplest problem of the type to be considered is the calculation of the electric and magnetic polarization of a sphere in a uniform static field. When a sphere of

* Original manuscript received by the IRE, March 15, 1955; revised manuscript received, July 14, 1955.

† Research Labs., Hughes Aircraft Co., Culver City, Calif.

[1] D. Polder, "On the theory of ferromagnetic resonance," *Phil. Mag.*, vol. 40, pp. 99–115; January, 1949.

[2] H. G. Beljers, "Measurements on gyromagnetic resonance of a ferrite," *Physica*, vol. 14, pp. 629–641; February, 1949.

[3] W. A. Yager and others, "Ferromagnetic resonance in nickel ferrite," *Phys. Rev.*, vol. 80, pp. 744–748; November, 1950.

[4] H. G. Beljers and J. L. Snoek, "Gyromagnetic phenomena occurring within ferrites," *Philips Tech. Rev.*, vol. 11, pp. 313–322; May, 1950.

[5] B. Lax and A. D. Berk, "Cavities with complex media," 1953 IRE Convention Record, Part 10, "Microwaves," pp. 65–73.

[6] J. O. Artman and P. E. Tannenwald, "Measurement of permeability tensor in ferrites," *Phys. Rev.*, vol. 91, pp. 1014–1015; August, 1953.

[7] A. A. Th. M. Van Trier, "Guided electromagnetic waves in anistropic media," *Appl. Sci. Res.*, B 3, pp. 305–371; 1953.

[8] J. H. Rowen and W. von Aulock, "Measurement of the complex tensor permeability of ferrites," *Phys. Rev.*, vol. 96, pp. 1151–1153; November, 1954.

permeability $\mu_0\kappa_m$ is placed in a uniform magnetic field $\boldsymbol{H}_0$, it is well-known that the field within the sphere will be uniform and equal to $3\boldsymbol{H}_0/(\kappa_m+2)$, while outside there will be a dipole field added to $\boldsymbol{H}_0$, with the dipole located at the center of the sphere.

This result will be approximately valid for a sphere in a nonuniform, or even time-varying field, provided that the sphere is so small that in its immediate neighborhood the applied field may be regarded as uniform and in the same phase.

Once this quasi-static approach is adopted, the electric and magnetic field problems are separated and we may confine ourselves to the latter. It is thus required to determine the diffraction of a uniform, quasi-static field by a ferrite sphere. It is clear from the form of $\mathfrak{u}$ that the response of the ferrite body to an incident field directed along the z axis is the same as that of an isotropic sphere of permeability μ_0, therefore, only the effect of an incident field in the xy plane is of interest. The x axis will then be chosen parallel to the incident field which will be denoted by H_0e_x, where H_0 is the magnitude of the magnetic field and e_x is the unit vector in the x direction. The field $\boldsymbol{H}$ to be determined must thus reduce to H_0e_x for large distances r, its tangential component must be continuous for $r=a$, the radius of the sphere; moreover, $\boldsymbol{B}=\mathfrak{u}\cdot\boldsymbol{H}$ must be solenoidal and $\boldsymbol{n}\cdot\boldsymbol{B}$, the normal component of $\boldsymbol{B}$ on the surface, must be continuous.

The quasi-static nature of the problem allows us to let $\boldsymbol{H}=\text{grad}\ \psi$. The potential ψ must be continuous everywhere, it must have first and second derivatives except for $r=a$, and for large r it should reduce to H_0x. In view of the solenoidal character of $\boldsymbol{B}$

$$\nabla^2\psi=0, \quad \text{for } r>a, \tag{2}$$

$$\text{div}\ (\mathfrak{u}\cdot\text{grad}\ \psi)=\mu\nabla^2\psi+(1-\mu)\frac{\partial^2\psi}{\partial z^2}=0, \quad \text{for } r<a. \tag{3}$$

The continuity of $\boldsymbol{n}\cdot\boldsymbol{B}$ on the sphere requires that

$$\boldsymbol{n}\cdot(\mu_0\ \text{grad}\ \psi)_+ = \boldsymbol{n}\cdot(\mathfrak{u}\cdot\text{grad}\ \psi)_-, \tag{4}$$

where the subscripts + and − indicate external and internal limits at the surface. Since the permeability tensor in spherical coordinates is

$$\mathfrak{u}=\mu_0\begin{pmatrix} 1+(\mu-1)\sin^2\theta & (\mu-1)\sin\theta\cos\theta & -j\alpha\sin\theta \\ (\mu-1)\sin\theta\cos\theta & 1+(\mu-1)\cos^2\theta & -j\alpha\cos\theta \\ j\alpha\sin\theta & j\alpha\cos\theta & \mu \end{pmatrix},$$

(4) takes the form:

$$\left(\frac{\partial\psi}{\partial r}\right)_+ = [1+(\mu-1)\sin^2\theta]\left(\frac{\partial\psi}{\partial r}\right)_- + (\mu-1)\frac{\sin\theta\cos\theta}{a}\left(\frac{\partial\psi}{\partial\theta}\right)_- - j\frac{\alpha}{a}\left(\frac{\partial\psi}{\partial\phi}\right)_-. \tag{5}$$

All the preceding conditions can be satisfied by the solution (suggested by the isotropic static problem):

$$\psi = \begin{cases} H_0x + D_1\dfrac{x}{r^3} + D_2\dfrac{y}{r^3}, & \text{for } r>a \\ A_1x + A_2y, & \text{for } r<a \end{cases}, \tag{6}$$

provided

$$\begin{aligned} D_1 &= (A_1 - H_0)a^3; \quad D_2 = A_2a^3, \\ A_1 &= 3H_0(\mu+2)[(\mu+2)^2-\alpha^2]^{-1}; \\ A_2 &= -3j\alpha H_0[(\mu+2)^2-\alpha^2]^{-1}. \end{aligned} \tag{7}$$

The internal magnetic field is thus

$$\boldsymbol{H}_- = A_1e_x + A_2e_y. \tag{8}$$

Because of the appearance of j in A_2, the x and y components of the field will be in time quadrature. Within the sphere the field will be uniform and elliptically polarized; outside the sphere there will be two perpendicular dipole fields in time-quadrature added to the original field e_xH_0. Note that the H field turned out to be solenoidal in the ferrite. This is a consequence of the simplicity of the field, for, in general,

$$\text{div}\ \boldsymbol{H} = j\frac{\alpha}{\mu}(\text{curl}\ \boldsymbol{H})_z + \frac{\mu-1}{\mu}\frac{\partial H_z}{\partial z}. \tag{9}$$

While a linearly-polarized external field was shown to excite an elliptically-polarized one in the ferrite, it is easy to show by superposition that a circularly-polarized external field $H_0(e_x \pm j\ e_y)$ excites a circularly-polarized field within the ferrite, which is given by

$$\boldsymbol{H}_- = \frac{3H_0(e_x \pm j\ e_y)}{\mu \pm \alpha + 2}. \tag{10}$$

The fields in a cavity are, of course, neither static nor uniform so that (8) and (10) are only approximations. From the classical problem of the diffraction of a plane wave by an isotropic sphere, one can show that

1. If the plane wave is traveling the static solution is a zeroth order approximation in (ka), k being the propagation constant, a, the radius of the sphere, whereas
2. If the plane wave is standing and the sphere is located at a maximum of the field, the static solution is a first order approximation in (ka).

It is intuitively clear the preceding statements prevail for anisotropic spheres also. Hence, keeping in mind the standing-wave character of cavity fields, one may conclude that the terms neglected in (10) are those in $(ka)^2$ and higher orders.

Field in a Cylinder

The case of a long, thin cylinder parallel to the z axis can be treated similarly. Considering the linearly polarized case first, we have, instead of (5),

$$\left(\frac{\partial\psi}{\partial r}\right)_+ = \mu\left(\frac{\partial\psi}{\partial r}\right)_- - j\frac{\alpha}{a}\left(\frac{\partial\psi}{\partial\phi}\right)_-, \tag{11}$$

and the potential on the outside becomes

$$\psi_+ = H_0 x + \frac{D_1' x}{r^2} + \frac{D_2' y}{r^2}, \tag{12}$$

while the form of the field within the cylinder is the same as in the spherical case. The coefficients A_1 and A_2 become

$$A_1' = \frac{2(\mu+1)H_0}{(\mu+1)^2-\alpha^2}, \quad A_2' = \frac{-j2\alpha H_0}{(\mu+1)^2-\alpha^2}, \tag{13}$$

furthermore,

$$D_1' = (A_1' - H_0)a^2, \quad D_2' = A_2' a^2.$$

When the applied field is circularly polarized, we have

$$\boldsymbol{H}_- = \frac{2H_0(e_x \pm j\, e_y)}{\mu \pm \alpha + 1}. \tag{14}$$

Ferrites in Cavities

One may readily show that the change in the resonant frequency of a cavity, due to the introduction of a small sample of material, is given by[9]

$$\omega - \omega_0 = j \frac{\int J_m \cdot H_0^* dv + \int J_e \cdot E_0^* dv}{\mu_0 \int \boldsymbol{H} \cdot \boldsymbol{H}_0^* dv + \epsilon_0 \int \boldsymbol{E} \cdot \boldsymbol{E}_0^* dv}, \tag{15}$$

where $J_e = j\omega(\epsilon - \epsilon_0)\boldsymbol{E}$ and $J_m = j\omega(\underline{\mu} - \mu_0)\cdot \boldsymbol{H}$ are the electric and magnetic polarization current densities, $\boldsymbol{E}_0$, $\boldsymbol{H}_0$ and ω_0 are the unperturbed fields and frequency of the cavity, $\boldsymbol{E}$, $\boldsymbol{H}$ and ω are the similar quantities in the presence of the material sample and ϵ, $\underline{\mu}$ are characteristics of the sample. The integrals are over the volume of the cavity. While the denominator of (15) may be replaced, for small perturbations, by $2\mu_0 \int |\boldsymbol{H}_0|^2 dv$, it is necessary to know the internal fields $\boldsymbol{E}$ and $\boldsymbol{H}$ for the evaluation of the numerator. For cases of practical interest, approximate expressions for these fields were obtained in the preceding sections.

Spherical Samples

We shall first consider cylindrical cavities (not necessarily circular) with spherical samples. In a practical case, the ferrite sphere is usually placed at a point where the electric field is zero, thus, $J_e = 0$. If, at this point, the unperturbed magnetic field is circularly polarized in the xy plane, we have $\boldsymbol{H}_0 = H_m(e_x \pm j\, e_y)$, and the internal field $\boldsymbol{H}$ is to be computed by means of (10). For sufficiently small samples, the numerator of (15) can be replaced by the product of v, the volume of the sample, and the integrand

$$J_m \cdot H_0^* = 2j\omega\mu_0 |H_m|^2 \frac{3(\mu - 1 \pm \alpha)}{\mu + 2 \pm \alpha}. \tag{16}$$

[9] *E.g.*, H. B. G. Casimir, "On the theory of electromagnetic waves in resonant cavities," *Philips Res. Rep.*, vol. 6, pp. 162–182; 1951.

The relative frequency shift is thus

$$\frac{\Delta\omega}{\omega} = -\frac{|H_m|^2 v}{\int_v |H_0|^2 dv} \frac{3(\mu - 1 \pm \alpha)}{\mu + 2 \pm \alpha} = -f \frac{3(\mu - 1 \pm \alpha)}{\mu + 2 \pm \alpha}, \tag{17}$$

where f is a constant of the cavity geometry.

Consider now a cylindrical cavity of length h with the axis parallel to the orienting field. If this cylinder has sufficient symmetry, it will permit TE modes with a circularly-polarized magnetic field at some points on the axis. One may show then that

$$f = q \frac{\beta^2}{k_0^2} \frac{v}{V}, \tag{18}$$

where $k_0^2 = \omega_0^2 \mu_0 \epsilon_0$, $\beta = n\pi/h$, n is an integer, V the volume of the cavity, q is a factor depending on the shape of the cross section. The situation is typified by cylinders of square and circular cross sections.

For a TE_{11n} mode of a circular cylinder

$$k_0^2 = \beta^2 + \left(\frac{\chi}{a}\right)^2, \quad q = [2(\chi^2 - 1)J_0^2(\chi)]^{-1} \simeq 2.08, \tag{19}$$

where a is the radius, $\chi = 1.84$, the first root of $J_1' = 0$. For a resonator of square cross section and with a mode consisting of the degenerate, TE_{01n} and TE_{10n} modes in time quadrature

$$k_0^2 = \left(\frac{n\pi}{h}\right)^2 + \left(\frac{\pi}{a}\right)^2, \quad q = 2, \tag{20}$$

where a is the side of the square cross section.

When losses are present μ, α and ω become complex: $\mu = \mu' - j\mu''$; $\alpha = \alpha' - j\alpha''$; $\omega = \omega' + j\omega''$. Separating (17) into real and imaginary parts and assuming small losses, one obtains for the real frequency shift

$$\frac{\Delta\omega}{\omega} = \frac{\omega' - \omega_0}{\omega'} = -f \frac{3(\mu' - 1 \pm \alpha')}{\mu' + 2 \pm \alpha'}, \tag{21}$$

while the $1/Q$ of the cavity increases by

$$\Delta \frac{1}{Q} = 2 \frac{\omega''}{\omega'} = 18 \frac{\mu'' \pm \alpha''}{(\mu' + 2 \pm \alpha')^2} f. \tag{22}$$

In the case of a nondegenerate cavity with a linearly-polarized unperturbed magnetic field $H_m e_x$ at the spherical sample the internal field must be calculated from (8). Then,

$$J_m \cdot H_0^* = \frac{3j\omega\mu_0[(\mu - 1)(\mu + 2) - \alpha^2]}{(\mu + 2)^2 - \alpha^2} |H_m|^2, \tag{23}$$

and the frequency shift is

$$\frac{\Delta\omega}{\omega} = -\frac{3}{2} \frac{|H_m|^2 v}{\int |H_0|^2 dv} \frac{(\mu - 1)(\mu + 2) - \alpha^2}{(\mu + 2)^2 - \alpha^2}. \tag{24}$$

Eq. (17), being a simpler expression than (24), indicates the advantage of using a circularly-polarized applied magnetic field at the sample.

Disc Samples

When the sphere of the preceding example is replaced by a thin disc whose *diameter is small* compared to that of the cavity and whose axis is perpendicular to the circularly-polarized rf magnetic field, the internal magnetic field equals the external field, (16) is replaced by

$$J_m \cdot H_0^* = 2j\omega\mu_0 |H_0|^2(\mu - 1 \pm \alpha) \tag{25}$$

and the relative frequency shift is

$$\frac{\Delta\omega}{\omega} = -(\mu - 1 \pm \alpha)f, \tag{26}$$

where the factor f has already been defined.

Cylindrical Samples

The case of a symmetrical rectangular cavity with a thin circular cylindrical post of ferrite placed along the axis of the cavity as shown in Fig. 1, is also of interest.

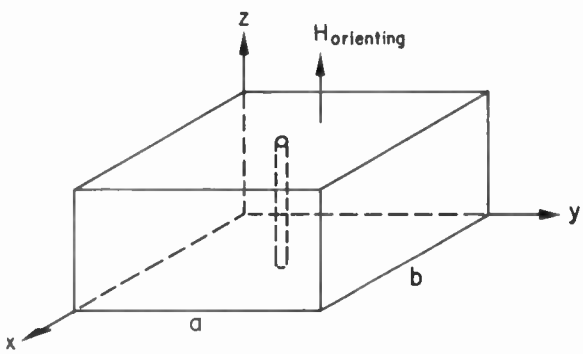

Fig. 1—Degenerate rectangular cavity with a circular ferrite post.

The circularly-polarized unperturbed magnetic field along the ferrite may be produced by superposing the TM_{120} and TM_{210} modes in time quadrature so that the electric field in the cavity is

$$E_0 = e_z\left(\sin\frac{2\pi x}{a}\sin\frac{\pi y}{a} - j\sin\frac{\pi x}{a}\sin\frac{2\pi y}{a}\right).$$

If (15) is applied to this case with the internal field calculated from (14), the frequency shift is

$$\frac{\Delta\omega}{\omega} = -\frac{16}{5}\frac{s}{a^2}\frac{\mu - 1 \pm \alpha}{\mu + 1 \pm \alpha}. \tag{27}$$

where s is the circular cross-sectional area of the ferrite.

In the more general case when the cavity is nondegenerate and the unperturbed field is linearly polarized

$$\frac{\Delta\omega}{\omega} = -\frac{|H_m|^2 v}{\int |H_0|^2 dv}\frac{(\mu - 1)(\mu + 1) - \alpha^2}{(\mu + 1)^2 - \alpha^2}. \tag{28}$$

Discussion: Some remarks on the merits of spherical and disc-shaped samples are in order. Rowen and von Aulock[8] gave the following expression for the frequency shift caused by a spherical sample of ferrite:

$$2\frac{\Delta\omega}{\omega} = \frac{(\mu - 1)(\mu + 2) - \alpha^2}{(\mu + 2)^2 - \alpha^2}C_1 \pm \frac{\alpha C_2}{(\mu + 2)^2 - \alpha^2}, \tag{29}$$

where C_1 and C_2 are constants of the geometry. According to our calculations, these constants are related, $C_2 = 3C_1$, no matter what the cross section of the cavity. As a consequence, (29) reduces to (17). Some of the disadvantages attributed to spherical samples by Rowen and von Aulock were probably overestimated, since their conclusions were based on (29) instead of the simpler (17). As we have already shown for moderate losses, one can readily separate the real and imaginary parts of the latter equation. Rowen and von Aulock give a two constant formula for disk-shaped samples also.[10] Here again, only one constant is necessary. We believe that the frequency perturbation formulas are applicable only to discs whose diameter is small compared to cavity dimensions because the disk should be restricted to a small area at the center of the cylinder base where the field is circularly polarized. Thus, the choice is to be made between a small sphere and a small disc rather than between a small sphere and a disc of arbitrarily large diameter. When $\mu+\alpha$ is small, say less than five, reasonably accurate determination may be made by means of a sphere. For larger values of $\mu+\alpha$ the frequency variation in (21) becomes quite insensitive to a change in $\mu+\alpha$. In this case, the disc shaped sample may be preferred in spite of the greater difficulty involved in making a sample.

One final word about the location of the sample. Experimentally, it would seem to be most convenient to place the sphere at the center of the bottom of the cavity. If this were done, the condition requiring homogeneity of the magnetic field around the sphere would be violated. The disturbing effect of the walls has been known for some time and has recently been commented on by Spencer and Le Craw.[11] While the use of a hemisphere in place of a sphere permits one to circumvent this difficulty, it is usually more convenient to support spherical samples in a nodal plane of the electric field away from the end walls.

Ferromagnetic Resonance

If losses are neglected, μ and α of (1), as given by Polder[1] are

$$\mu = 1 + \frac{\gamma^2 M_z H_z^i}{\gamma^2 H_z^{i^2} - \omega^2}; \quad \alpha = \frac{\omega\gamma M_z}{\gamma^2 H_z^{i^2} - \omega^2}, \tag{30}$$

[10] Casimir, *op. cit.*, eq. (3).

[11] E. G. Spencer and R. C. Le Craw, "Wall effects on microwave measurements of ferrite spheres," *Jour. Appl. Phys.*, vol. 26, pp. 250–251; February, 1955.

where H_z^i is the internal orienting field (the steady field actually operating on the electrons), M_z is the z component of the magnetization and γ is the magnetomechanical ratio. In view of the denominator of μ and α, ferromagnetic resonance might be expected to occur at $\omega=\gamma H_z^i$. However, the directly measurable resonance of such quantities as the field intensity or the magnetic flux density does not occur at $\omega=\gamma H_z^i$. In the case of a sphere, for example, the field intensity, obtained by substituting (30) in (10), is given by

$$H_- = \frac{\gamma H_z^i \pm \omega}{\gamma H_z \pm \omega}(e_x \mp j\, e_y) H_0. \tag{31}$$

Ferromagnetic resonance occurs, therefore, at $\omega=\gamma H_z$ where H_z is the external value of the orienting field. Similarly, ferromagnetic resonance of the ferrite cylinder considered in a previous section occurs at $\omega=\gamma(H_z+\frac{1}{2}M_z)$, and not at $\omega=\gamma H_z^i=\gamma H_z$ as it might be expected from (30). Thus, whether one utilizes Polder's permeability tensor and solves the quasi-static boundary value problem, as it is done in this paper, or follows Kittel's treatment[12] involving demagnetizing factors, one obtains the same expressions for the ferromagnetic resonance.

[12] C. Kittel, "On the theory of ferromagnetic resonance absorption," *Phys. Rev.*, vol. 73, pp. 155–161; January, 1948.

On the Principle and Design of a Trigger Circuit of a Signal-Seeking Radio Using "Difference-Voltage"*

CHIH CHI HSU†, ASSOCIATE, IRE

Summary—**The principle and design of the trigger circuit of a signal-seeking radio using the "difference-voltage" of an IF transformer is described in this paper. The "difference-voltage" is first expressed in a mathematical form, from which the "crossover points" can be found. Constant anticipation can be obtained if this "difference-voltage" is used as a trigger pulse to stop the seeking action. The amount of anticipation is related with the mixing index n and parameters of the IF transformer and it can be expressed in a simple form. The effect of the avc delay voltage in the described circuit does not affect the amount of anticipation. It only affects the proper trigger level. "Error-asymmetry" and the utilization of the property of detuning the output IF transformer in unidirectional seeker are discussed. Besides the error due to the improper trigger level, there are errors due to the nonlinearity of the tuner. This results in the so-called "error spread." Formulas for the amount of anticipation desired in terms of the tuner sweep characteristics and the stopping time are given. The design of the IF transformer with respect to errors due to components tolerances is fully discussed. Approximate formulas are derived for the error variations.**

Introduction

SIGNAL-SEEKING radios have two additional circuits beside other conventional radio circuits. They are (1) the seeking circuit and (2) the trigger circuit. The seeking circuit initiates the seeking action when the operator desires and stops when the trigger circuit orders so. The trigger circuit will issue such a command when a signal is reached. The seeking circuit usually consists of a relay with multiple contacts, a group of mechanical gears, cams, and switches, etc., and a mover, in the form of either a dc or an ac motor, or an electromagnet, or some energy-storing devices, such as springs, or some other transducers. In this paper, however, we will only deal with the trigger circuit, particularly a trigger circuit using the principle of the "difference-voltage." The difference-voltage between the secondary and primary voltages of the IF output transformer as the trigger pulse has the theoretical advantage of a sharper pulse than secondary voltage alone, and a constant anticipation regardless of the signal strength. A qualitative description of how the difference-voltage works has been given in the earlier literature[1] but no quantitive details were given. Section I of this paper will take up the quantitative details and formularize the results so that they can be used as a guide for future design. It will be assumed first that a linear tuner is used. The effect of a nonlinear tuner will be taken up in Section II, along with the proper choice of the amount of anticipation. In Section III, design considerations of the output IF transformer in a signal-seeking radio with respect to errors due to components tolerances will be explored.

I. On the Difference-Voltage, Crossover Point, Trigger Level and the Preliminary Design of the Trigger Circuit of a Signal-Seeking Radio Using Difference-Voltage

A. Difference-Voltage and Crossover Points

Fig. 1 (next page) shows IF output transformer and associated circuits. With the exception of grounding

* Original manuscript received by the IRE, June 6, 1955; revised manuscript received, August 16, 1955. This paper is based upon three reports written by the author at Bendix Radio Division, Bendix Aviation Corp., Baltimore, Md.

† Bendix Radio Division, Bendix Aviation Corp., Baltimore, Md.

[1] J. H. Guyton, "A signal-seeking automobile receiver," *Electronics*, vol. 26, pp. 154–158; May, 1953.

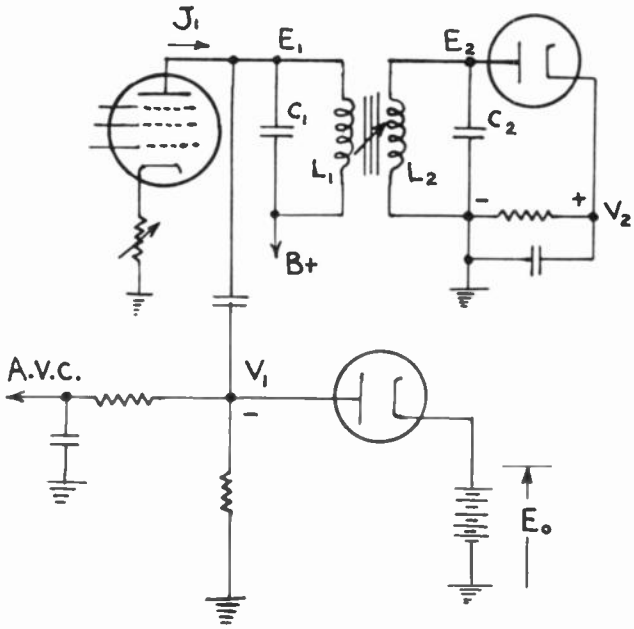

Fig. 1

point of the secondary detector diode, it is a very conventional one. If V_1 and V_2 are the magnitude of the rectified dc voltages due to the carriers (for simplicity we neglect the effect of modulation) of the primary and secondary of the output IF transformer respectively, then the difference-voltage is defined as

$$V_2 - nV_1, \tag{1}$$

where n (the mixing index) is a constant.

If the avc delay voltage $E_0 = 0$, then both V_1 and V_2 will be very close to the magnitude of their peak ac voltages E_1 and E_2, respectively. Hence we have

$$V_2 - nV_1 = E_2 - nE_1. \tag{2}$$

Both E_1 and E_2 are frequency dependent. For high Q cases, they can be expressed as follows:[2]

$$\frac{E_2}{J_1} = \frac{s\sqrt{R_1R_2}}{[(1+s^2)^2 - 2(s^2 - b/2)v^2 + v^4]^{1/2}} \tag{3}$$

$$\frac{E_1}{J_1} = \frac{R_1(1 + Q_2v^2/Q_1)^{1/2}}{[(1+s^2)^2 - 2(s^2 - b/2)v^2 + v^4]^{1/2}}, \tag{4}$$

where

R_1 = equivalent total loading of the primary,
R_2 = equivalent total loading of the secondary,
J_1 = input current to the IF transformer,
$2\pi f_0 = w_0 = 1/\sqrt{L_1C_1} = 1/\sqrt{L_2C_2}$,
$k = M/\sqrt{L_1L_2}$, the coefficient of coupling,
$s = k\sqrt{Q_1Q_2}$, the coupling index,
$\rho = Q_1/Q_2$, the Q ratio,
$b = \rho + 1/\rho = Q_1/Q_2 + Q_2/Q_1$,
$v = \sqrt{Q_1Q_2}(w/w_0 - w_0/w)$, the frequency variable.
E_1 = the primary voltage,
E_2 = the secondary voltage.

The expression for the Difference-Voltage will be

$$E_2 - nE_1 = J_1\left[\frac{s\sqrt{R_1R_2} - nR_1\sqrt{1+v^2Q_2/Q_1}}{[(1+s^2)^2 - 2(s^2-b/2)v^2 + v^4]^{1/2}}\right]. \tag{5}$$

Such an expression is difficult to visualize. However, it is useful. Fig. 2 is an actual photo of the primary, secondary and the Difference-voltage of a particular circuit. It is obvious difference-voltage in Fig. 2 can be obtained from sketches as shown in Fig. 3 (opposite).

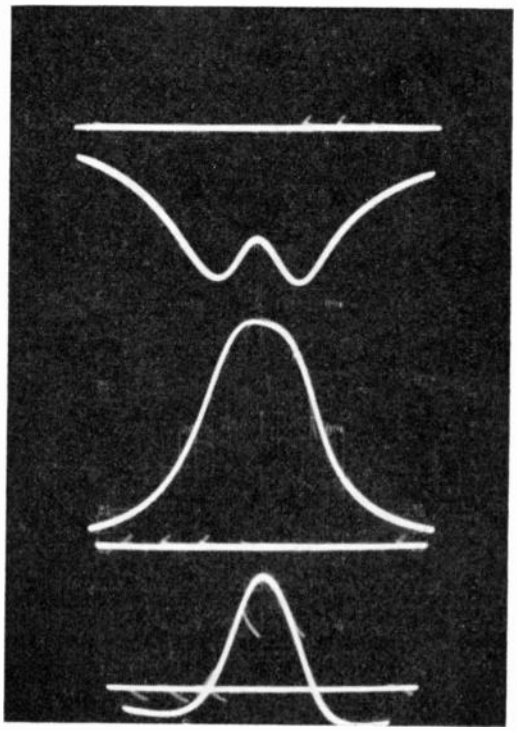

Fig. 2—From top to bottom; primary, secondary, and difference voltages.

The single peaked secondary voltage as shown in Fig. 2 may become double peaked if the coupling is too tight. The primary response is usually double peaked but under certain conditions it may also be a single peaked one. But in any event, the secondary response is more selective (narrow) than the primary response.

The Crossover points are the points at which $E_2 = nE_1$, such as the points a and b in Fig. 3. As the input signal strength changes, the secondary response will increase and decrease with the primary response in the same proportion. Hence the crossover points will move up and down with the secondary response as signal strength varies, but not along the frequency axis as in Fig. 4(a) (opposite). The points at which the difference-voltage crosses over the zero axis as shown in Fig. 4(b) will therefore always be the same. If the trigger level of the stopping circuit is set at those crossover points, constant anticipation will be obtained independent of the signal strength. The amount of anticipation

[2] G. E. Valley, Jr., and H. Wallman, "Vacuum tube amplifiers," MIT Rad. Lab. Ser., No. 18, McGraw-Hill Book Co., Inc., New York, N. Y., pp. 202–210; 1948.

is the difference between the frequency of the crossover point and the center frequency f_0.

The frequency at which the crossover point occurs can be obtained by setting (5) equal to zero, or

$$E_2 - nE_1 = 0. \tag{6}$$

Then

$$s\sqrt{R_1R_2} - nR_1\sqrt{1 + v^2Q_2/Q_1} = 0. \tag{7}$$

This can be reduced to

$$v = \sqrt{\frac{s^2}{n^2}\frac{C_1}{C_2} - \frac{Q_1}{Q_2}} \tag{8}$$

or

$$\Delta f = \frac{f_0}{2\sqrt{Q_1Q_2}}\sqrt{\frac{s^2C_1}{n^2C_2} - \frac{Q_1}{Q_2}}. \tag{9}$$

If the trigger level is set at the crossover point then Δf will be the amount of anticipation.

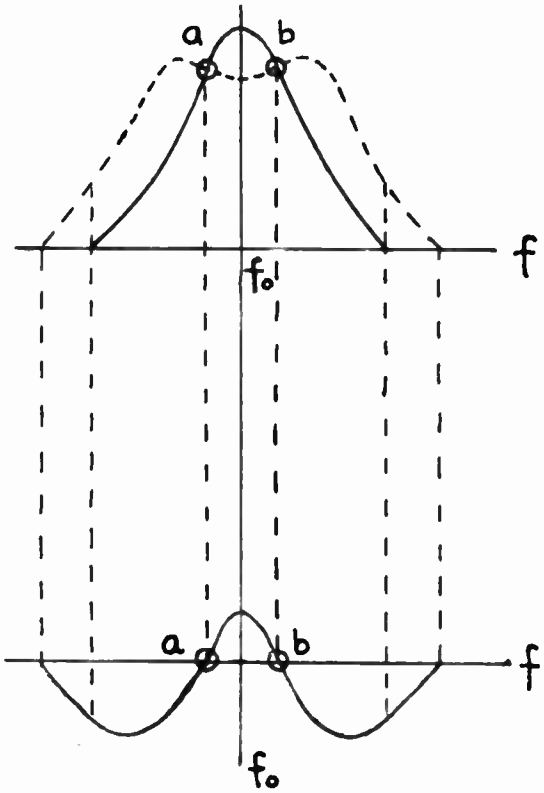

Fig. 3

B. Anticipation, Trigger Level, and the AVC Delay Voltage

So far we have assumed that the primary avc delay voltage $E_0=0$. If $E_0\neq 0$, then $E_1\neq V_1$. Instead, we have

$$V_1 = 0, \qquad \text{when } E_1 \leqq E_0 \tag{10}$$

$$V_1 = E_1 - E_0, \quad \text{when } E_1 \geqq E_0. \tag{11}$$

The difference-voltage will be

$$V_2 - nV_1 = E_2, \qquad \text{when } E_1 \leqq E_0 \tag{12}$$

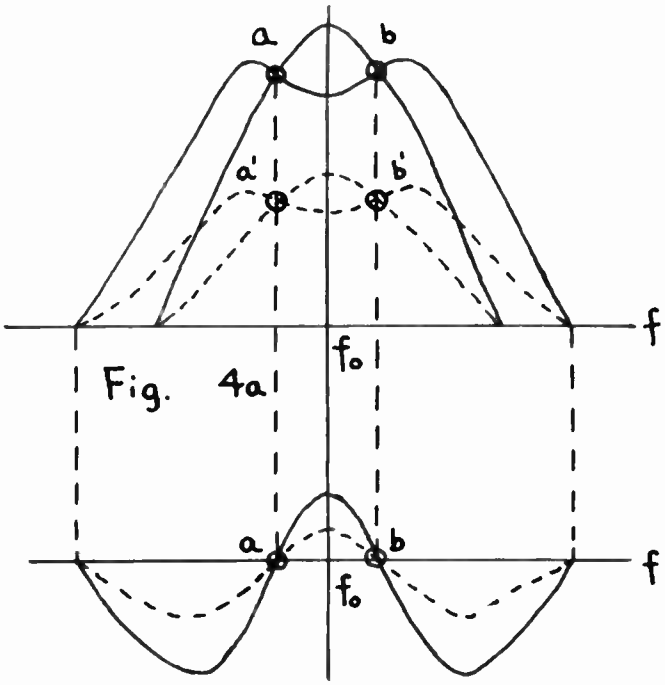

Fig. 4

$$V_2 - nV_1 = E_2 - n(E_1 - E_0), \quad \text{when } E_1 \geqq E_0. \tag{13}$$

From (13) we have:

$$V_2 - nV_1 = (E_2 - nE_1) + nE_0, \quad \text{where } E_1 \geqq E_0. \tag{14}$$

Eq. (12) is easy to interpert. It merely says that when the avc delay voltage is not exceeded, the difference-voltage is simply the secondary voltage. Eq. (14), however, is not easy to visualize immediately. If we compare (14) with (2), we find that the only difference is the constant term nE_0. If we set

$$E_2 - nE_1 = 0, \tag{6}$$

then (14) becomes

$$V_2 - nV_1 = nE_0 = \text{constant}. \tag{15}$$

Since E_2 and E_1 increase and decrease together, if equation (6) is true for one signal strength, it will be true for all signal strength. Hence equation (15) will also be true for all signal strength as long as $E_1 \geqq E_0$. In other words, when the delay voltage is exceeded, there will be crossover points. The crossover points will be at a constant level nE_0. If the trigger level of the stopping circuit is set at nE_0, then the anticipation will be independent of the signal strength when $E_1 \geqq E_0$.

Fig. 5 (next page) illustrates the above conclusion. Fig. 5(a) shows that the effect of the avc delay is the same as shifting the primary voltage curve downward by an amount of nE_0. The difference-voltage in the region of interest is shown in Fig. 5(b). The effect of the avc delay voltage shifts the difference-voltage upward by an amount of nE_0. Fig. 5(c) shows the difference-voltage at two different signal strengths. Notice that the difference-voltages without avc delay crossover

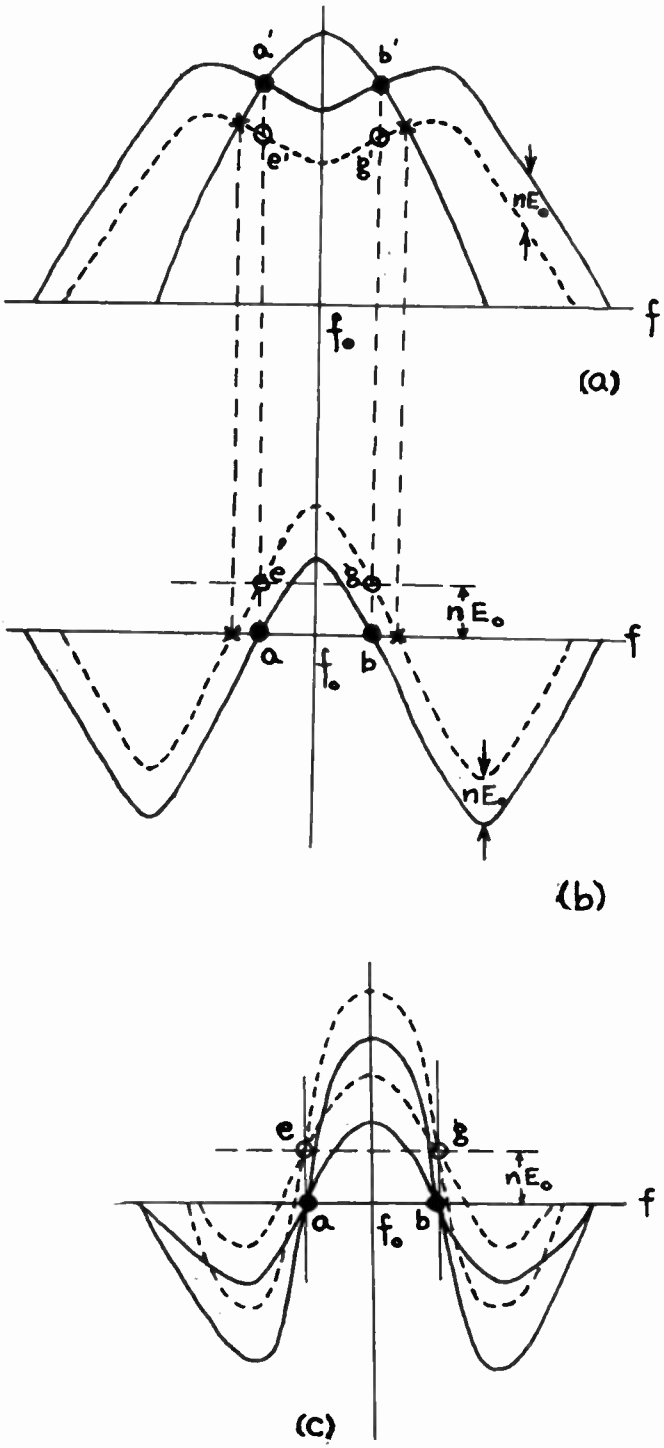

Fig. 5—Solid line: without avc delay.
Broken line: with avc delay.

at points a and b, while with avc delay, they cross over at points e and g.

It is evident here that the crossover points in which we are interested are the points at which the difference-voltages at different signal strength cross over one another. It is not necessarily the point at which the difference-voltage crosses over the zero axis. In the case of no delay voltage, however, they are the same.

The calculation of anticipation with avc delay voltage is therefore the same as that of the case without avc delay. [Use (9).]

Fig. 6 and Fig. 7 are photos of the difference-voltages for two different values of the avc delay voltage. The avc delay voltage of Fig. 7 is double that of Fig. 6. It can be seen clearly that the crossover level of Fig. 7 is also double that of Fig. 6. The distances between the two crossover points in each picture are equal. This bears out that the anticipation is not effected by the avc delay voltage.

More discussions on the avc delay voltage will be given later.

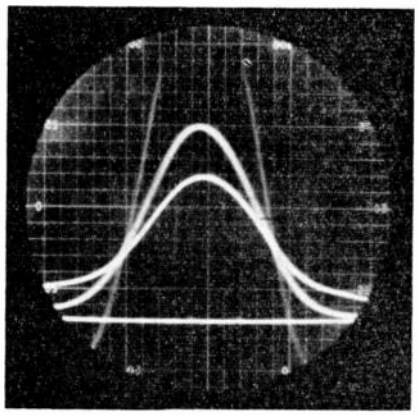

Fig. 6

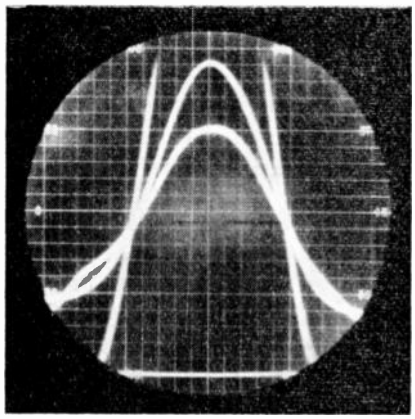

Fig. 7

C. Limitation of Mixing n and the Effect of Selective Circuits Ahead of the Output IF Transformer

Rewriting (9), we have

$$\Delta f = \frac{f_0}{2\sqrt{Q_1Q_2}} \sqrt{\frac{s^2}{n^2}\frac{C_1}{C_2} - \frac{Q_1}{Q_2}}. \tag{9}$$

If our output IF transformer is designed according to the performance in the listen position, then f_0, s, C_1, C_2, Q_1 and Q_2 are all fixed. The only variable is the mixing index. It is obvious that there will be no real solution for (9) if the term under the radical sign is less than zero.

In other words, there will be anticipation only if

$$\frac{s^2C_1}{n^2C_2} - \frac{Q_1}{Q_2} > 0, \tag{16}$$

or

$$n^2 < \frac{C_1Q_2}{C_2Q_1} s^2. \tag{17}$$

Since n cannot be negative, hence

$$n < \sqrt{\left(\frac{C_1}{C_2}\right)\left(\frac{Q_2}{Q_1}\right)}\, s, \tag{18}$$

or

$$n < \sqrt{\frac{R_2}{R_1}}\, s. \tag{19}$$

Although (19) is simpler, (18) is more convenient to use. It can be written as:

$$\text{Mixing Index} < \sqrt{(\text{Step up ratio})(Q \text{ ratio})} \times \text{Coupling Index}$$

The physical meaning will be even more clear if we notice that

$$\sqrt{\left(\frac{C_1}{C_2}\right)\left(\frac{Q_2}{Q_1}\right)}\, s = \frac{E_2}{E_1} \text{ at } f=f_0. \tag{20}$$

Hence (18) becomes

$$n < (E_2/E_1)_{\text{at } f=f_0},$$

or at $f=f_0$,

$$nE_1 < E_2. \tag{21}$$

Hence there is an upper limit for n, above which there will be no crossover points. Fig. 8 (right) shows the anticipation vs the mixing index for the equal Q case.

What about the lower limit of n? From (9), it will be obvious that the smaller the mixing index n, the larger will be the amount of anticipation. When $n \to 0$, $\Delta f \to \infty$. Such a result is obviously not true. The reason we have such a result is because we have made the assumption that the input is a constant current generator independent of frequency. In the actual case, we will have front end selectivity and the input IF selectivity so that the input to the output IF transformer will be a constant current generator but dependent on frequency. It is therefore obvious that the maximum anticipation will be limited by the bandwidth of stages preceding the output IF transformer. From the standpoint of obtaining as much anticipation as possible, the design of the IF transformers should be such that the input IF transformer should have less selectivity and the output IF transformer should have more selectivity if the overall selectivity is kept the same. This would call for a high Q output IF transformer. However, if the anticipation needed is less than 5 kc or so, a medium Q output IF transformer will be sufficient.

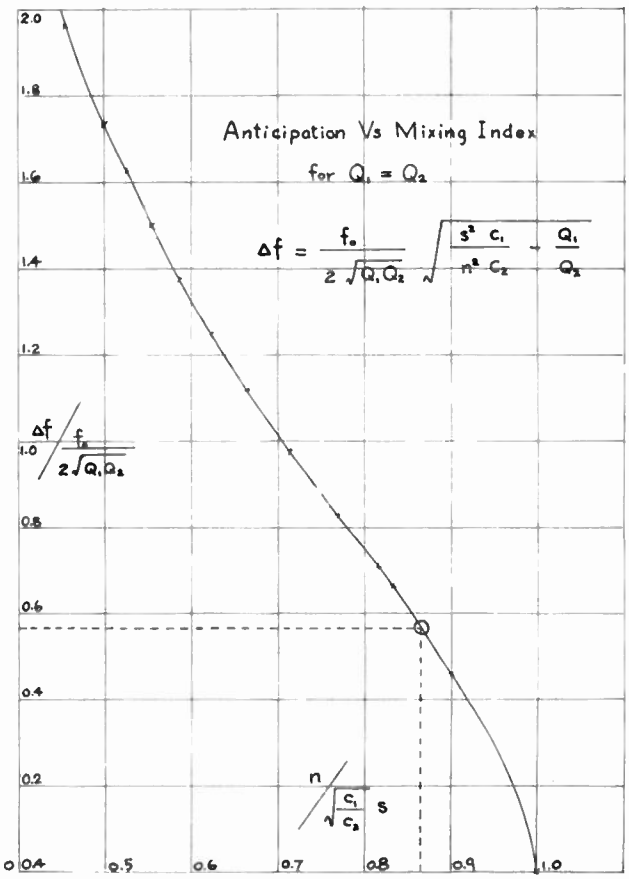

Fig. 8

The effect of the selectivity of the circuits ahead of the IF output transformer on the crossover points of the difference-voltages should be theoretically none, since the crossover points are independent of the signal strength. Of course, it is true only if the frequency of the crossover points are within the maximum anticipation obtainable.

D. The Peak of the Difference-Voltage

The peak of the difference-voltage is a very useful quantity to know. With the peak of the difference-voltage and the crossover points known, we can readily sketch the difference-voltage. The peak of the difference-voltage for zero avc delay voltage can be obtained by setting $v=0$ in (5). If we denote the peak by A, then

$$A = J_1 \frac{s\sqrt{R_1R_2} - nR_1}{1+s^2}, \tag{22}$$

or simply

$$A = (E_2 - nE_1)_{\text{at } f=f_0}. \tag{23}$$

From (20) and (23) we then have

$$A = \left[s\sqrt{\left(\frac{C_1}{C_2}\right)\left(\frac{Q_2}{Q_1}\right)} - n\right] E_{1\,\text{at } f=f_0}. \tag{24}$$

Eq. (24) is more convenient to use because E_1 at $f=f_0$ can be measured at listen position with great ease.

When the avc delay voltage is not zero, from (14) and (24), the peak A from the zero level will be

$$A = \left[s \sqrt{\left(\frac{C_1}{C_2}\right)\left(\frac{Q_2}{Q_1}\right)} - n \right] E_{1 \text{ at } f=f_0} + nE_0. \tag{25}$$

Since nE_0 is the crossover level, hence if the peak of the difference-voltage is measured from the crossover level, regardless of with or without avc delay voltage we will have

$$A_{\text{ from the crossover level}} = \left[s \sqrt{\left(\frac{C_1}{C_2}\right)\left(\frac{Q_2}{Q_1}\right)} - n \right] E_{1 \text{ at } f=f_0}. \tag{26}$$

From (24) and (26), it can also be shown that

$$A_{\text{ from the crossover level}} = s\sqrt{\frac{C_1}{C_2}} \left[\sqrt{\frac{Q_2}{Q_1}} - \frac{1}{\sqrt{\frac{4Q_1Q_2(\Delta f)^2}{f_0^2} + \frac{Q_1}{Q_2}}} \right] E_{1 \text{ at } f=f_0}. \tag{27}$$

For the same output IF transformer, it is obvious from (27) that the smaller the anticipation Δf, the smaller will be the value of A. If the trigger level is not set correctly, this may cause skip of the station.

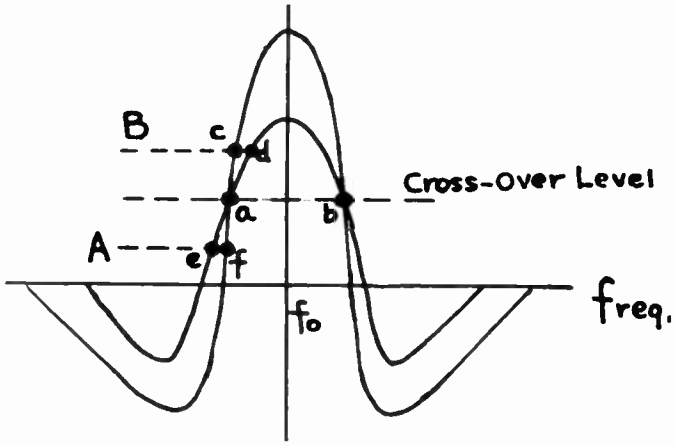

Fig. 9

E. Error Caused by the Trigger Level Variation and Error Asymmetry

The difference-voltage is used to trigger a relay. Amplifiers may be cascaded before the control (or the trigger) tube. The gain of the amplifier should be as to match the trigger level of the control tube to the crossover level of the difference-voltage. If the trigger level does not match the crossover level, error will result. The nature of the error variation caused by the improper trigger level can be seen from the sketch of Fig. 9.

If the gain of the trigger amplifier is too high or the trigger is set at the level A as shown in Fig. 9, then the anticipation will not be constant with respect to the signal strength. It will show the tendency to under-shoot. The weaker the signal, the larger the amount of undershoot. If, however, the system is over-shooting at point a (the crossover point) to start with, then the operation at the level A will show an improvement of seeking error. The improvement will, however, depend on the signal strength. On the other hand, if the gain of the trigger amplifier is too low or the trigger level is set at the level B (Fig. 9), the anticipation will again not be a constant with respect to the signal strength. It will show the tendency of over-shoot. The weaker the signal the larger the amount of over-shoot. If the system is over-shooting at point a to start with, then the trigger at the level B will result in more error. If, however, the system is under-shooting at point a to start with, then the trigger level B will show error improvement again. But the amount of improvement will again depend upon the signal strength. The nature of the error variation due to improper trigger level can be utilized to adjust the trigger amplifier gain so that the circuit will be triggered at the crossover level.

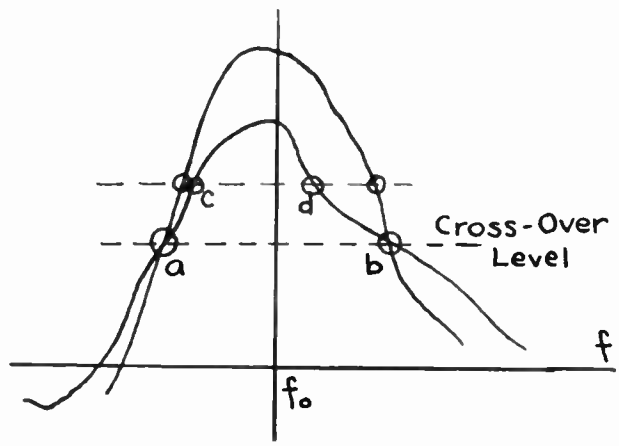

Fig. 10—Point c and point d are not equidistant from the f_0 axis.

If the front end and the input IF transformer are not well aligned, or the front end selectivity is nonsymmetrical with respect to the center frequency in the interested region, then we may not have such nice symmetrical difference-voltage such as shown in Fig. 9. Instead, we may have an asymmetrical difference-voltage such as those shown in Fig. 10. As discussed above, trigger at wrong level will give seeking error. The amount of error depends upon the signal strength. For a given signal strength, the error will be the same whether the signal seeking action is from the high frequency toward the low frequency or the other way, as long as the difference-voltage is symmetrical as shown in Fig. 9. But in the case of Fig. 10, even for the same signal strength, it will produce different error depending on whether it is seeking toward the high-frequency end or the low-frequency end. This we may refer to as error asymmetry.

Error asymmetry also can be caused by misalignment

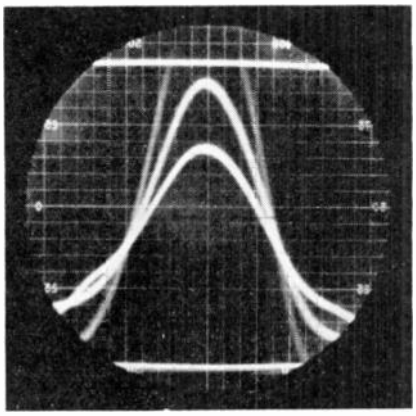

Fig. 11

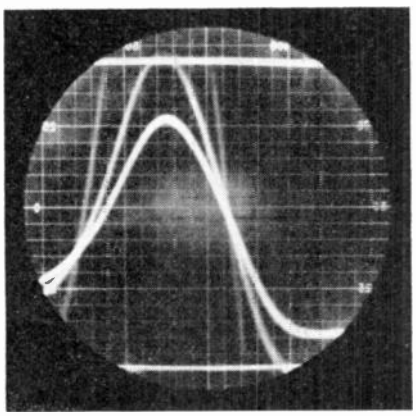

Fig. 12

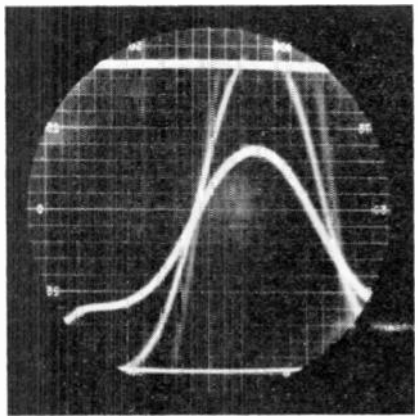

Fig. 13

or detuning of the output IF transformer. Figs. 11, 12 and 13 will clarify this point. Fig. 11 shows a photo of the difference-voltages when the output IF transformer is well aligned. It shows good symmetry. Fig. 12 and Fig. 13 show the detuning effect of the output IF transformer in one way and another. The two crossover points are not at the same level. If the trigger level is set at either one of the two crossover points, the error seeking in one direction may be zero but the error seeking in the other direction will not be zero.

It would be proper to point out here that the Error Asymmetry caused by detuning of the output IF transformer as shown in Fig. 12 and Fig. 13 does not arise as a problem for unidirectional seeking radio. In fact there are two distinct facts indicated by these two photos that detuning the output IF transformer can be used for advantages. The facts are

1. There are still crossover points.
2. The crossover points are shifted to one side or another. Fact one suggests that the same principle can be used for unidirectional signal seeking radio. Fact 2 suggests that we can take advantage of the shifting of the crossover point to get: a) more anticipation than the limit imposed by the front end and input IF transformer selectivity as discussed before, b) less anticipation without too much sacrifice of the peak A. (As previously pointed out in relating with (27), A will decrease as anticipation is reduced.) This will give less error due to signal level effect.

For bidirectional signal seeking radio, the shifting of the crossover points will cause errors, unless some other arrangements are used. This will be highly impractical. But that does not mean that a bidirectional signal-seeking radio is worse than a unidirectional one. There are error asymmetries in a bidirectional signal-seeking radio, but they can be reduced to within 0.5 kc or less. On the other hand it does not have the jerky, annoying sound of fly-back that a unidirectional signal seeking radio usually has.

Error asymmetry can also be caused by other reasons such as unequal braking action and others, but they will not be discussed further here.

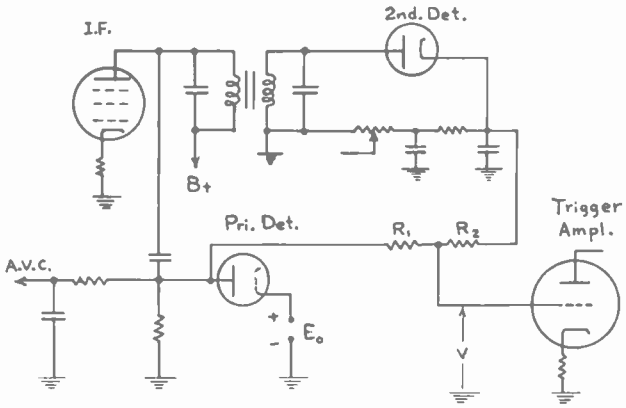

Fig. 14

F. Example: Preliminary Design of a Trigger Circuit of a Signal-Seeking Radio

It is decided to convert a certain model of conventional automobile radio into a signal-seeking radio using the principle of the difference-voltages. There are many possible trigger circuits but a circuit such as that above in Fig. 14 is decided upon. The IF frequency is 265 kc.

1. If an anticipation of 2.5 kc is desired, what should be the ratio R_2 to R_1?
2. What will be the crossover level if the avc delay voltage is six volts?
3. What will be the minimum trigger sensitivity?

4. Sketch the difference-voltages in the neighborhood of the crossover level.

1. The design of the output IF transformer will be discussed in Section III. For the present let us assume that the output IF transformer has the following parameters:

Circuit Q's : $Q_1 = Q_2 = 30$
Capacitances : $C_1 = 114$, $C_2 = 134$
Coupling index : $s = 0.85$

Since the anticipation $\Delta f = 2.5$ kc and $f_0 = 265$ kc, the mixing index n can be calculated from (9). Or we may use the curve on Fig. 8.

$$\frac{\Delta f}{\dfrac{f_0}{2\sqrt{Q_1Q_2}}} = \frac{(2.5)(2)(30)}{265} = 0.566$$

From Fig. 8 we have

$$\frac{n}{s\sqrt{\dfrac{C_1}{C_2}}} = 0.865$$

But

$$s\sqrt{\frac{C_1}{C_2}} = 0.85\sqrt{\frac{114}{134}} = 0.784.$$

Hence

$$n = (0.865)(0.784) = 0.68.$$

The mixing network used in Fig. 14 is actually an adder network. If R_1 and R_2 are relatively high value resistors, then the loading effect of these resistors on the IF output transformer can be neglected. With good approximation, Fig. 15 can be used to represent the

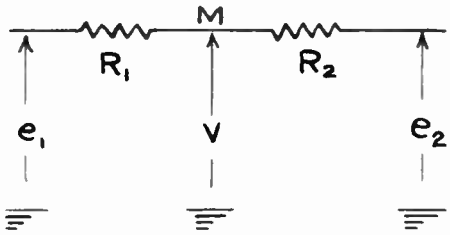

Fig. 15

mixing network. If

$$R_2/R_1 = n$$

then

$$V = \frac{1}{1+n}(e_2 + ne_1). \tag{28}$$

Now

$$e_2 = E_2$$
$$e_1 = -(E_1 - E_0),$$

hence

$$V = \frac{1}{1+n}(E_2 - nE_1 + nE_0). \tag{29}$$

Comparing the right side of the equation (29) with that of (14), we find that they are the same except the factor $1/(1+n)$. Hence

$$R_2/R_1 = n = 0.68.$$

If

$$R_1 = 10 \text{ megohms} \quad \text{then} \quad R_2 = 6.8 \text{ megohms}$$

2. The factor $1/(1+n)$ can be included in the gain of the amplifier following the mixing circuit; then the crossover level will still be nE_0. However, if the crossover level is measured at the point M, then

$$\text{crossover level} = \frac{n}{1+n}E_0. \tag{30}$$

If $E_0 = 6$v., $n = 0.68$, The crossover level $= (0.68)(6)/(1+0.68) = 2.43$ v.

3. To find the minimum trigger sensitivity, it is necessary to know the front end gain. The front end gain varies with the signal frequency. However, for a well-designed receiver, the variation in gain is not much. Assume that the receiver has an average front end and IF gain as follows:

$$E_{1\,\text{peak}} = (6.3)(67)(9)(108)(\sqrt{2}E_{\text{antenna effective}})$$

Or

$$E_1 = 590{,}000\, E_{\text{antenna}} \tag{31}$$

Before avc takes over, e_1 in (28) will be zero and (28) becomes

$$V = E_2/(1+n). \tag{32}$$

The minimum trigger sensitivity will be the sensitivity at which, $V = (E_2 \text{ at } f = f_0)/(1+n) =$ crossover level,

or

$$(E_{2\,\text{at}\,f=f_0})/(1+n) = nE_0/(1+n)$$

or

$$E_{2\,\text{at}\,f=f_0} = nE_0 \tag{33}$$

Substitute (20) into (33):

$$\sqrt{\left(\frac{c_1}{c_2}\right)\left(\frac{Q_2}{Q_1}\right)}\, sE_{1\,\text{at}\,f=f_0} = nE_0. \tag{34}$$

Substitute (31) into (34):

$$E_{\text{antenna}} = \frac{nE_0}{\sqrt{\left(\dfrac{C_1}{C_2}\right)\left(\dfrac{Q_2}{Q_1}\right)} \times s \times 590{,}000} \text{ volts,}$$

or

$E_{\text{antenna}} = 8.8$ micro-volts— The minimum trigger sensitivity.

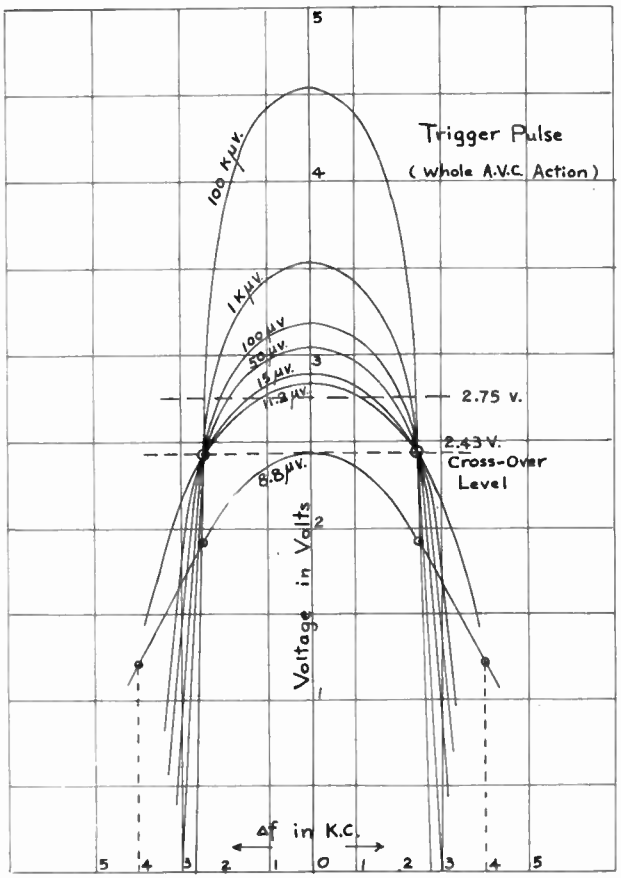

Fig. 16

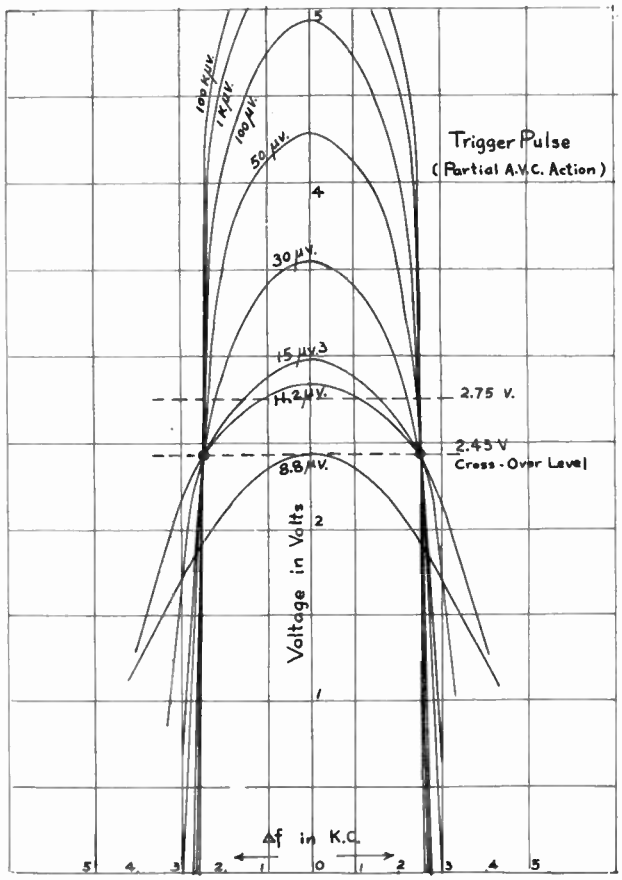

Fig. 17

4. To sketch the difference-voltage, it is necessary to know the selectivity. But for rough sketches, we may assume that the two times down bandwidth is about 8 kc. The difference-voltage for $E_{\text{antenna}} = 8.8$ microvolts can then be sketched, as shown in Fig. 16. At 2.5 kc from the center frequency of this curve, voltage is 1.92 volts. Hence the minimum sensitivity to have crossover point at this point should be approximately:

$$(2.43)(8.8)/1.92 = 11.2 \text{ micro-volts.}$$

The corresponding $E_{1 \text{ at } f=f_0}$ will be

$$(0.59)(11.2) = 6.6 \text{ volts.}$$

From (26) and the factor $1/(1+n)$, we have

$$A = \frac{1}{1+n}\left[\sqrt{\left(\frac{C_1}{C_1}\right)\left(\frac{Q_2}{Q_1}\right)}\, s - n\right] E_{1\,(\text{at } f=f_0)} + \frac{nE_0}{1+n}. \tag{35}$$

Hence for the present case we have

$$A = 0.062\, E_{1\,(\text{at } f=f_0)} + 2.43 \text{ volts.} \tag{36}$$

If the following avc characteristics are assumed: $E_0 = 6$ volts

Input (micro-volts)	15	50	100	1k	100k
E_1 at $f=f_0$ (volts)	8.0	10	12	18	34

Then the peak of the difference-voltages can be computed by using (36):

Input (micro-volts)	15	50	100	1k	100k
A (the peak) (volts)	2.9	3.05	3.18	3.55	4.54

The difference-voltages can then be sketched as shown in Fig. 16. They are based upon the avc characteristics at listen condition. However, at actual seeking condition, the sweep speed may be so fast that the time constant of the avc circuit is relatively large. For example, with sweep speed of 300 kc per second, the time to cover 3 kc is only 10 milliseconds. If the time constant of the avc citcuit is 100 ms, it is obvious that no appreciable avc voltage is reached at time of trigger action; unless there is a very strong signal. Hence we can say that under the seeking condition, avc action is only partial.

There will be no change due to this partial avc action before the avc takes over for the sketches in Fig. 16. At small signal the effect on those sketches is also negligible. Let us assume the following avc characteristics due to this partial avc action:

Input (micro-volts)	15	30	50	100	1k	100k
$E_{1 \text{ at } f=f_0}$	9	18	30	40	50	60

Then the peak of the difference-voltages will be

Input (micro-volts)	15	30	50	100	1k	100k
A (the peak) (volts)	2.99	3.54	4.29	4.91	5.43	6.15

The difference-voltages under such conditions are sketched as shown in Fig. 17 (page 1599).

Comparing Fig. 16 and Fig. 17, we notice that the 15 microvolt pulse does not change much but the 50 microvolt pulse has been changed tremendously. Suppose the trigger amplifier gain variation causes the trigger level to be 2.75 volts instead of the crossover level 2.43 volts. Then for 50 microvolts input, it will give an error of approximately 1 kc in the case of Fig. 16, while the error will be negligible in the case of Fig. 17. Hence the partial avc action actually helps the accuracy of the seeking action. But to obtain the accuracy by purposely using longer avc time constant may result in "skip" of weak stations immediately after the strong station. One thing is definitely clear though; that is, the higher the front end sensitivity, the better will be the seeking accuracy.

The sketches shown in Fig. 16 and Fig. 17 are only approximate ones to show that we can roughly get such kind of trigger pulse before we start any experimental work. The actual pulse is more complicated. For instance, due to double-peaked nature of the primary voltage, it is possible that the primary voltage at 11.2 microvolts does exceed the delay voltage at the 2.5 kc off the center frequency as shown in Fig. 16 and Fig. 17, but at the center frequency it may be less than the delay voltage. The result will be a flatter peak near the center frequency than that shown by the sketches at 11.2 microvolts input.

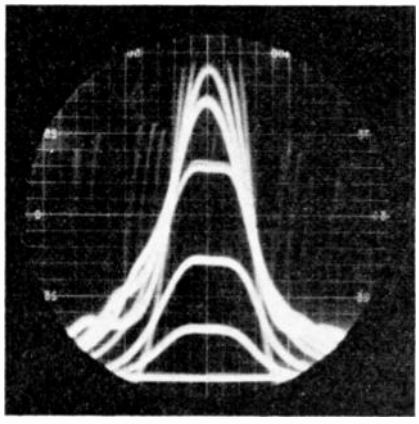

Fig. 18

Fig. 18 is a photo of the difference-voltages. Notice that at very weak signal input, the difference-voltage is the flatter-peak secondary voltage. When the signal is strong, the sharp-peak difference pulse appears. One of the difference-voltages shows that it passes the crossover point but the primary voltage is still not large enough at the center frequency; hence it still has the flat-peak.

II. On the "Error-Spread" and the Amount of Anticipation Desired for the Design of the Trigger Circuit of a Signal Seeking Radio

In Section I of this paper, we have assumed that the tuner is a linear one. However, in actual case, it is not. This will introduce another kind of error which varies over the broadcast band. We will call this "the error-spread over the band" or simply "the error-spread." Section II will discuss this error-spread and the amount of anticipation desired for the design of the trigger circuit of a signal-seeking radio.

A. The Desired Anticipation for a Linear Tuner

The anticipation is required because of the lagging of the stopping circuit response. The stopping circuit here includes the circuit associated with the relay, the tuner carriage, the motor or its equivalent, as well as the gear trains between them. If we define that

h = the anticipation in kc

a = sweep speed (in kilocycles per second) of the tuner

t_m = total effective mechanical delay time in millisecond,

θ = the error in kc,

then the error will be

$$\theta = at_m(10)^{-3} - h. \tag{37}$$

Hence, if

$$h < at_m(10)^{-3},$$

we have $\theta > 0$—over-shoot or if $h > at_m(10)^{-3}$, we will have: $\theta < 0$—under-shoot, Therefore, for $\theta = 0$, we only have to choose

$$h = at_m(10)^{-3}. \tag{38}$$

However, the tuner we have in actual case is usually a nonlinear one. The factor a in (38) will therefore not be a constant over the whole broadcast band. Fig. 19 shows a typical tuner characteristic. If t_m is the same, then, it will be obvious that the value of h chosen to satisfy (38) at one frequency of the band will upset the equality at another frequency. This results in the so-called "error-spread over the band." Hence, what is the desired amount of anticipation for the design of the trigger circuit of the signal seeking radio will depend upon not only the total effective mechanical delay time t_m, but also the characteristics of the tuner.

B. The Total Effective Mechanical Delay Time

The factor t_m—the total effective mechanical delay time in milliseconds—is not a simple one. The stopping system usually undergoes the following steps of action:

1. Relay contacts open—disconnects the driving source from the motor.
2. Fly-over period—the motor is coasting on its mechanical inertia.
3. Relay contacts closed—braking is applied to the motor.

Suppose we have specified that the relay vendors should supply a relay in our circuit and that the time

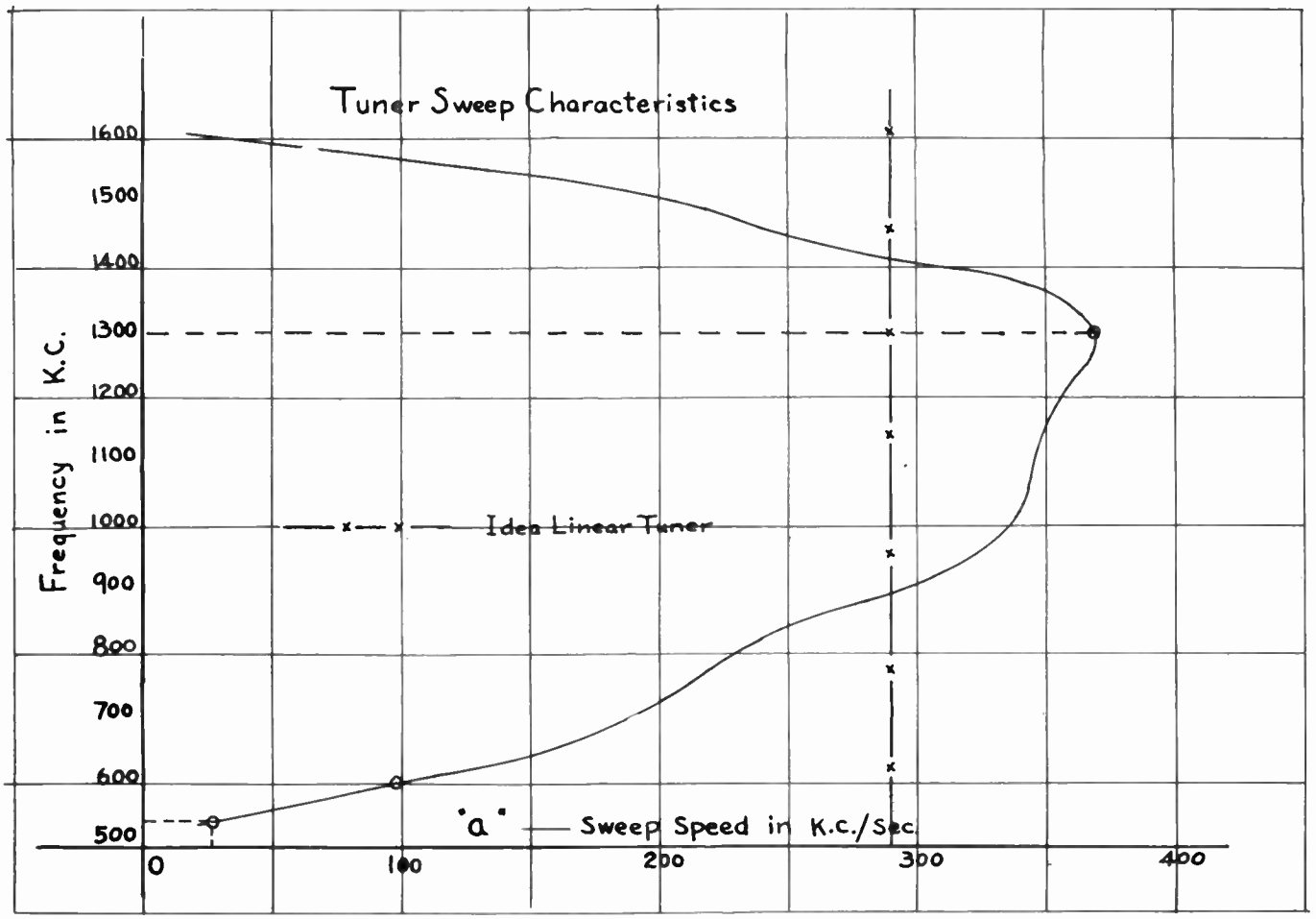

Fig. 19

from the commanding of the trigger action to the end of the fly-over period be t_1 (say for example 5 milliseconds), then we have:

$$t_m = \text{relay opening time } t_1 + \text{effective motor stopping time } t_2 \tag{39}$$

The effective motor stopping time is not the actual motor stopping time. During the motor stopping period, the speed of the motor changes. Before the braking is applied, we assume that the speed change is not large. But after the braking is applied the speed of the motor will change at a very fast rate. Hence, although we may use the relay opening time in (39) for approximation, we cannot use the actual motor stopping time after braking is applied. This actual time must be converted into the effective motor stopping time.

If the actual motor stopping time after braking is in terms of the number of revolutions the motor coasts between the instant when the braking is applied and the instant when the motor is completely at standstill, the calculation of the effective motor stopping time will be easier. Suppose the motor stops in p revolutions which corresponds to q inches movement of the tuner carriage, and the tuner sweep speed during the seeking is $1/r$ inches per second, then the effective motor stopping time in milliseconds will be

$$t_2 = qr(10)^3 \tag{40}$$

or

$$t_2 = dpr(10)^3, \tag{41}$$

where d is the conversion factor including the gear train ratio in inches of the carriage movement per revolution of the motor.

Substituting (41) into (39), we have

$$t_m = t_1 + dpr(10)^3. \tag{42}$$

As an example: if $t_1 = 5$ ms and if the motor stops within 2/3 of a revolution after the braking is applied, then we have $p = 2/3$. If $d = 0.001$ inch per 0.6 revolution, $r = 6$ seconds per inch, then $t_2 = dpr(10)^3 = (2/3)(0.001/0.6)(6)(10)^3 = 6.7$ ms. Hence

$$t_m = t_1 + t_2 = 5 + 6.7 = 11.7 \text{ m.s.} \tag{43}$$

C. Error-Spread Due to Nonlinear Tuner

Substituting (42) into (37), we have

$$\theta = a(t_1 + dpr(10)^3)(10)^{-3} - h. \tag{44}$$

Since t_m does not depend upon electrical characteristic of tuner over band, it will be a constant once t_1, p, d, and r are fixed. If we rewrite (37) into the form

$$\theta = -h + at_m(10)^{-3}, \tag{45}$$

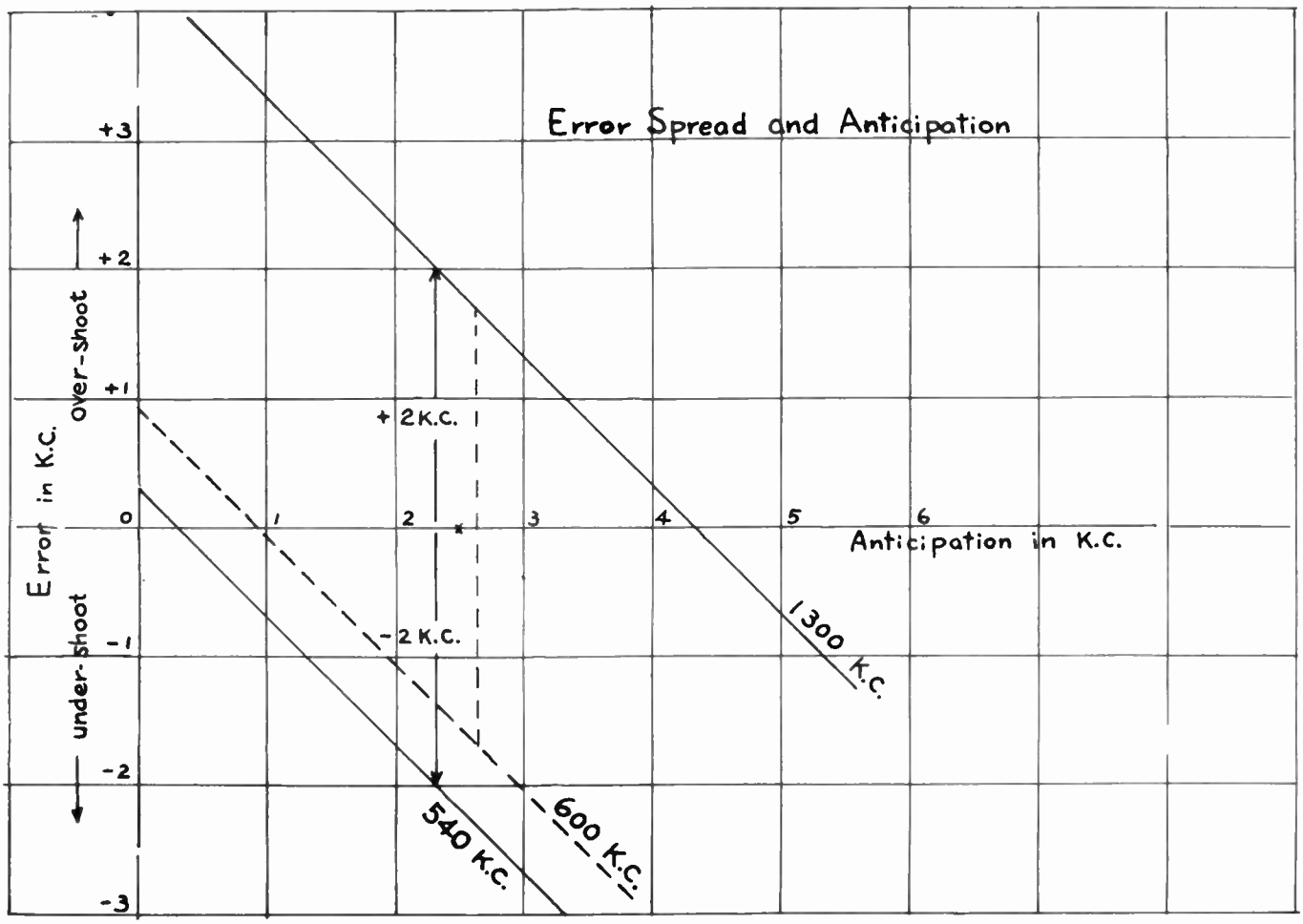

Fig. 20

then at any particular frequency in the band where the factor a will be a fixed value, the plot of θ versus h will be a straight line. For the error over the band we will have a family of straight lines with a as a parameter. The slope of those lines is negative unity.

If the tuner has a nonlinear characteristic as shown in Fig. 19, then the two boundary cases for the tuner will be at 540 kc and 1,300 kc respectively. The factor a will have the following values:

At 540 kc, a = 26.6 kilocycles per second

At 1,300 kc, a = 370 kilocycles per second.

If the stopping circuit gives total effective mechanical delay time t_m, 11.7 ms as shown by (43), then at 540 kc,

$$\theta = -h + (26.6)(11.7)(10)^{-3}; \tag{46}$$

at 1,300 kc,

$$\theta = -h + (370)(11.7)(10)^{-3}. \tag{47}$$

The plot of (46) and (47) is shown in Fig. 20 (above). It is obvious that if amount of anticipation is 2.3 kc, error-spread will be ± 2 kc (a total error-spread at 4 kc). Hence the assumption of 2.5 kc for anticipation in the example of Section I is adequate.

D. Analytical Expression for the Desired Anticipation and the Error-Spread

From (37), we have

$$\theta_1 = -h + a_1 t_m (10)^{-3} \tag{48}$$

$$\theta_2 = -h + a_2 t_m (10)^{-3}, \tag{49}$$

where the subscripts 1 and 2 indicate the two extreme cases of the nonlinear tuner. Let us also assume that a_1 be greater than a_2, then for the same amount of anticipation, the case of (48) will be easier to over-shoot than the case of (49). If it is desired that

$$\theta_1 = -b\theta_2, \tag{50}$$

where b can be any constant, then, we have

$$-h + a_1 t_m (10)^{-3} = -b(-h + a_2 t_m (10)^{-3}). \tag{51}$$

After simplification, we have

$$h = \frac{(a_1 + ba_2)}{(1 + b)} t_m (10)^{-3}. \tag{52}$$

Substitute (52) into (49) and (48):

$$\theta_1 = \frac{b}{1 + b} (a_1 - a_2) t_m (10)^{-3} \tag{53}$$

$$\theta_2 = \frac{-1}{1+b}(a_1 - a_2)t_m(10)^{-3}. \tag{54}$$

The total error-spread will be $\theta_1 - \theta_2$, hence

$$\text{total error-spread} = (a_1 - a_2)t_m(10)^{-3}. \tag{55}$$

Notice that the total error-spread is independent of the value of b. If $b=1$, that is if we wish that the over-shoot and the under-shoot of the error-spread be equal, then the proper anticipation should be

$$h = \frac{(a_1 + a_2)}{2} t_m(10)^{-3}. \tag{56}$$

The error-spread will be

$$\pm \frac{a_1 - a_2}{2} t_m(10)^{-3}. \tag{57}$$

III. Design Considerations of the Output IF Transformer of a Signal-Seeking Radio with Respect to Errors due to Components Tolerances

In the example of Section I of this paper, the circuit Q's of the IF output transformer are assumed to be 30. This corresponds to a coil Q of 50 in a typical set. IF transformer with Q of that range is relatively cheap. From the standpoint of seeking error variation, high Q output IF transformer will be more advantageous. But a high Q output IF transformer will require a too low Q input IF transformer if the over-all selectivity is kept the same. This will again cost money. However, if the cost is of secondary interest, then the IF output should be designed with respect to the seeking errors due to components tolerances. If the coupling factor, base capacitors are fixed, then the IF transformer design will be fixed if the Q's of the transformer are known. What kind of Q should we choose? What will be the seeking error caused by the variation of components associated with the output IF transformer? This section is intended to answer these questions. It will offer a way to tell approximately what amount of error we will have once our design is done. We will first assume that there is no Q-variation and then, later on, we will see what will happen when Q varies. Approximations are used wherever possible.

A. Variation of Error When the Amount of Anticipation Desired Is Fixed

Rewrite (9) into

$$f_c = \frac{f_0}{2\sqrt{Q_1Q_2}} \sqrt{\frac{s^2}{n^2}\frac{C_1}{C_2} - \frac{Q_1}{Q_2}}, \tag{58}$$

where f_c is the anticipation in kc, f_0 is the IF frequency, and n is the mixing index, and the rest are the conventional symbols. If we denote

$$u = \sqrt{\frac{s^2}{n^2}\frac{C_1}{C_2} - \frac{Q_1}{Q_2}}. \tag{59}$$

then

$$f_c = \frac{f_0}{2\sqrt{Q_1Q_2}} v. \tag{60}$$

Let us simplify the expression of (59) by defining

$$\frac{s^2}{n^2}\frac{C_1}{C_2} = x^2 \tag{61}$$

and

$$\frac{Q_1}{Q_2} = m^2; \tag{62}$$

then

$$u = \sqrt{x^2 - m^2}. \tag{63}$$

If we let m be a constant, then any percentage variation in s or $\sqrt{C_1/C_2}$ will be equivalent to the variation of x and any percentage variation in n will be equivalent to the variation of $1/x$.

If the variation is not large, we can make the following approximation:

$$\Delta f_c = \frac{df_c}{dx}\Delta x, \tag{64}$$

or

$$\Delta f_c = \frac{df_c}{du}\frac{du}{dx}\Delta x. \tag{65}$$

From (60)

$$\frac{df_c}{du} = \frac{f_0}{2\sqrt{Q_1Q_2}}. \tag{66}$$

From (63),

$$\frac{du}{dx} = \frac{x}{\sqrt{x^2 - m^2}}; \tag{67}$$

hence

$$\Delta f_c = \frac{f_0}{2\sqrt{Q_1Q_2}} \frac{x}{\sqrt{x^2 - m^2}}\Delta x. \tag{68}$$

But from (60),

$$\frac{f_0}{2\sqrt{Q_1Q_2}} = \frac{f_c}{u}; \tag{69}$$

therefore

$$\Delta f_c = \frac{f_c}{u} \frac{x}{\sqrt{x^2 - m^2}}\Delta x. \tag{70}$$

Substituting (63) into (70), we have

$$\frac{\Delta f_c}{f_c} = \frac{x}{x^2 - m^2}\Delta x. \tag{71}$$

If now

$$\Delta x = \pm M\%x.$$

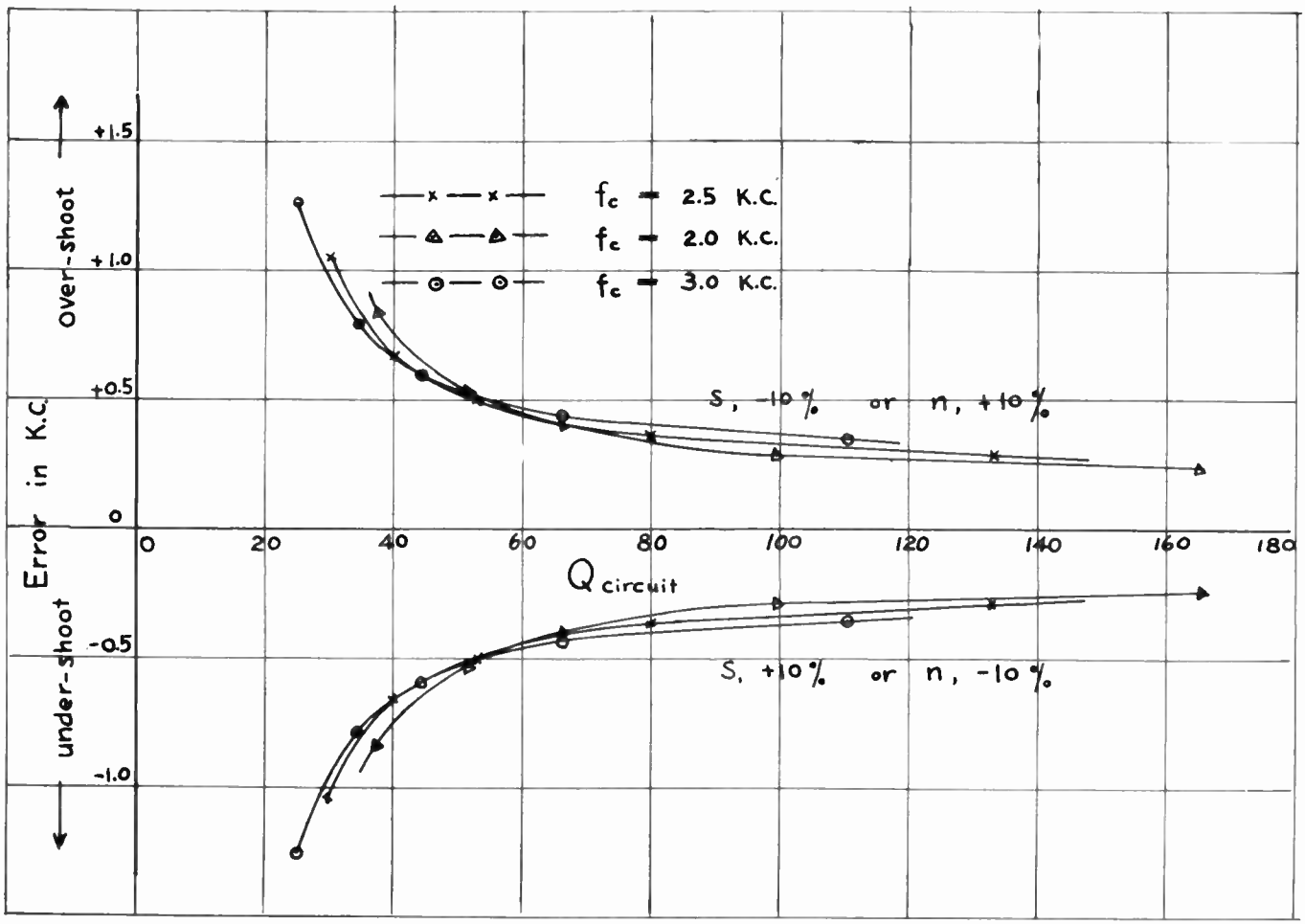

Fig. 21—Calculated error variation with fixed anticipation. For approximation use (76) and (80).

then

$$\frac{\Delta f_c}{\pm M\% f_c} = \frac{x^2}{x^2 - m^2}. \tag{72}$$

From (63) we have

$$v^2 = x^2 - m^2$$

or

$$x = \sqrt{v^2 + m^2}. \tag{73}$$

Hence

$$\frac{\Delta f_c}{\pm M\% f_c} = \frac{v^2 + m^2}{v^2} = 1 + \frac{m^2}{v^2}. \tag{74}$$

If we denote

$$v = \alpha m, \tag{75}$$

then

$$\boxed{\frac{\Delta f_c}{\pm M\% f_c} = 1 + \frac{1}{\alpha^2}}. \tag{76}$$

Substitute (75) into (60),

$$f_c = \frac{f_0}{2\sqrt{Q_1 Q_2}}\alpha m. \tag{77}$$

Substitute (62) into (77):

$$f_c = \frac{\alpha f_0}{2\sqrt{Q_1 Q_2}}\sqrt{\frac{Q_1}{Q_2}} = \frac{\alpha f_0}{2\sqrt{Q_2^2}}$$

or

$$\boxed{f_c = \frac{\alpha f_0}{2Q_2}}; \tag{78}$$

Hence

$$\boxed{Q_2 = \frac{\alpha}{2}\frac{f_0}{f_c}}. \tag{79}$$

From (76) and (79), it is clear that the larger the α the smaller the error, which corresponds to a higher Q_2.

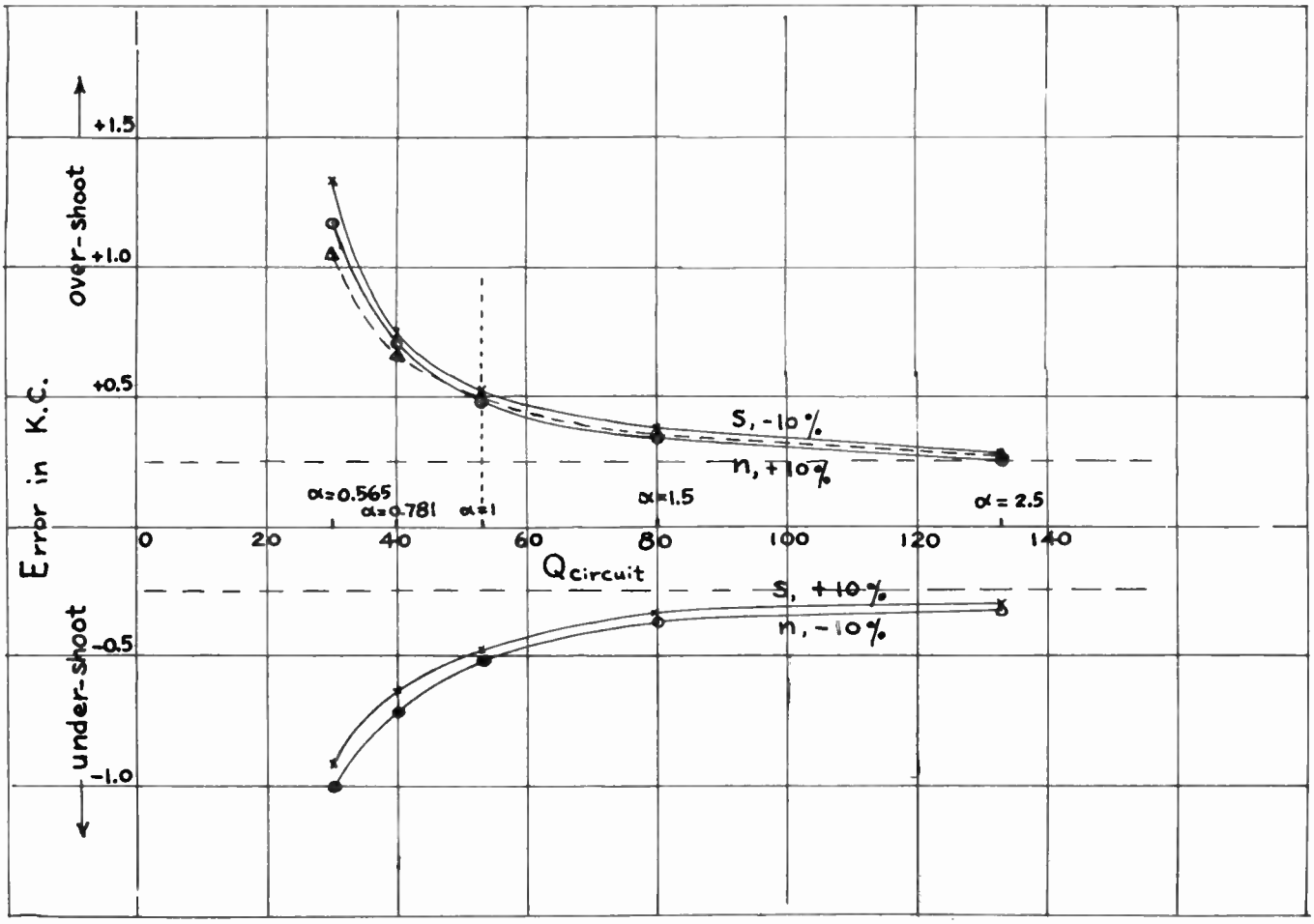

Fig. 22—Error variation with fixed anticipation. $f_c = 2.5$ kc.
– – – △ – – – approximation use (76) and (80).

Eq. (79) can also have another form:

$$\boxed{\alpha = \frac{2Q_2 f_c}{f_0}}. \tag{80}$$

From (80) and (76), the error curve due to different Q_2 can be plotted. If $C_1 = 114$ mmf, $C_2 = 134$ mmf, $s = 0.85$, $f_0 = 265$ kc and $Q_1 = Q_2 = Q$, three sets of curves are shown on Fig. 21 (page 1604) corresponding to $f_c = 2$ kc, $f_c = 2.5$ kc, and $f_c = 3$ kc respectively.

In order to check the accuracy of the above approximation formula, calculations by exact method are used for the case of $f_c = 2.5$ kc and the result is shown in Fig. 22. It shows that in the region of interest, the accuracy is very good.

From the above curves, it is evident that high Q case is better. However, the improvement above $Q = 80$ is not very much. Even at $\alpha = 1$, or $Q = 53$, it is not too far from the ideal minimum.

The result of Δf_c due to $\Delta(1/x)$ can be derived similarly. The final expression is the same except the sign. The details will not be shown here.

B. The effect of Unequal Q

Although the examples given above are for the cases with $Q_1 = Q_2 = Q$, the results apply as well to the unequal Q cases as to the equal Q cases. However, the Q's in Fig. 21 and Fig. 22 should be Q_2 in the unequal Q cases. This is because from (76), for the same amount of $\Delta f_c/(\pm M$ per cent $f_c)$, α has to be the same. From (79), if α is the same, then Q_2 has to be the same. Of course, when $m \neq 1$, the value of n is not the same as the value of n with $m = 1$. Table I, showing results from the exact calculation, should make the point clear.

TABLE I
$f_c = 2.5$ kc, $s = 0.85$

m	Q_1	Q_2	α	n	Error in kc			
					s, +10 per cent	s, −10 per cent	n, +10 per cent	n, −10 per cent
1	80	80	1.5	0.435	−0.34	0.38	0.34	−0.37
2	320	80	1.5	0.216	−0.35	0.37	0.33	−0.38
0.5	20	80	1.5	0.867	−0.34	0.38	0.34	−0.37

It is evident here that there is no advantage for $m > 1$. For $m < 1$ the primary Q can be lowered if the

waveform is not disturbed too much due to the misalignment of IF.

C. Error Due to Q-Tolerance and Loading Variation

Both the coil-Q tolerance and the loading variation will change the circuit Q and result in seeking errors. If a set of center-design components are used, and if C_1, C_2, k, and n are all center-design values, then the information about the error due to the deviation of circuit Q's from the center-design values will be valuable.

When Q_1 deviates from the center-design value. From (78), we know that if α and Q_2 are the center-design values, the anticipation will not be changed even when Q_1 is deviated from the center-design value. The point will be more clear if we put k, the coefficient of coupling, into (78). Then it can be shown that

$$f_c = \frac{f_0}{2}\sqrt{\frac{k^2c_1}{n^2c_2} - \frac{1}{Q_2^2}}. \tag{81}$$

Since Q_1 does not appear in (81), the deviation of Q_1 from the center-design value will not affect the accuracy of seeking. This result relieves the worry of the possible seeking error by the primary loading variation with the signal strength due to the primary avc loading, provided the detuning effect is negligible.

When Q_2 deviates from the center-design value. If the deviation $\Delta Q_2 = \pm M$ per cent Q_2 is relatively small, then

$$\Delta f_c = \pm M \text{ per cent } Q_2(\partial f_c/\partial Q_2). \tag{82}$$

From (81), it can be shown that

$$\partial f_c/\partial Q_2 = (f_0^2/4f_c)(1/Q_2^3). \tag{83}$$

Hence

$$\Delta f_c = \pm M \text{ per cent } (f_0^2/4f_c)(1/Q_2^2). \tag{84}$$

The error due to the deviation of Q_2 from the center-design value is therefore inversely proportional to the square of Q_2. This result again favors a high Q_2 output IF transformer. If volume control is the load of the transformer secondary, then the tolerance of the volume control specification should be tightened.

The accuracy of (84) depends upon the amount of deviation from the center-design value. For deviation less than 5 per cent it gives very good results. Even with a deviation of 10 per cent, it gives a fairly good approximation. The following results are computed according to (84) for $f_c = 2.5$ kc, $f_0 = 265$ kc, and $\pm$M per cent $= \pm 10$ per cent.

Q_2	30	40	50	60	70	80	100	120
Error in kc	0.78	0.44	0.28	0.2	0.15	0.11	0.07	0.05

It is evident that the improvement above $Q_2 = 60$ is not very much.

Conclusions

1. The equation for the "difference-voltage" with no avc delay voltage is

$$E_2 - nE_1 = J_1\left[\frac{s\sqrt{R_1R_2} - n\,R_1\sqrt{1 + v^2Q_2/Q_1}}{[(1+s^2)^2 - 2(s^2 - b/2)v^2 + v^4)^{1/2}}\right]. \tag{5}$$

2. The crossover points have a frequency deviation from the center frequency

$$\Delta f = \frac{f_0}{2\sqrt{Q_1Q_2}}\sqrt{\frac{s_2}{n^2}\frac{C_1}{C_2} - \frac{Q_1}{Q_2}}. \tag{9}$$

3. The avc delay effects only the crossover level but not the frequency of the crossover point.

4. If the trigger level of the stopping circuit is adjusted to the same as the crossover level of the trigger circuit, constant frequency anticipation can be obtained for a linear tuner. The amount of anticipation is equal to the frequency deviation of the crossover point.

5. There is an upper limit for the mixing index n, above which there will be no crossover points. The limit is

$$n < \sqrt{\frac{C_1}{C_2}\frac{Q_2}{Q_1}}\,s. \tag{19}$$

6. The maximum amount of anticipation obtainable depends upon the selective characteristics of the circuits ahead of the output IF transformer. Within the maximum anticipation obtainable, the effect of the front end selectivity on the crossover points should be none. However, it may cause error asymmetry if the trigger level is not the crossover level.

7. If the over-all selectivity of the receiver is kept the same, from the standpoint of obtaining as much anticipation as possible, the Q's of the output IF transformer should be high. However, if the anticipation desired is less than 5 kc or so, a medium Q output IF transformer will be sufficient.

8. The crossover level depends upon the avc delay voltage and the mixing index. Or,

$$nE_0 = \text{constant} \tag{15}$$

9. The peak of the difference-voltage from the crossover level is independent of the avc delay voltage once the avc delay voltage is exceeded.

$$A_{\text{from the crossover level}} = \left[s\sqrt{\frac{C_1}{C_2}\frac{Q_2}{Q_1}} - n\right]E_{1\text{ at } f-f_0}. \tag{26}$$

10. The smaller the amount of anticipation, the smaller will be the peak of the difference voltage from the crossover level.

11. The variation of the trigger level will cause "level effect"—the amount of seeking error depends upon the signal strength. The nature of the error variation due to improper trigger level can be utilized to

adjust the trigger amplifier gain so that the circuit will be triggered at the crossover level.

12. "Error Asymmetry" refers to the fact that in a bidirectional signal seeking radio with ideal tuner, the seeking error produced with the same input signal depends upon whether it is seeking toward the high frequency end or the low frequency end of the broadcasting band.

13. Error asymmetry can be caused by the misalignment of the front end, the input IF transformer, and the output IF transformer. It can also be caused by the unequal braking characteristics of the moving system and others.

14. Detuning of the output IF transformer shifts the crossover points. However, we can utilize this property in a unidirectional signal seeking radio to obtain

(a) more anticipation than the limit imposed upon by the front end and the input IF transformer selectivity.

(b) less anticipation without too much sacrifice of the peak of the difference-voltage from the crossover level.

15. High front end gain during seeking is desired for a signal seeking radio to reduce the seeking error due to the level effect.

16. The partial avc action helps the seeking accuracy. Hence long time constant for the avc circuit is desirable. But if it is too long, it may result in "skip" of weak stations immediately after the strong station.

17. Error-spread over the broadcast band is due to the nonlinear characteristic of the tuner system. To reduce the error-spread, the tuner sweeping characteristic should be made as linear as possible (i.e., the sweeping rate in kilocycles per second should be a constant throughout the broadcast band). This can be done either by a proper design of the tuner coil or a variable speed drive such that the resultant tuner sweeping characteristic is the one desired.

18. The faster the stopping circuit and the stopping action, the less the amount of anticipation required, and the less will be the error-spread.

19. If a_1 and a_2 ($a_1 > a_2$) are the two extreme sweep speed in kc per second of the tuner, the total error-spread will be:

$$(a_1 - a_2)t_m(10)^{-3}. \tag{55}$$

20. The shifting of error-spread depends upon the amount of anticipation.

$$h = \frac{(a_1 + ba_2)}{1 + b} t_m(10)^{-3}, \tag{52}$$

where the errors at the two extreme frequencies are related by

$$\theta_1 = -b\theta_2. \tag{50}$$

21. If Q's are constants and if the $\pm$M per cent variation of $\sqrt{C_1/C_2}$, s and n are not very large, the seeking error will be approximately

$$\Delta f_c/(\pm M \text{ per cent } f_c) = 1 + 1/\alpha^2, \tag{76}$$

where

$$\alpha = 2Q_2 f_c/f_0. \tag{80}$$

Hence for small error, high Q_2 output IF transformer will be required.

22. As long as Q_2 is the same,

(a) $Q_1 < Q_2$ does not give less error due to the per cent variation of C_1/C_2, s and n than the case with $Q_1 = Q_2$. (Although it does give a larger difference-voltage, but it may give more asymmetry for the same amount of misalignment.)

(b) There is no advantage for $Q_1 > Q_2$.

23. If a set of center-design components are used and if C_1, C_2, k, n are all center-design values, then the deviation of Q_1 from the center-design value does not affect the seeking accuracy.

24. However, when Q_2 is deviated from the center-design value, there will be seeking error. If the deviation is not large, the error will be approximately:

$$\Delta f_c = \pm M \text{ per cent } (f_0^2/4f_c)(1/Q_2^2). \tag{84}$$

25. It is evident from the results that some errors are positive while others are negative. It is therefore possible to use the error caused by one kind of component variation to compensate for the errors caused by other kinds of component variations.

26. In the example given, it will be more expensive to either:

(a) tighten the IF transformer tolerance and the volume control tolerance specifications,

(b) have high-coil-Q IF transformer, or

(c) to have special variable coupling IF transformer.

Hence to pick different mixing resistors for compensation of the tolerances of the IF and other associated components will be more practical and cheaper.

27. To utilize the maximum secondary coil Q of the IF output transformer, reflex detector may be used provided that the distortion is tolerable.

Acknowledgments

The author wishes to express his appreciation to Messrs. G. W. Randolph, C. S. Lerch, Jr., B. Hooten, J. F. Slack and other members of the signal-seeking radio development group at Bendix Radio for their cooperation. The author is particularly indebted to Mr. F. E. Churchill for his numerous laboratory check-ups and discussions.

IRE Standards on Graphical and Letter Symbols for Feedback Control Systems, 1955*

COMMITTEE PERSONNEL

Committee on Feedback Control Systems, 1952–1955

W. M. Pease, *Chairman*, 1952–1954

J. E. Ward, *Chairman*, 1954–1955

M. R. Aaron
G. S. Axelby
G. A. Biernson
R. E. Graham
V. B. Haas
R. J. Kochenburger
D. P. Lindorff
W. K. Linvill
D. L. Lippitt
J. C. Lozier
T. Kemp Maples
W. M. Pease
E. A. Sabin
P. Travers
J. E. Ward
R. B. Wilcox
S. B. Williams
F. R. Zatlin

Standards Committee, 1955–1956

E. Weber, *Chairman*

M. W. Baldwin, Jr., *Vice-Chairman*

R. F. Shea, *Vice-Chairman*

L. G. Cumming, *Vice-Chairman*

J. Avins
W. R. Bennett
J. G. Brainerd
P. S. Carter
P. S. Christaldi
A. G. Clavier
J. E. Eiselein
A. W. Friend
V. M. Graham
R. A. Hackbusch
H. C. Hardy
P. J. Herbst
Hans Jaffe
Henry Jasik
A. G. Jensen
J. L. Jones
J. G. Kreer, Jr.
E. A. Laport
A. A. Macdonald
Wayne Mason
D. E. Maxwell
K. R. McConnell
H. R. Mimno
M. G. Morgan
G. A. Morton
H. L. Owens
P. A. Redhead
C. H. Page
R. Serrell
R. M. Showers
H. R. Terhune
J. E. Ward
W. T. Wintringham

Measurements Co-ordinator

R. F. Shea

I. Introduction

1.1 Standardization of symbols is considered important for the exposition of feedback control concepts. The purpose is to establish forms for representing letter symbols and graphical symbols used in block diagrams.

In the preparation of this standard, it was found that there was no complete and self-consistent set of symbols in use that appeared to fulfill the requirements of the IRE. It was also found that there is a wide variation in the symbols used by different industries and professional societies so that it is difficult to choose symbols with a universal acceptance in all fields. Therefore, a compromise has been made among existing symbols used in the electrical field.

* Reprints of this Standard, 55 IRE 26.S1, may be purchased while available from The Institute of Radio Engineers, 1 East 79 Street, New York 21, N. Y., at $0.25 per copy. A 20 per cent discount will be allowed for 100 or more copies mailed to one address.

II. Graphical Symbols for Block Diagrams

2.1 *Transfer Element*

2.1.1 A transfer element represents the functional relationships (g_{12}) between a single input signal (x_1) and a single output signal (x_2), in which the input signal, indicated by the arrow, is the independent variable.

2.2 *Mixing Point*

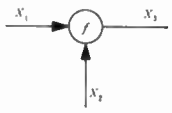

2.2.1 The indicated relationship is $x_3=f(x_1, x_2)$.

2.3 *Summing Point*

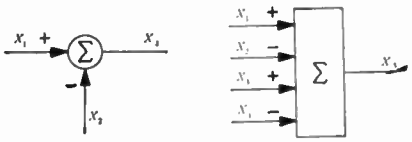

2.3.1 The indicated relationships are $x_3=x_1-x_2$ and $x_5=x_1-x_2+x_3-x_4$. A summing point is a special case of the mixing point and indicates the algebraic addition of two or more signals to produce one output signal. An algebraic sign should be indicated at the arrowhead for each signal to be added. If the number of input signals to be added is large the rectangular symbol should be used.

2.4 *Multiplication Point*

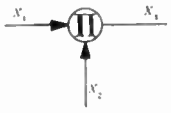

2.4.1 The indicated relationship is $x_3=x_1x_2$. A multiplication point is a special case of the mixing point.

2.5 *Branch Point*

2.5.1 A branch point, which indicates that a signal is distributed to two or more points in a block diagram is represented by a heavy dot. Example:

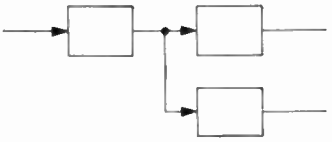

2.6 Graphical symbols added to a block diagram for mathematical purposes shall be shown dotted to indicate that they do not represent components of the physical system.

III. Standard for Letter Symbols

3.1 *Essential Features of the System of Symbols*

3.1.1 *Signals*

Signals are represented by a single letter symbol with a single subscript denoting its physical or mathematical meaning. The letter x has been chosen as the preferred symbol for generalized signals. Lower case represents the time domain. Upper case represents the complex frequency domain.

3.2 *Transfer Functions*

Transfer functions are represented by a single letter symbol with a double subscript, the first letter or number of which is the subscript of the symbol for the input signal and the second of which is the subscript of the symbol for the output signal. The symbol g has been chosen. Lower case represents the time domain. Upper case represents the complex frequency domain.

IV. Examples

4.1 Application of the standard graphical symbols and the standard form for letter symbols are illustrated in the typical block diagrams below:

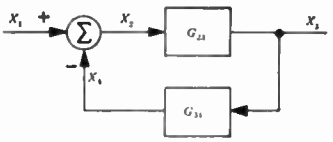

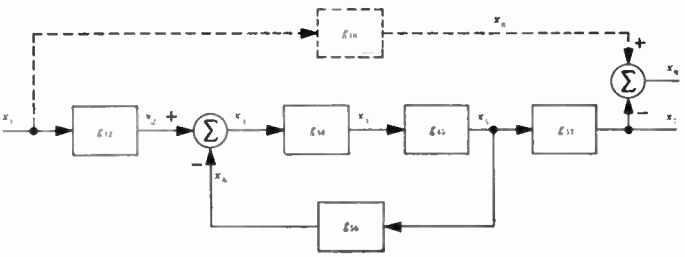

IRE Standards on Pulses: Methods of Measurement of Pulse Quantities, 1955*

COMMITTEE PERSONNEL

Subcommittee on Pulse Modulated Transmitters

H. Goldberg, *Chairman*

Ross Bateman
L. L. Bonham
W. F. Cook
H. Kohler
G. F. Montgomery
A. E. Newlon
W. K. Roberts
B. D. Smith

Committee on Radio Transmitters, 1953–1955

P. J. Herbst, *Chairman* H. Goldberg, *Vice-Chairman*

T. E. Ahlstedt
J. Battison
T. J. Boerner
M. R. Briggs
A. Brown
H. R. Butler
W. R. Donsbach
L. K. Findley
T. M. Gluyas, Jr.
J. B. Heffelfinger
H. E. Goldstine
A. E. Kerwien
L. A. Looney
J. F. McDonald
S. M. Morrison
J. Ruston
H. B. Seabrooks
G. W. Sellers
B. Sheffield
N. B. Tharp
I. R. Weir

Standards Committee, 1955–1956

E. Weber, *Chairman*
M. W. Baldwin, Jr., *Vice-Chairman* R. F. Shea, *Vice-Chairman*
L. G. Cumming, *Vice-Chairman*

J. Avins
W. R. Bennett
J. G. Brainerd
P. S. Carter
P. S. Christaldi
A. G. Clavier
J. E. Eiselein
A. W. Friend
V. M. Graham
R. A. Hackbusch
H. C. Hardy
P. J. Herbst
Hans Jaffe
Henry Jasik
A. G. Jensen
J. L. Jones
J. G. Kreer, Jr.
E. A. Laport
A. A. Macdonald
Wayne Mason
D. E. Maxwell
K. R. McConnell
H. R. Mimno
M. G. Morgan
G. A. Morton
H. L. Owens
P. A. Redhead
C. H. Page
R. Serrell
R. M. Showers
H. R. Terhune
J. E. Ward
W. T. Wintringham

Measurements Co-ordinator

R. F. Shea

I. Introduction

1.1 Definition of a Pulse (51 IRE 20. S1)

A pulse is defined as "a variation of a quantity whose value is normally constant; this variation is characterized by a rise and a decay, and has a finite duration.

Note 1: The word 'pulse' normally refers to a variation in time; when the variation is in some other dimension, it shall be so specified, such as 'space pulse.'

Note 2: This definition is broad so that it covers almost any transient phenomenon. Features common to all 'pulses' are rise, finite duration, and decay. It is necessary that the rise, duration, and decay be of a quantity that is constant (not necessarily zero) for some time before the pulse and has the same constant value for some time afterwards. The quantity has a normally constant value and is perturbed during the pulse. No relative time scale can be assigned."

* Reprints of this Standard, 55 IRE 15.S1, may be purchased while available from The Institute of Radio Engineers, 1 East 79 Street, New York 21, N. Y., at $0.60 per copy. A 20 per cent discount will be allowed for 100 or more copies mailed to one address.

1.2 Zero Axis

It is important to realize that since a pulse is defined as a variation of a quantity, the variation is zero at the start and end of the pulse. Therefore, in these standards the graphical representation of the normally constant value will be called the "zero axis" of a pulse.

1.3 Delineation of Pulses

It should be noted that the variation considered to be the pulse may be accompanied by other variations that are not of interest. For example, spikes, overshoots, and polarity reversals may be present, but may be ignored if they are not pertinent to the measurement being taken. The word "pulse" as used in these standards refers to that portion of a waveform delineated as the pulse, after exclusion of those portions of the waveform determined to be nonpertinent. This determination of the nonpertinent portions of a waveform may depend upon the function of the pulse in a particular circuit or system. For example, a negative excursion following a positive pulse may be ignored in the measurement of Pulse Decay Time if it is determined that this negative excursion has no important effect upon the operation of the circuit or system under consideration. The portion of a waveform delineated as pulse may also be determined by a time interval of interest outside of which the waveform is not considered part of the pulse. These standards have been written with as much generality as possible and are applicable to pulses with or without spikes, overshoots, or polarity reversals. Whether or not these are considered part of the pulse is a decision which is left up to the individual user. The delineation of the pulse should be made arbitrarily only if *a priori* knowledge is not available, and in either case the results should be clearly stated.

1.4 Definition of a Pulse Train (51 IRE 20. S1)

A pulse train is defined as "a sequence of pulses."

1.5 Delineation of Pulse Trains

Measurements of pulse trains often require knowledge of the component pulses making up the pulse train. A picture of the pulse train alone may not permit the component pulses to be determined.

The following trains are given as examples of the difficulty of measuring the characteristics of a pulse train unless delineation of the component pulses is made.

Example 1. Rectangular Pulses

In example 1, the pulse train could be either a sequence of short positive pulses, long negative pulses, or alternating short positive and long negative pulses depending upon what constitutes the component pulses. Example 2 presents the same difficulty as example 1, with the additional complication that several types of

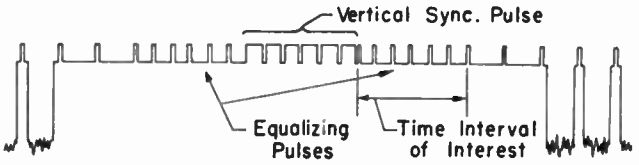

Example 2. Television Signal

component pulses are present. Even if it is known that this is a television signal, the determination of the characteristics of particular component pulses, for example the equalizing pulses, requires the additional concept of an interval of interest, which will be used frequently in these standards. For example, to determine the repetition rate of the equalizing pulses, one might choose a a time interval of interest as shown in the example. If one were required to determine the repetition rate of the vertical sync. pulses, another time interval of interest would have to be chosen. The determination of the characteristics of a complex pulse train may require the delineation of more than one type of component pulse and the use of more than one time interval of interest. The delineation of the component pulses and choice of an interval of interest should be made arbitrarily only if *a priori* knowledge is not available, and in either case the results should be clearly stated.

2. General Considerations

Although the methods of measurement given below cover a wide variety of pulse quantities, many of these methods involve the same measuring instruments, the same general techniques, and the same precautions. The following preface discusses some of these general precautions and techniques in greater detail than would have been possible under each separate method of measurement.

2.1 The Oscillograph

A pulse is best described graphically. The oscillograph, which provides pictorial representations of electrical quantities as functions of time, is commonly and constantly employed in pulse work. The term "oscillograph" as it is used here includes the entire family of devices such as cathode-ray oscilloscopes, ink-writing recorders, etc., which give either a permanent or nonpermanent record of an electrical quantity. It will be understood that the pulse may be current, power, frequency, etc. Since the oscillograph is usually voltage operated, a conversion device (transducer) may be required in connection with the oscillograph to convert the quantity being measured to a voltage. The transfer characteristics (amplitude and time scale factors, linearity, response function, etc.) of the test setup, the transducer, and the oscillograph must be known to enable measurements of the desired quantity to be made in terms of the calibrated deflections of the oscillograph.

In many cases it will be convenient and desirable to select a transducer having simple transfer character-

istics (for example, linear, wide-band devices), so that conversion from the oscillograph deflections to the quantities being measured can be readily obtained. It is recommended that the instruments used and their transfer characteristics be stated when reporting the results of measurement.

Some other type of instrument (for example, a vacuum-tube voltmeter, elapsed time meter, calorimeter, etc.) may provide a more convenient or accurate means of measurement than an oscillograph. However, in order to avoid possible serious errors, it is usually necessary first to observe and measure the desired quantity with an oscillograph.

Many oscillographs have features that aid in presenting a stable picture of the pulse and provide amplitude and time scale calibrations. These are very helpful in pulse work and should be used whenever accurate measurements are desired.

2.2 Bandwidth and Phase Response

The accuracy of measurement of a pulse quantity depends on the bandwidth and phase response of the measuring instrument and any associated transducer. Accuracy is usually improved by increasing the upper frequency limit and decreasing the lower frequency limit. In order to determine a minimum required upper frequency limit, it is generally necessary to decide upon a minimum time resolution. If the required minimum time resolution is T_1, then the upper frequency limit (3db) of the measuring instrument should be approximately $1/(2T_1)$, to give a minimum acceptable degree of accuracy in measuring the pulse quantity. For example, if in a certain circuit the constants are such that disturbances less than 0.1 microsecond in duration will not influence the operation, the required upper frequency limit is 5 megacycles. In many applications the minimum time resolution is determined by the bandwidth of the circuits associated with the pulse to be observed. The time resolution may also be determined by the degree of detail of a pulse the observer requires. For example, a pulse with a sharp spike requires a measuring instrument having a shorter resolution time (higher frequency limit) than does a pulse with no such spike or one in which the pulse spike is to be ignored.

In order to determine the required lower frequency limit, it is necessary to decide upon a time interval of interest. If T_2 is the time interval of interest, then the lower frequency limit (3db) is K/T_2, where K is the maximum error (or fractional droop) that can be tolerated. For example, if a 1 per cent accuracy is required and the time interval of interest is 1,000 microseconds, then the lower frequency limit should be at least as low as 10 cycles per second.

For proper response the phase characteristic of the instrument should be such that the time of transmission of all significant frequency components is constant (in other words, linear phase shift with frequency).

2.3 Precautions

In pulse measurements, the precautions generally necessary in rf work may be required. These include attention to such matters as (a) adequate shielding of measuring equipment to prevent undesired coupling to other parts of the circuit; (b) detuning or loading effects caused by measuring equipment input admittance; (c) lead length which may introduce resonance effects; (d) proper terminations; (e) choice of components to function properly at the frequencies encountered (e.g., the use of noninductive resistors); (f) residual parameters in circuit elements (e.g., inductance present in capacitors); (g) proper physical location of ground leads; and (h) the nonlinear behavior of circuit elements.

2.4 Units

The units (volts, amperes, coulombs, seconds, etc.) should be specified in reporting the results of a measurement.

2.5 Operating Conditions

The equipment or circuits on which the pulse measurements are to be made should be in normal operating condition unless otherwise specified, but in any case the operating conditions should be stated.

3. Methods of Measurement

3.1 Average Absolute Pulse Amplitude

3.1.1 Definition (51 IRE 20. S1)

The average of the absolute value of the instantaneous amplitude taken over the pulse duration.

Note: By "absolute value" is meant the arithmetic value regardless of algebraic sign.

3.1.2 Method of Measurement

1. Obtain a calibrated (time and amplitude) picture of the waveform including the pulse. Delineate the pulse by excluding those portions of the waveform determined to be nonpertinent.
2. Draw the zero axis of the pulse and mark the end points of the pulse duration on the picture. (*See* 3.11)
3. Determine the areas between the end points above and below the zero axis, taking into account any nonlinearity of scales.
4. Add the areas without regard to sign.
5. Divide the sum of the areas by the pulse duration to obtain the average absolute pulse amplitude.

3.1.3 Pictorial Examples

$$\text{Average Absolute Pulse Amplitude} = \frac{\text{Area 1} + \text{Area 2} + \text{Area 3}}{\text{Pulse Duration}}$$

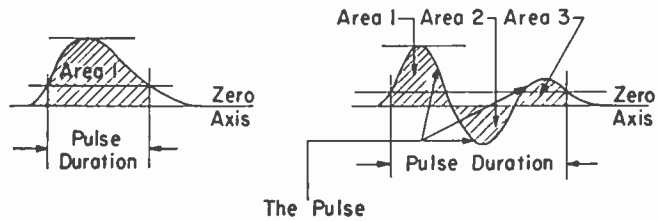

3.2 Average Pulse Amplitude

3.2.1 Definition (51 IRE 20. S1)

The average of the instantaneous amplitude taken over the pulse duration.

3.2.2 Method of Measurement

1. Obtain a calibrated (time and amplitude) picture of the waveform including the pulse. Delineate the pulse by excluding those portions of the waveform determined to be nonpertinent.
2. Draw the zero axis of the pulse and mark the end points of the pulse duration on the picture. (*See* 3.11)
3. Determine the areas between the end points above and below the zero axis taking into account any nonlinearity of scales.
4. Add the areas with regard to sign; that is, areas on opposite sides of the zero axis have opposite signs.
5. Divide the net area by the pulse duration to obtain the average pulse amplitude.

3.2.3 Pictorial Examples

$$\text{Average Pulse Amplitude} = \frac{\text{Area 1} - \text{Area 2}}{\text{Pulse Duration}}$$

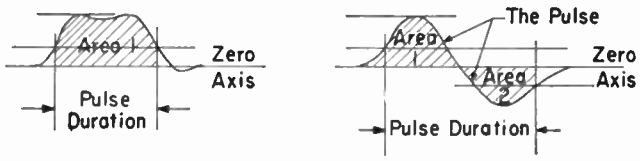

$$\text{Average Pulse Amplitude} = \frac{\text{Area 1} - \text{Area 2} + \text{Area 3}}{\text{Pulse Duration}}$$

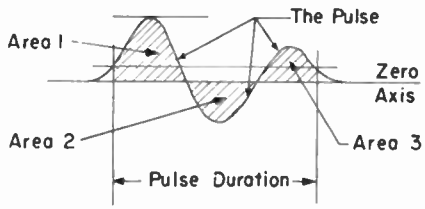

3.3 Crest Factor of a Pulse

3.3.1 Definition (51 IRE 20. S1)

The ratio of the peak pulse amplitude to the rms pulse amplitude.

3.3.2 Method of Measurement

1. Measure the peak pulse amplitude. (*See* 3.7)
2. Measure the rms (effective) pulse amplitude. (*See* 3.15)
3. Divide the peak pulse amplitude by the rms pulse amplitude to obtain the crest factor of the pulse.

3.4 Leading Edge Pulse Time

3.4.1 Definition (51 IRE 20. S1)

The time at which the instantaneous amplitude first reaches a stated fraction of the peak pulse amplitude.

3.4.2 Method of Measurement

1. Obtain a calibrated (time and amplitude) picture of the waveform including the pulse. Delineate the pulse by excluding those portions of the waveform determined to be nonpertinent.
2. Draw the zero axis of the pulse.
3. Find the peak pulse amplitude. (*See* 3.7)
4. Draw two lines parallel to the zero axis, spaced on each side of the zero axis by the stated fraction of the peak pulse amplitude. The time of the first point of intersection of the pulse trace and either line is the Leading Edge Pulse Time.

Note: The stated fraction may not correspond to that used in the measurement of Trailing Edge Pulse Time.

3.4.3 Pictorial Examples

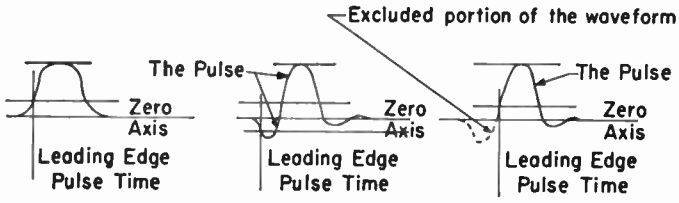

3.5 Trailing Edge Pulse Time

3.5.1 Definition (51 IRE 20. S1)

The time at which the instantaneous amplitude last reaches a stated fraction of the peak pulse amplitude.

3.5.2 Method of Measurement

1. Obtain a calibrated (time and amplitude) picture of the waveform including the pulse. Delineate the pulse by excluding those portions of the waveform determined to be nonpertinent.
2. Draw the zero axis of the pulse.
3. Find the peak pulse amplitude. (*See* 3.7)
4. Draw two lines parallel to the zero axis, spaced on each side of the zero axis by the stated fraction of the peak pulse amplitude. The time of the last point of intersection of the pulse trace and either line is the Trailing Edge Pulse Time.

Note: The stated fraction may not correspond to that used in the measurement of Leading Edge Pulse Time.

3.5.3 Pictorial Examples

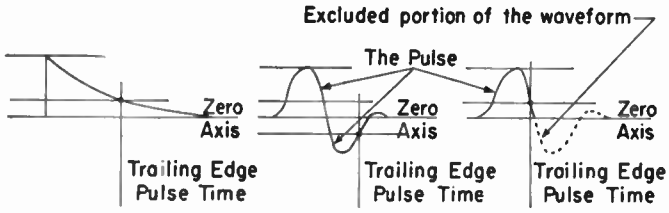

3.6 Mean Pulse Time

3.6.1 Definition (51 IRE 20. S1)

The arithmetic mean of the Leading Edge Pulse Time and the Trailing Edge Pulse Time.

Note: For some purposes the importance of a pulse is that it exists (or is large enough) at a particular instant of time. For such applications the important quantity is the Mean Pulse Time. The Leading Edge Pulse Time and the Trailing Edge Pulse Time are significant primarily in that they may allow a certain tolerance in timing.

3.6.2 Method of Measurement

1. Measure the Leading Edge Pulse Time. (*See* 3.4)
2. Measure the Trailing Edge Pulse Time. (*See* 3.5)
3. Calculate the arithmetic mean of the Leading Edge Pulse Time and the Trailing Edge Pulse Time. The result is the Mean Pulse Time, which is midway between the Leading Edge Pulse Time and the Trailing Edge Pulse Time when the pulse is portrayed graphically.

3.7 Peak Pulse Amplitude

3.7.1 Definition (51 IRE 20. S1)

The maximum absolute peak value of the pulse, excluding those portions considered to be unwanted, such as spikes.

Note: Where such exclusions are made, pictorial illustration of the amplitude chosen is desirable.

3.7.2 Method of Measurement

1. Obtain a calibrated (time and amplitude) picture of the waveform including the pulse. Delineate the pulse by excluding those portions of the waveform determined to be nonpertinent.
2. Draw the zero axis of the pulse.
3. Find the maximum departure of the pulse trace from the zero axis (regardless of sign). This departure is the peak pulse amplitude.

3.7.3 Pictorial Examples

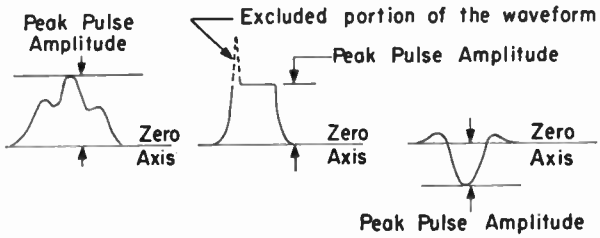

3.8 Pulse Spectrum (Pulse frequency spectrum)

3.8.1 Definition (51 IRE 20. S1)

The frequency distribution of the sinusoidal components of the pulse in relative amplitude and relative phase.

Note: The definition of this term was phrased to convey the idea that the spectrum is a complex (phasor) function of frequency and to express this function most nearly in a manner which corresponds to the method of measuring it (i.e., measuring amplitude and phase separately).

3.8.2 Method of Measurement

1. *Amplitude spectrum*

If only the amplitude spectrum is desired, and if the pulse can be repeated periodically to form a pulse train, the amplitude spectrum of the pulse train may be obtained with a spectrum analyzer using the method given under Pulse Train Spectrum. The envelope of the amplitude spectrum of the pulse train is the amplitude spectrum of the single pulse for positive frequencies.

Note: The pulse repetition period should be long in comparison with the pulse duration, so as to provide sufficient density of the spectrum lines to determine the envelope to the desired degree of accuracy.

2. *Amplitude and phase spectrum*

a. Obtain a calibrated (time and amplitude) picture of the waveform including the pulse. Delineate the pulse by excluding those portions of the waveform determined to be nonpertinent.

b. Obtain the Fourier transform of the waveform to obtain the amplitude and phase spectrum.

3.8.3 Pictorial Examples

Note: This example applies to Method 1 only.

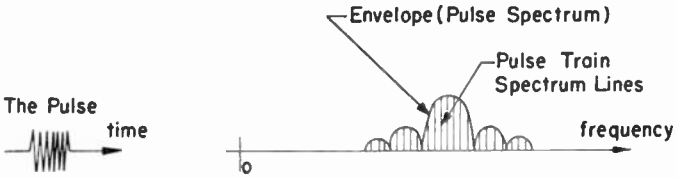

3.9 Pulse Bandwidth

3.9.1 Definition (51 IRE 20. S1)

The smallest continuous frequency interval outside of which the amplitude of the spectrum does not exceed a prescribed fraction of the amplitude at a specified frequency.

Caution: This definition permits the amplitude of the spectrum to be less than the prescribed amplitude within the interval.

Note 1: Unless otherwise stated, the specified frequency is that at which the spectrum has its maximum amplitude.

Note 2: This term should really be "Pulse Spectrum Bandwidth," because it is the spectrum and not the pulse itself that has a bandwidth. However, usage has caused the contraction and for that reason the term has been accepted.

Note 3: Unless otherwise stated, only positive frequencies are to be considered.

3.9.2 Method of Measurement

1. Obtain a calibrated picture of the amplitude spectrum. (*See* 3.8)
2. Determine the amplitude at the specified frequency.
3. Draw a line parallel to the zero axis spaced from the zero axis by the prescribed fraction of the amplitude at the specified frequency.
4. The first and last points of intersection (consider only positive frequencies) of the spectrum trace and the line determine the frequency limits outside of which the amplitude of the spectrum does not exceed the pre-

scribed fraction. The difference between these two limits is the Pulse Bandwidth.

3.9.3 Pictorial Examples

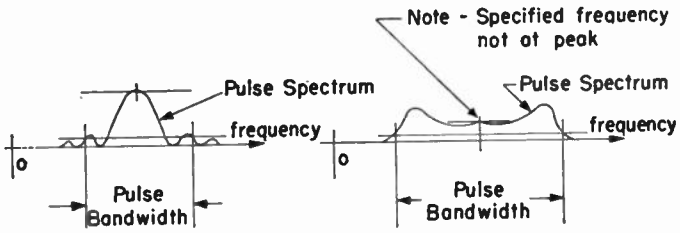

3.10 Pulse Decay Time

3.10.1 Definition (51 IRE 20. S1)

The interval between the instants at which the instantaneous amplitude last reaches specified upper and lower limits, namely, 90 per cent and 10 per cent of the peak pulse amplitude unless otherwise stated.

3.10.2 Method of Measurement

1. Obtain a calibrated (time and amplitude) picture of the waveform including the pulse. Delineate the pulse by excluding those portions of the waveform determined to be nonpertinent.
2. Draw the zero axis of the pulse.
3. Find the peak pulse amplitude. (*See* 3.7)
4. Draw two lines parallel to zero axis spaced on each side of zero axis by 90 per cent (or stated fraction) of peak pulse amplitude, and two parallel lines spaced on each side of zero axis by 10 per cent (or stated fraction) of peak pulse amplitude. Time interval between last point of intersection of pulse trace and either 90 per cent line and last point of intersection of pulse trace and either 10 per cent line is Pulse Decay Time.

3.10.3 Pictorial Examples

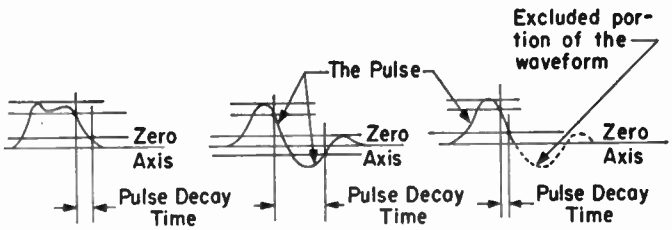

3.11 Pulse Duration

3.11.1 Definition (51 IRE 20. S1)

The time interval between the first and last instants at which the instanteous amplitude reaches a stated fraction of the peak pulse amplitude.

3.11.2 Method of Measurement

1. Obtain a calibrated (time and amplitude) picture of the waveform including the pulse. Delineate the pulse by excluding those portions of the waveform determined to be nonpertinent.
2. Draw the zero axis of the pulse.
3. Find the peak pulse amplitude. (*See* 3.7)
4. Draw two lines parallel to the zero axis, spaced on each side of the zero axis by the stated fraction of the peak pulse amplitude. The time interval between the first and last points of intersection of the pulse trace and either line is the Pulse Duration.

3.11.3 Pictorial Examples

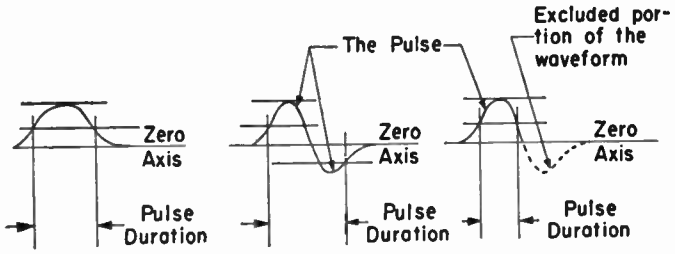

3.12 Pulse Duty Factor

3.12.1 Definition (51 IRE 20. S1)

The ratio of the average pulse duration to the average pulse spacing.

Note 1: This is equivalent to the product of the average pulse duration and the pulse repetition rate.

Note 2: The terms "average pulse duration" and "average pulse spacing" imply a time interval over which the averaging takes place. In the method of measurement below, this time interval is called the time interval of interest.

Note 3: The above definition defines pulse duty factor basically as a ratio of time "on" to total time. This is not in agreement with the use of the term "duty factor" as a ratio of average to peak power, except in special cases, such as that of a rectangular pulse. Care should be taken not to confuse the two meanings of "duty factor" when dealing with unusual pulse shapes.

Note 4: If the Pulse Duty Factor desired is that of a sub-group within a complex train (for example, vertical sync. pulses in a TV signal, channel pulses in a time-division multiplex system, etc.), the particular subgroup must be specified.

3.12.2 Method of Measurement

1. Measure the pulse duration (*see* 3.11) of each individual pulse in the pulse train included in the time interval of interest.
2. Divide the sum of the pulse durations by the time interval to obtain the pulse duty factor.

3.13 Average Pulse Duration

3.13.1 Definition

The average, over the time interval of interest, of the durations of the individual pulses of a pulse train.

3.13.2 Method of Measurement

1. Decide on the time interval of interest.
2. Measure the pulse duration (*see* 3.11) of each pulse in this time interval.
3. Find the average pulse duration by dividing the sum of the individual pulse durations by the number of pulses in the time interval of interest.

3.14 Pulse Rise Time

3.14.1 Definition (51 IRE 20. S1)

The interval between the instants at which the instantaneous amplitude first reaches specified lower and upper limits, namely, 10 per cent and 90 per cent of the peak pulse amplitude unless otherwise stated.

3.14.2 Method of Measurement

1. Obtain a calibrated (time and amplitude) picture of the waveform including the pulse. Delineate the pulse by excluding those portions of the waveform determined to be nonpertinent.
2. Draw the zero axis of the pulse.
3. Find the peak pulse amplitude. (*See* 3.7)
4. Draw two lines parallel to the zero axis and spaced on each side of the zero axis by 90 per cent (or stated fraction) of the peak pulse amplitude, and two parallel lines spaced on each side of the zero axis by 10 per cent (or stated fraction) of the peak pulse amplitude. The time interval between the first point of intersection of the pulse trace and either 10 per cent line and the first point of intersection of the pulse trace and either 90 per cent line is the Pulse Rise Time.

3.14.3 Pictorial Examples

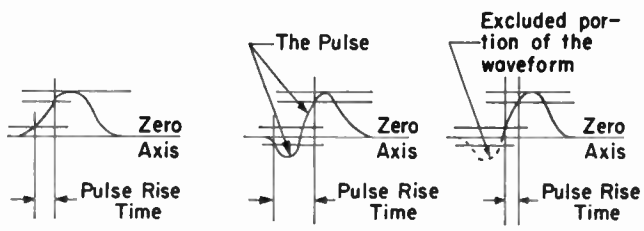

3.15 RMS Pulse Amplitude

3.15.1 Definition (51 IRE 20. S1)

The square root of the average, over the pulse duration, of the square of the instantaneous amplitude.

3.15.2 Method of Measurement

1. Obtain a calibrated (time and amplitude) picture of the waveform including the pulse. Delineate the pulse by excluding those portions of the waveform determined to be nonpertinent.
2. Draw the zero axis of the pulse and mark the end points of the pulse duration on the picture. (*See* 3.11)
3. Plot the square of the instantaneous amplitude between the end points and measure the enclosed area.
4. Divide the area by the pulse duration to obtain the mean-square amplitude.
5. Take the square root to obtain the RMS Pulse Amplitude.

3.15.3 Pictorial Examples

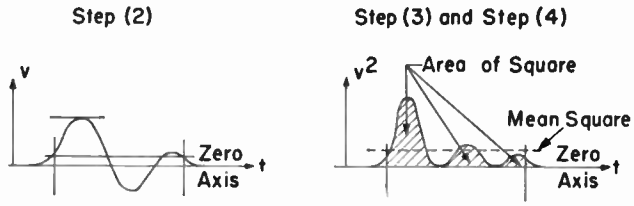

3.16 Average Pulse Repetition Rate

3.16.1 Definition

The number of pulses in the time interval of interest divided by that time interval.

Note 1: The time interval of interest must be clearly understood or stated, since it affects the results of measurement in many cases.
Note 2: If the Average Pulse Repetition Rate desired is that of a subgroup within a complex train (for example, vertical sync. pulses in a TV signal, channel pulses in a time-division multiplex system (etc.) the particular subgroup must be specified.

3.16.2 Method of Measurement

1. Decide upon the time interval of interest.

Note: A picture of the pulses may be needed in order to decide upon this time interval.

2. Determine the number of pulses in the time interval.

Note: There are instruments that may be used to count the number of pulses automatically, such as a gated counter. It may also be possible to determine the number of pulses by comparison with an oscillator generating a known number of cycles or pulses during the time interval.

3. Divide the number of pulses by the time interval to obtain the Average Pulse Repetition Rate.

3.17 Pulse Spacing (Pulse Interval)

3.17.1 Definition

The interval between the corresponding pulse times of two pulses.

Note 1: The two pulses should be clearly specified, whether consecutive or not. The particular pulse time used should be stated.
Note 2: The term "pulse interval" is deprecated because it may be taken to mean the duration of the pulse. Neither term means the space between pulses (Pulse Separation).

3.17.2 Method of Measurement

1. Measure the pulse times of the pulses.
2. The difference in time of the corresponding pulse times is the Pulse Spacing.

3.17.3 Pictorial Examples

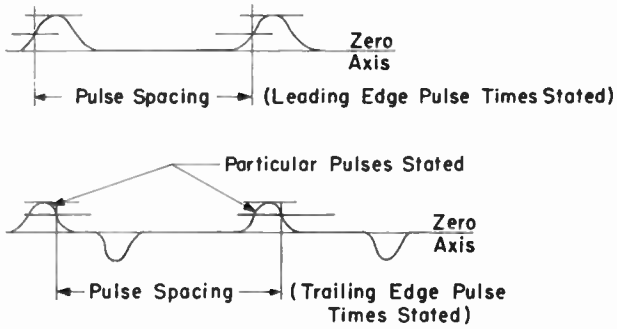

The Cascade Backward-Wave Amplifier: A High-Gain Voltage-Tuned Filter for Microwaves*

M. R. CURRIE†, ASSOCIATE, IRE, AND J. R. WHINNERY‡, FELLOW, IRE

Summary—**The characteristics of a backward-wave circuit as a beam modulator and as a beam demodulator are investigated theoretically and experimentally. A basic modulator-demodulator configuration, consisting of two periodic circuits (e.g., helices) separated by an arbitrary transducer section, constitutes the basis for a new class of backward-wave tubes. These "cascade backward-wave amplifiers" behave as narrow-band amplifiers whose pass bands can be tuned electronically over a wide range of frequencies. They overcome most of the inherent disadvantages of the simple single-circuit backward-wave amplifier and feature high gain well removed from the oscillation region, high off-signal rejection, internal circuit terminations which smooth out variations in operating characteristics with frequency, and provision for adjusting bandwidth electronically. The characteristics of an experimental model at *S*-band are presented and compared with theory. Analysis indicates that a minimum noise figure in the same range as that of a conventional traveling-wave tube, i.e., about 6 db, should be attainable.**

Introduction

THE PRACTICAL importance of the backward-wave oscillator has imparted considerable impetus to the detailed study of its characteristics. Calculations of start-oscillation conditions, measurements of efficiency and work on various types of periodic circuits for operation over frequency ranges embracing the whole microwave spectrum have progressed since the recent announcement of this novel device.[1] However, some important aspects of backward-wave interaction have received little or no attention, e.g., the use of a backward-wave tube as a narrow-band electronically tunable amplifier. Its characteristics complement those of the conventional traveling-wave tube and are of potential importance in certain types of microwave systems. From a more fundamental point of view no effort has been directed towards a broad examination of the interaction mechanism when boundary conditions other than those presented by the simple oscillator configuration are imposed.

This paper presents the characteristics of a backward-wave circuit when considered as a beam modulator or as a beam demodulator. A new class of backward-wave tubes based on a simple modulator-demodulator configuration is evolved from these basic considerations. These tubes, termed cascade backward-wave amplifiers, can be regarded roughly as extensions of the klystron concept to nonresonant circuits. The study shows that they overcome some inherent practical limitations of the conventional or single-section backward-wave amplifier.

Following a qualitative description of the basic model and its potential advantages, some typical performance curves obtained with an experimental tube are presented and compared with theory. The analysis of the modulator-demodulator model is presented in the final section of the paper. Both the theoretical and experimental studies indicate that the cascade backward-wave amplifier possesses considerable flexibility as a voltage-tuned filter or as a swept amplifier.

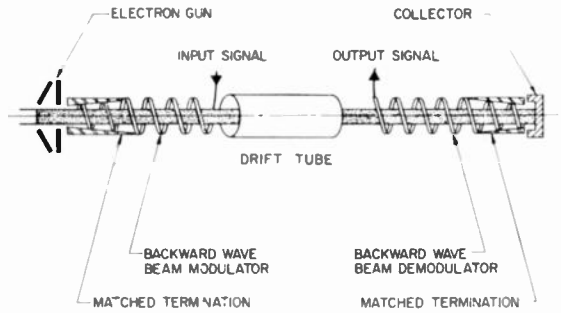

Fig. 1—The basic model of a cascade backward-wave amplifier. The first helix modulates the electron beam; the second helix acts as a beam demodulator. The extreme ends of the tube are matched internally. Other backward-wave structures than helices could be employed. The drift tube is not an essential part of the model but can be used as a gain equalizer. Note the analogy between this configuration and that of a klystron amplifier.

The Basic Model and Its Potential Usefulness

The model of primary concern to this discussion is pictured in Fig. 1. An electron beam is first modulated by a section of helix or other slow-wave structure interacting with a backward wave. The input signal is introduced at the collector end of the first helix and is amplified as it travels toward the gun end of the tube. There the amplified signal is assumed to be dissipated in a matched helix termination which could be located in an external transmission line or on the circuit itself. In the general model, the modulated electron stream then passes through a drift tube (although this is not essential to the operation), and then into a second helix

* Original manuscript received by the IRE, April 29, 1955; revised manuscript received, June 15, 1955. Most of this research was carried out at the Electronics Research Laboratory, University of California, and was submitted by M. R. Currie as part of a doctoral dissertation. The work was sponsored by the U. S. Air Force under Contract AF33(616)-495. The noise analysis was carried out at the Electron Tube Laboratory, Hughes Aircraft Company.

† Res. and Dev. Labs., Hughes Aircraft Co., Culver City, Calif.
‡ Electronics Res. Lab., University of California, Berkeley, Calif.

[1] Backward-Wave Oscillators were first announced by R. Kompfner and B. Epzstein in papers presented at the Tenth Annual Conference on Electron Tube Research, Ottawa, Canada; June, 1952.

or other slow-wave circuit also interacting with a backward wave. The output signal is thus taken from the gun end of the second helix, with the collector end of this circuit matched. In the succeeding discussion the first helix will be referred to as the beam modulator; the second helix will be referred to as the beam demodulator, since it extracts energy from the beam, although it may leave the beam more bunched and spread out in velocity than before entering the helix.

As explained in the basic references on backward-wave interaction,[2,3] such a wave has group velocity and phase velocity in opposite directions. Thus, when the phase velocity is in the direction of the beam and in approximate synchronism with the beam so that energy interchange takes place much as in a conventional traveling-wave tube, energy flows and increases "backward" toward the gun end. There is also an inherent regeneration from the energy flow loops established by the oppositely directed movements of energy in the circuit and the beam. Thus, regenerative amplification is available below a certain critical or "start-oscillation" current, and oscillation above that current. Either the oscillation or the regenerative amplification is voltage tunable over a wide range because of the inherent dispersive character of the backward waves which may be supported by any geometrically periodic structure.[4]

The single-helix backward-wave amplifier, pictured in Fig. 2, has already been analyzed.[5] In this, the rf input is at the collector end and the rf output at the gun end, with operation below the start-oscillation current to yield the regenerative gain just described. A narrow-band amplifier of relatively high gain is thus obtainable with electrical tuning over a wide range. This characteristic is potentially very useful but there are certain disadvantages in the single-helix structure which restrict its practical usefulness. The most serious is that operation with reasonably high gain requires currents near the start-oscillation current, so that stable operation is difficult. Fig. 2, which gives the calculated gain of a single-helix backward-wave amplifier, shows that 20-db gain requires a current 90 per cent of the start-oscillation current; moreover, the slope of the curve is very steep in this region so that the gain is critically dependent on small changes in current. If the rf transitions to external circuitry are imperfect, the resulting internal reflections cause the value of starting current to fluctuate periodically about an ideally smooth curve as frequency changes, thus causing sharp gain fluctuations or possible excursions into the oscillation region as the amplifier is swept over a range of frequencies.

As will be shown by the calculated and measured curves of this paper, the two-circuit version of the backward-wave amplifier as sketched in Fig. 1 gives relatively high gain with operating currents only 50 to 70 per cent of start-oscillation current. The slope of the gain-versus-current curve is also much smaller for a given gain, so that stabler operation is possible over the band. Another important advantage of the cascade amplifier lies in the freedom to terminate one end of each circuit in an internal reflectionless match. With tapered terminations placed on the circuit, the operating characteristics can be made to vary smoothly with frequency, and design for almost constant gain over a large frequency range is possible.

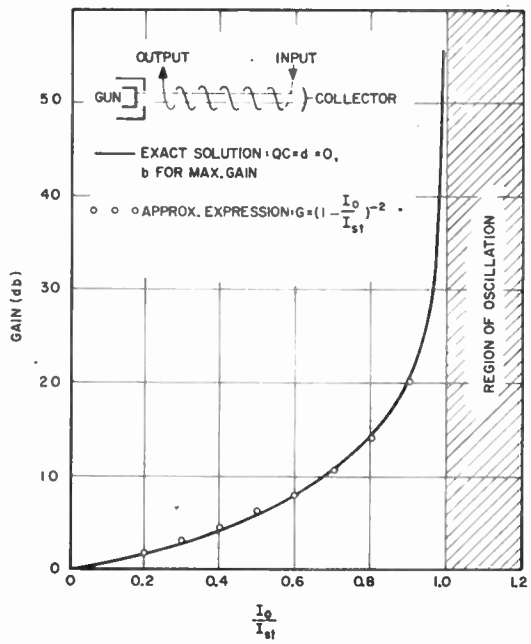

Fig. 2—Theoretical curve of gain vs current for a single-circuit backward-wave amplifier. The operating current I_0 is normalized with respect to the start-oscillation current I_{st}. The curve is for $QC=0$, $d=0$ and optimum b. It is fitted closely by the simple relationship shown.

A third advantage comes from the break between input and output circuits. Only a narrow band of frequencies whose corresponding backward-wave phase velocities are in approximate synchronism with the beam velocity can be coupled onto the output circuit; other signals are simply dissipated in the lossy termination on the input circuit. The off-signal rejection of the cascade amplifier is therefore very high, whereas the single-circuit backward-wave amplifier provides a direct feed-through path which must be broken artificially if adequate cold loss is to be introduced.

It is often desirable in filter applications to be able to adjust bandwidth. The cascade-circuit structure can, in a rough sense, be considered as two high-Q circuits coupled in series from input to output. Thus, the possibility of altering bandwidth by stagger tuning the sections exists. This can be done by operating them at slightly different potentials. The result is a filter whose center frequency and bandwidth both can be varied electronically.

[2] R. Kompfner and N. T. Williams, "Backward-wave tubes," Proc. IRE, vol. 41, pp. 1602–1611; November, 1953.
[3] H. Heffner, "Analysis of the backward-wave traveling-wave tube," Stanford E.R.L. Rep. No. 48; June 18, 1952.
[4] L. Brillouin, "Wave Propagation on Periodic Structures," McGraw-Hill Book Company, Inc., ch. V; 1948.
[5] H. Heffner, "Analysis of the backward-wave traveling-wave tube," Proc. IRE, vol. 42, pp. 930–937; June, 1954.

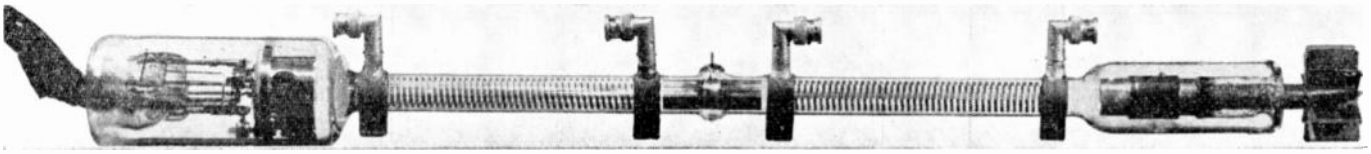

Fig. 3—Photograph of an experimental cascade backward-wave amplifier. This tube operates in the range 2–4 kmc, and employs a hollow electron beam. External connections were made to the gun end of the input helix and to the collector end of the output helix to lend added flexibility to the experiment.

Before leaving the general description, it is interesting to note the resemblance between the cascade backward-wave amplifier of Fig. 1 and a conventional two-cavity klystron. The first helix modulates the stream; there is a drift action in the drift tube (and in portions of the helices); and the second helix removes rf power from the beam. As will be noted in the later analysis, the tube actually has a very good figure of merit if compared with a klystron at a fixed frequency, but the distinct difference comes from the voltage tunability inherent in the backward-wave structure.

The model not only has application as a practical device, but also has fundamental interest in studying modulation of a beam and energy extraction from a beam by backward-wave interaction, or in the interaction of a backward wave on one helix with a forward wave on the other. Another model analyzed and recently built utilizes a third (floating) helix in place of the drift tube between the modulator and demodulator. Still other "space-charge wave transducers" could be used.

Performance Curves of the Amplifier

In this section it is desired to show certain calculated and measured performance curves for the cascade backward-wave amplifier following the model of Fig. 1. The calculated curves are from formulas derived in the final section of the paper. The measured curves were taken on a tube pictured in Fig. 3. This tube was designed for S-band, utilized a hollow-beam gun, tape helices for the backward-wave interaction structure, and a drift space between the helices as in the model of Fig. 1. Input and output helices are each $5\frac{1}{2}$ inches long, 0.545-inch inside diameter, and 0.125-inch pitch. The drift tube is $2\frac{1}{2}$ inches long (nominally $\frac{1}{8}$ plasma wavelength at the center of the 2–4 kmc band). All four ends of the helices were brought out to type BNC angle connectors to give added flexibility to the experiment. The hollow beam, used to secure strong interaction with the backward-wave (-1) component of the h_{10} helix mode,[6] has a radial thickness of 0.030 inch and is separated from the helix by approximately 0.025 inch. The measured cold isolation between the two helix sections was greater than 50 db.

The measured tuning curve of the experimental amplifier, Fig. 4, shows a tuning range from 2,000 to 4,000 mc with voltage variation from 270 to 4,000 volts.

[6] S. Sensiper, "Electromagnetic Wave Propagation on Helical Conductors," Sc.D. Dissertation, Mass. Inst. Tech., ch. II; 1951.

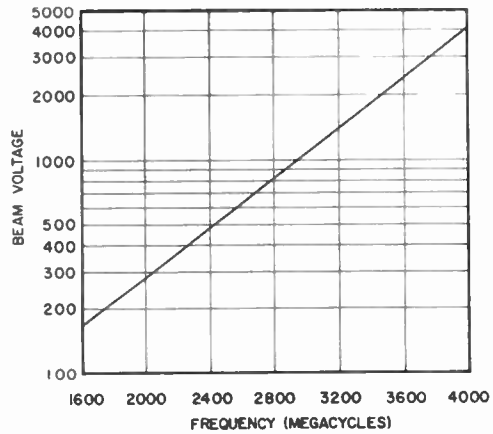

Fig. 4—Tuning curve showing the beam voltage at maximum gain vs frequency for the experimental tube described in this paper.

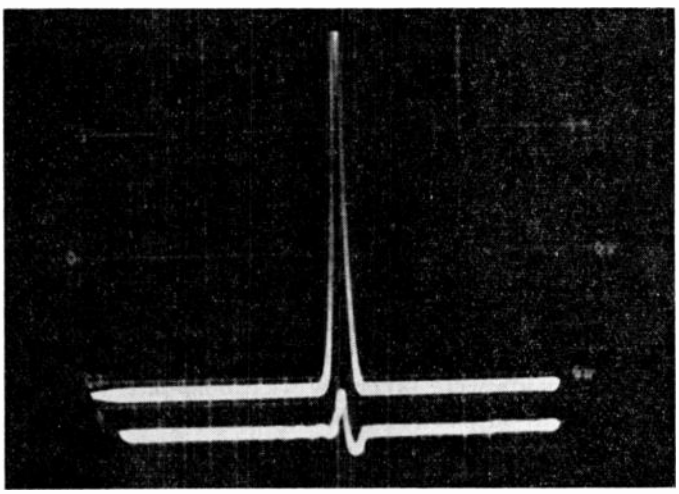

Fig. 5—Oscilloscope traces of output power as the cascade backward-wave amplifier is swept in voltage. The signal input is at 2,950 mc. The small gain spike was taken from the first helix and so represents the output of a single-circuit backward-wave amplifier. The large spike was taken from the second helix and demonstrates the increased gain produced by the composite tube. The same detection system was used to record each trace. The beam current was about $\frac{1}{4}$ the start-oscillation value. The basewidth of the large spike is about 60 mc.

Either frequency or voltage variation could be changed to some extent by modification of the helix design. Fig. 5 shows an oscilloscope comparison of the gain from the two-helix tube with that from one of the helices operating as a single-helix backward-wave amplifier at the same ratio of operating to starting current. The two traces were recorded successively with the same detection system and represent power output versus beam voltage as the tube was swept over a frequency

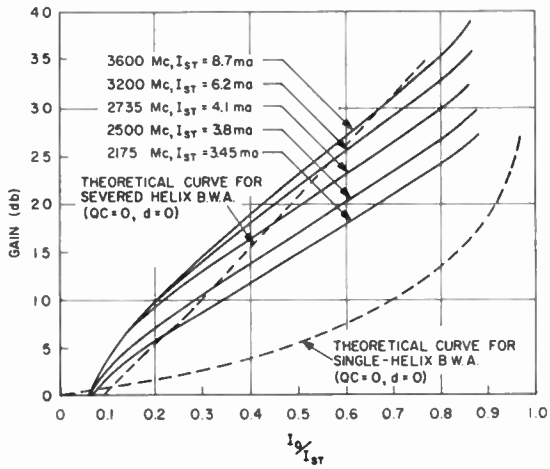

Fig. 6—Experimental curves of gain vs normalized current at several different frequencies. Theoretical curves for the single-helix backward-wave amplifier and for the idealized severed-helix amplifier (no drift tube) are shown for comparison. The frequency dependence of the experimental curves is caused by the drift tube.

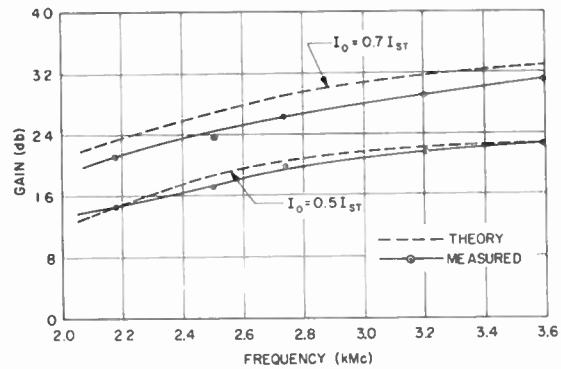

Fig. 7—Comparison of measured and theoretical gain as a function of frequency for the experimental cascade backward-wave amplifier. The curves are shown for two different ratios of operating current to the start-oscillation current. The calculated curves include the effects of the drift tube.

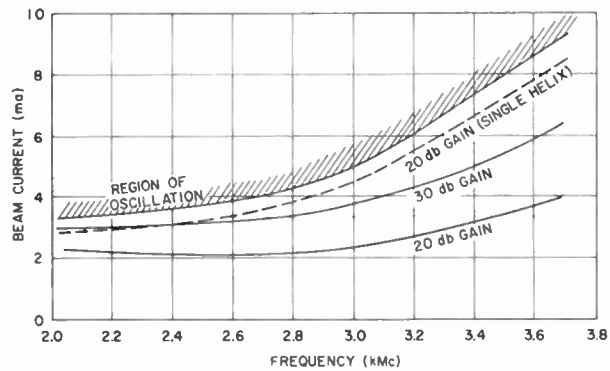

Fig. 8—Curves showing the current necessary to maintain constant gain as the experimental cascade amplifier was tuned in frequency. The actual curves were not smooth because of internal reflections due to poor matching.

range centered on 3,000 mc. The small gain spike was taken from the gun end of the signal launcher, and so represents the gain of the single-helix backward-wave amplifier. The base line of this trace represents the average power of the signal generator. The dip to the right of the gain spike is a region of negative gain in which the interaction has become degenerative. Other maxima and minima of the interference pattern decrease in amplitude as one departs farther from synchronism with the circuit wave. The large response curve was taken from the gun end of the second helix and shows the large and very clean response of the two-helix tube. Since no direct feed-through path exists from input to output, the reference line on this trace represents essentially zero power.

Fig. 6 shows measured values of gain vs current for the experimental tube, taken at several frequencies. Measurements were taken cw with bolometers located both at the output of the composite tube and at the output of the first helix. Tuning stubs were employed but were not adjusted during measurements at a particular frequency. Considerably greater apparent gain could be obtained by deliberate mismatching so as to reinforce the output signal by internal reflections. One of the theoretical curves shown for comparison is that for a single-helix amplifier, showing the much smaller gain for a given current. The other is the calculated curve for a two-helix tube with no drift space between helices (denoted severed-helix tube). Much of the variation with frequency is thus seen to come from the drift space, and in later calculations it is shown that the effect of the drift tube is to subtract increasingly from the over-all gain as the frequency is lowered. Note that for a single-helix amplifier, gain would be expected to increase with decreasing frequency because of increased space-charge at the low voltages, and this effect was observed in the output of the first section alone.

Fig. 7 shows gain vs frequency for two values of normalized current. Here the theoretical curves do take into account the effect of the drift region. Very close agreement between calculated and measured curves is shown, but as the calculations neglect the finite circuit loss and space-charge effects, this should not be taken too literally. There is a variation of gain with frequency for a given current setting, but this could be compensated for if required by a straightforward AGC circuit. Fig. 8 shows the required variation in current as a function of frequency for constant gains of 20 db and 30 db. The actual curve was not as smooth as shown because of poor matching at the extreme ends of the experimental tube. However, it serves to illustrate the role of the drift tube as a gain equalizer and the flexibility this element lends to the over-all design. A more recent tube has yielded an insertion gain flat within several db over a 50-per cent frequency range at S-band.

The frequency bandwidth was measured at several different frequencies and gains; the measured results were in fair agreement with those calculated from (33) and Fig. 14. For example, at 3,000 mc and 30-db gain, the bandwidth was about 9 mc corresponding to a Q of 330. The predicted Q was 360. The gain-bandwidth product was a strongly increasing function of gain. A

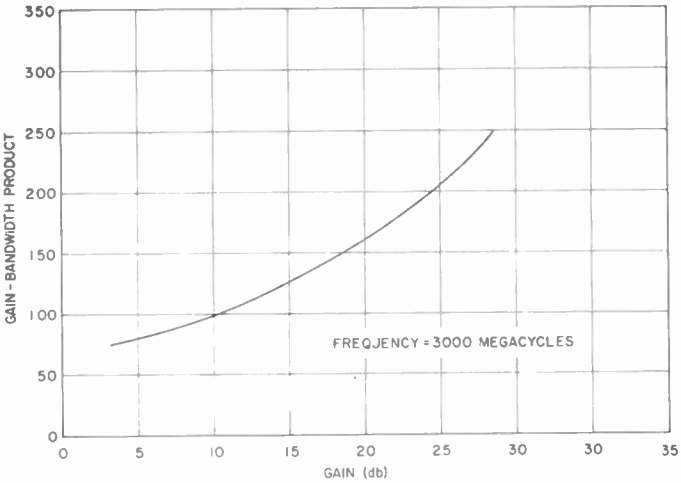

Fig. 9—Experimental curve of the voltage-gain times bandwidth (megacycles) product vs gain (db) at 3,000 mc. The gain-bandwidth product increases rapidly with gain level in the cascade amplifier.

typical curve is shown in Fig. 9. The gain-bandwidth product of a single-circuit backward-wave amplifier is much less dependent on gain and is almost constant. Thus, the bandwidth is largely fixed by the parameters of the input circuit; the increased gain-bandwidth product for the cascade configuration is due to its greatly increased gain at a given value of beam current.

The possibility of varying the bandwidth of the cascade amplifier by stagger tuning the input and output circuits (i.e., operating them at slightly different potentials so that synchronism between the circuit wave and the beam velocity occurs at slightly different frequencies in each section) is illustrated in Fig. 10. There, the input frequency was swept from 2.0 to 3.0 kilomegacycles with a backward-wave oscillator. The traces display output power vs frequency. With the modulator and demodulator circuits synchronized, the bandwidth at 2.7 kilomegacycles and 19-db gain was 10 megacycles. With a 30-volt potential difference between helices the gain dropped to about 11 db, and the bandwidth increased to 35 megacycles. The response resembles that of two tuned circuits which are stagger tuned. For smaller voltage differences it is possible to increase the gain-bandwidth product somewhat by this method. It appears that this feature could be very useful in applications where gain is only of secondary importance.

The noise figure was measured at one point and was about 24 db. This is in the same range as that of a typical forward-wave traveling-wave amplifier tube when no special effort is made to reduce the noise on the electron stream (e.g., by means of velocity jumps[7]); it is also in fair agreement with the calculated noise figure assuming space-charge limited flow from the cathode to the first helix and taking into account only the effects due to velocity fluctuations at the potential minimum.

[7] D. A. Watkins, "Traveling-wave tube noise figure," Proc. IRE, vol. 40, pp. 65–70; January, 1952.

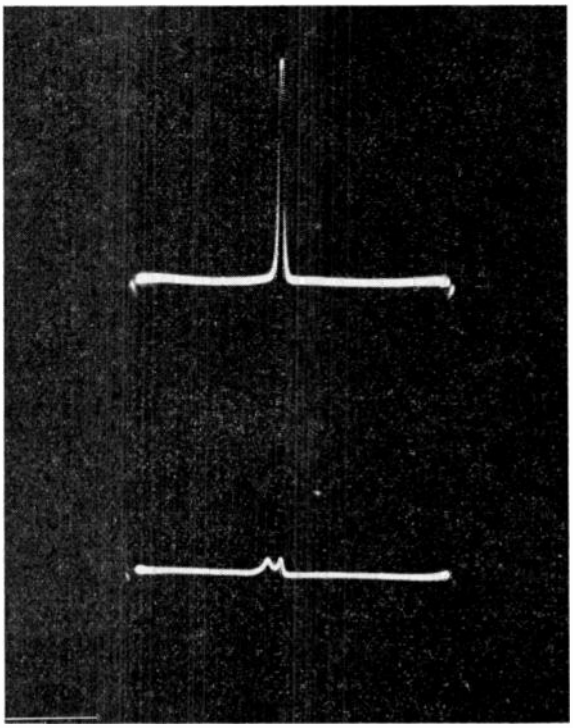

Fig. 10—Oscilloscope traces showing the effect of stagger tuning on bandwidth. The cascade amplifier was operated at fixed voltage and the input frequency was swept from 2 to 3 kmc by means of a backward-wave oscillator. The large response represents 19-db gain and 10 mc bandwidth and was taken with the input and output helices synchronized. The smaller response was for 30 volts between helices; it shows a gain of 11 db and a bandwidth of 38 mc and displays the double-humped shape characteristic of tuned circuits. The basewidths are approximately 48 and 142 mc, respectively.

This result lends confidence to the analysis to be presented and indicates that the noise figure can be reduced considerably with a suitable electron gun.

Other experiments were conducted with the two-helix tube, one of which will be mentioned briefly here. The first helix was made shorter than the other by means of resistive termination on the tube's envelope. Thus, it was possible to operate at a current which was below the oscillation region for the first helix but above start-oscillation for the other. The helices were held at different dc potentials. Under these conditions the first helix modulated the beam at the frequency of the input signal. The second operated as a backward-wave oscillator at a slightly different frequency. Electronic mixing of the two frequencies took place on the beam and it was possible to pick up a sharp signal at the difference frequency. The beat frequency could be varied over a large range by changing the potential difference between helices.

Analysis

Analysis of the General Model for Backward-Wave Interaction

Basic model to be analyzed is that of Fig. 11 (page 1622), in which beam is allowed to possess an arbitrary initial current and velocity modulation as it enters backward-wave circuit at $z=0$. The transmission-line ap-

proach is used, following Pierce's work.[8] The equations of motion and continuity are linearized (small signals) and motion only in the z-direction is allowed. Time dependence for rf quantities is assumed as $\exp(j\omega t)$. The resultant ballistic relation between rf convection current $i(z)$ and longitudinal field on the slow-wave circuit $E(z)$ is

$$\frac{d^2i(z)}{dz^2} + 2j\beta_e\frac{di(z)}{dz} + (\beta_q^2 - \beta_e^2)i(z) = \frac{-2j\beta_e C^3}{K}E(z). \quad (1)$$

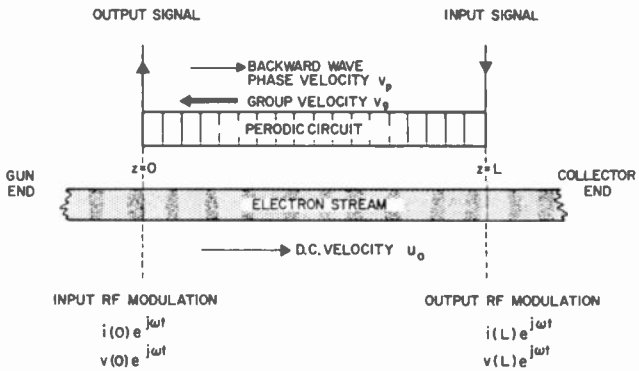

Fig. 11—The basic model for analysis. Beam is injected into the backward-wave circuit at $z=0$ with total velocity $u_0+v(0)e^{j\omega t}$ and total current $-I_0+i(0)e^{j\omega t}$. $v(0)$ and $i(0)$ are arbitrary both in magnitude and phase. The input signal is introduced at $z=L$.

Similarly, the modified telegrapher's equation, giving coupling between the circuit and stream, is

$$\frac{d^2E(z)}{dz^2} - \Gamma_0^2E(z) = -\Gamma_0 K\frac{d^2i(z)}{dz^2}. \quad (2)$$

In the absence of the electron beam the circuit wave propagates as $\exp(j\omega t - \Gamma_0 z)$; β_q is the effective plasma frequency wave number and β_e the electron stream wave number, K is the impedance presented by the circuit to the beam, and C is the gain parameter, both as defined by Pierce.[9]

A self-consistent solution of the composite beam-circuit model involves the simultaneous solution of the above equations. $E(z)$ and $i(z)$ are then solutions of fourth-order linear differential equations. The associated constants in the solutions must be fixed by four independent boundary conditions. The current and velocity modulation can be independently specified at $z=0$ and the applied circuit field at $z=L$ is known. The remaining constraint can be taken as a matched circuit termination at one end.

The solutions can be expanded in terms of exponentials (i.e., four waves) or as power series in z. The former method has been used extensively by Pierce.[10] The power series method was originally presented by Kompfner[11] and has been recently extended by Quate[12] to include the effects of space charge and circuit loss; it is convenient in numerical solutions where the effective circuit length is small ($CN<0.4$). Although both solutions were used in this work, only the results of the wave-type solution will be presented in this section. The reformulation of the solutions in terms of power series is summarized in Appendix A.

Employing the exponential method of solution, $E(z)$ and $i(z)$ are each expanded as the sum of four waves. Γ_n is defined as the propagation constant of the nth wave and is the solution of the characteristic equation obtained from (1) and (2). Since the phase velocities of the perturbed waves are close to the dc beam velocity the propagation constants for backward waves can be written

$$\Gamma_n = j\beta_e(1 + jC\delta_n) \quad (3)$$

$$\Gamma_0 = -j\beta_e(1 + Cb + jCd), \quad (4)$$

where b is the velocity parameter and d is the loss parameter, as defined by Pierce.[13] In terms of the incremental propagation constant δ_n, the determinantal equation is the cubic

$$(\delta_n^2 + 4QC)(\delta_n + jb - d) = +j. \quad (5)$$

Here, terms of order C have been neglected compared with unity. Assuming that the circuit is matched at one end, the boundary conditions take the form

$$\sum_{n=1}^{3} E_n e^{-\Gamma_n L} = E(L)$$

$$\sum_{n=1}^{3} \frac{(\Gamma_n^2 - \Gamma_0^2)}{-\Gamma_0\Gamma_n^2 K}E_n = i(0)$$

$$\sum_{n=1}^{3} \frac{(\Gamma_n - j\beta_e)(\Gamma_n^2 - \Gamma_0^2)}{j\beta_e\Gamma_0\Gamma_n^2 K} = \rho_0 v(0). \quad (6)$$

The dc linear charge density is ρ_0.

After considerable manipulation and employing the following relations, derived from (5),

$$\delta_1 + \delta_2 + \delta_3 = -jb + d,$$

$$(\delta_1 + \delta_2)(\delta_2 + \delta_3)(\delta_3 + \delta_1) = -j, \quad (7)$$

the complete solutions for the "output" quantities can be written

$$E(0) = \frac{\kappa}{\Delta}E(L) - \frac{2V_0\beta_e C^2}{I_0}\frac{\Phi}{\Delta}i(0) + j\frac{u_0\beta_e C}{\eta}\frac{\chi}{\Delta}v(0) \quad (8)$$

$$i(L) = j\frac{I_0}{2V_0\beta_e C^2}\frac{\chi}{\Delta}E(L) - \frac{\Lambda}{\Delta}i(0) - j\frac{I_0}{u_0 C}\frac{\Psi}{\Delta}v(0) \quad (9)$$

$$v(L) = -\frac{\eta}{u_0\beta_e C}\frac{\Phi}{\Delta}E(L) + j\frac{u_0 C}{I_0}\frac{\Omega}{\Delta}i(0) - \frac{\Lambda}{\Delta}v(0). \quad (10)$$

[8] J. R. Pierce, "Traveling-Wave Tubes," D. Van Nostrand Co., New York; 1950.
[9] J. R. Pierce, *loc. cit.*, p. 17.
[10] J. R. Pierce, *loc. cit.*, ch. VII.
[11] R. Kompfner, "Traveling-wave tubes—centimetre-wave amplifier," *Wireless Eng.*, vol. 24, pp. 255–267; September, 1947.
[12] C. F. Quate, "Power Series Solution of Traveling-Wave Tube Equations," Bell Tel. Lab. Tech. Memo 53-1 500-36; October, 1953.
[13] J. R. Pierce, *loc. cit.*, ch. VIII.

The coefficients are functions of the dc conditions of the beam, velocity b, circuit loss d, space-charge QC and circuit length. The following functions are defined

$$\kappa = (\delta_1 - \delta_2)(\delta_2 - \delta_3)(\delta_3 - \delta_1)$$

$$\chi = \sum_{i=1}^{3} (\delta_j - \delta_k)e^{2\pi CN\delta_i}$$

$$\Phi = \sum_{i=1}^{3} \delta_i(\delta_j - \delta_k)e^{2\pi CN\delta_i}$$

$$\Delta = \sum_{i=1}^{3} (\delta_i^2 + 4QC)(\delta_j - \delta_k)e^{2\pi CN\delta_i}$$

$$\Psi = e^{-j2\pi N} \sum_{i=1}^{3} (\delta_j^2 - \delta_k^2)e^{2\pi CN(\delta_j+\delta_k)}$$

$$\Lambda = e^{-j2\pi N} \sum_{i=1}^{3} \delta_i(\delta_j^2 - \delta_k^2)e^{2\pi CN(\delta_j+\delta_k)}$$

$$\Omega = e^{-j2\pi N} \sum_{i=1}^{3} \delta_i^2(\delta_j^2 - \delta_k^2)e^{2\pi CN(\delta_j+\delta_k)},$$

where i, j, k are taken as cyclic permutations of 1, 2, 3. N is the number of electronic wavelengths in circuit length L.

The linear relationships (8–10) express the output quantities in terms of the velocity, current and field which are impressed on the system. The coefficients constitute a general matrix for application in the succeeding calculations.

Simple Backward-Wave Amplifier

In this situation a smooth beam is injected from an electron gun directly into the interaction space; that is, no rf current or velocity modulation exists on the beam at the gun end of the circuit. As a result of the interaction process the circuit field builds up from its initial impressed value at $z=L$ to a maximum value at $z=0$ while the modulation induced on the beam increases in magnitude in the direction of electron flow. Analysis of this model applies to a single-helix amplifier or oscillator as well as to a beam modulator.

The power associated with the circuit is (for $C \ll 1$)

$$P(z) = \frac{1}{2\beta_e^2 K} E(z)E(z)^*. \tag{11}$$

From (8) an expression for the power gain of the above model can be written.

$$G = \frac{P(0)}{P(L)} = \left| \frac{\kappa}{\Delta} \right|^2. \tag{12}$$

For a fixed amount of space charge QC and circuit loss d it is possible to adjust the beam velocity b and the electrical length of the circuit CN so that the denominator in the above expression vanishes. This condition of infinite small-signal gain is unstable and is taken as the point at which oscillations start. Start-oscillation conditions have been computed for a wide range of operating parameters by others.[14–16]

The gain was plotted in Fig. 2 for values of beam current (I_0) below that at start-oscillation. Zero space charge and circuit loss were assumed for this representative curve and the gain has been optimized with respect to the velocity parameter b. The curve is fitted closely by the empirical relationship.

$$G = \left(1 - \frac{I_0}{I_{st}}\right)^{-2}. \tag{13}$$

It is seen that the backward-wave amplifier is capable of yielding very high values of gain. Because of the regenerative action, the tube characteristically possesses a very sharp frequency response, observed values of quality factor Q in the thousands having been reported.[17] The limitations on this amplifier have been discussed in an earlier section of the paper.

Backward-Wave Beam Modulator

Consider now the backward-wave circuit as a device for modulating a beam. From (9) and (10) the rf current and velocity modulation which are induced on the beam as a result of the interaction process are related to the input field by

$$i(z) = j\frac{I_0}{2V_0\beta_e C^2} \frac{\chi(z/L\,CN)}{\Delta(CN)} E_{in} \tag{14}$$

$$v(z) = \frac{-\eta}{u_0\beta_e C} \frac{\Phi(z/L\,CN)}{\Delta(CN)} E_{in}. \tag{15}$$

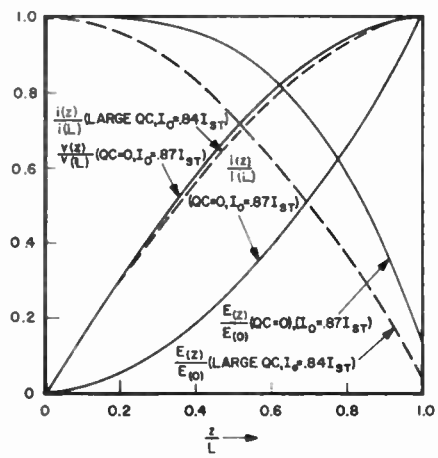

Fig. 12—Curves showing the build-up of current modulation and circuit field as a function of distance in a backward-wave modulator. The solid curves were calculated for $QC=0$, $d=0$. The dashed curves are approximate for large QC.

The relative values of rf current and field are shown as a function of distance in Fig. 12 (above) for the special

[14] H. Heffner, *loc. cit.*

[15] H. R. Johnson, "Backward-Wave Oscillators," Hughes Aircraft Company Tech. Memo. No. 361; May, 1954.

[16] W. A. Harman, "Backward-Wave Interaction in Helix-Type Tubes," Stanford E.R.L. Report No. 13; April, 1954.

[17] H. Heffner, "Backward-Wave Tubes," *Electronics*, vol. 26, pp. 135–137; Oct., 1953.

case of zero space charge and circuit loss. The curves are for a current of about 87 per cent of the starting value ($CN=0.30$) and for a value of b which optimizes the gain of the device as an amplifier.

As the circuit length is decreased and the current increased (in order to stay at a given value of CN) the inter-electronic Coulomb forces become more pronounced and some sort of limiting behavior might be expected. For large values of QC and zero circuit loss the incremental propagation constants assume particularly simple forms. The results show physically that only two waves need be considered. The interaction process can be described in terms of coupling between the circuit wave and the slow space-charge wave only. Limiting expressions for large values of QC (greater than about 0.25) are

$$E(z) \cong E(0) \cos\left[\frac{\pi}{2}\frac{CN}{\overline{CN}}\frac{z}{L}\right] \tag{16}$$

$$|i(z)| \cong \frac{C}{\beta_e K}\frac{1}{\sqrt{2b}}\frac{\sin\left[\frac{\pi}{2}\frac{CN}{\overline{CN}}\frac{z}{L}\right]}{\cos\left[\frac{\pi}{2}\frac{CN}{\overline{CN}}\right]}|E(L)| \tag{17}$$

$$|v(z)| = \frac{2C^2}{\rho_0\beta_e K}\sqrt{\frac{b}{2}}\frac{\sin\left[\frac{\pi}{2}\frac{CN}{\overline{CN}}\frac{z}{L}\right]}{\cos\left[\frac{\pi}{2}\frac{CN}{\overline{CN}}\right]}|E(L)| \tag{18}$$

where $\overline{CN}$ is the value of CN at start-oscillation,[18]

$$\overline{CN} \cong \left(\frac{QC}{16}\right)^{1/4} \quad \text{and} \quad \frac{CN}{\overline{CN}} \cong \left(\frac{I_0}{I_{st}}\right)^{1/4}. \tag{19}$$

Eqs. (16) and (17) are shown in Fig. 12 for operation at about 84 per cent of starting current. The ratio of $E(z)$ at $z=0$ and $z=L$ is just the voltage gain of the model when regarded as an amplifier. The curves indicate that the effect of space charge is to increase gain somewhat for a given (I_0/I_{st}). This effect is verified by more extensive calculations based on the exact relation (12).

The curves in Fig. 12 emphasize the fact that where the current modulation is weak the circuit field is strong, and vice versa; this is inherent in the nature of the interaction and differs markedly from the case of forward-wave interaction. These considerations suggest that backward-wave interaction is a relatively inefficient process. In particular, we are led to speculate on the possibility of securing a stronger reciprocal action between the beam and the circuit by somehow placing initial modulation on the beam so that interaction can commence with relatively large rf energy associated with both electrons and circuit. This is the situation to be discussed in the following section.

It is of interest to examine the nature of the modulation just as it leaves the interaction space. A descriptive parameter is the dimensionless ratio

$$\sigma(z) = \frac{Ci(z)}{\rho_0 v(z)} = \frac{j\chi(z/L\,CN)}{\Phi(z/L\,CN)}. \tag{20}$$

$\sigma(L)$ is shown in Fig. 13 (below) as a function of CN for $QC=0$, $d=0$ and optimum b. As effective length CN of interaction space increases the magnitude of $\sigma(L)$ also increases. The current modulation leads the velocity

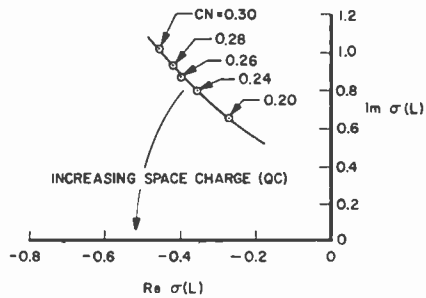

Fig. 13—The modulation on a beam at the output end ($z=L$) of a backward-wave modulator is described by the parameter $\sigma(L) = Ci(L)/\rho_0\sqrt{(L)}$. This parameter is shown on the σ-plane as a function of CN for $QC=0$, $d=0$. For this case the value of CN at start-oscillation is 0.314. The curve moves toward the (negative) real axis for increasing space charge (QC).

modulation (in the time sense) by an angle greater than 100 degrees, indicating that there is power carried by the stream. This is in contrast to a klystron in which the angle is 90 degrees and no rf power is carried by the stream. For the limiting case of large QC,

$$\sigma(L) \to -\frac{1}{b}, \tag{21}$$

where, in this case,

$$b \cong \sqrt{4QC}. \tag{22}$$

Therefore, increased current density causes the phase angle between current and velocity modulation at the end of the interaction space to increase and $|\sigma(L)|$ to decrease.

Backward-Wave Beam Demodulator

Referring to the model in Fig. 11, the case is now considered in which a beam is injected into the interaction space with both velocity and current modulation whose magnitudes and relative phases are arbitrary. The collector end of the circuit is assumed to be passively terminated in a matched load. Here we are primarily interested in the circuit field which is induced on the helix and, in particular, its value at the output terminals. From (8) and (20),

$$E(0) = -\frac{2V_0\beta_e C}{I_0}\frac{\rho_0 v_{in}}{\Delta}[\sigma_{in}\Phi + j\chi], \tag{23}$$

where v_{in} and σ_{in} describe the input modulation.

Since the induced field is strongly dependent upon the parameter σ_{in} and hence on the nature of the system employed in the original modulation of the beam, we

[18] W. A. Harman, *loc. cit.*, ch. III.

shall examine several specific cases which are conceptually susceptible to experiment. First compare the backward-wave circuit with the output cavity of a klystron amplifier. In a simple klystron the cavity is located at a point of maximum current modulation along the stream. The bunched beam then induces a current flow in the cavity walls and excites it to resonance. An equivalent shunt resistance of the cavity can then be defined[19] which relates the power delivered to the resonator to the fundamental convection current component in the stream,

$$R_{sh} = \frac{2P}{i^2}. \tag{24}$$

A figure of merit for the cavity is usually taken as the ratio

$$\frac{R_{sh}}{Q} \sim \text{gain} \times \text{bandwidth}.$$

An upper limit for this ratio is roughly 100 with $R_{sh} \sim 100{,}000$ and $Q \sim 1{,}000$. R_{sh} can be increased at the expense of bandwidth, and vice versa.

Now consider a situation in which the klystron cavity is replaced by a backward-wave structure. The two arrangements are similar in several important respects. Both devices are narrow-band; both absorb energy from a bunched beam. The systems are on one hand resonant and on the other hand strongly regenerative in nature. For contrast it is of interest to define an effective shunt resistance for the backward-wave circuit for the case of pure current modulation at its input and to compare the resulting figure with that obtainable from a klystron cavity. From (11) and (23) the following expression is obtained:

$$(R_{sh})_{\text{eff.}} = \left(\frac{V_0}{2I_0}\right)^{2/3} K^{1/3} \frac{\Phi\Phi^*}{\Delta\Delta^*}. \tag{25}$$

Substitution of some conservative parameters ($V_0 \sim 500$ volts, $I_0 \sim 3$ ma, $K \sim 5$ ohms, $I_0 = 0.7\ I_{st}$) into the above relation indicates that an effective shunt impedance of 10^5 ohms can easily be obtained in practice. It will be shown that the corresponding Q in this range of operation is typically of the order of 400. As in the case of a klystron $(R_{sh})_{\text{eff.}}$ can be increased at the expense of bandwidth. A length of backward-wave circuit therefore represents a conceptual improvement over a re-entrant-type resonator on the basis of their relative figures of merit. This is not surprising when the cumulative nature of the distributed interaction is considered; however, it does illustrate the effectiveness of a backward-wave demodulator in extracting energy from a bunched beam.

From these considerations it is seen that, in principle, an amplifier could be constructed which utilizes a re-entrant cavity to modulate a beam and a periodic circuit as the output structure. Indeed, such an amplifier is entirely feasible and would appear to possess some advantages. This concept is important to the point of view which is developed in this paper.

The denominator in the expression for the field at the output of the demodulator is exactly the same as that which appears in the gain expression for a simple backward-wave amplifier. This implies that, for identical circuits, the condition of instability (i.e., start-oscillation) occurs at the same point and is independent of externally applied fields.

The Severed-Helix Backward-Wave Amplifier

We shall now examine the behavior of a demodulator section when the input modulation has the same characteristic as that possessed by a beam at the output of a backward-wave modulator. The model to be analyzed is that of Fig. 1, discussed earlier, but with the drift distance approaching zero. The principal idealization is then that the two helices are completely isolated from one another and that no coupling between them exists in the absence of the electron beam.

The power output of the second helix is found to be

$$P_{\text{out}} = \frac{1}{(2K)^{1/3}} \left(\frac{V_0}{I_0}\right)^{4/3} |\rho_0(v_{\text{in}})_2|^2 \frac{|(\sigma_{\text{in}})_2\Phi_2 + j\chi_2|}{|\Delta_2|^2}, \tag{26}$$

where the added subscripts (2) denote quantities pertaining to the second helix and $(\sigma_{\text{in}})_2$ describes the beam modulation at its entrance. From (15) the velocity modulation at the output of the first helix is

$$|\rho_0(v_{\text{out}})_1|^2 = (2K)^{1/3} \left(\frac{I_0}{V_0}\right)^{4/3} \left|\frac{\Phi_1}{\Delta_1}\right| P_{\text{in}}, \tag{27}$$

and, in this case, with no separation between circuits and no velocity jump, the continuity of velocity and current is expressed by

$$(\sigma_{\text{out}})_1 = (\sigma_{\text{in}})_2, \quad (\rho_0 v_{\text{out}})_1 = (\rho_0 v_{\text{in}})_2. \tag{28}$$

The gain expression for the severed-circuit amplifier becomes

$$G = \left|\frac{\chi_1\Phi_2 + \chi_2\Phi_1}{\Delta_1\Delta_2}\right|^2. \tag{29}$$

The simplest case results when both helices are the same physical length (it has been assumed implicitly that they are identical in all other respects). This is also the case of greatest interest. Since the start-oscillation point is the same for each section, unequal lengths would mean that one section is operating closer to oscillation than the other. This is usually undesirable. For operation at a specified fraction of starting current, maximum gain will be obtained for equal circuit lengths and synchronous tuning. In this case the over-all gain is

$$G = \left|\frac{2\Phi\chi}{\Delta^2}\right|^2. \tag{30}$$

[19] K. R. Spangenberg, "Vacuum Tubes," McGraw-Hill Book Co., New York, p. 535; 1948.

For stagger-tuning or dissimilar input and output circuits, (29) can be used to compute gain. The gain expressions in terms of power series can be found from Appendix A.

Gain is shown as a function of the velocity parameter b in Fig. 14 for $QC=0$, $d=0$. The curves are plotted for various lengths (CN) of the circuits. For CN greater than about 0.24 ($I_0>0.5I_{st}$) the magnitude of b at maximum gain is fairly constant. Maximum gain therefore occurs at approximately constant percentage deviation of the beam velocity from that of the unforced circuit wave, regardless of the gain level. The curves also display a lack of symmetry around the point of maximum gain which has been experimentally observed.

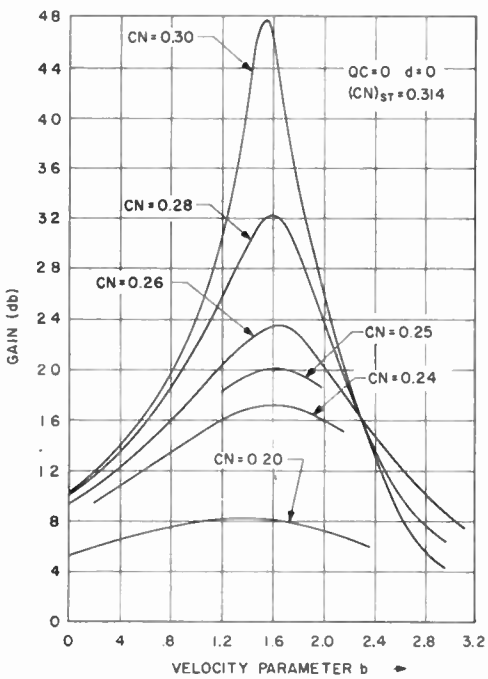

Fig. 14—Curves showing the gain of a severed-helix backward-wave amplifier (zero drift length between input and output circuits) as a function of the velocity parameter b. The input frequency is held constant. These curves are for $QC=0$, $d=0$; CN at start-oscillation is equal to 0.314. Identical input and output circuits are assumed.

Since there is a one-to-one correspondence between velocity and frequency, Fig. 14 illustrates the reciprocal relation between gain and bandwidth. From the definition of b,

$$\Delta b \cong \frac{1}{C}\frac{\Delta v_p}{v_p} \sim \frac{1}{C}\frac{\Delta f}{f}, \tag{31}$$

so that the velocity width Δb is proportional to the bandwidth. For a tape helix the phase velocity of the domiuant backward-wave harmonic is[20]

$$v_p \cong \frac{ka\sqrt{\mu\epsilon}\tan\psi}{D-ka},$$

where ψ is the pitch angle of the helix, ka is the ratio of circumference to free-space wavelength and D is the dielectric loading factor.[21] Therefore

$$\Delta b \cong \frac{D}{ka}\frac{\Delta(ka)}{(D-ka)}, \tag{32}$$

and the bandwidth becomes

$$\Delta f \cong Cf\left(1-\frac{ka}{D}\right)\Delta b, \tag{33}$$

where Δb is interpreted as the spread of the gain curves at the half-power points.

An equivalent Q of the amplifier can be defined

$$Q = \frac{f}{\Delta f} \cong \frac{1}{C\left(1-\frac{ka}{D}\right)\Delta b}. \tag{34}$$

For example, at $ka=0.5$, $I_0=0.7\ I_{st}$, $C=0.01$ and $D=1$, an equivalent Q of approximately 400 will be realized. A higher Q at a given gain level can be obtained by decreasing the beam-helix coupling and going to longer lengths of helix (at the same CN). Alternatively, operation at higher beam voltages, lower currents, and the use of more dispersive backward-wave circuits could be employed.

For the case of large space charge (QC), the circuit field at the output of the demodulator section can be written

$$E_{out} \sim \frac{\beta_e K}{2C^2}(\rho_0 v_{in})_2\sqrt{\frac{2}{b}}\tan\left[\frac{\pi}{2}\frac{CN}{\overline{CN}}\right]. \tag{35}$$

Using (18), the over-all gain then becomes approximately

$$G \cong \tan^4\left[\frac{\pi}{2}\left(\frac{I_0}{I_{st}}\right)^{1/4}\right]. \tag{36}$$

In Fig. 15 (opposite page), gain of severed-helix tube, optimized with respect to b, is shown as a function of current for limiting cases of large and small space charge (zero loss). The curves are universal. That is, starting current I_{st} can be separately calculated as a function of frequency in any specific case. The rapid rise of the curves from the region of negative gain indicates the strong interaction which occurs in the demodulator. A curve for $L_1=\frac{1}{2}L_2$ illustrates the desirability of using circuits of equal length.

A comparison of the characteristics of the idealized severed-helix tube with those of the simple backward-wave tube has already been given. A typical calculation ($I_0=0.7\ I_{st}$, $QC=0$, $d=0$) shows that where the latter device produces a gain of 11 db, the "gain" of the modulator-demodulator configuration is about 32 db. In order to put the comparison on a fairer basis it should be rec-

[20] M. R. Currie, "The Electronic Impedance Characteristics of Waves on a Helix," Tech. Rep. No. 60, E.R.L., University of California; April 1, 1954.

[21] P. K. Tien, "Traveling-wave tube helix impedance," Proc. IRE, vol. 41, pp. 1617–1623; November, 1953.

ognized that the composite system employs two circuits each having an electrical length equal to that of the single circuit in the conventional tube. It might be more realistic to compare the gain of the composite structure with the gain obtained when two single-circuit tubes are cascaded. A comparison on this basis shows that the former arrangement still offers higher gain, 32 db as compared with 22 db. This comparison is valid for equal values of operating current if the circuits are identical in each case.

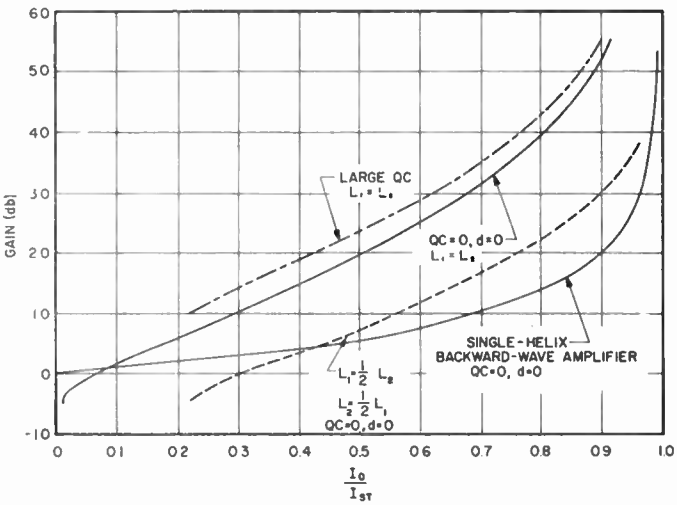

Fig. 15—Gain curves for the severed-helix backward-wave amplifier as a function of current normalized to the start-oscillation current. L_1 and L_2 denote the lengths of the input and output circuits, respectively. The gain has been optimized with respect to the velocity parameter b. The gain of a single-circuit backward-wave amplifier is shown for comparison.

The physical explanation of this behavior follows from Fig. 12 and the earlier discussion. In the usual case an unmodulated beam enters the interaction space where the circuit wave is strongest; conditions for strong interaction are not optimum. In the modified arrangement the modulation induced during the beam's transit through the first circuit is immediately placed in the region of maximum field on the second circuit. An enhanced reciprocal interaction between the beam and this circuit results.

Cascade Backward-Wave Amplifier with Drift Space

The idealized model probably could not be realized very closely in practice. Two circuits placed immediately adjacent to each other would prohibit good input and output matching and their fringing fields would not yield the high degree of cold isolation which is desired. In a more practical model to be considered, the circuits are separated by an arbitrary structure. A general configuration is shown in Fig. 16(a). The function of the new element or transducer is not only to isolate the input and output circuits but also to transform the velocity and current modulation which exist on the beam at the end of the first section so as to optimize the output signal. In the general case the transducer could consist of any combination of propagating and nonpropagating circuits.

The simplest transducer section consists of a region in which the electrons drift at constant velocity, as was considered in Fig. 1. Although this constitutes an analogy with the klystron, the drift tube here is not essential to the bunching mechanism. The effect of the drift tube on the over-all gain can be simply determined under the assumption that only one mode is excited in this region by the input modulation (denoted i_a and v_a). In this case the transformation to new values i_b and v_b can be described in terms of the space-charge waves of a single mode; the drift region can be regarded as a passive and lossless two-terminal pair network. The validity of the above assumption depends upon the particular geometry of the structure. For a helix circuit and a hollow beam it appeared to be good experimentally.

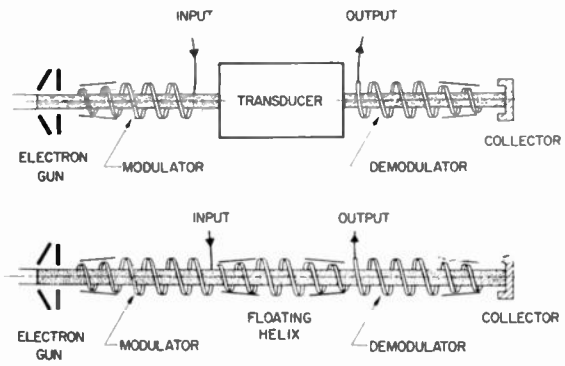

Fig. 16—Schematic models of the cascade backward-wave amplifier. (a) A general configuration in which the modulator and demodulator sections are separated by an arbitrary structure or space-charge wave transducer. (b) The floating helix amplifier in which the center section consists of a circuit terminated at each end. The helices could be replaced by any periodic circuits.

The output modulation is related to the input modulation by the following equations:

$$i_b = i_a\left[\cos\theta_q - j\frac{\sigma_0}{\sigma_a}\sin\theta_q\right], \tag{37}$$

$$\rho_0 v_b = \rho_0 v_a\left[\cos\theta_q - j\frac{\sigma_a}{\sigma_0}\sin\theta_q\right]; \tag{38}$$

where

$$\theta_q = \frac{\omega_p}{u_0}Rd \text{ (radian length of drift tube)},$$

$$\sigma_a = \frac{Ci_a}{\rho_0 v_a},$$

$$\sigma_0 = -\left(\frac{C}{R}\frac{\omega}{\omega_p}\right). \tag{39}$$

The particular beam and drift-region configuration is accounted for by the plasma frequency reduction factor R. This parameter is evaluated in Appendix B for the case of a hollow beam possessing modulation characteristic of the backward wave on a helix. If σ_0 is regarded

as the "characteristic impedance" of the drift region, i_a, v_a, and σ_a transform exactly as voltage, current and impedance along a transmission line; the usual calculation techniques (e.g., Smith chart) can be applied.

For the simple case of identical input and output circuits the over-all gain is given by

$$G = \left| \frac{2\Phi\chi}{\Delta^2} \right|^2 HH^*, \tag{40}$$

where

$$H = \cos\theta_q - j\frac{\sin\theta_q}{2}\left(\frac{\sigma_a}{\sigma_0} + \frac{\sigma_0}{\sigma_a}\right). \tag{41}$$

The first factor in (40) is just the gain of the idealized severed-helix tube; the factor HH^* represents the effect of the drift region on the over-all gain of the device.

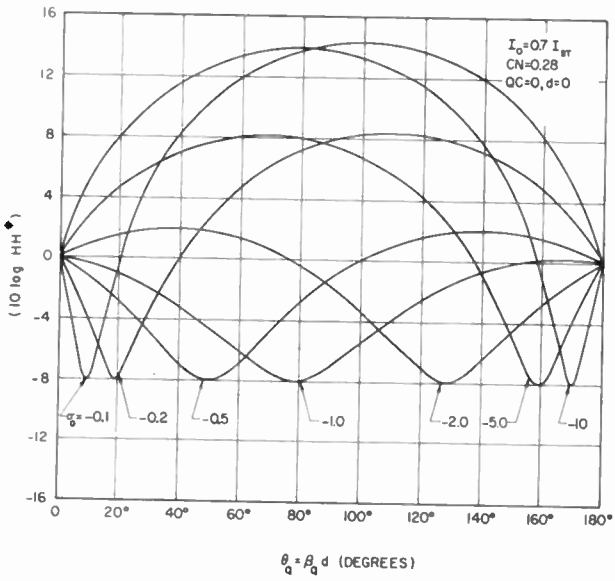

Fig. 17—Curves showing the effect of a drift region on the gain of a cascade backward-wave amplifier. The ordinate is the db correction to the gain of the severed-helix amplifier; the abscissa is the length of the drift region in degrees (one plasma wavelength is equal to 360 degrees). The parameter is the drift-tube "characteristic impedance" $\sigma_0 = -(C\omega/\omega_q)$. Identical input and output circuits are assumed and the calculations are for $I_0 = 0.7\ I_{st}$, $QC = 0$, and $d = 0$.

In Fig. 17 some representative curves of HH^* (expressed in db) are given as a function of drift tube length for various σ_0. Although these curves are for operation at 70 per cent of starting current it is found that they do not change significantly with the ratio I_0/I_{st}. It is apparent that a drift tube can increase the over-all gain for magnitudes of σ_0 either much greater or much smaller than unity. The former condition could only be met at the higher frequencies (e.g., X-band and above) and with the beam grazing the drift tube so as to lower the value of R.

For typical operation of helix-type backward-wave tubes at S-band, σ_0 may have a value near -1. In this range nearly all drift lengths result in a subtraction from the net gain. However, the magnitude of gain is often only of secondary importance in such a tube. For example, in the application of the tube as a swept amplifier it may be more important to maintain reasonably constant gain as a function of frequency at a constant value of beam current. The gain of the severed-helix tube (at small QC) is a function only of normalized current (I_0/I_{st}). Since I_{st} generally increases with frequency the gain at constant current will decrease at the higher frequencies. The choice of drift distance therefore lends an additional degree of freedom to the design of the tube. In particular, referring to Fig. 17, it is seen that this region can be made to compensate the above effect and the over-all gain can be made more constant with frequency. This compensating action was observed in the experimental amplifier discussed earlier. In this sense, the drift region can be regarded as a gain equalizer.

The Floating Helix Model

Another simple transducer section consists of a backward-wave circuit terminated at each end in a lossy match as shown in Fig. 16(b). In analogy to the floating cavity klystron this configuration is termed the floating helix amplifier. The analogy is only superficial since, in this case, the floating helix plays an active role in the energy balance. It absorbs energy while imparting further modulation to the beam. In the limit, this configuration may consist of an arbitrary number of floating circuits between the modulator and demodulator with each contributing to the over-all gain of the tube. The bandwidth can be adjusted to some degree by stagger tuning these elements.

For the case in which the floating circuit is identical to the input and output circuits, the over-all gain is given by

$$G = \left| \frac{2\Phi\chi}{\Delta^2} \right|^2 JJ^*, \tag{42}$$

where

$$J = \frac{1}{\Delta}\left[-\Lambda + \frac{1}{2}\left(\frac{\Phi^2\Psi + \chi^2\Omega}{\Phi\chi}\right)\right]. \tag{43}$$

The factor JJ^* expresses the contribution of the floating circuit to the gain of the idealized model. Numerical calculations for small QC show that at $I_0/I_{st} = 0.5$ the gain is increased by about 9 db and, at $I_0/I_{st} = 0.7$, the new element adds about 19 db. Calculations for unequal circuit lengths or multiple floating circuits can be readily formulated in matrix notation based on the linear relationships (8), (9) and (10).

Noise Figure

In considering the application of the cascade backward-wave amplifier as a small-signal device it is important to know its noise figure, i.e., its capability of detecting extremely low signal levels. The minimum detectable signal is limited by random fluctuations of

the electrons and the conversion of these fluctuations to noise power on the circuit at the tube's output. A theoretical minimum noise figure for conventional traveling-wave tubes has been calculated recently[22,23] and actually has been exceeded in practice (this discrepancy is attributed to incomplete knowledge of conditions at the potential minimum). A similar analysis will be presented for the cascade amplifier.

Noise figure can be defined[24] as the ratio of the noise-to-signal power ratio at the output N_0/S_0, to that at the input N_i/S_i, i.e.,

$$F = \frac{N_0/S_0}{N_i/S_i} = \frac{N_0}{N_i G}, \tag{44}$$

where G is the over-all gain. The tube is assumed to be matched to a source at temperature T; N_i is the available thermal noise power

$$N_i = kTB,$$

where k is Boltzmann's constant and B is frequency bandwidth. The total noise power at the output is

$$N_0 = N_{0b} + N_{0t}.$$

N_{0b} is power due to noise on the beam and N_{0t} is thermal noise power. For the cascade amplifier

$$N_{0t} = kTBG + kT_2B_2G_2. \tag{45}$$

The second term represents the contribution of the output circuit when considered as a single-circuit backward-wave amplifier *per se*. Its input (collector end) is matched to a temperature T_2; B_2 and G_2 are, in general, different than the corresponding values for the composite tube. Another term would be required for the case of a floating circuit tube. The noise figure becomes

$$F = 1 + \frac{B_2G_2T_2}{BGT} + \frac{1}{kTB}\frac{N_{0b}}{G}. \tag{46}$$

Assuming a single-valued-velocity flow, the output power due to rms velocity fluctuations $\bar{v}$ and current fluctuations $\bar{\imath}$ at the input of the modulator section can be calculated from equations previously given. Two sources of noise exist at the potential minimum near the cathode, namely, velocity fluctuations

$$\bar{v}_a = \sqrt{4-\pi}\left(\frac{\eta kT_cB}{I_0}\right)^{1/2},$$

and full shot noise.

$$\bar{\imath}_a = \sqrt{2eI_0B}.$$

Under the assumption that these are completely uncorrelated, each will set up fluctuations in velocity and current at the entrance to the interaction space; the fluctuations due to the two noise sources will be uncorrelated and will produce powers which add at the tube's output. The resultant noise figure of the drift-tube configuration can be written

$$F = 1 + \frac{B_2G_2T_2}{BGT} + \frac{I_0}{4V_0CkTB} \sum_{i=1,2} \left| \left(\frac{\mu_0}{\eta}\right) \frac{(\Phi\Psi - \chi\Lambda) + \frac{1}{\sigma_0}\tan\theta_q(\chi\Psi + \sigma_0^2\Phi\Lambda)}{2\Phi\chi + \frac{1}{\sigma_0}\tan\theta_q(\chi^2 - \sigma_0^2\Phi^2)}\bar{v}_i + j\left(\frac{2V_0C}{I_0}\right)\frac{(\chi\Omega - \Phi\Lambda) - \frac{1}{\sigma_0}\tan\theta_q(\chi\Lambda + \sigma_0^2\Phi\Omega)}{2\Phi\chi + \frac{1}{\sigma_0}\tan\theta_q(\chi^2 - \sigma_0^2\Phi^2)}\bar{\imath}_i \right|^2, \tag{47}$$

where the subscripts $i = 1, 2$ represent quantities due to $\bar{v}_a$ and $\bar{\imath}_a$, respectively.

In order to evaluate the noise figure the quantities $\bar{v}_1$, $\bar{\imath}_1$ and $\bar{v}_2$, $\bar{\imath}_2$ must be related to the noise sources at the potential minimum. This can be done in any specific case by means of the Llewellyn-Peterson equations. The noise figure is then a function of the electron gun dimensions and of the distance from the final anode to the circuit entrance. This procedure has been generalized[25,26] by assuming an arbitrary lossless space-charge-wave transducer between the potential minimum and the circuit entrance. If the noise figure is written in the form

$$F = 1 + \frac{I_0}{4V_0CkTB} \cdot \sum_{i=1,2} \left| \left(\frac{\mu_0}{\eta}\right)\alpha\bar{v}_i - j\left(\frac{2V_0C}{I_0}\right)\sqrt{4QC}\,\beta\bar{\imath}_i \right|^2, \tag{48}$$

then F can be minimized with respect to the transducer's characteristic parameters. The formal analyses given in the above references are applicable to backward-wave amplifiers as well as to conventional forward-wave amplifiers. From the results of these analyses the following expression for minimum noise figure can be obtained:

$$F_{\min} = 1 + 2\frac{T_c}{T}\sqrt{4-\pi}\,|a_2b_1 - a_1b_2|, \tag{49}$$

where

$$\alpha = a_1 + ja_2; \qquad \beta = \frac{1}{\sqrt{4QC}}(b_1 + jb_2). \tag{50}$$

Slightly different forms for $F_{\min}$ result from choosing other methods of averaging the velocity fluctuations at the potential minimum.[27]

[22] J. R. Pierce and W. E. Danielson, "Minimum noise figure of traveling-wave tubes with uniform helices," *Jour. Appl. Phys.*, vol. 25, pp. 1163–1165; September, 1954.

[23] R. Peter and S. Bloom, "A minimum noise figure for the traveling-wave tube," *RCA Rev.*, vol. 15, pp. 252–267; June, 1954.

[24] R. W. Peter, "Direct-reading noise-factor measuring systems," *RCA Rev.*, vol. 12, pp. 269–281; June, 1951.

[25] J. R. Pierce and W. E. Danielson, *loc. cit.*

[26] R. Peter and S. Bloom, *loc. cit.*

[27] J. R. Pierce, "A theorem concerning noise in electron streams," *Jour. Appl. Phys.*, vol. 25, p. 931; August, 1954.

Comparison of (47) and (48) yields values of α and β appropriate for cascade amplifier. In usual range of operation, B_2 is slightly greater than B (at same current) and $G_2 \ll G$ (Fig. 15). Second term in (47) is small and thus can be neglected to good approximation.

The minimum noise figure has been computed for various values of circuit loss as a function of QC. In order to simplify the calculations, the tabulated conditions at start-oscillation were used. This procedure yields results which are strictly valid only at the point of infinite gain. The results are shown in Fig. 18. Certain features of the curves are worth comment. For zero loss the minimum noise figure is exactly the same as for a forward-wave amplifier, namely,

$$F = 1 + (0.9265)\frac{T_c}{T} \sim 6 \text{ db}.$$

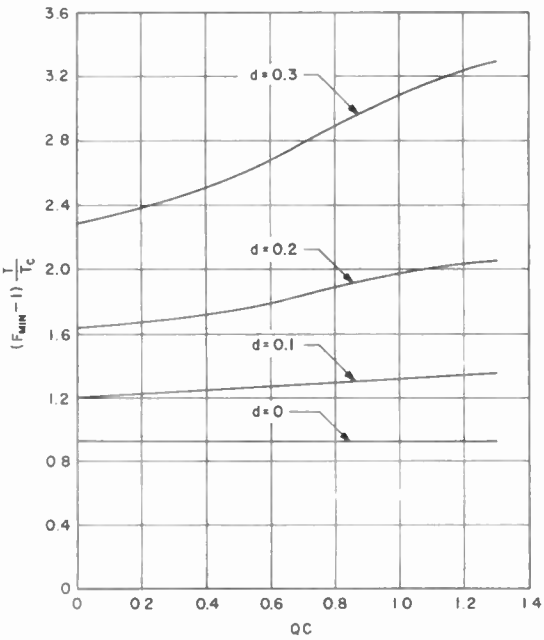

Fig. 18—The minimum noise figure $F_{\min}$ of the cascade backward-wave amplifier can be determined from the above curves. The curves are given for four values of the attenuation parameter d. Identical curves were obtained for drift lengths of 0, $\frac{1}{8}\lambda_q$, and $\frac{1}{4}\lambda_q$ and for a single-helix backward-wave amplifier.

But noise figure in backward-wave case is much more strongly dependent upon circuit loss than a forward-wave amplifier. Moreover, in the latter, $F_{\min}$ can be lowered by decreasing value of d over only first several circuit wavelengths; for backward-wave circuit, d must be minimized over its entire length.

In each case the curves were computed for three lengths of drift tube (0, $\frac{1}{8}\lambda_q$, $\frac{1}{4}\lambda_q$) and $\sigma_0 = -1$. Exactly the same values of $F_{\min}$ were obtained in each case. Thus, at high gain, the noise figure is determined only by the parameters of the modulator section (if the thermal noise of the output circuit is neglected). The signal-to-noise ratio is fixed as the beam leaves the modulator. Therefore, the curves also give the minimum noise figure of a single-circuit backward-wave amplifier. The latter has been recently computed independently[28] and agrees with the above results. Detailed calculations for operation at low gain levels indicate minimum noise figures slightly below those shown in Fig. 18.

Appendix A: Power Series Solutions

Quate[29] recently solved the traveling-wave tube differential equations by expanding the solutions in the form of power series. This type of solution is convenient for electrically short circuits where all three waves must be taken into account. It is therefore ideal for backward-wave tubes. When Quate's expressions are transformed to the case of backward waves and put into the same form as (8)–(10), the functions used in this paper can be replaced by power series as follows:

$$\frac{\kappa}{\Delta} = \frac{1}{S_a} \qquad \frac{\Lambda}{\Delta} = S_d - j\frac{S_b S_c}{S_a}$$

$$\frac{\Phi}{\Delta} = \frac{S_b}{S_a} \qquad \frac{\Psi}{\Delta} = S_e - j\frac{S_c^2}{S_a}$$

$$\frac{\chi}{\Delta} = \frac{S_c}{S_a} \qquad \frac{\Omega}{\Delta} = -\left[S_f + j\frac{S_b^2}{S_a}\right], \tag{51}$$

where the power series are given by

$$S_a = e^{-j(\tau b/2)}\left[e^{-j(\tau b/2)} + j\frac{\tau^3}{3!} - j\frac{\tau^5}{5!}\left(\frac{f^2}{2} + 4QC\right) - \frac{\tau^6}{6!}(1 - 4QCf) + \cdots\right]$$

$$S_b = \tau - j\frac{\tau^2}{2!}f - \frac{\tau^3}{3!}(f^2 + 4QC) + j\frac{\tau^4}{4!}(f^3 + 1 + 4QCf) + \frac{\tau^5}{5!}(f^4 + 2f + 4QCf^2 + (4QC)^2) + \cdots$$

$$S_c = \frac{\tau^2}{2!} - j\frac{\tau^3}{3!}f - \frac{\tau^4}{4!}(f^2 + 4QC) + j\frac{\tau^5}{5!}(f^3 + 1 + 4QCf) + \cdots$$

$$S_d = \cos(\tau\sqrt{4QC}) + j\frac{\tau^3}{3!} + \frac{\tau^4}{4!}f - j\frac{\tau^5}{5!}(f^2 + 8QC) - \cdots$$

$$S_e = \frac{1}{\sqrt{4QC}}\sin(\tau\sqrt{4QC}) + j\frac{\tau^4}{4!} + \frac{\tau^5}{5!}f - j\frac{\tau^6}{6!}(f^2 + 8QC) + \cdots$$

$$S_f = \sqrt{4QC}\sin(\tau\sqrt{4QC}) - j\frac{\tau^2}{2!} - \frac{\tau^3}{3!} f + j\frac{\tau^4}{4!}(f^2 + 8QC) + \frac{\tau^5}{5!}(f^3 + 8QCf + 1) + \cdots,$$

[28] T. E. Everhart, "Concerning the Noise Figure of a Backward-Wave Amplifier," Hughes Aircraft Co. Rep. 40-31-00-3; Oct., 1954.
[29] C. F. Quate, *loc. cit.*

where

$$\tau = 2\pi CN \quad \text{and} \quad f = b_d' + jd.$$

The series are particularly useful for zero loss and small QC. They converge fairly rapidly for $b<2.5$. Many of the exploratory calculations in this paper employed the series; the authors are indebted to C. F. Quate for pointing out this method of solution.

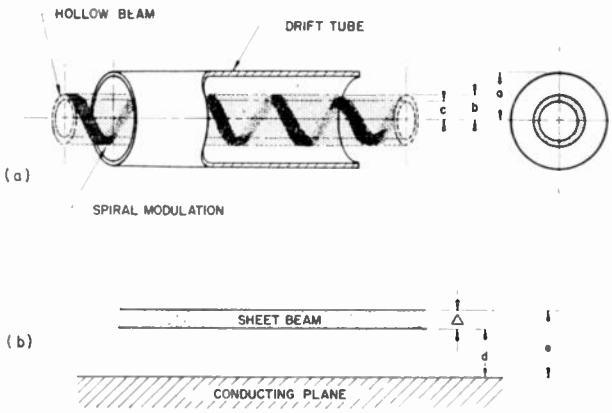

Fig. 19—Drift-tube configuration used for analysis. (a) The exact cylindrical model in which a hollow beam enters the drift tube with a spiral modulation pattern characteristic of interaction with the (-1) harmonic of a helix. (b) An approximate planar model in which a sheet beam passes close to a conducting plane.

Appendix B: Plasma Frequency Reduction Factor

The configuration of the beam and drift region entered the analysis implicitly in the plasma frequency reduction factor R. It accounts for the change in plasma frequency due to the finite size of the beam and the effects of charges induced on nearby metal surfaces. R is defined[30]

$$R = \frac{\omega_q}{\omega_p} = \left[\frac{1}{1+\dfrac{T^2}{\beta_e^2}}\right]^{1/2}, \tag{52}$$

where T is a characteristic value of the differential equation

$$\Delta_t^2 E_z + T^2 E_z = 0. \tag{53}$$

The T for the mode encountered with helix-type backward-wave tubes has not been previously evaluated and is given here. The modulation induced on the beam by interaction with the backward space harmonic of the helix is not axially symmetric; the fields of this component propagate as $\exp j[\omega t - |\beta_{-1}| z - \theta]$. If viewed in a plane of constant z the fields have a sinusoidal variation with azimuth. As the beam enters the drift region it possesses a spatial modulation pattern which is a spiral as shown above, Fig. 19(a). It is assumed that only fields having this same angular variation will be excited in the drift tube. The solution to (53) is then in terms of first-order Bessel functions and their derivatives; T is the solution of a transcendental equation involving these functions.

The complicated nature of the characteristic equation for T makes its extensive evaluation as a function of geometry and beam velocity difficult. For hollow beams of radial thickness small compared with diameter, it can be assumed that electrons will not experience drastic effects due to the curvature of the drift tube. An approximate model therefore consists of an infinite sheet beam passing close to a conducting plane, as in Fig. 19(b). The spiral modulation pattern is then replaced by a pattern characteristic of the (-1) harmonic on a developed helix, i.e., the wave propagates as $\exp j[\omega t - |\beta_{-1}| z + y/a]$ so that the fields repeat at $y = 2\pi na$. The determinantal equation then becomes simply

$$\tanh(\eta d) = \frac{\eta/T' \tan T'\Delta + 1}{T'/\eta \tan T'\Delta - 1}, \tag{54}$$

where $T' = \sqrt{T^2 - (1/a)^2}$, $\eta^2 \cong \beta e^2 + (1/a)^2$, and the equivalence between the cylindrical and planar models is given by

$$\frac{\Delta}{a} = \frac{b-c}{a}, \qquad \frac{d}{a} = 1 - b/a.$$

Eq. (54) can be shown to be the limiting form of the exact cylindrical equation when asymptotic approximations of the Bessel functions are inserted.

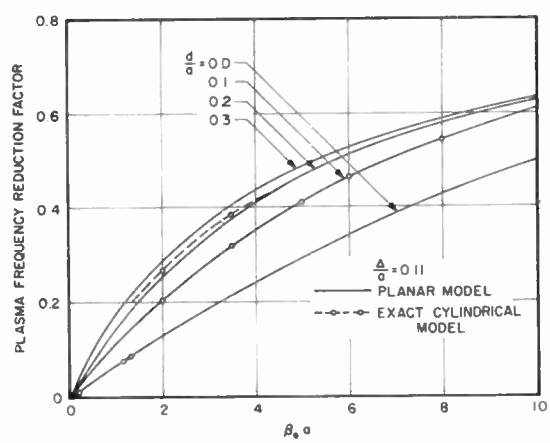

Fig. 20—Curves of plasma-frequency reduction factor versus ratio of helix diameter to electronic wavelength for various radial separations of the beam from the drift tube. The dimensions are defined in Fig. 19. Calculations based on the cylindrical and planar models show good agreement.

A typical curve of R as a function of $(\beta_e a)$ is shown in Fig. 20. The value of Δ/a corresponds to that of the experimental tube. The circled points were calculated from the cylindrical solution and illustrate the usefulness of the planar model. In the range of $(\beta_e a)$ typically encountered in helix-type backward-wave tubes (about 4 to 8) values of R under 0.5 are easily obtained and decrease as the beam is made to pass closer to the drift tube.

[30] S. Ramo, "The electronic wave theory of velocity modulation tubes," Proc. IRE, vol. 27, pp. 757–763; December, 1939.

Junction Transistor Blocking Oscillators*

J. G. LINVILL†, ASSOCIATE MEMBER, IRE, AND R. H. MATTSON†

Summary—**Blocking oscillators are useful as generators of rectangular pulses. Though junction transistors with alpha cutoff frequencies of a few megacycles have been most frequently used for low-frequency applications, they make surprisingly fast blocking oscillators. Rise times shorter than 0.1 microsecond have been analytically predicted and experimentally obtained.**

A simple but experimentally verified analysis indicates the proper transformer design for best rise time and prescribed pulse width. Using extensions of the primary results, one can evaluate triggering requirements and the effect of loading on the oscillator performance. Experimental results support these extensions.

Introduction

BLOCKING oscillators using triode junction transistors are useful for many applications. With only minor modifications, the basic blocking oscillator circuit can be used as a regenerative pulse amplifier, ring counter stage, pulse generator, or frequency divider stage. Junction transistors with alpha cutoff frequencies of a few megacycles ordinarily used for low-frequency applications make surprisingly fast blocking oscillators. Analysis predicts and experimental results confirm that such transistor blocking oscillators can provide output pulses with rise times of a tenth microsecond.

The crux of the design of a blocking oscillator, Fig. 1, which is essentially a one-stage amplifier with regenerative transformer coupling, is the choice of the feedback transformer. It is chosen to minimize the rise and fall times of the output pulse and deliver the desired pulse width.

This paper presents an analysis of transistor blocking oscillator performance, on the basis of which one can design a blocking oscillator for most rapid switching times and the desired pulse width. The analysis also compares the effectiveness of different trigger pulses in initiating the oscillator cycle. Finally an analysis of the effects of loading the blocking oscillator is shown.

The Blocking Oscillator and Its Network Approximants

A typical transistor blocking oscillator is shown in Fig. 1. It can be made either free-running or driven by choice of the voltage V_r. The essential elements found in blocking oscillators are the active element, in this case a transistor, and the transformer. There are a number of variations possible in the arrangement of the transformer connections which do not significantly alter the operation of the oscillator. For instance, the transistor can appear in a common-emitter orientation with feedback from collector to base. The emitter bias arrangement shown is another of the possibilities. The resistance R and the capacitance C are of significance in determining the frequency of operation and are chosen so as not to influence appreciably the performance of the oscillator during its output pulse. A pulse source is shown at the emitter of the transistor which is used either to trigger the transistor in the driven case or to synchronize it in the free-running case.

The presence of diode D_1 insures that the transistor never reaches the condition of saturation; it must always have a collector-to-base voltage of at least V_1. The prevention of saturation, effected by D_1, avoids difficulties associated with storage[1] of minority carriers in the base of the transistor in the condition of saturation and permits one to deal with the circuit as if the diodes are either open or short circuits and with the transistor as a simple linear amplifier when its emitter is carrying current in the forward direction. Diode D_2 protects the collector junction from high voltages caused by the inductance of the transformer at the termination of the output pulse.

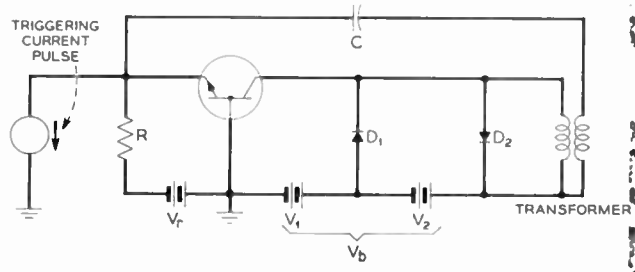

Fig. 1—A typical transistor blocking oscillator.

In terms of Fig. 1, the sequence of operations of the blocking oscillator for a cycle is as follows. At the end of the quiescent period, just as the trigger pulse starts, the emitter is back-biased and the collector voltage is V_b. The trigger pulse causes current to flow in the emitter, and at this point the transistor becomes active. After a short time the emitter current is substantially all collected by the collector and by virtue of the transformer a much larger emitter current is drawn in the same direction as that initiated by the trigger pulse. It is desirable to select a transformer with suitable turns ratio to lead to the fastest build-up of current in the transistor. As will be seen, the diffusion delay, collector capacitance, and leakage inductance, along with the transistor parameters all need to be considered. As the current build-up proceeds, the collector voltage drops from V_b until it reaches V_1 when diode D_1 begins con-

* Original manuscript received by the IRE, May 5, 1955; revised manuscript received, June 16, 1955.

† Bell Telephone Labs., Inc., Murray Hill, N. J.

[1] J. L. Moll, "Large-signal transient response of junction transistors," Proc. IRE, vol. 42, 1773–84; December, 1954.

duction. At this point the circuit regeneration is stopped and the sequence associated with switching ON is complete. The collector voltage remains at V_1 and the diode D_1 merely carries an amount of current to satisfy Kirchhoff's current law at the collector node. However, one observes that the magnetizing inductance of the transformer is in parallel with D_1 and at this stage has a steady voltage V_2 across it. Therefore, the current through this magnetizing inductance simply builds up linearly and there is a corresponding decrease in the current carried by D_1. The end of the ON period of the pulse comes when the current in D_1 has dropped to zero. At this point the remainder of the circuit cannot support the growing current required by the magnetizing inductance at the voltage V_2, so this voltage starts to decrease. D_1 opens and the collector voltage starts to rise. There follows in reverse the sequence of events that came with the switching action just described, and the result is that the transistor is switched off. When the voltage at the collector is back again to V_b, diode D_2 prevents any further rise and the magnetizing inductance is discharged through it. By virtue of the charge stored on the condenser C during the pulse, the emitter is again biased off even in the free-running case and a recharging from V_r through R must occur before the cycle is repeated.[2] In the case of the driven blocking oscillator, the value of V_r is such that the transistor will not begin to conduct again until a new triggering pulse is applied.

On the basis of the preceding discussion, it is clear that the blocking oscillator goes through three distinct operations during a cycle. There are the switching periods when the circuit is regenerative and unstable, the ON period when D_1's current is being transferred to the magnetizing inductance, and there is the OFF period when the transistor is quiescent and the external circuit is relaxing in preparation for the next cycle. In each of these portions of the cycle simplifications can be made which reduce the complexity of analysis of the circuit and lead to simple relationships.

Approximant for the Switching Periods

A circuit which approximates the blocking oscillator during the switching portion of the cycle is shown in Fig. 2. It is assumed at the outset that once the triggering pulse has been applied the emitter is forward-biased and the circuit behaves in an essentially linear manner. The circuit of Fig. 2 should exhibit natural frequencies corresponding to growing transients. In particular, it will be the purpose of the analysis shown later to determine this natural frequency and to permit its maximization by proper choice of the transformer turns ratio. The transistor is approximated to have negligible emitter resistance, negligible collector conductance, and a unity low-frequency alpha, or current gain. Typical values of base resistance, collector capacitance and alpha cutoff frequency for junction triodes are shown in Fig. 2. It is assumed that the bias circuit on the emitter acts substantially like an open circuit and that the diodes connected to the collector also behave like open circuits during this portion of the cycle. The assumptions just indicated seem drastic but the end use of the circuit approximant is to determine suitable values of the turns ratio. The simplification of analysis makes the results easy to apply and experimental results provide substantial checks on the analysis.

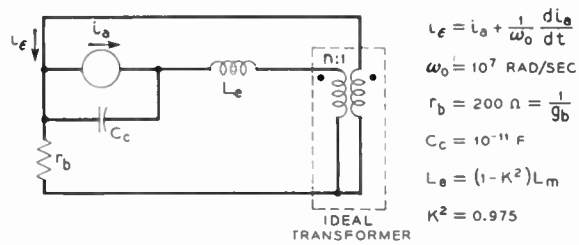

Fig. 2—Approximant of blocking oscillator for switching period.

Approximant for the ON Period

An approximant for the blocking oscillator during the ON period of the pulse is shown in Fig. 3. During the ON period current is transferring from the diode D_1 to the magnetizing inductance of the transformer. In the ON period the current gain of the transistor can be approximated as being constant and the effect of the leakage inductance and the collector capacitance can be neglected. The diode D_1 behaves approximately like a short circuit and diode D_2 like an open circuit.

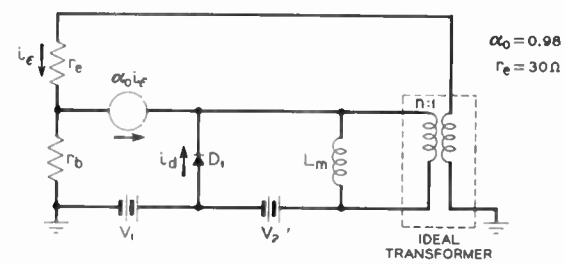

Fig. 3—Approximant for blocking oscillator during ON period.

Analysis of the Switching Part of the Cycle

As far as the performance of a blocking oscillator is concerned, one of the most significant characteristics is the rapidity with which the switching is accomplished. Blocking oscillators are interesting ordinarily because of the rectangular pulses which they can generate. It is of particular interest to determine how short the rise time can be in terms of the parameters of the transistor and to determine what values of turns ratio of the transformer should be employed to obtain fast response. These matters are most conveniently studied in terms of the approximant shown in Fig. 2.

[2] It is assumed for simplicity that the discharge of C requires longer than the discharge of the magnetizing inductance through D_2. This will not always be so and the relaxation time can in some cases be determined by the inductance discharge.

Once the triggering pulse has brought the transistor into its active region, the blocking oscillator responds in an essentially linear manner, exhibiting transient components in its response corresponding to the natural frequencies of the circuit. Because of the positive feedback of the blocking oscillator one finds that in this period the blocking oscillator is unstable; at least one of its natural frequencies corresponds to a growing transient. The growing transient component initiated by the trigger pulse becomes more significant in time than the other components, which decay. Thus it is clear that the switching time is related to the unstable natural frequency. The larger this natural frequency is, the more rapid the growth of the transient; hence the shorter the rise time. In addition it is apparent that the initial value of the growing transient is determined by the nature and value of the triggering pulse. The trigger pulse can be viewed as a means of establishing initial conditions in the blocking oscillator which in turn establish the transients to follow. One would like to have the trigger pulse establish a large component of the growing transient in order that a short time required for the remainder of the switching transient be completed by the oscillator on its own. In this connection it is clear that there are other triggering points than the one shown at the emitter which need to be considered. Differing trigger points provide different impedances to the trigger pulse; it is possible to trigger the blocking oscillator at some points with smaller expenditure of energy than is required at others.

The first problem of switching to consider is the determination of the natural frequencies of the blocking oscillator during the switching period, and in particular to determine how the unstable natural frequency can be maximized. To evaluate the natural frequencies of the approximant shown in Fig. 2, write the force-free nodal or loop equations and equate the system determinant to zero. This gives the characteristic equation

$$p^3 + \left[\omega_0 + \frac{(n-1)^2}{g_b L_e}\right] p^2 + \left[\frac{\omega_0(n-1)^2}{g_b L_e} + \frac{1}{C_c L_e}\right] p - \frac{\omega_0(n-1)}{C_c L_e} = 0. \quad (1)$$

For n greater than unity, one of the coefficients in the characteristic equation is negative and by Descartes' rule of signs the equation must have a positive real root, indicated as p_1. It turns out that this is the only root corresponding to a growing transient. An estimate of the rise time of the output pulse in terms of the positive root p_1 can be obtained from the following reasoning. Where other roots have negative real part and p_1 has a positive real part, it is clear that following the application of a trigger pulse, the transient component corresponding to p_1 increases while the others decrease. At the termination of the pulse rise, the growing transient is ordinarily the predominant component by far. A reasonable measure of rise time is the amount of time required for that component to have changed from 10 per cent to 100 per cent of its value at the end of the rise. Thus, since t must increase by $2.3/p_1$ for $\epsilon^{p_1 t}$ to increase tenfold, the rise time is approximately $2.3/p_1$.

In the design of the transformer, one ordinarily specifies the turns ratio and the magnetizing inductance. It is accordingly convenient to replace L_e in (1) by $(1-K^2)L_m$, where L_m is the magnetizing inductance and K is the coefficient of coupling, leading to

$$(1-K^2)p^3 + \left[(1-K^2)\omega_0 + \frac{(n-1)^2}{g_b L_m}\right] p^2 + \left[\frac{\omega_0(n-1)^2}{g_b L_m} + \frac{1}{C_c L_m}\right] p - \frac{\omega_0(n-1)}{L_m C_c} = 0. \quad (2)$$

If one has a transformer in which the coefficient of coupling is very close to unity, it is clear that the characteristic equation reduces essentially to a quadratic having for $n>1$, one positive and one negative root. Further, since all of the coefficients of p are positive, for any value of n, the positive root decreases as K decreases. Thus for fast rise times one should use as good coefficient of coupling as possible.

It is of interest to determine the relationship of the postive root of (2) to ω_0, the radian cutoff frequency of alpha. Thus we define a new variable

$$x = \frac{p}{\omega_0}. \quad (3)$$

in terms of which one rewrites (2) as follows:

$$(1-K^2)x^3 + \left[(1-K^2) + \frac{(n-1)^2}{g_b \omega_0 L_m}\right] x^2 + \left[\frac{(n-1)^2}{g_b \omega_0 L_m} + \frac{1}{\omega_0^2 C_c L_m}\right] x - \frac{(n-1)}{L_m C_c \omega_0^2} = 0. \quad (4)$$

In (4) the parameters which are subject to design control are L_m and n. The same parameters, as is shown later, are significant in specification of the pulse width. For small ferrite transformers a typical value of $(1-K^2)$ is .975; for typical grown-junction triode transistors $\omega_0 = 10^7$ rad/sec, $g_b = .005$ mhos, and $C_c = 10^{-11}$ farads. It is possible to plot in $L_m - n$ plane the loci of points which solve (4) for various values of x and the parameters typical of the transistor. This is done simply by obtaining from (4) an expression for L_m in terms of x and n:

$$L_m = \frac{-\dfrac{(n-1)^2 x^2}{g_b \omega_0} - \left[\dfrac{(n-1)^2}{g_b \omega_0} + \dfrac{1}{\omega_0^2 C_c}\right] x + \dfrac{n-1}{C_c \omega_0^2}}{(1-K^2)x^3 + (1-K^2)x^2}. \quad (5)$$

On the same plane one can show the loci of points which correspond to desired constraints as far as pulse width is concerned, as will be seen subsequently.

In Fig. 4 (opposite page) are shown loci of values of L_m and n which solve (4) for particular values of x. The figure contains, implicitly, information regarding

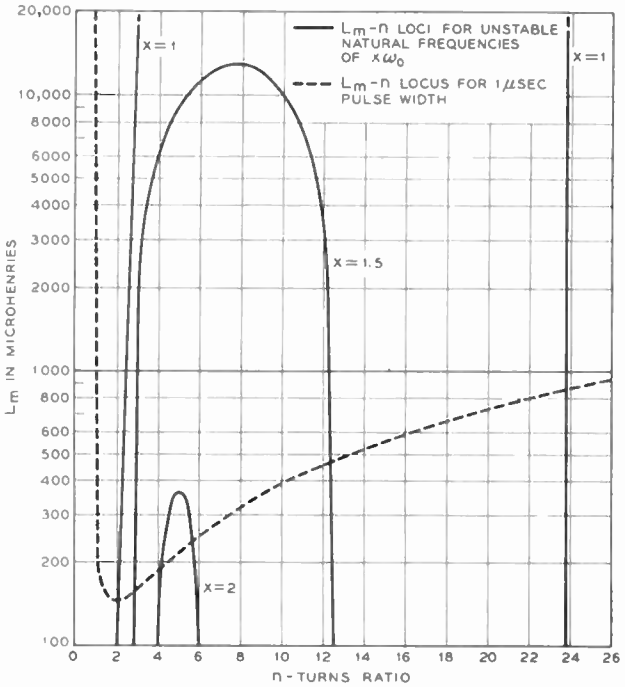

Fig. 4—Loci in $L_m - n$ plane for constant natural frequencies and for 1 μsec pulse width.

switching speeds of blocking oscillators with transistors having the parameter values quoted above. Moreover, it makes possible the selection of the optimum turns ratio for fastest operation.

Fig. 4 reveals an interesting possibility of transistor blocking oscillators. It shows that for appropriate turns ratios growing transients with exponents twice as large as $\omega_0 t$ occur for typical junction triode blocking oscillators. This is interesting in comparison to the maximum growing transients found in Eccles-Jordan type of transistor circuits in which the maximum exponent of the growing transient is $\omega_0 t$.[3]

Clearly the limiting x for positive L_m's is obtained for $L_m = 0$ and for the point on the loci of constant x in the $L_m - n$ plane with zero slope. It is simple to find the values of n where zero slope of the loci for constant x occur from (5).

$$\frac{dL_m}{dn} = \frac{-\dfrac{2(n-1)x^2}{g_b\omega_0} - \dfrac{2(n-1)}{g_b\omega_0}x + \dfrac{1}{C_c\omega_0^2}}{(1-K^2)x^3 + (1-K^2)x^2} = 0. \quad (6)$$

Thus

$$\frac{dL_m}{dn} = 0 \quad \text{where} \quad n = 1 + \frac{g_b}{2C_c\omega_0(x^2+x)}. \quad (7)$$

For typical junction triode transistor parameters and $x = 2$ one finds that n should be, by (7), about 5.3. A following section reveals that this turns ratio in combination with a suitable magnetizing inductance gives pulses with 0.1 microsecond rise times and 2 microsecond duration.

[3] J. V. Linvill, "Nonsaturating two transistor pulse circuits," Proc. IRE, vol. 43, pp. 826–834; July, 1955.

From (5) one can determine the fastest possible blocking oscillator through finding the value of x which gives $L_m = 0$ when n is the optimum value. From (5), $L_m = 0$ when

$$\frac{g_b(n-1)}{C_c\omega_0} - (n-1)^2(x^2+x) - \frac{g_b x}{\omega_0 C_c} = 0. \quad (8)$$

By (7) one obtains, with (8),

$$\frac{g_b^2}{2C_c^2\omega_0^2(x^2+x)} - \frac{g_b^2}{4C_c^2\omega_0^2(x^2+x)} - \frac{g_b x}{C_c\omega_0} = 0, \text{ or} \quad (9)$$

$$x^3 + x^2 = \frac{g_b}{4C_c\omega_0}. \quad (10)$$

The value of x, solving (10), is designated as x_m and represents an upper limit on the normalized unstable natural frequency of the blocking oscillator. For $g_b = .005$, $C_c = 10^{-11}$ and $\omega_0 = 10^7$, x_m is 2.03, which corresponds to a rise time of $(2.3/2.03) \times 10^{-7}$ sec.

Analysis of ON Portion of Cycle

At the termination of the switching period, the magnetizing inductance is not carrying appreciable current, Fig. 3, but it has a voltage of V_2 across it. The emitter current is easily seen to be

$$i_e = -\frac{V_2}{n[r_e + r_b(1-\alpha_0)]}. \quad (11)$$

The current entering the transformer must be i_e/n. Thus diode D_1 at the outset carries a current

$$i_d = \frac{V_2}{n[r_e + r_b(1-\alpha_0)]}\left[\alpha_0 - \frac{1}{n}\right]. \quad (12)$$

The pulse width T is the amount of time required for this amount of current to build up in the magnetizing inductance L_m. During the pulse, the transfer of current from the diode to the inductor occurs linearly with no effect on the remainder of the circuit.

$$T = \frac{(\alpha_0 n - 1)L_m}{n^2[r_e + r_b(1-\alpha_0)]}. \quad (13)$$

The locus of values of L_m and n corresponding to 1 microsecond pulse lengths is shown on Fig. 4, where values of α_0 of .98 and r_e of 30 ohms are used in (13).

On the basis of the curves shown on Fig. 4 one observes that the optimum turns ratio is about 5 and that one gets here a growing transient with an exponent of $2\omega_0 t$, leading to 0.1 microsecond rise time.

Experimental Results on Rise Time and Pulse Width

Two B.T.L. *n-p-n* grown-junction transistors with parameter values very nearly equal to typical values previously mentioned were used in circuit configuration shown in Fig. 5(a) (page 1636). Using a transformer with a 5 to 1 turns ratio and a 500 microhenry magnetizing inductance, rise times of about 0.10 and 0.11 microseconds were measured at the collector. The pulse

widths measured were 2.1 and 2.4 microseconds. These results compare favorably with the predicted values of 0.1 microsecond rise time, and 2.0 microsecond pulse width. Fig. 5 shows the circuit configuration and photographs of the response. Note that this circuit is not triggered by an input pulse, but by a charging condenser. A step trigger might cause a better rise time.

The design equations have also been worked out using typical parameter values for *p-n-p* alloy junction transistors with frequency cutoff values of about 3 megacycles. When using appropriate transformers, rise times of 0.07 microsecond and pulse widths of 0.75 microsecond have been obtained. These results are in good agreement with predicted results.

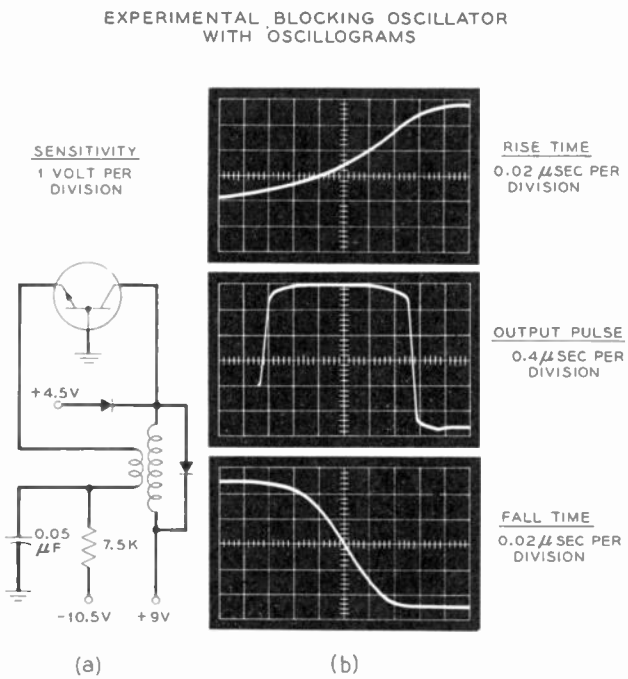

Fig. 5—Experimental blocking oscillator with oscillograms.

The Triggering Problem

In the foregoing analysis of the switching period, principal emphasis is placed on the growing transient component of response. While it is true that practically any pulse which removes the reverse bias of the emitter initiates all transient components including the unstable one, the growing component dominates after a short period of time.

It is interesting to compare results for pulses applied in different places. Different triggering points are best supplied by pulse sources of different internal impedance. Moreover, one finds that to develop a given size of the growing transient requires more energy for certain triggering points than others.

Three possible triggering points are shown in Fig. 6 along with suitable forms of triggering pulses. Each of the pulses can be assumed to take the transistor immediately into its active region. For this reason it is appropriate to use the approximant for the blocking oscillator shown in Fig. 2. Each of the triggering pulses excites all of the transient modes of the circuit but with increasing time the unstable transient greatly dominates the others. For parameters of the typical grown-junction triode and for the 5:1 turns ratio selected on the basis of the preceding sections one finds that within 50 millimicroseconds the growing transient is multiplied by 2.7 while the decaying components are multiplied by .02 and .00003. A convenient means of comparing different pulsing points is to consider responses to 50 millimicrosecond pulses. One should select for each pulsing point such an amplitude as will cause a standard magnitude of growing exponential. The amounts of energy required for three points can then be compared.

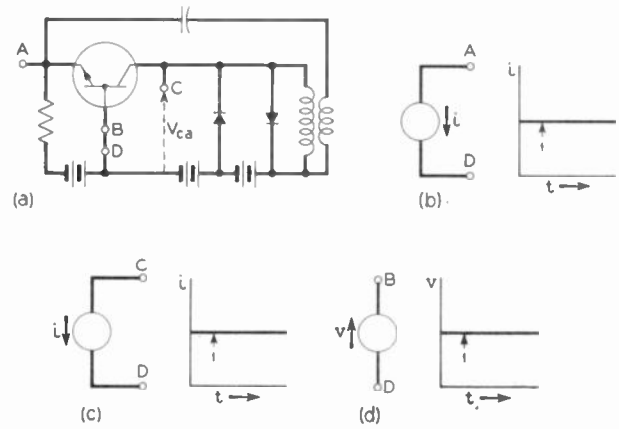

Fig. 6—Blocking oscillator and pulses with which it can be triggered. (a) Blocking oscillator with terminals for application of triggering pulses. (b) Current pulse for emitter triggering. (c) Current pulse for collector triggering. (d) Voltage pulse for base triggering.

Fig. 7 (opposite page) shows calculated responses to steps of current or voltage applied at points indicated in Fig. 6. On the basis of these response calculations one can determine what energy is required of the trigger source to bring the growing transient component of collector voltage to the value (1 volt) indicated on Fig. 7 in 50 millimicroseconds. One observes by rough graphical integration of $\int i_{source} v_{source} dt$ from Fig. 7 that for the case of emitter triggering this is about 3.5×10^{-11} joules; for the case of the collect triggering the energy is about 3.3×10^{-11} joules and for the case of base triggering the energy is about 6×10^{-11} joules. For the case of emitter triggering the ratio of source voltage to source current changes, starting at 200 ohms, dropping to 40 ohms, and rising again to 200 ohms. For the case of collector triggering, the voltage-current ratio begins at 200 ohms and rises to more than 5,000 ohms at the end of the 50 mμs period. For the case of base triggering with voltage source, the voltage-current ratio after an initial drop becomes 250 ohms throughout the 50 mμs period.

The foregoing discussion is highly idealized and naturally is expected to yield only order of magnitude answers. When trigger-pulse sources of finite impedance rather than the infinite or zero impedance sources used for Fig. 7 are employed, these influence the natural frequencies of the circuit and influence the rise times

and energies in a way which is neglected in the above analysis. Second, the blocking oscillator does not become instantaneously active and linear as indicated in the analysis. Rather the transition is a gradual one as current builds up in the emitter, its incremental resistance at first being very high. Thus at first the circuit behaves differently from its subsequent behavior. The energies indicated above are significant only for comparison purposes since the analysis gives really no indication of what the minimum energy is which can be used to trigger the circuit reliably. It does indicate that the differences in energy for triggering in the various points is not widely different but the best source impedances to be used in different places is quite different.

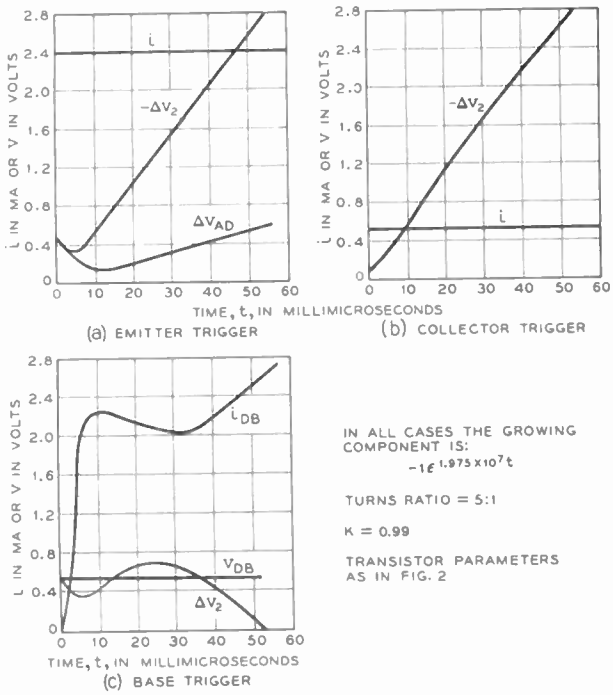

Fig. 7—Calculated responses of blocking oscillator to three triggers as in Fig. 6.

Experimental Results on Triggering

An *n-p-n* grown-junction transistor with typical parameter values was investigated in the circuit configuration shown in Fig. 8(a). Fig. 8(b) shows the calculated and measured responses to the three types of triggers. Other transistors and various trigger pulses were also investigated, and correlation between calculated and experimental results was good.

Fig. 8(b), Position 1, is a plot of the response voltage vs time when the emitter has a 5 milliampere current trigger impressed. The dotted curve is the calculated curve. The discontinuities in this curve are due to the fact that the 50 millimicrosecond trigger pulse was assumed to have zero rise and fall times. The measured response could not have such sharp discontinuities because it is a physical rather than a mathematical system. However, the shape of the curves is very similar. Note that at the end of 50 millimicroseconds the trigger is no longer feeding energy into the system. The circuit is responding by itself at a rate determined by its natural frequencies.

Fig. 8(b), Position 2, is the response vs time when an one milliampere current trigger is impressed at the collector. Note the similarity between Positions 1 and 2 in Fig. 8(b). This indicates that the main difference between the emitter and collector trigger is the 5 to 1 transformer. About the same amount of energy in each case will give the same response.

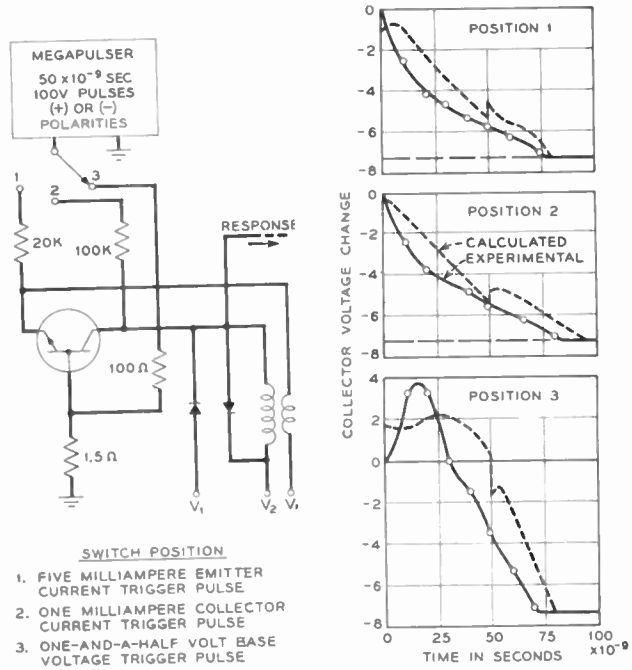

Fig. 8—Circuit and responses for triggering studies.

The calculated and experimental responses to a 1.5 volt trigger impressed at the base are shown in Fig. 8(b), Position 3. Again note the general shapes of the curves are very similar, although the sharp discontinuities are not present in the experimental curve.

In all figures the dashed curves are the calculated results and the solid curves are the experimental results. Note that all of the responses are deviations of the collector voltage from an original or quiescent voltage.

The Effect of Loading on Blocking Oscillator Performance

To this point the blocking oscillators described have been considered to work into infinite impedances. Ordinarily blocking oscillators are required to provide some useful output power. Hence it is interesting to determine how results obtained in the foregoing are altered by application of a load. The analysis of a loaded blocking oscillator is much like that of an unloaded one; many of the preceding results are altered in a simple manner. One would expect the application of a load to slow the switching time somewhat and to alter the transformer design for optimum speed. The following analysis substantiates these expectations in a quantitative way.

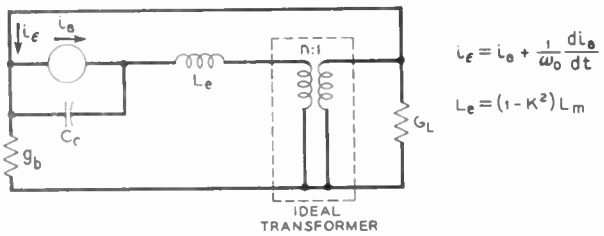

Fig. 9—Approximant for loaded blocking oscillator during switching.

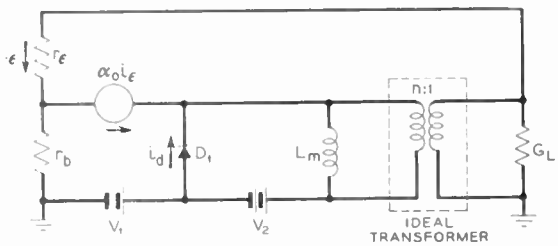

Fig. 10—Approximant for loaded blocking oscillator during ON period.

An approximant for switching to the blocking oscillator circuit with a conductive load connected to the collector is shown in Fig. 9.[4] The characteristic equation for this approximant where one uses a normalized frequency variable is [compare (4)]

$$(1-K^2)x^3+\left[(1-K^2)+\frac{(n-1)^2}{L_m\omega_0(g_b+G_L)}\right]x^2$$
$$+\left[\frac{(n-1)^2}{(g_b+G_L)L_m\omega_0}+\frac{1}{L_mC_c\omega_0^2}\right]x-\frac{g_b(n-1)}{L_mC_c\omega_0^2(g_b+G_L)}=0. \quad (14)$$

One observes that every g_b in (4) is replaced by g_b+G_L and the negative constant with which the positive root varies significantly is decreased. One can plot loci of constant x-values which solve (14) in the L_m-n plane as was done before with similar kinds of curves resulting. The analog to (5) is

$$L_m = \frac{\dfrac{g_b(n-1)}{(g_b+G_L)\omega_0^2C_c}-\dfrac{(n-1)x^2}{\omega_0(g_b+G_L)}-\left[\dfrac{(n-1)^2}{(g_b+G_L)\omega_0}+\dfrac{1}{C_c\omega_0^2}\right]x}{(1-K^2)x^3+(1-K^2)x^2}. \quad (15)$$

The turns ratio corresponding to maximum x for $L_m=0$ is found by the same process as used in the unloaded case, to give in place of (10),

$$x^3+x^2=\frac{g_b^2}{4C_c\omega_0(g_b+G_L)}. \quad (16)$$

The turns ratio which gives $dL_m/dn=0$ is given by (7) without change for the loaded case

$$n=1+\frac{g_b}{2C_c\omega_0(x^2+x)}. \quad (17)$$

[4] Alternately, a series load could be applied. A generally similar analysis to that which follows could be applied for the series case.

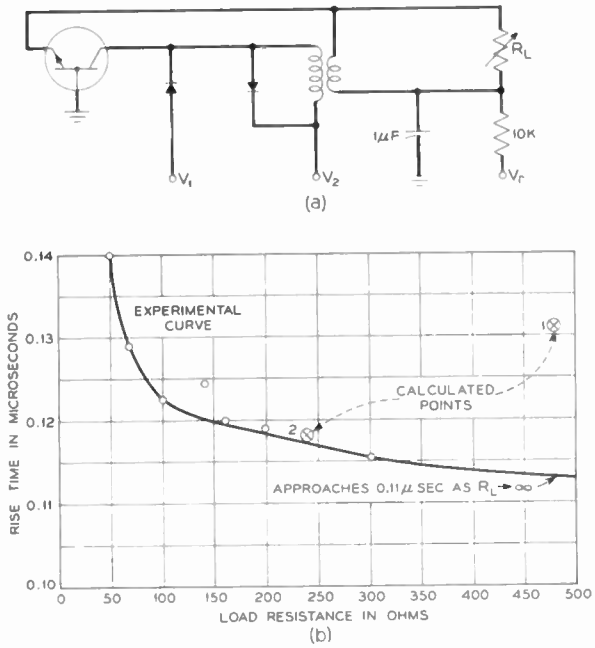

Fig. 11—Circuit and response for loading studies.

On the basis of (16) one can determine the amount of loading which will reduce the speed of the growing transient by any desired amount. By (17) one can determine approximately the appropriate turns ratio for the transformer.

Suppose one wishes to determine how much loading is permitted if x is to be 1.5 rather than the value 2 found for typical triode parameters in the unloaded case. Eq. (16) reveals that G_L, if $x=1.5$ is

$$G_L = 1.2g_b \text{ or } \frac{1}{G_L} = 166 \text{ ohms}. \quad (18)$$

For this case the turns ratio, by (17), should be approximately 6.7. One would obtain approximately the same results with a loading resistor from collector to ground of 7,500 ohms.

The effect of a load on the pulse width of the blocking oscillator can be evaluated through considering the approximant of Fig. 10. An analysis precisely like that leading to (13) for the unloaded case leads to

$$T = L_m\left[\frac{\alpha_0 n-1}{n^2[r_e+(1-\alpha_0)r_b]}-\frac{G_L}{n^2}\right] \quad (19)$$

for the loaded case.

Experimental Results with Loading

Fig. 11(a) shows the experimental circuit configuration for the investigation of the loading problem. Fig. 11(b) is a graph of rise time vs load resistance using a

7 to 1, one millihenry transformer. Two calculated values of rise time can be obtained for checking purposes. The first value is for a no-load condition ($G_L=0$). By interpolation from Fig. 4, a 7 to 1, one millihenry transformer corresponds to an x of about 1.8. This corresponds to a rise time of 0.13 microsecond which gives the point labeled (1) on Fig. 11(b). The second value of rise time is for a loaded condition. Knowing the turns ratio and the transistor parameters, (17) can be solved for the value of x. This value of x substituted into (16) gives a value of G_L. The value of x can be used to solve for the rise time with this particular load. Thus, a second point can be calculated and it is labeled (2) on Fig. 11(b).

Previously it was shown that a 5 to 1 turns ratio resulted in the fastest rise time for the unloaded case. If the circuit is loaded as shown in Fig. 11(a), the rise time will become slower because the load robs some of the feedback current. However, by increasing the turns ratio the rise time may be shortened by restoring some of the feedback current. From (16) and (17) it is possible to calculate either the optimum turns ratio for a given load or the optimum load for a given turns ratio. Fig. 11(b) shows that the calculated and experimental value of optimum load for a given turns ratio are about the same.

Eq. (20) shows how the pulse width changes with the load conductance. Experimental measurements confirm this variation.

Theory of Shot Noise in Junction Diodes and Junction Transistors*

A. VAN DER ZIEL†, SENIOR MEMBER, IRE

Summary—**A theory of shot noise in junction diodes and transistors is presented, based upon a transmission line analogy. The noise is caused by the randomness in the diffusion of the minority carriers and the randomness in the recombination of minority and majority carriers. In transmission line analogy, first process corresponds to distributed noise emf's in series with transmission line, and second process corresponds to distributed noise current generators in parallel to transmission line. After magnitude of these equivalent distributed noise sources has been determined, noise problem is solved by standard methods. It is found that theoretical results for a junction diode agree with experimental work published earlier.**

An equivalent circuit describing the noise in transistors is presented. It contains two partially correlated noise current generators i_{p1} and i_{p2}, i_{p1} connected across the emitter junction and i_{p2} connected across the collector junction. $\langle i_{p1}^2\rangle_{av}$, $\langle i_{p2}^2\rangle_{av}$ and $\langle i_{p1}^* i_{p2}\rangle_{av}$ are calculated. At low frequencies emitter and collector current show full shot effect and i_{p1} and i_{p2} are almost completely correlated; at higher frequencies the correlation becomes less complete.

The noise can also be described by an emf e_s in series with the emitter and a current generator i_p in parallel to the collector junction. $\langle e_s^2\rangle_{av}$, $\langle i_p^2\rangle_{av}$ and $\langle e_s^* i_p\rangle_{av}$ are calculated. At low frequencies e_s and i_p are uncorrelated, but some correlation is expected at higher frequencies. Low-frequency results resemble earlier equivalent circuits of Montgomery, Clark, and van der Ziel, and of Giacoletto.

Introduction

IN THE past, diffusion problems have been solved occasionally with the help of a transmission line analogy. Recently Dr. D. O. North, RCA Laboratories, showed the author that the same method could be extended to noise problems in diodes and transistors.[1]

This idea, for which Dr. North deserves the credit, is applied in this paper. To put the paper in a self-consistent form and to help readers that are unfamiliar with the method, we first develop the analogy, then apply it to derive known diode and transistor formulas, and finally extend it to noise problems.

The noise mechanisms discussed in this paper do not refer to the IF noise mechanism which predominates at low frequencies. For good transistors the IF noise is important below 1,000 cycles, for poorer transistors its influence extends even to higher frequencies. The noise mechanisms discussed here are thus those that predominate at higher frequencies, at which the influence of the IF noise is negligible.

I. The Transmission Line Analogy of Diffusion Problems in Semiconductors

The differential equations for a distributed line with negligible distributed self-inductance are

$$\partial E/\partial x = -RI,$$
$$\partial I/\partial x = -GE - C\partial E/\partial t, \qquad (1)$$

where E is the voltage, I the current and R, G, and C the resistance, conductance and capacitance per unit length. We shall show that the diffusion equations for current carriers in a semiconductor can be written in a form that is identical with (1).

Consider the one-dimensional diffusion of minority carriers injected into semiconducting material, such as occurs in junction diodes and in the base region of junction transistors. Let "drift" of the minority carriers be negligible in comparison with "diffusion." Further

* Original manuscript received by the IRE April 21, 1955; revised manuscript received, June 6, 1955, this work was supported by the U. S. Signal Corps.

† Dept. of Elec. Engrg., Univ. of Minnesota, Minneapolis, Minn.

[1] D. O. North, 1955 Conference on Semiconductor Device Research, Philadelphia, Pa.; June, 1955; and earlier discussions.

let the material be n-type, so that the minority carriers are holes. Let the material have a cross-sectional area A and a length w. If we integrate over the cross-sectional area A, we have the diffusion equations

$$\partial p/\partial t = -(p - p_n)/\tau_p - (1/e)\partial i_p/\partial x$$
$$i_p = -eD_p\partial p/\partial x, \tag{2}$$

where D_p is the hole diffusion coefficient, τ_p the hole lifetime, e is the electronic charge, i_p is the hole current and p_n is the equilibrium hole concentration, whereas p is the actual hole concentration (both per unit length, of course). Introducing the excess hole concentration $p' = (p - p_n)$, we rewrite (2) as

$$\partial p'/\partial x = -(1/eD_p)i_p$$
$$\partial i_p/\partial x = -(e/\tau_p)p' - e\partial p'/\partial t, \tag{2b}$$

which shows a complete analogy with (1). We thus have the following correspondences: E corresponds to the excess hole concentration p', I corresponds to the hole current i_p, R corresponds to $(1/eD_p)$ G corresponds to (e/τ_p) and C corresponds to e. To solve the problem of hole flow in n-type material, we solve the corresponding transmission line problem by standard methods and then translate back to the original problem.

Two important quantities in transmission line theory are the characteristic impedance $Z_0 = R^{1/2}/(G+j\omega C)^{1/2}$ and the propagation constant $\gamma = R^{1/2}(G+j\omega C)^{1/2}$. In the diffusion problem the corresponding quantities are

$$Z_0 = [e^2D_p(1 + j\omega\tau_p)/\tau_p]^{-1/2}:$$
$$\gamma = a + jb = [(1 + j\omega\tau_p)/D_p\tau_p]^{1/2}. \tag{2c}$$

We shall call these quantities the *characteristic impedance* and the *propagation constant* of the semiconductor. For low frequencies these quantities reduce to:

$$Z_0 = Z_{00} = [e^2D_p/\tau_p]^{-1/2} \quad \gamma = \gamma_0 = (D_p\tau_p)^{-1/2}, \tag{2d}$$

so that (2c) may be written

$$Z_0 = Z_{00}/(1 + j\omega\tau_p)^{1/2}: \quad \gamma = \gamma_0(1 + j\omega\tau_p)^{1/2}. \tag{2e}$$

II. Application to p-n Junctions

Consider a p-n junction in which the current is all carried by holes and in which the n-region is infinitely long for all practical purposes (that is, the length w of the n-region is such that practically none of the holes injected at one end reach the electrode at the other end). We put the origin of our co-ordinate system at the point at which the holes are injected into the n-region. If no voltage is applied to the junction, the concentration at $x=0$ is equal to the equilibrium concentration p_n. If a voltage V is applied to the diode, the hole concentration at $x=0$ becomes:

$$p = p_n \exp(eV/kT). \tag{3a}$$

The hole concentration follows the applied voltage almost instantaneously. If in particular a dc voltage V_0 and a small ac voltage $V_1 \exp(j\omega t)$, $(eV_1/kT \ll 1)$ are applied, we may write

$$p = p_n + p_0' + p_1' \exp(j\omega t), \tag{3b}$$

where

$$p_0' = p_n[\exp(eV_0/kT) - 1]:$$
$$p_1' = p_n(eV_1/kT)\exp(eV_0/kT) \tag{3c}$$

For an infinite transmission line of characteristic impedance Z_0 an applied voltage E gives rise to an input current E/Z_0. Applying this directly to our p-n junction, we have for the dc hole current at $x=0$,

$$I_p = p_0'/Z_{00} = I_{p0}[\exp(eV_0/kT) - 1]:$$
$$I_{p0} = ep_n(D_p/\tau_p)^{1/2}. \tag{4}$$

In the same way we have for the ac hole current at $x=0$,

$$i_p = I_1 \exp(j\omega t) = p_1' \exp(j\omega t)/Z_0$$
$$= G_0(1 + j\omega\tau_p)^{1/2}V_1 \exp(j\omega t). \tag{5}$$

Consequently, ac admittance of junction becomes

$$Y = G + jB = I_1/V_1 = G_0(1 + j\omega\tau_p)^{1/2}, \tag{6a}$$

where G_0 is the dc conductance of the junction

$$G_0 = (e/kT)e(D_p/\tau_p)^{1/2}p_n \exp(eV_0/kT)$$
$$= (e/kT)(I_p + I_{p0}). \tag{6b}$$

Eq. (6a) may be rewritten as

$$G = G_0[\tfrac{1}{2}(1 + \omega^2\tau_p^2)^{1/2} + \tfrac{1}{2}]^{1/2}$$
$$B = G_0[\tfrac{1}{2}(1 + \omega^2\tau_p^2)^{1/2} - \tfrac{1}{2}]^{1/2}. \tag{6c}$$

Finally, we obtain for the dc hole concentration in the n-region,

$$p'(x) = p_0' \exp(-\gamma_0 x) = p_0' \exp[-x/(D_p\tau_p)^{1/2}]. \tag{7}$$

We have thus derived all well-known formulas of junction diode theory.

III. Application to Junction Diode Noise Problems

Let the junction be short-circuited as far as ac is concerned, then, according to (3c), the ac hole concentration at $x=0$ is zero. The fluctuating hole *current* at $x=0$ is not zero, however, and the noise current in the external short-circuit is equal to it. We thus have to calculate the mean square value of this fluctuating hole current at $x=0$.

The noise in the p-n junction is caused by two mechanisms: fluctuations in the hole concentration at all points of the n-region due to diffusion, and to recombination. Both mechanisms are independent; their effects should, therefore, be added quadratically. For that reason, both effects are discussed separately. We assume again that all current is carried by holes and the n-region is infinitely long for all practical purposes.

We first turn to the random processes of hole-electron pair creation and recombination. We split the semiconductor into sections of length Δx. According to (2b), the above process corresponds to a dc hole current ($\partial p'/\partial t = 0$ for stationary current flow):

$$e(p' + p_n)\Delta x/\tau_p - ep_n\Delta x/\tau_p,$$

disappearing between x and $(x+\Delta x)$. The first term is due to hole-electron pair recombination and the second term is due to hole-electron pair creation. Since pair recombination and pair creation are independent random processes, the two currents fluctuate independently: because the individual events are independent and random, and because the chance of recombination within the interval Δx is very small, one would expect full shot effect for these currents. The mean square value of the Fourier component Δi_{px} is, therefore,

$$\langle \Delta i_{px}^2 \rangle_{av} = 2edf[e(p' + p_n)\Delta x/\tau_p + ep_n\Delta x/\tau_p] \quad (8)$$
$$= 2e^2df(p' + 2p_n)\Delta x/\tau_p.$$

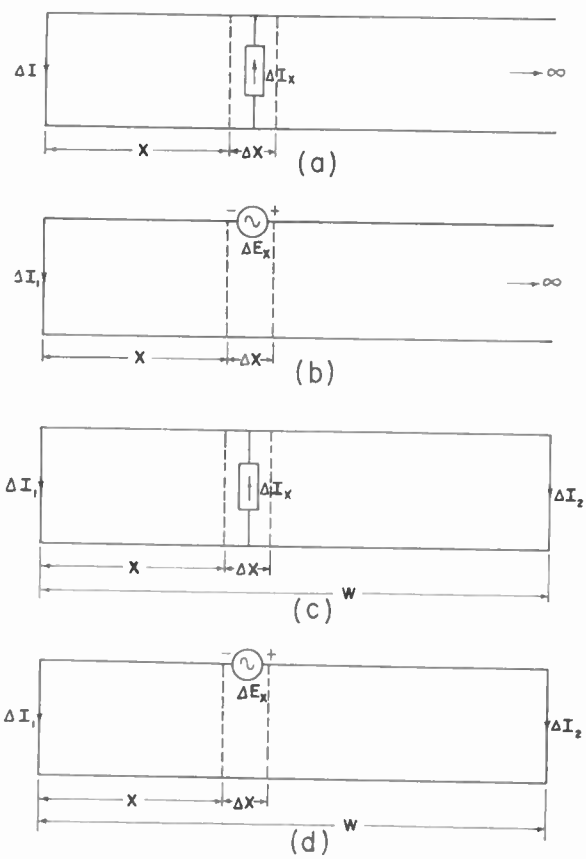

Fig. 1—Transmission line equivalent circuits of semi-conductor noise. (a) Equivalent circuit of recombination fluctuations in a junction diode. (b) Equivalent circuit of diffusion fluctuations in a junction diode. (c) Equivalent circuit of recombination fluctuations in a transistor. (d) Equivalent circuit of diffusion fluctuations in a transistor.

In our transmission line analogy, a current generator ΔI_x connected across the line at a distance x from the input gives rise to a current ΔI in the lead short-circuiting the input (Fig. 1(a)):

$$\Delta I = \Delta I_x \exp(-\gamma x).$$

Applying this to our $p-n$ junction, we find for the mean square value of the hole current in the lead short-circuiting the input, due to the hole current generator Δi_{px},

$$\langle \Delta i_p^2 \rangle_{av} = \langle \Delta i_{px}^2 \rangle_{av} \exp(-2ax)$$
$$= [2e^2df(p' + 2p_n)\Delta x/\tau_p] \exp(-2ax), \quad (9a)$$

where a is the real part of γ:

$$a = [(1 + \omega^2\tau_p^2)^{1/2} + 1]^{1/2}/(2D_p\tau_p)^{1/2} = \gamma_0(G/G_0). \quad (9b)$$

We now turn to the effect of the random diffusion processes. We split the semi-conductor into sections of length Δx and calculate the density fluctuations δp in these sections. Making a Fourier analysis of these fluctuations, we find for the mean square value of the Fourier components Δp_x of δp:

$$\langle \Delta p_x^2 \rangle_{av} = 4(p' + p_n)\Delta x df/D_p. \quad (10)$$

An indirect proof of this formula is given at the end of this section.

In our transmission line analogy a fluctuating emf ΔE in series with line between x and $(x+\Delta x)$ produces a current ΔI in lead short-circuiting input [Fig. 1(b)]:

$$\Delta I = (\Delta E/Z_0) \exp(-\gamma x). \quad (11)$$

Therefore, the mean square value of the Fourier component of the fluctuating hole current in the lead short-circuiting the input of the junction is

$$\langle \Delta i_p^2 \rangle_{av} = [\langle \Delta p_x^2 \rangle_{av}/|Z_0|^2] \exp(-2ax)$$
$$= [4e^2df(p' + p_n)\Delta x/\tau_p](1 + \omega^2\tau_p^2)^{1/2}$$
$$\cdot \exp(-2ax). \quad (12)$$

We now add (9a) and (12) and integrate with respect to x. This yields for the mean square value of the Fourier component i_p of the hole current fluctuation at $x=0$ (equal to the current fluctuation in the external circuit):

$$\langle i_p^2 \rangle_{av} = (2e^2df/\tau_p)\left[\int_0^\infty (p'+2p_n) \exp(-2ax)dx\right.$$
$$\left. + 2(1+\omega^2\tau_p^2)^{1/2}\int_0^\infty (p'+p_n) \exp(-2ax)dx\right]$$
$$= 2edf[I_p(-1+2G/G_0)+I_{p0}(2G/G_0)]$$
$$= 4kTGdf - 2eI_pdf. \quad (13a)$$

The noise is thus represented by a current generator i_p in parallel to the junction. The final result in (13a) follows from substituting (7), putting

$$(1+\omega^2\tau_p^2)^{1/2} = -1+2(G/G_0)^2; \quad \gamma_0+2a = \gamma_0(1+2G/G_0);$$
$$Z_{00}/(\gamma_0\tau_p) = 1/e \quad (13b)$$

and finally substituting (4).

Equating

$$\langle i_p^2 \rangle_{av} = 2eI_{eq}df. \quad (14a)$$

we find for the equivalent saturated diode current I_{eq} of the junction,

$$I_{eq} = I_p(-1 + 2G_1G_0) + I_{p0}(2G/G_0). \quad (14b)$$

For low frequencies $G \simeq G_0$, and (14b) reduces to

$$I_{eq} = (I_p + 2I_{p0}). \quad (14c)$$

This allows a very simple interpretation; the noise is just as if two currents (I_p+I_{p0}) and $-I_{p0}$ were flowing across the p-n barrier, each showing full shot effect.[2] That this interpretation gives the correct result, however, is accidental; it does not describe the physical mechanism and it would give erroneous results at higher frequencies. Equating

$$\langle i_p^2\rangle_{av} = n\cdot(4kTGdf), \tag{15a}$$

we find, for the noise ratio of the junction,

$$n = 1 - (1/2)(G_0/G)I_p/(I_p + I_{p0}). \tag{15b}$$

For low frequencies $G\simeq G_0$, and (15b) reduces to the well-known formula

$$n = n_0 = (1/2)(I_p + 2I_{p0})/(I_p + I_{p0}), \tag{15c}$$

which follows immediately from combining (14c) and (6b). At very high frequencies the noise ratio rises from the low-frequency value n_0 to the limiting value $n_\infty = 1$. This agrees very well with the experimental results.[3] The calculations thus give a simple explanation of the fact that n is relatively independent of frequency and also explain the finer details of the experiments.

For $I_p=0$ we find $n=1$ at all frequencies, as would be expected from Nyquist's theorem. Note that this result is only achieved because of (10). Any other expression would have resulted in a violation of Nyquist's theorem for $I_p=0$. Our final result thus gives an indirect verification of (10) for $p'=0$. Since the random diffusion processes affect the equilibrium hole concentration p_n and the excess hole concentration p' in the same manner, p' and p_n have to occur in the formula in the same way. We therefore conclude, even without a detailed proof, that (10) must be correct. Up to now we have not yet been able to give a *direct* proof of (10).

It is sometimes convenient to know the noise resistance R_n of the junction. Since R_n is a measure for the noise emf in series with the junction, we find its value by putting

$$4kTR_ndf = \langle i_p^2\rangle_{av}/|Y|^2, \tag{16a}$$

where Y is the junction admittance. This yields

$$R_n = (1/2G_0)[2(G/G_0)(I_p + I_{p0}) - I_p] \cdot\{(I_p + I_{p0})[2(G/G_0)^2 - 1]\}^{-1}: \tag{16b}$$

for low frequencies $(G\simeq G_0)$ this reduces to the well-known formula,

$$R_n = R_{n0} = (1/2G_0)(I_p + 2I_{p0})/(I_p + I_{p0}). \tag{16c}$$

We thus see that R_n decreases with increasing frequency.

[2] The result obtained at low frequencies is, therefore, identical with what would be expected from the emission theory (compare: A. van der Ziel, "Noise," Prentice-Hall, New York, 1954: p. 216). An earlier treatment appears in V. F. Weisskopf, "On the Theory of Noise in Conductors, Semi-conductors, and Crystal Rectifiers." NDRC 14-33, May 15, 1943.

[3] R. L. Anderson and A. van der Ziel. "On the shot effect of p-n junctions," TRANS. IRE, vol. EO-1, pp. 20–24; November, 1952.

IV. Dc and Ac Operation of Transistors

We now apply our theory to p-n-p transistors and assume again that all current is carried by holes. The difference with the junction diode case is that the n-region is now much shorter. It corresponds to a transmission line of finite length. Let w be the width of the n-region.

In our calculations we often have to apply emf's to the emitter junction and (or) to the collector junction. Since the base layer (n-layer) has a true base resistance r_b', this is not quite equivalent to applying these emf's between the emitter and base electrodes and (or) between the collector and base electrodes, respectively. For the same reason, short-circuiting the emitter and collector junction is not quite equivalent to putting short-circuiting connections between the emitter and base electrodes and between the collector and base electrodes, respectively. This is important for the equivalent circuit that is going to be developed.

If we have a transmission line of length w, with a voltage E_s at the sending end and a voltage E_R at the receiving end, then the voltage distribution along the line is

$$E(x) = E_s[\sinh\gamma(w - x)/\sinh\gamma w] + E_R(\sinh\gamma x/\sinh\gamma w), \tag{17}$$

and the input and output currents are

$$I_s = E_s/(Z_0\tanh\gamma w) - E_R/(Z_0\sinh\gamma w)$$
$$I_R = E_s/(Z_0\sinh\gamma w) - E_R/(Z_0\tanh\gamma w). \tag{18}$$

We can apply this directly to the n-region of our p-n-p transistor. Let V_e be the dc signal applied across the emitter junction and V_c the dc signal applied across the collector junction. If p_n is the equilibrium hole concentration in the n-region, then the excess hole concentration $p_{e0'}$ at the emitter junction $(x=0)$ and the excess hole concentration p_{c0}' at the collector junction $(x=w)$ are given by the equations

$$p_{e0}' = p_n[\exp(eV_e/kT) - 1];$$
$$p_{c0}' = p_n[\exp(eV_c/kT) - 1]. \tag{19}$$

$p_{c0}'\simeq -p_n$ if the collector is properly biased.

If small ac signals

$$v_e = V_{e1}\exp(j\omega t) \quad\text{and}\quad v_c = V_{c1}\exp(j\omega t)$$

are applied across the emitter and the collector junction, respectively, the ac hole densities at the emitter junction $(x=0)$ and at the collector junction $(x=w)$ are

$$p_{e1}'\exp(j\omega t) = (e/kT)V_{e1}\exp(j\omega t)\cdot p_n\exp(eV_e/kT),$$
$$p_{c1}'\exp(j\omega t) = (e/kT)V_{c1}\exp(j\omega t)\cdot p_n\exp(eV_c/kT),$$

because the hole densities at $x=0$ and at $x=w$ readjust themselves almost instantaneously to the applied voltages. $p_{c1}'\simeq 0$ if the collector is properly biased. This is usually the case and we shall assume that it is true here.

We thus have for the dc excess hole density distribution in the n-region, according to (17),

$$p'(x) = p_{e0}'[\sinh \gamma_0(w - x)/\sinh \gamma_0 w] + p_{c0}'(\sinh \gamma_0 x/\sinh \gamma_0 w); \quad (20)$$

whereas the dc hole currents at $x=0$ and $x=w$ are

$$I_e = p_{e0}'/(Z_{00} \tanh \gamma_0 w) - p_{c0}'/(Z_{00} \sinh \gamma_0 w).$$
$$I_c = p_{e0}'/(Z_{00} \sinh \gamma_0 w) - p_{c0}'/(Z_{00} \tanh \gamma_0 w). \quad (21a)$$

If $V_c=0$, then $p_{c0}'=0$ and, consequently,

$$I_e = I_{ee}[\exp(eV_e/kT)-1]; \; I_{ee} = p_n/(Z_{00} \tanh \gamma_0 w). \quad (21b)$$

If $V_e=0$, then $p_{e0}'=0$ and, consequently,

$$I_c = -I_{cc}[\exp(eV_c/kT)-1]; \; I_{cc} = p_n/(Z_{00} \tanh \gamma_0 w). \quad (21c)$$

In that case $I_c \simeq I_{cc}$ if the collector is properly biased. $I_{cc}=I_{ee}$ if p_n is uniform in the n-region; we tacitly assumed this to be the case. The base current I_b is, if $p_{c0}' \simeq -p_n$,

$$I_b = (I_e - I_c) = (1 - \alpha_0)[I_e - I_{cc}(1 + \alpha_0)]; \quad (21d)$$

where

$$\alpha_0 = 1/(\cosh \gamma_0 w) \quad (21e)$$

is a quantity that is close to unity if the width w of the n-region is small. Hence,

$$I_e = I_{cc}(1 + \alpha_0) \quad (21f)$$

for the case of zero base current (floating base). This does not seem to agree with experiments which seems to require a much larger emitter current for floating base. Leakage currents are partly responsible for this discrepancy.[4]

We now apply small ac voltages across the two junctions and neglect effects due to the change in width w of the junction; we shall take that into account later. We also assume that the collector is biased such that p_{c1}' is negligible. We then have at the emitter side

$$i_e = p_{e1}' \exp(j\omega t)/(Z_0 \tanh \gamma w) = V_{e1} \exp(j\omega t) Y_e, \quad (22)$$

and at the collector side,

$$i_c = p_{e1}' \exp(j\omega t)/(Z_0 \sinh \gamma w) = \alpha V_{e1} \exp(j\omega t) Y_e = \alpha i_e; \quad (23a)$$

where

$$\alpha = 1/(\cosh \gamma w) = 1/\cosh[\gamma_0 w(1 + j\omega\tau_p)^{1/2}]. \quad (23b)$$

α is the current amplification factor: its value α_0 for low frequencies was already introduced by (21e). The emitter junction admittance Y_e is

$$Y_e = (p_{e1}/V_{e1})/(Z_0 \tanh \gamma w) = (e/kT)p_n \exp(eV_e/kT)/(Z_0 \tanh \gamma w). \quad (24a)$$

For low frequencies this expression reduces to

$$Y_e = g_{e0} = (e/kT)p_n \exp(eV_e/kT)/(Z_{00} \tanh \gamma_0 w) = (e/kT)[I_e + (1 - \alpha_0)I_{cc})], \quad (24b)$$

so that the expression for high frequencies may be written

$$Y_e = g_{e0}(1+j\omega\tau_p)^{1/2} \tanh \gamma_0 w/\tanh[\gamma_0 w(1+j\omega\tau_p)^{1/2}]. \quad (24c)$$

We have thus verified the well-known transistor formulas by this method. We note that our problem reduces to the junction diode problem mentioned previously if $w \to \infty$, this corresponds to $\alpha_0 \to 0$.

We now turn to the effects caused by the change in width of the n-region due to the ac voltages V_e and V_c applied across the emitter and the collector junction, respectively. These effects occur because the width of the transition region of a p-n junction depends upon the voltage applied across the junction. Usually the effects of the fluctuating boundary at the emitter side can be neglected but the effects of the fluctuating boundary at the collector side have to be taken into account. This has three effects:[5]

1. It modulates the true resistance r_b' of the base region; described by an emf $\mu_{bc}V_c$ in series with r_b'.
2. It modulates the current amplification factor α, this gives rise to a collector junction admittance Y_c'.
3. It modulates the current flow across the emitter junction; this can be described by a fluctuating emf $\mu_{ec}V_c$ in series with Y_e.

In addition true capacitance C_c of collector junction is in parallel to Y_c'. Equivalent circuit is shown in Fig. 2. At high frequencies μ_{ec} and Y_c' may be complex.

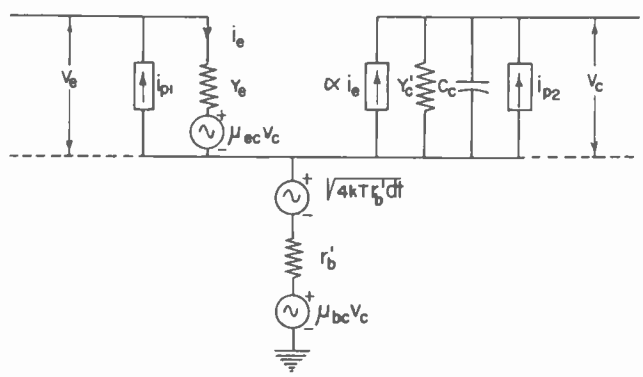

Fig. 2—Equivalent circuit of noise in junction transistors. The noise is described by two partially correlated current generators i_{p1} and i_{p2}, the feedback properties by two emf's $\mu_{ec}v_c$ and $\mu_{bc}v_c$.

V. Application to Noise Problems in Transistors

We now want to calculate the noise currents flowing across the emitter and collector junctions when both junctions are short-circuited. Our diffusion problem

[4] L. J. Giacoletto, private communication.

[5] J. M. Early, "Effects of space-charge layer widening in junction transistors," Proc. IRE, vol. 40, pp. 1401–1406; November, 1952.
L. J. Giacoletto, "Study of p-n-p alloy junction transistor from dc through medium frequencies," *RCA Rev.*, vol. 15, pp. 506–562; December, 1954.

thus corresponds to a transmission line with input and output short-circuited.

We divide the n-region of the transistor into small sections of length Δx. The noise due to hole-electron pair creation and recombination in the region between x and $(x+\Delta x)$ may then again be represented by a parallel current generator Δi_{px} and the noise due to random diffusion processes may be represented by a fluctuating hole density Δp_x between x and $(x+\Delta x)$. According to Section III,

$$\langle \Delta i_{px}^2 \rangle_{av} = 2e^2 df(p' + 2p_n)\Delta x/\tau_p;$$
$$\langle \Delta p_x^2 \rangle_{av} = 4(p' + p_n) df \Delta x/D_p. \tag{25}$$

We now apply the same reasoning as in Section III; the only difference is that we now have an equivalent transmission line of finite length w, short-circuited at both ends, and that we have to know the short-circuit currents at both the input and the output.

In our transmission line case, a parallel-connected current generator ΔI_x between x and $(x+\Delta x)$ produces currents ΔI_1 and ΔI_2 in input and output [Fig. 1(c)]:

$$\Delta I_1 = \Delta I_x \sinh \gamma(w - x)/\sinh \gamma\, w;$$
$$\Delta I_2 = \Delta I_x \sinh \gamma x/\sinh \gamma w|; \tag{26}$$

and an emf ΔE_x connected between x and $(x+\Delta x)$ produces currents $\Delta I_1'$ and $\Delta I_2'$ in input and output [Fig. 1(d)]:

$$\Delta I_1' = -(\Delta E_x/Z_0) \cosh \gamma(w - x)/\sinh \gamma w;$$
$$\Delta I_2' = +(\Delta E_x/Z_0) \cosh \gamma x/\sinh \gamma w. \tag{27}$$

We thus have for our diffusion problem,

$$\Delta i_{p1} = \Delta i_{px} \sinh \gamma(w - x)/\sinh \gamma w - (\Delta p_x/Z_0) \cosh \gamma(w - x)/\sinh \gamma w$$
$$\Delta i_{p2} = \Delta i_{px} \sinh \gamma x/\sinh \gamma w + (\Delta p_x/Z_0) \cosh \gamma x/\sinh \gamma w. \tag{28}$$

Since Δi_{px} and Δ_{px} are uncorrelated, Δi_{p1} and Δi_{p2} will be only *partially* correlated.

We find, therefore, that the noise of the transistors can be represented by two partially correlated current generators i_{p1} and i_{p2} across the emitter and collector junctions, respectively. These quantities are obtained by summing the effects of the individual sections Δx. Since fluctuations in different intervals are independent and since Δi_{px} and Δp_x are independent also, the fluctuations have to be added quadratically. Replacing the summation by an integration, we obtain

$$\langle i_{p1}^2 \rangle_{av} = \sum \langle \Delta i_{p1}^2 \rangle_{av} = \int_0^w \langle \Delta i_{px}^2 \rangle_{av} |\sinh \gamma(w-x)/\sinh \gamma w|^2 + \int_0^w \langle \Delta p_x^2 \rangle_{av} |\cos \gamma(w-x)/\sinh \gamma w|^2/|Z_0|^2 \tag{29}$$

$$\langle i_{p2}^2 \rangle_{av} = \sum \langle \Delta i_{p2}^2 \rangle_{av} = \int_0^w \langle \Delta i_{px}^2 \rangle_{av} |\sinh \gamma x/\sinh \gamma w|^2 + \int_0^w \langle \Delta p_x^2 \rangle_{av} |\cosh \gamma x/\sinh \gamma w|^2/|Z_0|^2 \tag{30}$$

$$\langle i_{p1}^* i_{p2} \rangle_{av} = \sum \langle \Delta i_{p1}^* \Delta i_{p2} \rangle_{av} = \int_0^w \langle \Delta i_{px}^2 \rangle_{av} [\sinh \gamma^*(w-x) \sinh \gamma x/|\sinh^2 \gamma w|] - \int_0^w \langle \Delta p_x^2 \rangle_{av} [\cosh \gamma^*(w-x) \cdot \cosh \gamma x/|\sinh^2 \gamma w|]/|Z_0|^2. \tag{31}$$

The problem of noise in transistors is hereby solved in principle for all frequencies. For small w the term with $\langle \Delta p_x^2 \rangle_{av}$ predominates; that is, diffusion is the most important effect. In that case, the correlation coefficient for i_1 and i_2 is almost equal to -1, except at the highest frequencies (See Section VI).

The quantities i_{p1} and i_{p2} represent the effect of shot noise in transistors. Besides these two current generators, one has to introduce the thermal noise emf $(4kTr_b'df)^{1/2}$ of the true base resistance r_b'. The full equivalent circuit, as far as noise is concerned, is, therefore, as given in Fig. 2.

VI. Further Discussion of Transistor Noise

For relatively low frequencies we may put $\gamma = \gamma_0$ and $Z_0 = Z_{00}$, this simplifies the integrations in (29)–(31). Introducing (25) for $\langle \Delta i_{px}^2 \rangle_{av}$ and $\langle \Delta p_x^2 \rangle_{av}$, substituting (20) for $p'(x)$, carrying out the integrations in (29)–(31), substituting the expressions for I_e, I_c and I_{cc} and bearing in mind that $p'_{c0} \simeq -p_n$ in practice, we obtain:

$$\langle i_{p1}^2 \rangle_{av} = 2e[I_e + 2I_{cc}(1 - \alpha_0)]df \tag{32}$$
$$\langle i_{p2}^2 \rangle_{av} = 2eI_c df \tag{33}$$
$$\langle i_{p1}^* i_{p2} \rangle_{av} = -2e[I_c - I_{cc}(1 - \alpha_0)]df. \tag{34}$$

The emitter and collector current thus show full shot effect; the correlation coefficient c of the emitter current and the collector current fluctuations is

$$c = \langle i_{p1}^* i_{p2} \rangle_{av}/[\langle i_{p1}^2 \rangle_{av} \cdot \langle i_{p2}^2 \rangle_{av}]^{1/2} \simeq -(I_c/I_e)^{1/2} \simeq -\alpha_0^{1/2}; \tag{34a}$$

the latter part of the equation holds if we neglect a few small terms of the order $I_{cc}(1-\alpha_0)$. The correlation coefficient is thus closely equal to -1 at low frequencies.

Except perhaps for very small currents, the terms containing the quantity I_{cc} may be neglected at low frequencies. We would have obtained that approximation also, if we had neglected the terms p_{c0}' and p_n in $\langle \Delta i_{px}^2 \rangle_{av}$ and $\langle \Delta p_x^2 \rangle_{av}$. This should still be a reasonable approximation at very high frequencies, even though it may not be as accurate as at low frequencies. By substituting

$$p'(x) = p_{e0}' \sinh \gamma_0(w - x)/\sinh \gamma_0 w; \qquad \gamma = a + jb;$$
$$a = \gamma_0[\tfrac{1}{2} + \tfrac{1}{2}(1 + \omega^2\tau_p^2)^{1/2}]^{1/2};$$
$$b = \gamma_0[-\tfrac{1}{2} + \tfrac{1}{2}(1 + \omega^2\tau_p^2)^{1/2}]^{1/2} \tag{35}$$

into (29)–(31) and carrying out the integrations, we obtain

$$\langle i_{p1}^2\rangle_{av} = 2eI_c df[-1 + \tanh \gamma_0 w\,(a \sinh 2aw + b \sin 2bw)/(\gamma_0 |\sinh^2 \gamma w|)] \tag{36}$$
$$\langle i_{p2}^2\rangle_{av} = 2eI_c df \tag{37}$$
$$\langle i_{p1}^* i_{p2}\rangle_{av} = -2eI_c df[\gamma \sinh \gamma_0 w/(\gamma_0 \sinh \gamma w)]. \tag{38}$$

Introducing the emitter junction admittance $Y_e = g_e + jb_e$ [(24)], and bearing in mind that $I_c = \alpha_0 I_e$ and that $Y_e = g_{e0} = eI_e/kT$ at low frequencies, these equations may be written:

$$\langle i_{p1}^2\rangle_{av} = 2eI_c df(-1 + 2g_e/g_{e0}) = 2kTdf\cdot(2g_e - g_{e0}) \tag{36a}$$
$$\langle i_{p2}^2\rangle_{av} = 2eI_c df = 2kTdf\cdot\alpha_0 g_{e0} \tag{37a}$$
$$\langle i_{p1}^* i_{p2}\rangle_{av} = -2kTdf\cdot\alpha Y_e \tag{38a}$$

Eq. (36a) is equivalent to (13a) of the junction diode.

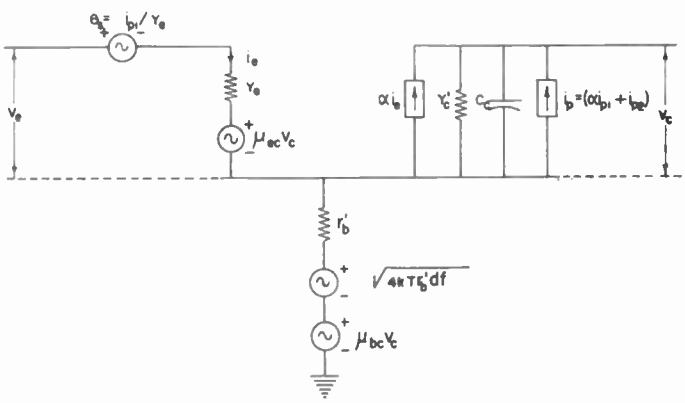

Fig. 3—Other form of equivalent circuit. The noise is now described by an emf $e_s = i_{p1}/Y_e$ in series with the input and a current generator $i_p = (i_{p2} + \alpha i_{p1})$ in parallel to the collector junction. This circuit is completely equivalent to the one shown in Fig. 2.

Our next step is to modify the equivalent circuit of Fig. 2. We observe that it is formally equivalent to circuit shown in Fig. 3 (above), where noise is represented by a noise emf $e_s = i_{p1}/Y_e$ in series with the input and a noise current generator $i_p = (i_{p2} + \alpha i_{p1})$ in parallel to the collector admittance. Applying (32)–(34) and neglecting a few small terms of the order $I_{ce}(1 - \alpha_0)$, we obtain at low frequencies:

$$\langle e_s^2\rangle_{av} = \langle (i_{p1}/Y_e)^2\rangle_{av} = 2kTr_{e0}df \tag{39}$$
$$\langle i_p^2\rangle_{av} = \langle (i_{p2} + \alpha_0 i_{p1})^2\rangle_{av} = 2e\alpha_0(1 - \alpha_0)I_e df \tag{40}$$
$$\langle e_s^* i_p\rangle_{av} = \langle i_{p1}^*(i_{p2} + \alpha_0 i_{p1})\rangle_{av} r_{e0} = 0, \tag{41}$$

where r_{e0} is the emitter junction resistance at low frequencies. Hence e_s and i_p are practically uncorrelated. Except for the term due to the shot effect of the collector saturated current I_{c0}, the equivalent circuit of Fig. 3 shows resemblance with a phenomenological equivalent circuit published earlier.[6]

At higher frequencies this is no longer the case; e_s and i_p have a complex correlation coefficient $c \neq 0$ and their mean square values differ from the corresponding low-frequency values. Applying (36)–(38), we obtain:

$$\langle e_s^2\rangle_{av} = \langle i_{pi}^2\rangle_{av}/|Y_e|^2 = 2kTdf\cdot(2g_e - g_{e0})/(g_e^2 + b_e^2) \tag{42}$$
$$\langle i_p^2\rangle_{av} = 2eI_c(1 - |\alpha|^2/\alpha_0)df = 2kTdf\cdot\alpha_0 g_{e0}(1 - |\alpha|^2/\alpha_0) \tag{43}$$
$$\langle e_s^* i_p\rangle_{av} = 2kTdf\cdot\alpha(1 - g_{e0}/Y_e^*). \tag{44}$$

At low frequencies (42) reduces to (39), (43) reduces to (40), and (44) reduces to (41).

In the phenomenological equivalent circuit the emf e_s was ascribed to "shot noise" and the current generator i_p was ascribed to "partition noise"; the latter meant that the noise is caused by fluctuations in the recombination processes. To show that at low frequencies the recombination fluctuations predominate over diffusion fluctuations in i_p, we apply (28) and write

$$i_p = \sum(\Delta i_{p2} + \alpha\Delta i_{p1}) = \alpha\sum(\Delta i_{px}\cosh \gamma x + \Delta p_x \sinh \gamma x/Z_0),$$

where the summation extends over all sections Δx of the base region. Consequently,

$$\langle i_p^2\rangle_{av} = |\alpha^2|\left[\int_0^w \langle \Delta i_{px}^2\rangle_{av}|\cosh^2 \gamma x| + \int_0^w \langle(\Delta p_x/Z_0)^2\rangle_{av}|\sinh^2 \gamma x|\right]. \tag{45}$$

The first term in this equation is due to recombination fluctuations and the second is due to diffusion fluctuations. For good junction transistors α_0 is close to unity and $|\cosh^2 \gamma x| \gg |\sinh^2 \gamma x|$ at low frequencies; therefore the recombination fluctuations predominate in i_p at low frequencies. In the same way it may be shown that diffusion fluctuations predominate in e_s at low frequencies.

The present calculation does not verify the existence of a noise term due to the shot effect of the collector saturated current. Further experimental and theoretical work is needed to clarify that situation.

The equivalent circuit also contains two feedback emf's $\mu_{ec}v_c$ and $\mu_{bc}v_c$. A calculation shows that these emf's, which are important for the amplification properties of the transistor, hardly alter the noise figure; they may therefore be omitted as far as noise considerations are concerned. This indicates that the "base resistance r_b" in the earlier phenomenological equivalent circuit actually should be the "true" base resistance r_b' of the new equivalent circuit. The numerical value for r_b that

[6] H. C. Montgomery and M. A. Clark, "Shot noise in junction transistors," *Jour. Appl. Phys.*, vol. 24, pp. 1397–1398; November, 1953.
A. van der Ziel, "Note on shot and partition noise in junction transistors," *Jour. Appl. Phys.*, vol. 25, pp. 815–816; June, 1954.

was used by Montgomery and Clark in their calculation of the noise figure actually represented the true base resistance of their transistor.[7]

It is also possible to change the equivalent circuit of Fig. 2 by replacing the emf $\mu_{ec}v_c$ by a current generator $Y_{ec}v_c$, where $Y_{ec}=\mu_{ec}Y_c$, the current generator αi_e by a current generator $Y_{ce}v_e$, where $Y_{ce}=\alpha Y_e$, and the admittance Y_c' by an admittance:

$$Y_c'' = Y_c' + \alpha\mu_{ec}Y_e \tag{46}$$

(Y_c' is the collector junction admittance for open emitter junction and Y_c'' the collector junction admittance for short-circuited emitter junction). The circuit thus obtained closely resembles a phenomenological circuit proposed by Giacoletto.[8]

VII. Noise Figure

Let a signal source of internal impedance $Z_s=(r_s+jX_s)$ be connected to the input and let the thermal noise of the signal source be represented by an emf $(4kTr_sdf)^{1/2}$ in series with Z_s. Let the output terminals be open and let $\langle v_{ct}^2\rangle_{av}$ and $\langle v_{cs}^2\rangle_{av}$ represent the mean square value of the noise voltage across the collector junction due to transistor noise and the thermal noise of the signal source, respectively. Since $(Y_c'+j\omega C_c)$ is a small admittance, we may in first approximation assume that the noise voltages developed in the base resistance are small in comparison with the noise voltage across $(Y_c'+j\omega C_c)$. The noise figure F may then be defined as:

$$F = 1 + \langle v_{ct}^2\rangle_{av}/\langle v_{cs}^2\rangle_{av} \tag{47}$$

Calculating v_{ct} and v_{cs}, introducing the emitter junction impedance $Z_e=1/Y_e=(r_e+jX_e)$ and putting $Z_{tot}=(Z_e+Z_s+r_b')$, we obtain:

$$F = 1 + r_b'/r_s + \langle(-e_s + i_pZ_{tot}/\alpha] \cdot(-e_s^* + i_p^*Z_{tot}^*/\alpha^*)\rangle_{av}/(4kTr_sdf). \tag{48}$$

This does not contain any reference to the feedback emf's, indicating that feedback does not affect the noise figure in this approximation.

It may be shown that F is a minimum if:

$$X_s + X_e = -X_e/(-1+\alpha_0/|\alpha|^2) \tag{49}$$

$$r_s = \{[(-1+\alpha_0/|\alpha|^2)(r_e+r_b')+r_e]^2 - (\alpha_0/|\alpha|^2)(r_e^2+X_e^2)\}^{1/2}/(-1+\alpha_0/|\alpha|^2)^{1/2} \tag{50}$$

in which case:

$$F = F_{\min} = [(-1+\alpha_0/|\alpha|^2)(r_e+r_b')+r_e]/r_{e0} + \{[(-1+\alpha_0/|\alpha|^2)(r_e+r_b')+r_e]^2/r_{e0}^2 - (\alpha_0/|\alpha|^2)(r_e^2+X_e)^2/r_{e0}^2\}^{1/2} \tag{51}$$

For low frequencies $\alpha=\alpha_0$, $r_e=r_{e0}$ and $X_e=0$, so that:

$$F_{\min} = \{[1+(1-\alpha_0)r_b'/r_{e0}] + \sqrt{[1+(1-\alpha_0)r_b'/r_{e0}]^2-\alpha_0}\}/\alpha_0 \tag{52}$$

The minimum noise figure at low frequencies is thus mainly determined by the quantity $(1-\alpha_0)r_b'/r_{e0}$; for low noise figure this quantity should be small. At higher frequencies the noise figure increases because the current amplification factor α goes to zero and $\langle i_p^2\rangle_{av}$ increases from the low-frequency value $2eI_c(1-\alpha_0)df$ to the high-frequency value $2eI_cdf$.

Conclusion

The above developments show that the transmission line analogy can be successfully applied to the solution of noise problems in junction diodes and transistors. It is interesting to note that at low frequencies the new theory shows resemblance with older phenomenological equivalent circuits. Besides, the theory also gives the hf noise behavior of the devices, a result that could not be obtained by the old method. The earlier experimental results on noise in junction diodes find hereby an adequate theoretical explanation.

The theory is a *one-dimensional* theory and the recombination is assumed to be volume recombination. Actually most recombination occurs at the surface and the problem is multi-dimensional. Deviations between theory and experiment might thus be expected in some cases. A research program is under way at the University of Minnesota to check this theory with experiment.

Acknowledgment

The author is indebted to Dr. D. O. North, RCA Labs., Princeton, N. J., for suggesting the method and for helpful criticism during the preparation of the paper; to Prof. R. E. Burgess, University of British Columbia, Vancouver, B. C., Canada, for discussions on the problem; to Dr. M. J. O. Strutt, Swiss Federal Institute of Technology, Zürich, Switzerland, for suggesting the equivalence of the equivalent circuits of Figs. 2 and 3 and for sending a pre-publication copy of a paper by W. Guggenbühl and M. J. O. Strutt on noise in transistors; and to Dr. L. G. Giacoletto, RCA Labs., Princeton, N. J., for important improvements in the manuscript.

[7] H. C. Montgomery, private communication.

[8] L. J. Giacoletto, Semiconductor Devices Conference. Minneapolis, Minn., June, 1954.

Multiple Frequency Shift Teletype Systems*

D. B. JORDAN†, ASSOCIATE, IRE, H. GREENBERG‡, ASSOCIATE, IRE,
E. E. ELDREDGE§, SENIOR MEMBER, IRE AND W. SERNIUK||, SENIOR MEMBER, IRE

Summary—**Radio teletype transmission is of such a nature that once the signal goes far enough into noise, reliable reception rapidly deteriorates. This paper calls attention to a system for radio teletype communication that has advantages that have been demonstrated both theoretically and experimentally. A new system for teletype communication is described that involves the use of several frequencies instead of the two, called "mark and space," used in convention frequency shift keying (FSK) operation. By so doing, longer pulses are allowed for equivalent transmission rates, and as a result smaller detection bandwidths are possible. The main advantage is a greater correlation between received signal plus noise and the transmitted signal. Probability of error from information theory is used to find the theoretical gain of two multiple frequency shift (MFS) systems over the conventional FSK system. Coding, filters, and special circuitry are described. An experimental comparison of one MFS system and conventional FSK operation is presented on the basis of error counts using both white and impulse noise superimposed on the signal. Theoretical gains are checked by the laboratory experimental work.**

Introduction

IN FREQUENCY shift telegraphy the carrier frequency is shifted rather than interrupted for the transmission of intelligence, that is, the "mark" and "space" signals are transmitted by two radio frequencies differing by an audio frequency. Frequency shift keying is, therefore, analogous to frequency modulation of a carrier with square waves.

A basic advantage of the frequency shift method over on-off keying of a continuous wave carrier is that the former is capable of handling large and rapid changes in signal amplitude with less distortion than the latter method, particularly in the case of long-distance radio telegraphy in the high frequency range. Also, the fact that there is a signal being received at all times permits the frequency shift method to make more effective use of agc circuits than is possible with on-off keying.

Estimates of the gain of frequency shift over "on-off" keying range from 6 to 10 decibels. This paper describes a system which gives further improvement in signal-to-noise ratio and for which improved performance under multipath conditions is to be expected. An added feature of the system is a carrier pulse which simplifies automatic frequency control and permits synchronous operation. This paper includes a discussion of both the theoretical development and experimental verification of system performance.

* Original manuscript received by the IRE, February 18, 1955; revised manuscript received, June 6, 1955.
† Republic Aviation Corp., Guided Missile Div., Hicksville, N. Y.
‡ Ramo-Wooldridge Corp., Los Angeles, Calif.
§ Electronic Defense Laboratory, Sylvania Electric Products, Inc., Mountain View, Calif.
|| Physics Lab., Sylvania Electric Products, Inc., Bayside, N. Y.

Theoretical Development

Commercial frequency shift keying (FSK) radio teletype operators have found in the past that, during high noise conditions, reception is considerably improved by a reduction in rate of transmission. Alternatively the operator repeats the message in the hope that by so doing it may be understood in its entirety. Both these schemes, slower transmission and redundancy, are undesirable when traffic is heavy. By slowing down transmission speed, the operator actually increases the pulse time. This method would thus be advantageous if a reduction in keying speed could be accomplished without the corresponding undesirable and costly reduction in traffic. Such is possible through the use of a multiple frequency shift (MFS) system in which the carrier frequency is shifted to one of several alternate values for a longer time rather than to only one of two frequencies for a short period, as in FSK. Standard transmitters and existing teletypewriter equipment are adaptable to these systems through the use of a coder and decoder, and the change is kept entirely within the transmitter-receiver section of the communication system (Fig. 1). The experimental work on one such system is described below.

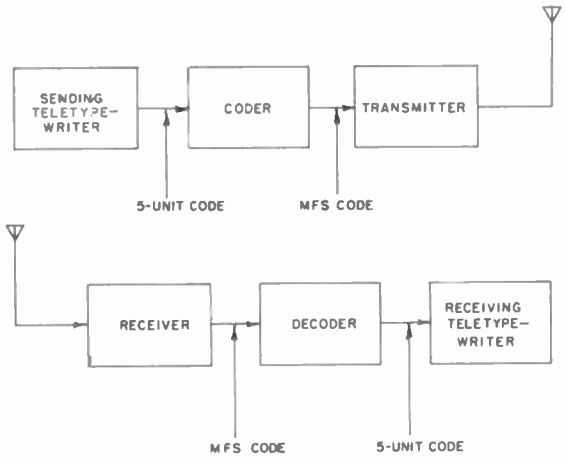

Fig. 1—Block diagram of communication system employing MFS.

Of course new coding schemes will be necessary when MFS systems are employed. To calculate the coding necessary, use will be made of the logarithmic measure of information:

$$H = \log_2 N,$$

where $\log_2$ indicates taking the logarithm to the base 2,

N is the number of possible messages, and H is the amount of information, in bits, of each message.[1]

Standard teletype communication uses 32 information symbols or "messages," (26 for letters plus six extra symbols for carriage shift, line feed, etc.) which means that each contains five bits of information, since $\log_2 32 = 5$. The symbols of each system must, therefore, each contain not less than this amount. From the expressions

binary FSK (2 channel) : $5 \log_2 2 = 5$

quadruple MFS (4 channel) : $3 \log_2 4 = 6$
sextuple MFS (6 channel) : $2 \log_2 6 = 5.17$
single-pulse MFS (32 channel): $1 \log_2 32 = 5$,

it can be seen that the conventional binary FSK system satisfies this requirement by using 5 information pulses per symbol. MFS systems using 4, 6 and 32 alternate frequency positions or "channels" would thus need three, two, or one information pulses per symbol respectively. Also note that the quadruple (4-channel) system is wasteful of information when used with standard teletype equipment, and for this reason it will not be further discussed here.

It was stated that MFS systems employ pulses which are longer in time than those used by the conventional FSK system. MFS systems gain their advantage from the fact that a pulse of twice the length requires one-half the bandwidth for the same resolution, and since random noise power varies as the bandwidth, the signal-to-noise power ratio is doubled. In so doing, the rate of transmission of information is not reduced. As a standard of comparison, consider the conventional FSK system running at 60 words per minute. This corresponds to a keying speed of 42 bauds or a transmission rate of 163 milliseconds per letter. In the following discussion this figure of 163 milliseconds per letter will be used as the standard of comparison. For binary transmission this figure is divided into a 22 millisecond "start pulse," five information pulses, each 22 milliseconds long, and a "stop pulse" of 31 milliseconds. Since the start pulse only serves the purpose of releasing a clutch mechanism in the receiving teletypewriter, it will be unnecessary in MFS transmission, as this action can be supplied by the decoder. However, the stop pulse will be held for synchronization purposes and the operation of automatic frequency control. Since this stop pulse will have its own frequency channel, its length, and thus its bandwidth, can be prescribed separately in the over-all system design. If it is matched with the transmission pulse in the sextuple MFS system, then it will add only one-sixth to the *total* systems bandwidth. This is a separate consideration to transmission-channel bandwidth.

Fig. 2 indicates those frequencies to which the carrier frequency is shifted for the purpose of sending information in three systems. The binary system does not use the carrier frequency but rests on the mark frequency whereas the MFS systems will use the carrier frequency as a "stop" signal for time synchronization and automatic frequency control.

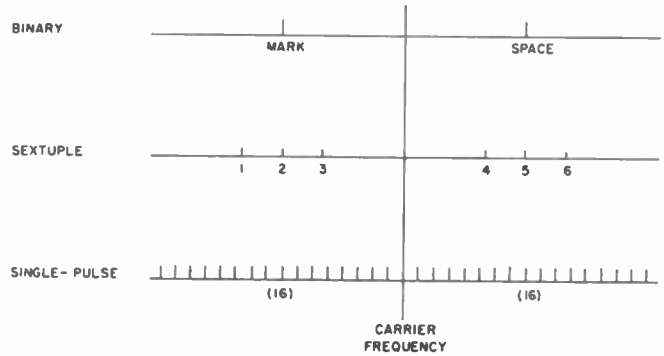

Fig. 2—Frequency band division for three systems.

The transmission of a message using the sextuple system at a similar word-per-minute rate as the binary system is shown diagramatically in Fig. 3.

It is seen that for the same information transmission rate the keying speed has been considerably cut down in MFS transmission. The pulses of the sextuple system are 66 milliseconds long and those of the single-pulse system would be 132 milliseconds long. These increases in time indicate a reduction in bandwidth per channel of three and six times, resulting in a like increase in the signal-to-noise power ratio. As for bandwidth economy, the single-pulse 32-shift system is costly since this system requires a total bandwidth of almost three times the total bandwidth required by the binary system, whereas the sextuple system requires approximately the same bandwidth as the binary system, as is shown later.

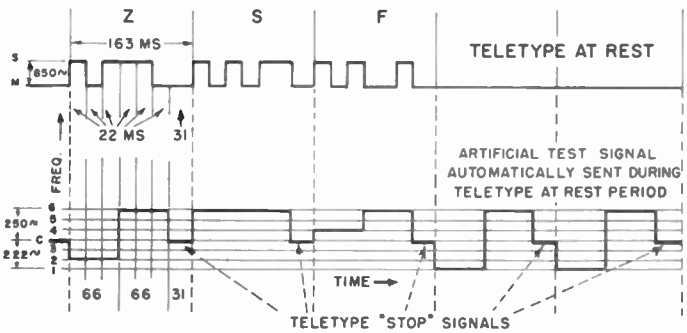

Fig. 3—Comparison of sextuple code and teletype code. Note that the "stop" signals occur at the assigned carrier frequency which is the center of the transmitting band. It is used for carrier frequency control (AFC) as well as decoder motor synchronization. Time period based on 60wpm teletype operation.

Considerable gains have been achieved in the laboratory through a narrowing of the FSK "mark" and "space" bandwidths presently used; however, in the theoretical analysis, bandwidths will be normalized to those used by the binary system for comparison purposes.

[1] For convenience in the comparison calculations, it is assumed here that the messages are all equally probable.

Application of Probability Theory

To show the theoretical gains realizable for MFS systems, it is possible to analyze the probability of transmission error under standard noise conditions. The resultant envelope is detected when noise or noise plus signal is passed through a narrow band-pass filter. Thus, after demodulation, a level of voltage amplitude will be received in each channel for either the binary or multiple systems. A signal voltage V received in a given channel will be registered as a correct signal if xV volts or greater is received, where x is some multiplier of V. Thus we have set a "bias level" such that everything received above xV volts is considered a signal while everything received below xV volts is not. In envelope detection, the bias level is represented by a circle of radius xV. An error will occur if no signal is sent in a channel, i.e., no signal with the proper frequency for the given channel, and through the addition of noise, a voltage of greater than xV volts is received. Error may also occur in signal channel if there is subtractive effect due to noise, and resultant voltage reads below bias level.

The transition probabilities of error for a single letter, assuming white noise having a Gaussian voltage distribution, will be derived for the binary and multiple shift systems. The envelope of the noise will then have a bivariate normal distribution.

The probability of error for the signal channel is given by the probability the vector sum of noise and signal is less than xV. This probability is given by

$$P_V = \frac{1}{V_n^2} \int_0^{xV} v e^{-(v^2+V^2)/2V_n^2} I_0\left(\frac{vV}{V_n^2}\right) dv,$$

where V_n is the root mean square noise voltage and I_0 is a modified Bessel function of the first kind. The probability of registering a signal in a channel in which no signal is sent will be given by

$$P_0 = \frac{1}{V_n^2} \int_{xV}^{\infty} v e^{-v^2/2V_n^2} dv = e^{-(x^2/2)\cdot(S/N)}$$

where $S/N = (V/V_n)^2$ is the signal-to-noise power ratio.

It is now necessary to consider the error in a symbol for comparison between the frequency shift systems. Consider any arbitrary system of m channels using n pulses per symbol. The probability that a signal is received in the desired channel is $(1-P_V)$, and the probability that a signal, through the addition of noise, is not received in the other channels is $(1-P_0)^{m-1}$. Thus, the probability that all n pulses are received correctly is given by $(1-P_V)^n(1-P_0)^{n(m-1)}$ where the joint probabilities are the products of the simple probabilities.

Probability of error in a symbol for any system is

$$P_m = 1 - (1 - P_V)^n(1 - P_0)^{n(m-1)}.$$

The conventional FSK system uses five pulses per symbol and two channels; thus

$$P_2 = 1 - (1 - P_V)^5(1 - P_0)^5.$$

The sextuple system uses two pulses per symbol; thus

$$P_6 = 1 - (1 - P_V)^2(1 - P_0)^{10}.$$

The 32-channel system with one pulse per symbol gives

$$P_{32} = 1 - (1 - P_V)(1 - P_0)^{31}.$$

These expressions depend on signal-to-noise ratio, and on bias level xV. It may be expected that there exist optimum values of x such that probability of error is minima for each signal-to-noise ratio value.

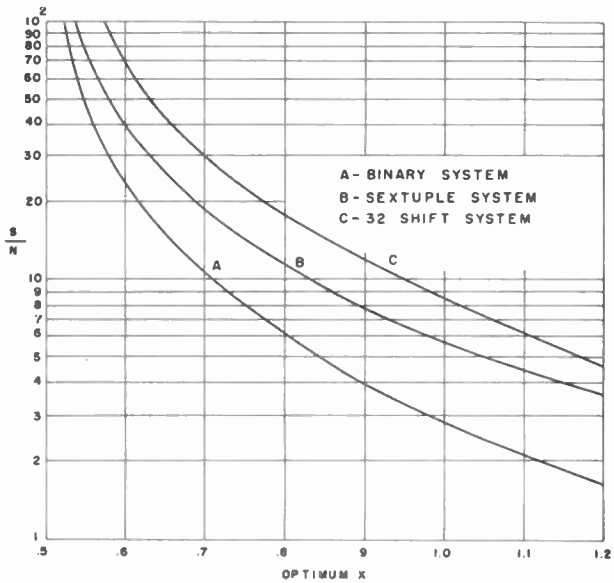

Fig. 4—Optimum bias level for various S/N ratios.

Fig. 4 gives the optimum value of x, determined through graphical means, for each system. Fig. 5 (next page) shows the probability of error, in the binary, 6- and 32-channel systems respectively, plotted for optimum bias levels. Note that these curves are plotted using the probability of error equations for pre-detection signal-to-noise. The true probabilities of error must then be found for post-detection signal-to-noise. This means that for $S/N=8$ in the binary system the probability of error is 80 per cent; the probability of error in the sextuple system in also 80 per cent with $S/N=2$.

More important is the fact that for the same noise conditions the probability of error is reduced in the multiple shift systems through the improvement in the S/N ratio. For example, $S/N=8$ produces a probability of error of 80 per cent in the binary system. The ratio $S/N=8$ in the binary system is equivalent to $S/N=24$ in the sextuple system and produces a probability of error of only 10 per cent. Then, under the same noise conditions, a signal-to-noise improvement is obtained which reduces the probability of error from 80 per cent to 10 per cent. Similarly, the 32-channel system operates at a signal-to-noise ratio of one-sixth of that at which binary system operates for same probability of error.

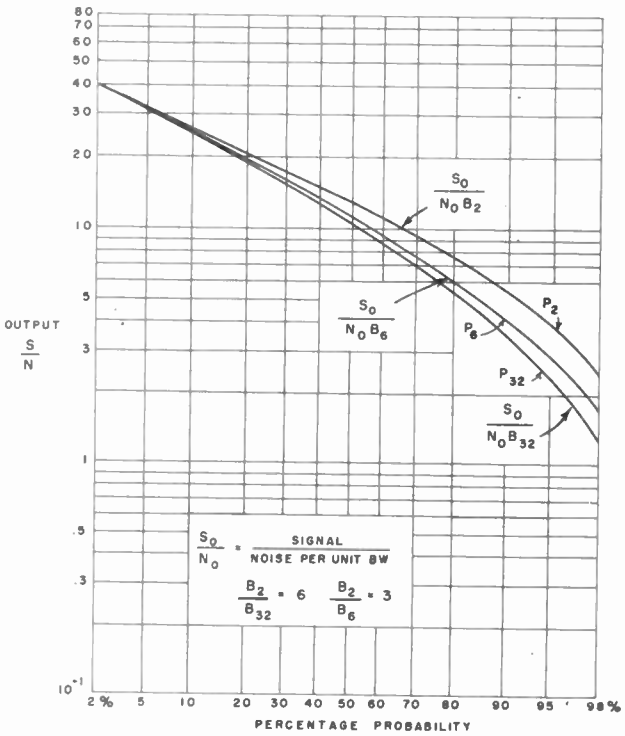

Fig. 5—Probability of error in 2-, 6- and 32-shift systems.

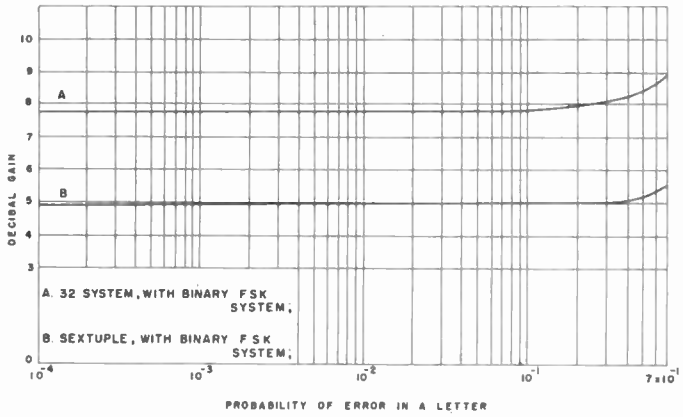

Fig. 6—Comparison of systems.

An indication of the improvement through MFS is obtained from the decibel power gain calculation, as shown in Fig. 6. The sextuple system shows about 5 decibels gain over the binary system, while the 32 system shows 7–8 decibels gain over the binary system.

The words given in Table I (below) indicate improvement in reliability of reception of signals sent by two MFS systems discussed here over those sent by the conventional FSK system. These words were taken from Di-

TABLE I

IMPROVEMENT IN RELIABILITY OF RECEPTION OF SIGNALS SENT BY MFS SYSTEMS OVER THOSE SENT BY FSK SYSTEM

Letter	FSK	Sextuple	32-Shift
DEDUCE	xExxxx	DEDUCE	DEDxCE
WORKSHOP	WxxxxxOx	WxRKSHOP	WORKSHOP
EACH	EAxx	EAxH	EACH
FAREWELL	xxxxWExx	FARxWxLL	FAREWELL
OF	xx	Ox	OF
FROM	FRxx	xxOM	FROM
WALK	xxxx	WALx	WALK
SIMPLE	SxxPxx	SxMxLx	SIMPLE
ROOST	RxxSx	ROOx	ROOST
VALUES	xxxxxx	VxLxES	VALUES
DEBT	xxBx	DEBT	DxxT
DECISIVE	xxxxxIxx	DxCISIVx	DESICIVE
SHEIK	xxxxx	SHxIx	SHEIK
HOSE	xOxE	HxSE	HOSE
AMALGAMATED	AMxxGAxxxxx	xMALxAMxTEx	AMALxAMATED
WEAVE	WxxxE	WxAVE	WEAVE
PROCEDURE	xxxxxxUxx	PROCEDUxE	PRxCEDURE
FACT	xxCx	xxxx	FxCT
FORTHWITH	xOxxxxIxH	FORTxxxTH	FORTHWITH
APPROXIMATELY	APxxxxxMxxxxx	APPROXIMATELY	APPROXIMATExY
SHRUG	SxRUx	SHRUG	SHRUG
THE	xxx	THE	THE
FRESH	xxxSx	xRESH	FRESH
FIFE	xxxx	xIFE	FIFE
RIDGE	xxxGE	RIDxE	RIDGE
PRICE	xxxCE	PRICE	PRICE
CLAWS	xxAxx	CLxWS	CLAWS
GRAPE	Gxxxx	GRAPE	GRAPE
SACK	xxxx	SxCx	SACK
THEME	TxxMx	THExE	THEME
CHOSE	CxOSE	CHOxE	CHOSE
DUKE	Dxxx	DUKE	DUKE
SPLASH	xPxxxH	SxLASx	SPLxSH
Corresponding probability of error	$P_2 = .75$	$P_6 = .21$	$P_{32} = .03$

Toro's paper[2] presented at the 1952 Airborne Electronics Conference, and they were chosen because wrong letters can only be guessed at from the context of the word rather than from that of the sentence. In this Table, errors (indicated by X's) have been simulated using random number tables[3] with the corresponding probability of error shown thereon.

Experimental Verification

Because the sextuple MFS system theoretically offers a gain of almost five decibels in signal-to-noise over FSK without an increase in over-all bandwidth and without necessitating the large number of filters needed for the 32-frequency system, it was decided to concentrate on the sextuple system for the initial laboratory verification of the theoretical benefits of MFS. Although the sextuple system actually employs seven frequencies, it was so named because the six shift frequencies are used for code information while the carrier is used for synchronization only. To simplify the comparison of the sextuple system with the standard FSK system as many components as possible were made common to both systems.

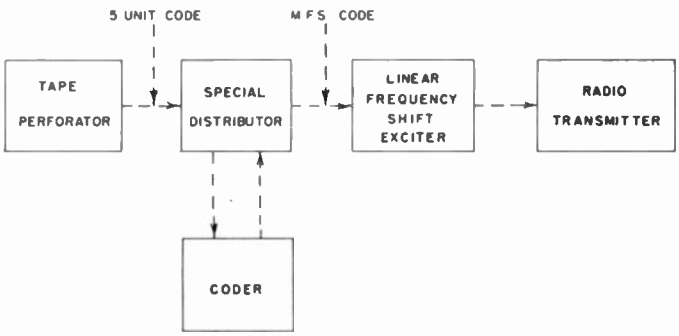

Fig. 7—Multiple frequency shift teletype transmitting system.

Fig. 7 is a block diagram of the MFS teletype transmitting system. A standard teletype distributor was modified for use with the MFS system. Information to be transmitted is fed into the transmitter-distributor on punched teletype tape. Five contacts are mechanically controlled in accordance with the pattern of holes on the tape. The movements of these five contacts control the operation of five encoder relays. The standard seven segment teletype commutator has been replaced by a unit consisting of a stop segment and two code unit segments. This gives a total time period of 163 milliseconds divided into a 31 millisecond carrier or stop pulse and two 66 millisecond information pulses. Operation of the encoder relays determines which of six fixed voltages is applied to each code unit segment. When the segment voltages are applied to the frequency shift keyer through the rotor of the transmitter distributor, a shift in frequency results. The voltages are adjusted so that three frequencies are set on each side of the "stop" or carrier center frequency. As the brushes move back to the "stop" segment, a cam operated by the motor shaft causes a microswitch to open, breaking the encoder relay energizing circuit. The microswitch closes again as soon as the brushes move past the rest position so that the encoder relays can be re-energized to set up the next character.

The linear frequency shift exciter is a standard exciter keyed by the output of the special distributor. The output of the exciter is used to drive the radio transmitter, which normally has a class-C amplifier in the output stage. Fig. 8 is a block diagram of the MFS teletype

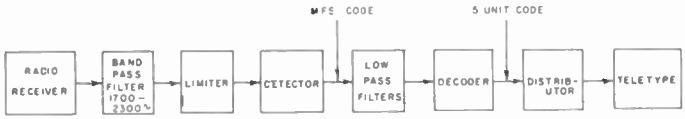

Fig. 8—Multiple frequency shift teletype receiving system.

receiving system. The receiver may be a conventional communications type of receiver using a beat frequency oscillator to produce an audio output, usually in the range between 2,000 and 3,000 cycles. The receiver should have automatic volume control and a degree of selectivity depending upon the particular bandwidth requirement of the system. Normally communication receivers use a bandwidth of from 3,000 to 4,000 cycles in the intermediate frequency section. The band-pass filter that is used following the receiver is sufficiently wide to encompass the frequencies that are used in the system. In the case of the sextuple system, a frequency band from 1,700 to 2,300 cycles is satisfactory for this purpose. The limiter is of the normal type, limiting both the positive and negative peaks, and is usually set for 40 to 50 decibels of limiting. The detector for the MFS system uses a number of selective filters. In the sextuple system, 7 filters are used, one of which is the carrier filter. The selectivity curves of these filters are shown in Fig. 9 (next page). Following the filters, the signal is amplified and then is rectified by means of half-wave rectifiers.

During the course of experimental development, filter shaping and effect on signal-to-noise ratios in both the standard FSK and MFS systems were checked in some detail. The total pre-detection bandwidth of the sextuple system with a spacing of 80 cycles between center frequencies of adjacent channels is about 535 cycles per second at the three decibel points. The pre-detection bandwidth must be wide enough to encompass the range of the seven channel filters. The 80-cycle spacing of channel filters is a compromise based on criteria of pulse definition, signal-to-noise ratio, drift, filter design,

[2] M. J. DiToro, "Distant Radio Communication Theory," IRE Conference on Airborne Electronics, 1952 Abstract of Papers, pp. 37–47, Dayton, Ohio.

[3] See, for example, W. J. Dixon and F. T. Massey, "Introduction to Statistical Analysis," McGraw-Hill Book Co., Inc., New York, N.Y., p. 290; 1951.

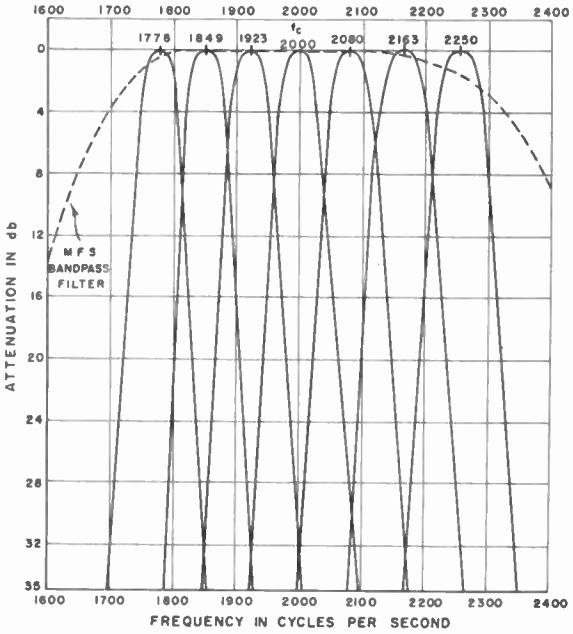

Fig. 9—Measured channel filter selectivity.

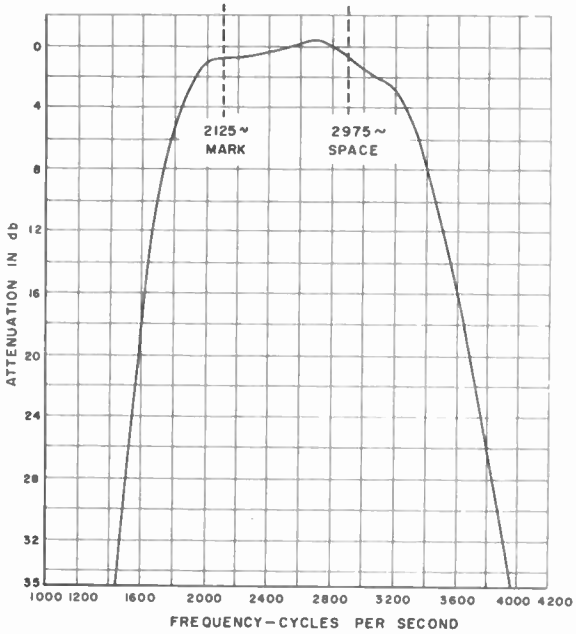

Fig. 10—Band-pass filter for standard laboratory frequency shift tests.

and deviation ratio. Deviation ratio is defined by

$$\text{Deviation Ratio} = \frac{\text{Frequency Shift}}{2 \times \text{Keying Speed}}.$$

Davey and Matte[4] have shown that satisfactory separation of mark and space signals in the FSK system is possible for a deviation ratio as low as 4.7. For a 70 cycle shift the deviation ratio is 4.7 and, of course, increases for greater frequency shifts, so that the 80 cycle shift being used is acceptable from this standpoint.

In one of his texts,[5] Goldman calculates that the optimum bandwidth for the reception of a single pulse from a signal-to-noise and pulse definition standpoint is approximately three quarters of the reciprocal of the pulse time. In the sextuple system this means a channel filter bandwidth of approximately 12 cycles for a 66-millisecond pulse duration. In practice, some bandwidth allowance must be made for drift in the transmitters and receiver. In the final analysis the precise spacing of the filters was determined by the availability of filters which met the above criteria. Since the keying speed has been reduced by a factor of three, the post-detection bandwidth has been reduced by the same factor with a resultant improvement in signal-to-noise ratio.

Test Equipment

Previous investigations of FSK systems have shown that significant improvement in reception in the presence of noise results from the use of a band-pass filter between the receiver and the limiter. In order to test the effect of filter bandwidth on performance, a filter switching unit was constructed. By means of this circuitry either the MFS bandpass filter, a standard FSK filter, a simple comb filter for FSK, or a resistance pad could be switched into the circuit between the receiver output and the limiter input.

The standard FSK band-pass filter is of the type commonly used in commercial systems. The filter frequency response is shown in Fig. 10. The simple comb filter was used in order to test the effect of further pre-detection narrowbanding in the FSK system. This filter was laboratory constructed and its frequency response is given in Fig. 11 (opposite). Resistance pad was used in place of a filter when making measurements of receiver power output, in order to have the receiver working into the same output load regardless of the system being tested.

The effect of the band-pass filter on system performance is shown in Fig. 12 (opposite). Note that the comb filter gives an improvement in signal-to-noise ratio of approximately 2 decibels over the standard filter which is, in turn, approximately $2\frac{3}{4}$ decibels better than operation with the resistance pad. These results lead to the conclusion that an FSK system should use the narrowest possible input filter consistent with keying speeds. A frequency shift of 850 cycles per second is wasteful of band space, particularly at the relatively low keying speed of 60 words per minute.[4] The tests indicate that the best input filter for an 850-cycle shift would have a frequency response similar to that shown for the comb filter used in these tests. The curves of Fig. 12 show the usual sharp breaking characteristic of a frequency shift system using a limiter. The error rate goes from zero to an unusable rate of 10 per cent or more with a 3-decibel decrease in signal-to-noise ratio.

[4] J. R. Davey and A. N. Matte, "Frequency-shift telegraph radio and wire applications," *Trans. AIEE*, vol. 66, pp. 479–493; 1947.

[5] S. Goldman, "Frequency Analysis Modulation and Noise," McGraw-Hill Book Co., Inc., New York, N.Y., p. 99; 1948.

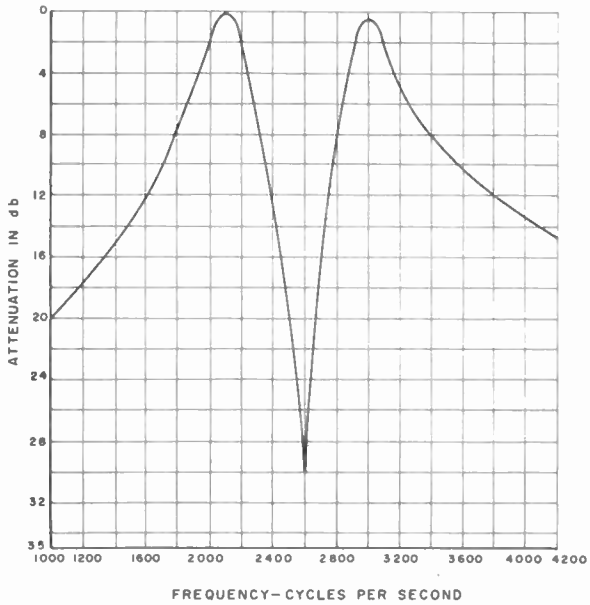

Fig. 11—Comb type filter for standard laboratory frequency shift tests.

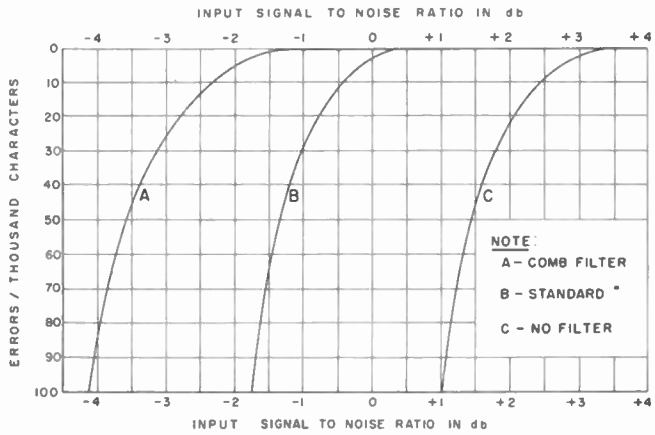

Fig. 12—Effect of band-pass filter on FSK system performance in presence of random noise (40-cycle low-pass filter).

Modern frequency shift systems generally use low pass filters after the detector, with upper cutoff in the region of 75 cycles. For laboratory test purposes a low pass filter was constructed which could be adjusted for operation with cutoff at either 40 cycles or 80 cycles. Although the 40-cycle low pass filter was found to improve the signal-to-noise ratio, it also introduced telegraph bias into the system so that the maximum noise improvement could not be obtained. Best operation should result from using an 80-cycle filter under normal operating conditions to avoid telegraph bias distortion, but switching to a 40-cycle filter under high noise conditions.

Referring again to Fig. 8, it will be noted that the MFS code is still being used through the low pass filter. The decoder is used to transform the MFS code to the normal five unit teletype code. The decoder has a bank of thyratrons whose output is in the five unit teletype code. This output feeds the distributor which runs at the normal speed of a teletype distributor. The teletype is driven by the distributor and receives 22-millisecond information pulses as well as the 22-millisecond "start" pulse and the 31-millisecond "stop" pulse. The "start" for the distributor is obtained from the decoder. The teletype now is no longer a decision instrument and the distributor is a form of regenerative repeater. No bias distortion is possible in the teletype in this system.

The carrier channel is used to maintain synchronization between the receiver and transmitter. The carrier channel rectifier is so connected that when a carrier signal is present a negative voltage is applied to the grid of a carrier relay driver, causing the carrier relay to be de-energized and breaking the relay contacts. When the received signal shifts off the carrier frequency, the grid of the relay driver becomes less negative and the carrier relay is energized. One contact of the carrier relay controls the operation of the receiver-distributor motor start circuit that maintains the receiving equipment in synchronism with the transmitter. A second contact of the carrier relay is used to clear the letter set-up in the thyratron bank.

Because of the narrow pass band of the channel filters the MFS system is comparatively intolerant of frequency drift. An automatic frequency control system has to be included which will keep the receiver locked on the carrier frequency. By maintaining the proper carrier frequency output from the receiver, all other channel frequencies will also be maintained at their proper values, provided the proper shifts are maintained in the frequency shift exciter.

A synchronizing pulse is necessary to maintain the receiver in synchronism with the transmitter. A television horizontal synchronization circuit can be modified to give improved automatic keying rate control. By the application of such a correlation technique it should be possible to reduce the length of the synchronization pulse and increase the length of the code unit pulses to further improve the ability of the system to operate in the presence of noise and multipath conditions.

The encoder and decoder used in this system have been described as using relays and thyratrons of the receiving type. Designs for an encoder and a decoder which will allow the sextuple system to transmit and receive all thirty-two teletype characters have been developed.

The initial decoder design required multiple contact relays with fast operate and release times. Acceptable relays were not readily available so that a satisfactory decoder could not be constructed. Published data on the multicontact wire relays developed by the Bell Telephone Laboratories indicated that they would be ideal for this application, but these relays were not readily available. A unit was therefore designed using thyratrons as electronic relays. More advanced techniques such as crystal diode matrices would undoubtedly lead to further simplification of the code translation circuitry.

Although the usual frequency shift teletype system operates in the high-frequency bands between 2 and 24 megacycles, the basic system can be tested for performance in noise with a much lower frequency which is more convenient for laboratory use. Consequently, a test set-up using 200 kilocycles as a carrier frequency was used. The transmitting end of this laboratory set-up consisted of the units shown in Fig. 7, with the exception of the radio transmitter. The frequency shift exciter, with an output of two to three watts, was used for this purpose, with the exciter being adjusted for operation at 200 kilocylces. In order to test perfromance when subjected to noise, two sources of noise were used; one a white noise generator and one an impulse noise generator utilizing a 60-cycle spark coil. The noise measurements were made using a thermal millimeter and all signal-to-noise ratios were measured on a root-mean-square basis. Separate gain control pads for the signal generator and the noise generators allowed various combinations of signal and noise to be used.

The receiving system comprised the units shown in Fig. 8 with the radio receiver being a simple 200-kilocycle converter having two tuned circuits in the input. The band-pass of the receiver was 3,800 cycles which approximates the usual pass band in a conventional communications receiver.

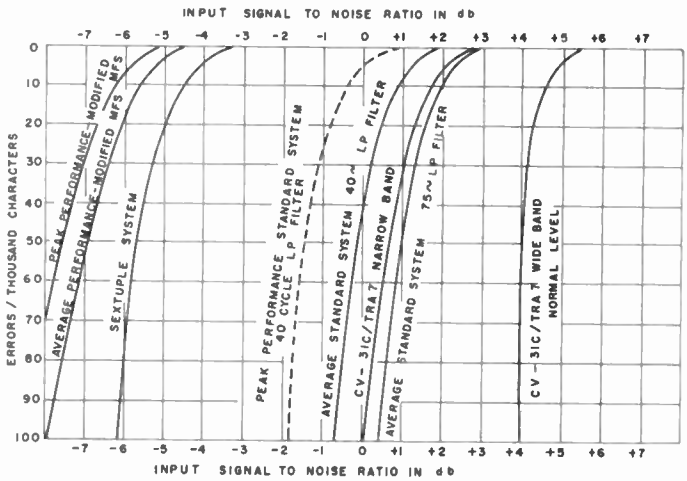

Fig. 13—Frequency shift performance in white noise.

Experimental Results

Fig. 13 above shows performance of system in white noise compared to operation of a normal frequency shift system using the five-unit teletype code. Study of the experimental results obtained with various test tapes on the FSK system showed that, at any given signal-to-noise ratio, "$R-Y$"[6] belts produced more errors than did word belts. These former belts were therefore used in evaluation of the signal-to-noise capabilities of the MFS system. Two types of frequency shift converters were used for the normal teletype tests; one being the standard type CV-31c/TRA7 that converts the input frequency shift signal to a signal centered around 50 kilocycles. In this unit the frequency shift is detected by means of a slope discriminator. The entire unit is self-contained with its own teletype driver. The other equipment comprised a frequency shift system whereby the signals from the reciever were at an audio frequency centered around 2,550 cycles, with mark 2,125 cycles and space 2,975 cycles. The usual elements of such a system were used including a band-pass filter, limiter, discriminator, and a teletype driver which drives the teletype unit. When the bandwidths of the two converters are substantially equal the results are much the same.

These curves again show the normal sharply-breaking characteristics of a frequency shift system using a limiter. The error rate has been shown to go from almost no errors to over 100 per 1,000 characters with a signal-to-noise ratio change of 3 decibels or less. In operating practice it has been found that a frequency shift system will give nearly perfect teletype copy provided the signal-to-noise ratio never falls below plus 6 decibels. The results shown on these curves substantiate this experience in that 6 decibels would allow a margin of 3 or 4 decibels before the system starts to break. The performance of the system using the sextuple code is substantially better than the usual frequency shift radio teletype. The systems improvement is 5 to 6 decibels, which compares well with the theoretical calculations.

Fig. 14 shows the performance of the systems under impulse noise. The improvement of the sextuple system is somewhat higher for impulse noise than it is for white noise. The gain is 9 to 10 decibels.

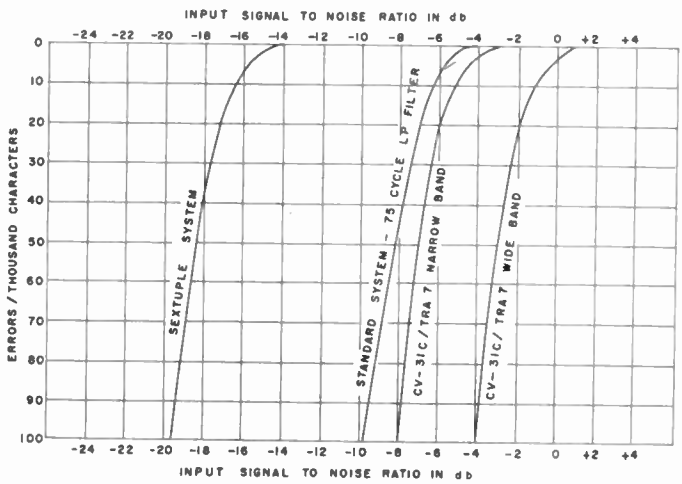

Fig. 14—Frequency shift performance in impulse noise.

Since the work described did not cover an actual air test no measurements have been made of multipath effects, but it is anticipated that marked improvements would result due to the long pulses that are used.

[6] Continuous circular tape on which letters R-Y-R-Y, etc. are punched in code. These put maximum load on switching circuit.

Conclusion

Laboratory performance tests of the sextuple MFS system clearly indicate the inherent superiority of MFS over FSK for the transmission of teletype information under white and impulse type noise conditions. The performance of the standard FSK system with the comb input filter was found to be approximately 2 decibels better than the same system with the standard input filter. Since the effective bandwidth of the comb filter is approximately the same as the bandwidth of the sextuple MFS input filter, it can be seen that the MFS system is about 4 decibels better than the FSK system with equivalent pre-detection bandwidths. This improvement is mainly due to a reduction of bandwidth which is permissible with the greater pulse duration in the MFS system. This greater pulse duration is achieved without a reduction in the speed of transmission of information. A slight additional improvement results from the simpler code used by the MFS system. Theoretical gains have been satisfactorily verified.

Acknowledgment

The authors wish to recognize Messrs. D. R. Meierdiercks, F. Picus, and W. Posner, for considerable aid in the theoretical and experimental efforts. The work described in this paper was sponsored by the U. S. Air Force under Contract AF33(038)-22536.

The Use of a Ring Array as a Skip Range Antenna*

J. D. TILLMAN†, MEMBER, IRE, W. T. PATTON†, MEMBER, IRE, C. E. BLAKELY†, AND F. V. SCHULTZ†, SENIOR MEMBER, IRE

Summary—**The problem involved here is the development of a shore antenna for shore-to-ship communications at distances from 40 to 500 miles. The difficulty at these distances is due to interference between ground-wave and sky-wave modes of propagation.**

The propagation factors involved are considered and it is shown that (1) A frequency less than 3.3 mc should be used, (2) The ground wave should be used during the day and (3), The sky wave should be used at night.

An azimuthally omnidirectional antenna is described which consists of vertical monopoles equally spaced around the circumference of a circle. The antenna can be excited in either of two ways, one of which concentrates the radiated energy along the ground for use with the ground wave, and the other of which gives maximum radiation at a polar angle of 30 degrees and a null in the ground plane for use with the skywave. The results of model tests at 30 mc and at 1,200 mc are given. Results of calculations showing the expected coverage for noon and midnight are included.

Introduction

IT IS THE purpose of this paper to describe an antenna system to be used to transmit signals over the range from 40 to 500 miles. This antenna is intended primarily for shore-to-ship communication, so that the ground paths involved will consist mainly of sea water. Reliable operation for 24 hours each day and for any season or geographical location is required.

Communication into the region within 500 miles of the transmitter is characterized by severe fading. This fading is the result of interference between ground-wave and sky-wave fields which are of the same order of magnitude over part of the region. The zone in which this severe fading and interference occurs is normally about 100 miles across, and is located at about 200 miles from the transmitter at night, and at about 600 miles during the day. The question of obtaining an adequate signal-to-noise ratio is the same for this system as for any other, and the principal problem is one of eliminating interference between ground-wave and sky-wave modes of propagation. This is accomplished by the use of an antenna which can be excited in either of two ways:

1. A ground-wave phasing which gives a pattern concentrating the radiated energy along the surface of the earth for communication via the ground wave.
2. A sky-wave phasing which eliminates any ground wave by means of a null at zero degrees elevation angle and concentrates the radiated energy about an elevation angle of 60 degrees for communication via the sky wave.

In each case the radiation pattern is omnidirectional in azimuth. The ground-wave phasing is used to communicate during the day and for distances of less than about 200 miles at night. The sky-wave phasing is used at night for distances greater than about 100 miles.

Propagation Considerations

The antenna is to be used for a particular communication link, so that rather specific antenna requirements can be determined by a consideration of propagation factors. The important considerations are

1. Skip distance.
2. Ground-wave intensity-to-sky-wave intensity ratio.
3. Signal-to-noise ratio.

Since the reason for investigating these factors is to establish criteria for the design of the antenna, the methods of computing sky-wave field intensities and

* Original manuscript received June 17, 1955, revised manuscript received, August 8, 1955. The research reported in this paper has been sponsored by the Bureau of Ships, Dept. of the Navy.

† Electrical Engineering Dept., University of Tennessee, Knoxville, Tenn.

skip distances given in CRPL Circular No. 462[1] are considered to be sufficiently accurate. This circular also contains noise data which are adequate for this purpose. Ground wave field intensities can be found by using well known methods.[2] These factors must be used to select an operating frequency and to determine the required vertical radiation pattern of the antenna.

For daytime the use of a frequency near two megacycles per second is indicated, as both sky-wave interference and noise go through a minimum with respect to frequency in this range. The use of frequencies below about one megacycle per second is undesirable at night because a large number of fairly strong multi-hop sky-wave modes are excited simultaneously, and intermode interference is correspondingly severe. A further undesirable factor is the excessive size of the required antenna structure at these relatively low frequencies. An upper limit on the nighttime frequency can be set by stipulating that the skip distance must never exceed the distance that can be covered by the ground wave if there is no sky-wave interference. This insures coverage by one mode or the other. These distances for a sunspot minimum are plotted against frequency in Fig. 1, and it is seen that the highest frequency that may be used for all conditions is 3.3 megacycles per second. This frequency will be used for all following calculations in this paper.

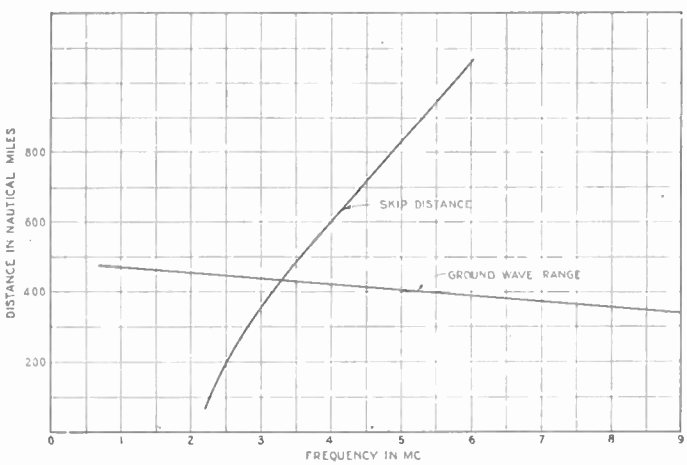

Fig. 1—Skip distance and ground wave range vs frequency. The ground-wave range is for a 5-kilowatt transmitter located 2 miles from a straight coast, and is based on no interfering sky wave.

Calculations of relative ground-wave and sky-wave field intensities show that for daytime conditions ionospheric absorption reduces sky-wave interference to a point where the ground-wave communication is satisfactory without requiring a pattern greatly sharper than that of a quarter-wave monopole. At night the sky wave is relatively unabsorbed, and is strong enough to override noise at distances greater than about 100 miles from the transmitter. To reduce the ground-wave intensity sufficiently so that it will not interfere with the sky wave requires a null in the antenna pattern at the ground plane, thus eliminating the ground wave. This null must exist for all azimuth angles or the region of interference-free coverage will be a narrow wedge-shaped area. This in turn implies that the azimuthal radiation pattern at all polar angles be omnidirectional unless excessively complicated antennas are used. Maximum radiation should be at about a 60-degree elevation angle, corresponding to a 1-HOP-F2 distance of about 200 nautical miles, thus concentrating the field in the desired area. The region out to the point where the sky wave is strong enough to override noise must be covered via the ground wave. Since the sky wave is relatively strong at night, the ground-wave phasing of the antenna should concentrate the enregy along the surface as much as possible to keep interference to a minimum.

The Antenna System

The antenna requirements set out above can be met by an array of vertical elements equally spaced around the circumference of a circle. The use of such an array to obtain patterns having little radiation at high angles was proposed by Chireix,[3] by Hansen and Hollingsworth,[4] and, in a somewhat different form, by Page.[5] This array can also be excited in such a way as to give the pattern desired for sky-wave communication.

It is shown in the Appendix that the pattern of such an array of quarter-wave monopoles is given by

$$E = I_0 J_n\left(\frac{2\pi\rho}{\lambda}\sin\theta\right)\frac{\cos\left(\frac{\pi}{2}\cos\theta\right)}{\sin\theta}\epsilon^{j(\omega t+n\phi)}, \qquad (1)$$

where each of the m elements has a current I_0/m, and there is a progressive phase difference $2\pi n/m$ between adjacent elements. $J_n(x)$ is the Bessel function of the first kind of order n. The angles θ and ϕ are shown in Fig. 7. The use of (1) assumes that m is larger than the critical value specified in the Appendix. In (1) choose $n=0$. A null in the ground plane (at $\theta=90°$) can then be obtained by setting $2\pi\rho/\lambda$ equal to any root of $J_0(x)=0$. The smallest radius giving this null is $\rho=0.383\lambda$. See pattern for this case in Fig. 2 (opposite). Inspection shows that this pattern meets the requirements for the sky-wave phasing. Since the phase difference between adjacent elements is $2\pi n/m$, and $n=0$, all of the currents are in phase for this method of excitation.

To obtain a vertical pattern giving better sky-wave suppression than given by the elements of the array, it is necessary that $2\pi\rho/\lambda$ be less than the value of x for the first maximum of $J_n(x)$. This insures that $J_n(2\pi\rho/\lambda \sin\theta)$ is a monotone increasing function of θ.

[1] "Ionospheric Radio Propagation," U. S. Dept. of Commerce, Nat. Bur. Standards Circ. No. 462; June, 1948.

[2] "Ground Wave Field Intensities," Signal Corps Propagation Unit, Tech. Rep. No. 3; June 1949.

[3] H. Chireix, "Antennes a rayonnement zenithal reduit," *L'Onde Elect.*, vol. 15, pp. 440–456; July, 1936.

[4] W. W. Hansen and L. M. Hollingsworth, "Design of 'flat-shooting' antenna arrays," Proc. IRE, vol. 27, pp. 137–143; Feb., 1939.

[5] H. Page, "Ring aerial systems," *Wireless Eng.*, vol. 25, pp. 308–315: October, 1948.

For $\rho = 0.383\lambda$, this requires that $n \geqq 2$. In an antenna of this size a value of $n > 3$ leads to undesirable super-gain characteristics.[6] Then the value of $n = 3$ is the best for the present purpose. This pattern is also shown in Fig. 2.

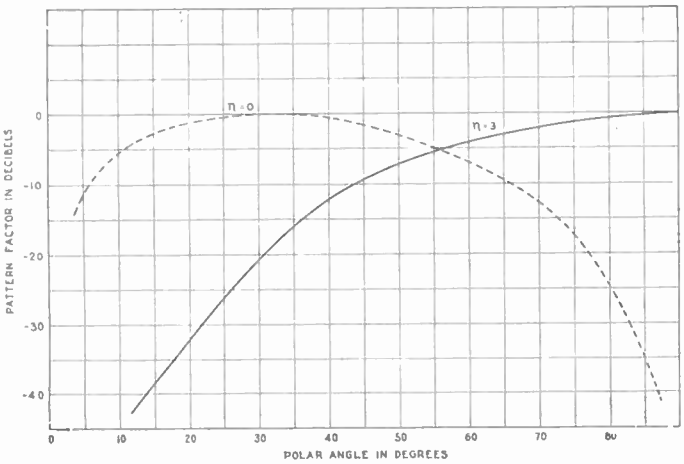

Fig. 2—Vertical pattern of a single-ring array of quarter-wave monopoles with a radius of 0.383 wavelength.

Eq. (18) in the Appendix can be used to fix m. Nine elements are needed for $\rho = 0.383\,\lambda$ and $n = 3$. Gains may be calculated by the method due to Page.[7] For $n = 0$, the gain is 5.94 decibels, and for $n = 3$ it is 2.57 decibels.

Experimental Verification

A model of the antenna was constructed and tested at 1,200 mc. Azimuthal patterns at a number of polar angles were obtained for both methods of excitation by means of a pattern recorder. Vertical patterns were obtained by point-by-point measurements. Experimental data together with calculated values are shown in Figs. 3–6 on the following page. The agreement with theory is seen to be quite good.

[6] L. J. Chu, "Physical Limitations of Omnidirectional Antennas," MIT Tech. Rep. No. 64, pp. 11–21; May, 1948.

[7] H. Page, "Radiation resistance of ring aerials," *Wireless Eng.*, vol. 25, pp. 102–109, April, 1948.

The final antenna will consist of nine folded monopoles equally spaced about the circumference of a circle. At 3.3 mc, the radius of the circle is 114 feet, and the elements are 75 feet high. It is planned to feed the elements with coaxial cables emanating from the center of the ring where the matching and phasing network are to be located. The antenna was also modeled at 30 mc to investigate these lumped circuit driving networks. This study showed that each phasing of the antenna could be excited by a network containing three T-sections, and that the current in each element could be set to within the required tolerance without undue difficulty.

Propagation Calculations

The probable ranges that can be covered using this antenna have been calculated. These calculations are based on a required signal-to-noise ratio of 10 decibels and a 10-decibel separation of ground-wave and sky-wave modes of propagation, both of which are adequate for teletype. Allowance has been made for fading, assuming a Rayleigh distribution for the sky-wave field intensity. The calculations were made for a transmitter power of 3 kw and an over-all efficiency of 50 per cent. The antenna was considered to be located two nautical miles inland from a straight coast line. Ranges for noontime conditions are shown in Table I and for midnight in Table II. The data in Table II are the range using the ground-wave phasing, and the inner and outer limits of coverage using the sky-wave phasing.

TABLE I

Ranges in Nautical Miles at Noon For a Single-Ring Array Located Two Miles from a Straight Coast

Calculations are based on 3 kw transmitter and a frequency of 3.3 mc.

Azimuth angle	Noise Grade 1	Noise Grade 2	Noise Grade 3	Noise Grade 4	Noise Grade 5
0	690	690	690	560	430
30	670	670	670	550	420
60	560	560	560	490	360

TABLE II

Ranges in Nautical Miles at Midnight for a Single-Ring Array Located Two Miles from a Straight Coast

Calculations are based on 3 kw transmitter and a frequency of 3 mc.

Azimuth angle	Antenna phasing	Noise Grade 1W	Noise Grade 2W	Noise Grade 3W	Noise Grade 4	Noise Grade 5
0	G	204	204	204	204	204
	S	40 / 1000+	61 / 930	91 / 630	148 / 420	N / N
30	G	195	195	195	195	195
	S	40 / 1000+	61 / 930	91 / 630	148 / 420	N / N
60	G	165	165	165	165	165
	S	40 / 1000+	61 / 930	91 / 630	148 / 420	N / N

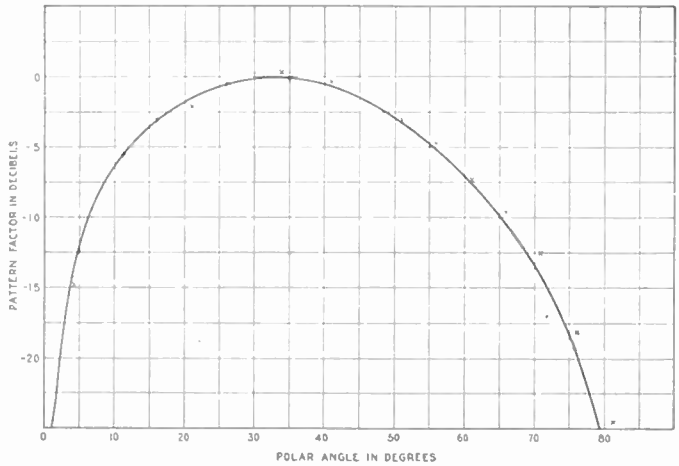

Fig. 3—Measured and calculated vertical patterns of a single-ring array of quarter-wave monopoles with a radius of 0.383 wavelength and $n=0$.

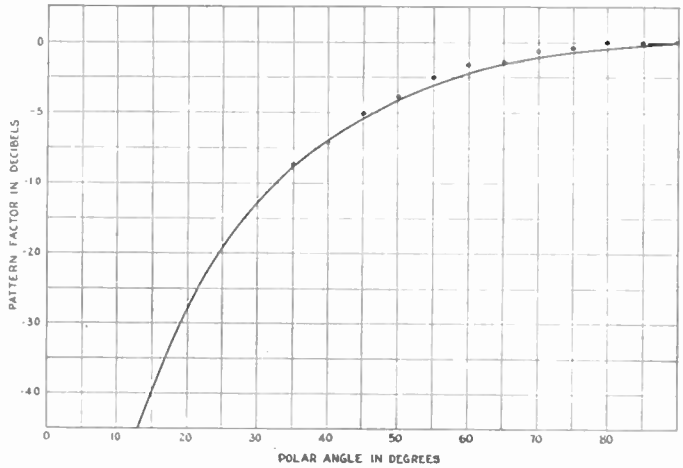

Fig. 4—Measured and calculated vertical patterns of a single-ring array of quarter-wave monopoles with a radius of 0.383 wavelength and $n=3$.

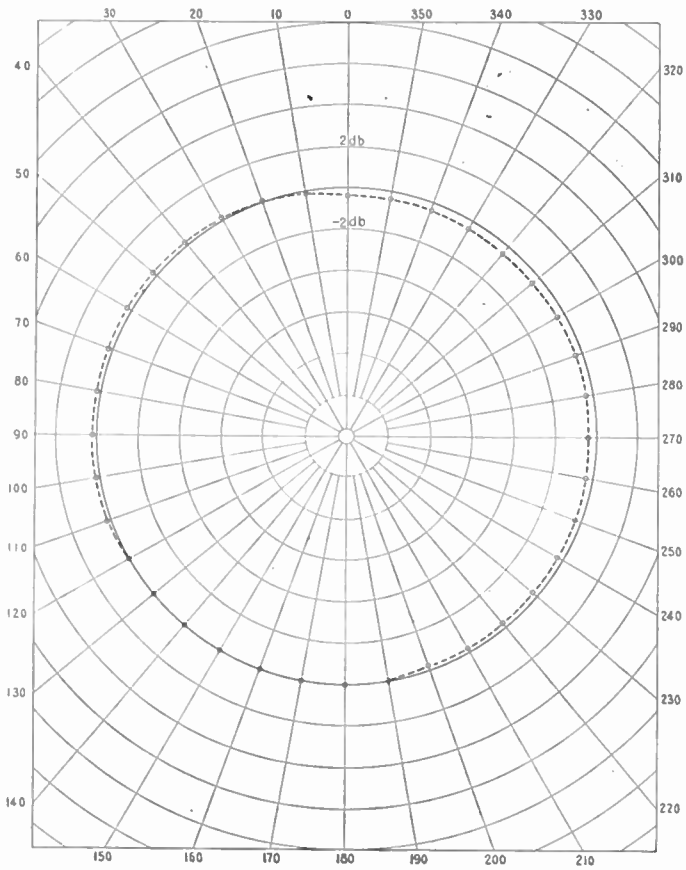

Fig. 5—Measured and calculated horizontal pattern at $\theta=30$ degrees of a single-ring array of quarter-wave monopoles with a radius of 0.383 and $n=0$.

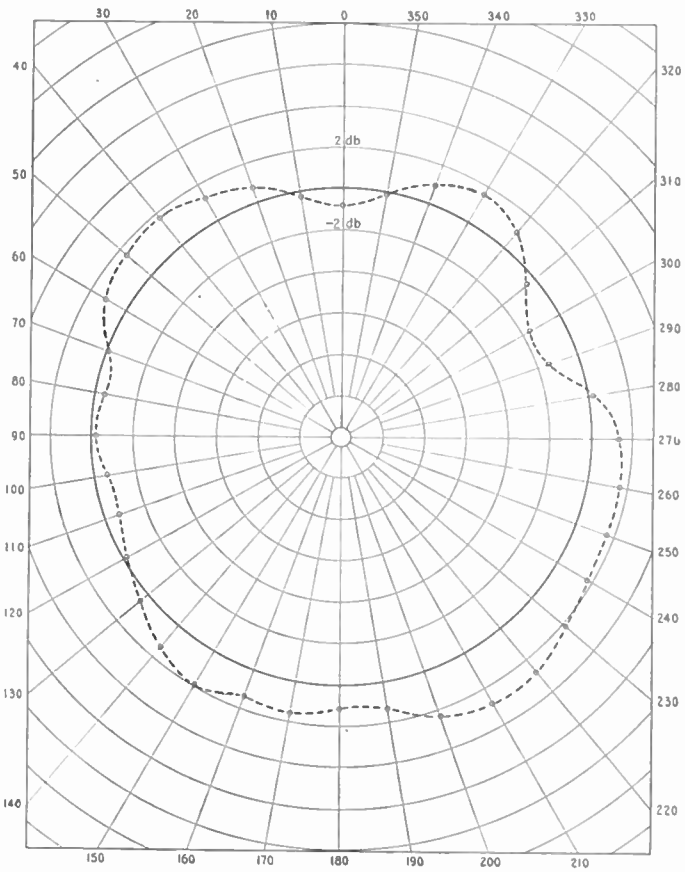

Fig. 6—Measured and calculated patterns of a single-ring array of quarter-wave monopoles with a radius of 0.383 wavelength and $n=3$.

The letter N is used to indicate that a signal-to-noise ratio of 10 decibels does not exist at any point in the 0-to-500-mile region. Calculations were also carried out for a large number of other cases. These include:

1. Sporadic E-mode present.
2. Ionospheric absorption abnormally high.
3. Twilight conditions.
4. Arctic ionospheric and noise conditions.

In each case the results are acceptable.

Conclusions

The antenna system described in this paper appears to offer a method of obtaining reliable shore-to-ship communication over distances of less than 500 miles without the customary fading caused by interference between ground-wave and sky-wave fields. This absence of interference is quite valuable where extreme accuracy of reception of the transmitted signal is required.

Appendix

Derivation of the Expression for the Array Factor

A plan view of the m element array is shown in Fig. 7. Establish a spherical co-ordinate system, with the polar axis perpendicular to the plane of the circle, and choose $\phi=0$ through element m. Let the radius of the circle be 7. To obtain patterns of the type desired let the current in the ith element be

$$I_i = \frac{I_0}{m} \epsilon^{j(\omega t+(2\pi n/m)i)}, \tag{2}$$

where n is any positive integer or zero. There is thus a uniform progressive phase shift between adjacent elements, with n complete cycles of phase shift around the ring. The field from the ith element is proportional to

$$E_i = \frac{I_0}{m} \epsilon^{j[\omega t+(2\pi n/m)i+2\pi\rho/\lambda \sin\theta \cos(\phi-(2\pi/m)i)]}. \tag{3}$$

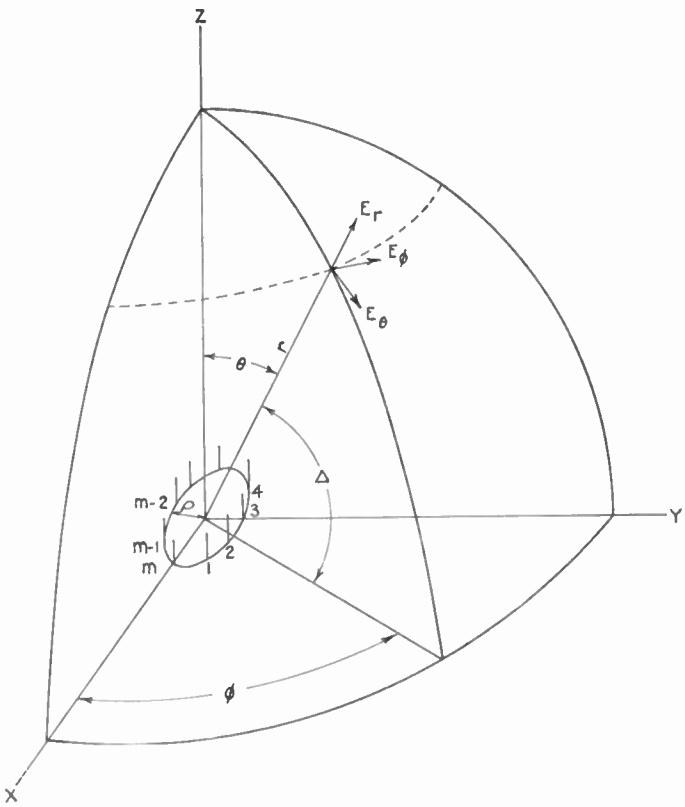

Fig. 7—View of a single-ring array lying in the r, ϕ, $\theta=0$ degrees plane of a spherical co-ordinate system.

The array factor is then found by summing E_i from 1 to m. This gives

$$E = \frac{I_0}{m} \epsilon^{j(\omega t+n\phi)} \sum_{i=1}^{m} \epsilon^{j(z\cos\eta_i - n\eta_i)}, \tag{4}$$

where

$$z = \frac{2\pi\rho}{\lambda} \sin\theta$$

$$\eta_i = \phi - \frac{2\pi}{m} i. \tag{5}$$

The summation in (4) has been investigated by Stenzel[8] for $n=0$ and m even, by Chireix,[9] for $n\neq 0$ and m even, and by Page[10] for $n=0$ and m even or odd. A general development follows that holds for each of these cases and also for $n\neq 0$ and m odd. We must investigate

$$S_m = \sum_{i=1}^{m} \epsilon^{j(z\cos\eta_i - n\eta_i)}. \tag{6}$$

This may be expanded in a series of Bessel functions,[11] giving

$$S_m = \frac{J_0(z)}{m} \sum_{i=1}^{m} \epsilon^{-jn\eta_i} + 2\sum_{i=1}^{m}\sum_{k=1}^{\infty} \epsilon^{-jn\eta_i}[(-1)^k \cos 2k\eta_i J_{2k}(z) + j(-1)^{k-1}\cos(2k-1)\eta_i J_{2k-1}(z)]. \tag{7}$$

Each term of (7) may be considered separately. Let

$$S_1 = \frac{1}{m}\sum_{i=1}^{m} \epsilon^{-jn\eta_i} J_0(z), \tag{8}$$

$$S_2 = \frac{2}{m}\sum_{i=1}^{m}\sum_{k=1}^{\infty} \epsilon^{-jn\eta_i}(-1)^k \cos 2k\eta_i J_{2k}(z), \tag{9}$$

$$S_3 = \frac{2}{m}\sum_{i=1}^{m}\sum_{k=1}^{\infty} \epsilon^{-jn\eta_i}(-1)^{k-1} \cos(2k-1)\eta_i J_{2k-1}(z). \tag{10}$$

Now in each case these sums reduce to geometric progressions. The first is

$$\begin{aligned} S_1 &= \frac{1}{m}\sum_{i=1}^{m} J_0(z)\epsilon^{-jn\phi}\epsilon^{j(2\pi n/m)i} \\ &= \frac{J_0(z)}{m}\epsilon^{-jn\phi}\sum_{i=1}^{m}\epsilon^{j(2\pi n/m)i} \\ &= \frac{J_0(z)}{m}\epsilon^{-jn\phi}\frac{\sin \pi n}{\sin(\pi n/m)}\epsilon^{j(m+1/m)\pi n}. \end{aligned} \tag{11}$$

If $m>n$, which is the only practical case, and $n\neq 0$, $S_1=0$. If $n=0$, $S_1=J_0(z)$. Thus,

$$S_1 = \begin{cases} J_0(z) & n=0 \\ 0 & n\neq 0. \end{cases} \tag{12}$$

For S_2 we obtain, by reversing the order of summation, and by a simple algebraic manipulation, that

$$S_2 = \frac{1}{m}\sum_{k=1}^{\infty}(-1)^k J_{2k}(z)\sum_{i=1}^{m}[\epsilon^{j(2k-n)\phi}\epsilon^{j(n-2k)(2\pi/m)i} + \epsilon^{-j(2k+n)\phi}\epsilon^{j(n+2k)(2\pi/m)i}]. \tag{13}$$

S_2 may now be expanded by the use of the expression for the sum of a geometric progression, giving

[8] H. Stenzel, "Über die richtcharakteristik von in einer Ebene Angeordneten Strahlern," *Electr. Nachr. Technik*, vol. 6, pp. 165–181; May, 1929.
[9] Chireix, *loc. cit.*
[10] Page, *loc. cit.*
[11] G. N. Watson, "Theory of Bessel Functions," Cambridge University Press, Cambridge, England, pp. 22–23; 1944.

$$S_2 = \frac{1}{m} \sum_{k=1}^{\infty} (-1)^k J_{2k}(z) \cdot \left[\epsilon^{j(2k-n)\phi} \epsilon^{j(m+1/m)(n-2k)\pi} \frac{\sin (n-2k)\pi}{\sin (n-2k)\pi/m} + \epsilon^{-j(2k+n)\phi} \epsilon^{j(m+1/m)(n+2k)\pi} \frac{\sin (n+2k)\pi}{\sin (n+2k)\pi/m} \right]. \quad (14)$$

In (14) n and m are integers and k takes on only integral values. Then the only values of k which give rise to nonzero terms are those for which

$$k = -\frac{lm - n}{2} \quad \text{or} \quad k = \frac{lm - n}{2}.$$

There are four cases: n odd, m odd; n even, m odd; n odd, m even; and n even, m even. The algebra for each of these cases is straightforward but tedious and will not be given here. The summation for S_3 can be carried out in the same way as for S_2. When this is done, the result obtained by adding S_1, S_2, and S_3 is the same for all four cases although different terms come from S_1, S_2, and S_3 for each case. The final expression for the array factor is

$$E = j^n I_0 J_n \left(\frac{2\pi\rho}{\lambda} \sin\theta \right) \epsilon^{j(\omega t + n\phi)} + I_0 \sum_{k=1}^{\infty} \left\{ j^{km-n} J_{km-n} \left(\frac{2\pi\rho}{\lambda} \sin\theta \right) \epsilon^{j[\omega t + (n-km)\phi]} + j^{km+n} J_{km+n} \left(\frac{2\pi\rho}{\lambda} \sin\theta \right) \epsilon^{j[\omega t + (km+n)\phi]} \right\}. \quad (15)$$

For $n = 0$, this reduces to

$$E = I_0 J_0 \left(\frac{2\pi\rho}{\lambda} \sin\theta \right) \epsilon^{j\omega t} + 2 I_0 \epsilon^{j\omega t} \sum_{k=1}^{\infty} j^{km} \cos km\phi J_{km} \left(\frac{2\pi\rho}{\lambda} \sin\theta \right). \quad (16)$$

The azimuthal pattern at polar angle θ will be circular if

$$J_{m-n} \left(\frac{2\pi\rho}{\lambda} \sin\theta \right) \ll J_n \left(\frac{2\pi\rho}{\lambda} \sin\theta \right), \quad (17)$$

where terms for $k \geqq 2$ are neglected because of the rapid decrease of $J_k(x)$ with increasing k. The peak-to-peak variation in the pattern in db is

$$\text{VAR} = 20 \log \frac{\left| J_n \left(\frac{2\pi\rho}{\lambda} \sin\theta \right) \right| + \left| J_{m-n} \left(\frac{2\pi\rho}{\lambda} \sin\theta \right) \right|}{\left| J_n \left(\frac{2\pi\rho}{\lambda} \sin\theta \right) \right| - \left| J_{m-n} \left(\frac{2\pi\rho}{\lambda} \sin\theta \right) \right|}. \quad (18)$$

If $n = 0$, (18) is valid for m even, but if m is odd the term for $k = 1$ is in quadrature with the principal term and

$$\text{VAR} = 10 \log \frac{\left[J_0 \left(\frac{2\pi\rho}{\lambda} \sin\theta \right) \right]^2 + \left[J_m \left(\frac{2\pi\rho}{\lambda} \sin\theta \right) \right]^2}{\left[J_0 \left(\frac{2\pi\rho}{\lambda} \sin\theta \right) \right]^2}. \quad (19)$$

If m is large enough so that the use of (18) or (19) shows that the azimuthal pattern is essentially a circle, the term for $k = 1$ can also be neglected and

$$E = j^n I_0 J_n \left(\frac{2\pi\rho}{\lambda} \sin\theta \right) \epsilon^{j(\omega t + n\phi)}. \quad (20)$$

This is the expression for the pattern of an array of isotropic radiators, and must be multiplied by the expression for the pattern of the individual elements to obtain the equation of the final pattern.

Microwave High-Speed Continuous Phase Shifter*

W. SICHAK†, MEMBER, IRE, AND D. J. LEVINE†, MEMBER, IRE

Summary—**A continuous phase shifter using circularly polarized helices in a circular waveguide is described. The phase shifter is smaller than previous types[1] and has an insertion loss of less than 0.2 db. Equations for the phase-shift error and the amount of amplitude modulation produced due to reflections and elliptical polarization are derived. Errors less than ±2° can be obtained over a 3 per cent frequency band. A 9,400-mc model designed to rotate at 3,600 rpm is 5½ inches long and 1 inch in diameter, excluding the motor drive.**

Theory of Operation

It can be shown that the phase of the output voltage of a circularly polarized antenna receiving a circularly polarized wave is directly proportional to the angle of rotation of the antenna about its longitudinal axis. In order to make a phase shifter, two circularly polarized antennas (each of the same screw sense) are mounted in a circular waveguide, and one antenna is rotated about its axis at the required rate.

Errors

Axial-Ratio Error: The relation between the maximum phase error and the axial ratios of the antennas is

$$\tan \Delta_{max} = \frac{K - 1}{2 \cdot K^{1/2}}, \tag{1}$$

$$K = \frac{A + B}{1 + AB},$$

where A and B are the axial ratios of the antennas and Δ is the error.

This relation is plotted in Fig. 1(a) for the case where the axial ratios are equal. An axial ratio of 2 db produces an error of less than 1 degree.

Standing-Wave Error: It can be shown that the maximum phase-shift error Δ_{max} is given by

$$\tan \Delta_{max} = \frac{2P^2(1 - P^4)^{1/2}}{1 - 2P^4}. \tag{2}$$

where P = reflection coefficient of each end.

This equation is plotted in Fig. 1(b). A standing-wave ratio of 1.2 at each end causes an error of about 1 degree.

Variation in Output Amplitude

The ratio of maximum to minimum received voltage obtained when an elliptically polarized antenna is rotated in an elliptically polarized field[2] is $(1+AB)/(A+B)$, where A and B are the axial ratios of the antennas.

For equal axial ratios, the percentage modulation m is $100\ (1-A)^2/(1+A)^2$. This equation is plotted in Fig. 1(c). Axial ratios of 2 db produce 1.3 per cent modulation.

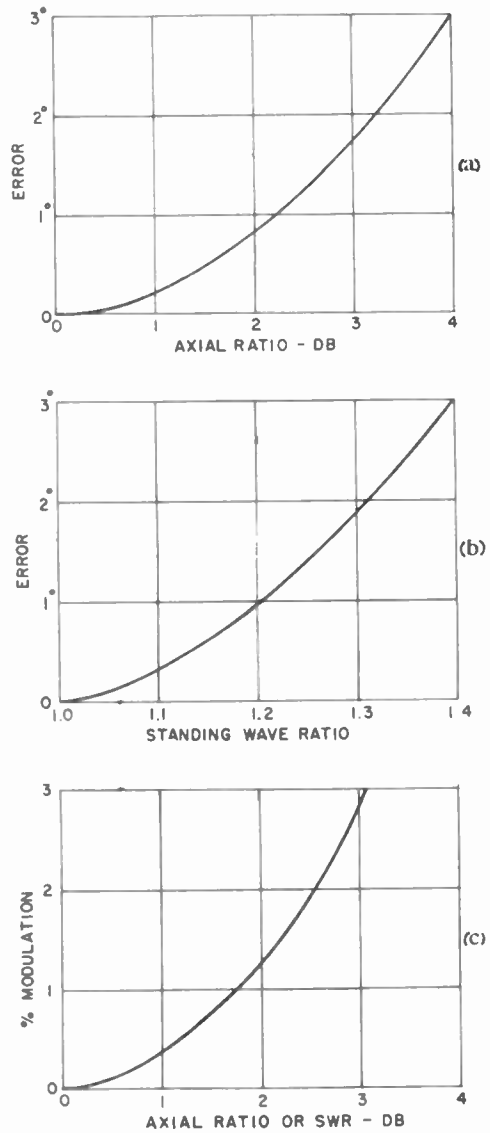

Fig. 1—(a) Phase-shift error vs axial ratio of each end. (b) Phase-shift error vs standing-wave ratio. (c) Percentage modulation of the phase-shifted wave vs axial ratio of each end or standing-wave ratio.

If the ends of the phase shifter are equally mismatched, the ratio of maximum to minimum volt-

* Original manuscript received by the IRE, May 29, 1951; revised manuscript received, January 10, 1952; resubmitted June 27, 1955. The work described in this paper was sponsored by the Bureau of Ordnance, Navy Department.

† Federal Telecommunication Laboratories, Inc., 500 Washington Ave., Nutley, N. J.

[1] A. G. Fox, "An adjustable wave-guide phase changer," Proc. IRE, vol. 35, pp. 1489–1498; December, 1947.

[2] "Reference Data for Radio Engineers," Federal Telephone and Radio Corp., New York, N. Y., third edition, page 366; 1949.

age is $(1+r^2)/2r$. The percentage modulation is 100 $(r-1)^2/(r+1)^2$.

The amplitude-modulation sidebands in the output are separated from the carrier by twice the rotational frequency of the phase shifter, since the input standing-wave ratio is the same whether the phase shift is θ or $180°+\theta$. The reflected wave consists of two parts: the first, due to the mismatch at the input end, is independent of rotation; the second, due to the mismatch at the load end, is shifted in frequency by twice the rotational frequency. If the load end of the phaseshifter, including the helix, is perfectly matched and has an axial ratio of unity, there are no amplitude or phase errors in the output.

For simplicity, the above analyses have considered the effects of axial ratio and standing-wave ratio separately. For small errors, the maximum errors due to each can be added directly.

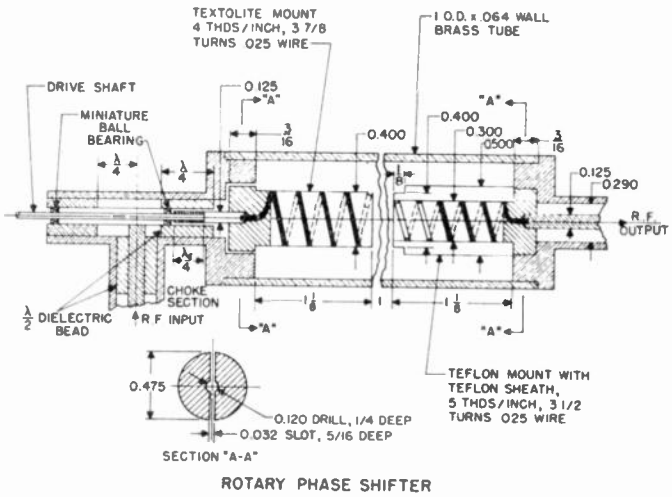

Fig. 2—Rotary phase shifter.

Rotary Phase Shifter

Description

The rotary phase shifter shown in Figs. 2 and 3 takes the form of a length of circular waveguide terminated in a helical circularly polarized H_{11}-mode launcher at each end. The 9,400-mc model is about $5\frac{1}{2}$ inches long and 1 inch in diameter, not including the motor. The mass of the rotating textolite helix and its drive shaft is 5 grams. The sense of each helix is the same. The exploded view of Fig. 3 illustrates two types of helices; the textolite unsheathed helix at the rotating end and a fixed sheathed teflon helix. The helix spacing is about one inch between ends. It was found that a shorter spacing resulted in direct coupling between the ends of the helices and resulted in large errors.

These phase shifters can be rotated at speeds higher than 3,600 rpm if desired. The phase-shift rate can be doubled by rotating the helices in opposite directions.

Helix Design and Construction

For use in this phase shifter, the helical-antenna design problem is complicated by the fact that the helix radiation field must be contained in a circular waveguide. It was decided to radiate an H_{11} mode in a circular waveguide dimensioned below cutoff for all higher modes. In this way, modes that introduce errors are avoided.

Several types of dielectric-mounted helices were built with axial ratios less than 2 db and vswr less than 2 on a 50-ohm line. These helices were tested by rotating a small probe on the periphery of a circular waveguide terminated in a crossed tapered resistive-strip load.

The helix dimensions fell within the limits of Kraus' data,[3] although they were found to be more critical than the air-supported-helix dimensions.

Experimental work on the helices indicated that the axial ratio was critically dependent on the length of wire used. For example, a $\frac{1}{8}$-inch change in wire length can result in a 2-db axial-ratio change. However, once the axial ratio is reduced to about 1 db and the impedance is properly matched, the complete helix assembly exhibits good frequency response. The typical response curves of Fig. 4 are for the teflon-mounted helix matched with a quarter-wave transformer.

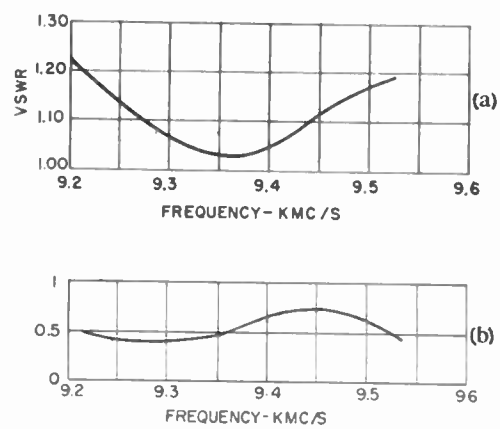

Fig. 4—(a) Standing-wave ratio of one helix vs frequency. (b) Axial ratio of one helix vs frequency.

The helix mounting method is quite important because of eccentricity errors. It was difficult to estimate the maximum permissible eccentricity, but if the helix end exhibits a peak-to-peak amplitude of less than 0.010

[3] J. D. Kraus, "Antennas," McGraw-Hill Book Co., New York, N. Y., chap. 7; 1950.

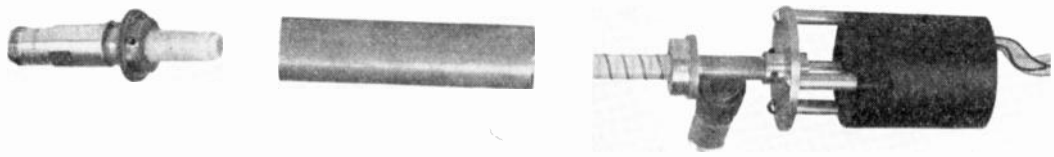

Fig. 3—Exploded view of phase shifter.

inch when the drive is rotated, then errors due to eccentricity should be small.

The total phase error to be expected from the use of this rotary phase shifter can be estimated from the apparent axial ratio (eccentricity and guide asymmetry give apparent axial ratios other than unity even if the helices are perfect) and the vswr seen from the phase shifter looking in each direction from the center of the circular waveguide. Note that this means the vswr plotted in Fig. 1 is the combined vswr of the helix and its load. Thus, referring to Fig. 4 and assuming that each helix has the same axial ratio and vswr, from Figs. 1(a) and 1(b), the sum of the two phase errors at 9.2 and 9.5 kmc is less than 1.5°.

The insertion loss of the phase shifter is less than 0.2 db, caused by vswr and normal wall losses.

Rotary-Phase-Shifter Tests

The phase-shifting characteristics were measured on a circuit similar to the usual phase-measuring arrangements but without using an air path.[4,5] These tests indicate very sharp (about 2° wide) resonant-absorption and phase-shift-discontinuity regions, 180° apart. This was attributed to a resonance of the small wrong-sense (for the helices) waves set up in the phase-shifter cavity. To suppress this, called for either ideal circular polarization launchers or a "wrong-sense" suppressor. The latter was tried in the form of loss-loaded slots cut in the circular waveguide so as to afford minimum interference with wall currents set up by the fields of the desired screw sense. The slots act as partial suppressors for the unwanted sense of rotation. Such a procedure reduced the amplitude of the transmission loss at the resonant points from 13 to 1.5 db. At nonresonant points, the transmission loss was less than 0.2 db.

[4] J. D. Kraus, "Antennas," McGraw-Hill Book Co., New York N. Y., p. 452; 1950.
[5] C. G. Montgomery, "Techniques of Microwave Measurements," McGraw-Hill Book Co., New York, N. Y., vol. 11, MIT Series, p. 916, Fig. 15.6; 1947.

Conclusion

A continuous rotary phase shifter employing helical circularly polarized H_{11} axial-mode launchers in a circular waveguide has been built and tested. Investigation of the errors involved and measurements indicate that the phase errors can be made less than ±2° maximum.

Acknowledgment

Acknowledgment is due to A. J. Lombardi for the mechanical design of the phase shifters and to A. T. Brown for making some of the measurements.

A Comparison of Two Radiometer Circuits*

S. J. GOLDSTEIN, JR.†, ASSOCIATE MEMBER, IRE

Summary—**The detection of weak thermal radiation and similar noise-like signals is often limited by the internal noise of the receiving apparatus. Dicke has described a method of detecting such signals. It employs a mechanical modulator at the input of a wide-band superheterodyne receiver. The detected output of the receiver is multiplied by a voltage of the same frequency as that which actuates the modulator, and filtered to produce a dc voltage when an external signal is present. Another method has been proposed which uses two independent receivers. The undetected output voltages are cross-correlated, and the correlator yields a dc voltage when a signal is applied to both receivers. Each method can be used to measure the intensity of signals small in amplitude compared to the noise of the receiver. A mathematical model of each of the circuits is presented, using, insofar as possible, the same assumptions; and equations derived for the least detectable signal power of each. The two-receiver method has, under the assumptions made, somewhat greater sensitivity. Engineering problems associated with each of the radiometers are discussed.**

Introduction

A RECEIVER designed to monitor near-sinusoidal signals can usually be made to have an adequate signal-to-noise ratio by narrowing the bandwidth to exclude the thermal and shot noise of the receiver. This process depends on the fact that the signal spectrum is sharply peaked while the noise has a nearly uniform spectrum. But shaping the band-pass of a receiver for thermal radiation or other noise-like signals has no such effect, because the spectra are practically indistinguishable.

The first of the methods to be described "identifies" the signal spectrum by modulating it before it is fed to the receiver. The second distinguishes between the signal and noise by virtue of the fact that the noise in independent receivers will be uncorrelated.

Radiometers of the kind described by Dicke have been widely used.[1–4] The model described in Dicke's 1946 paper[1] has a waveguide input to a balanced crystal mixer. A lossy dielectric wheel is rotated in and out of a slot in the waveguide at 30 cps, thus modulating the signal at that frequency. The receiver has a 30 mc intermediate frequency amplifier, a diode second detector followed by a 30 cps band-pass filter, and a phase-sensitive detector to which a voltage of the modulation frequency is also applied. Final detector output is

* Original manuscript received by the IRE, September 17, 1954; revised manuscript received, July 13, 1955.
† Stanford University, Stanford, Calif.

[1] R. H. Dicke, "The measurement of thermal radiation at microwave frequencies," *Rev. Sci. Instr.*, vol. 17, pp. 268–275; July, 1946.
[2] R. H. Dicke and R. Beringer, "Microwave radiation from the sun and moon," *Astrophys. Jour.*, vol. 103, pp. 375–376; May, 1946.
[3] A. E. Covington, "Microwave solar noise observations," *Nature*, vol. 159, pp. 405–406; March 22, 1947.
[4] R. H. Dicke, R. Beringer, R. L. Kyhl, and A. B. Vane, "Atmospheric absorption measurements," *Phys. Rev.*, vol. 70, pp. 340–348; September, 1946.

sent through a low-pass filter, yielding a dc voltage when a signal is present. A fluctuating voltage caused primarily by receiver noise is superimposed on dc signal.

The two-receiver radiometer cross-correlates the undetected receiver outputs with a multiplying circuit followed by a low-pass filter. If superheterodyne receivers are used, the local oscillators must be synchronized. The signal is supplied to each receiver through some sort of isolating device that prevents the noise at the input of one receiver from reaching the other. This leads to the requirement of separate antennas for most applications. The receiver noises will be uncorrelated, while the signal voltages in the two receivers are highly correlated. The output of the correlator has a dc component caused by the signal and a random component due to receiver noise, just as in the Dicke circuit. The output signal-to-noise ratio in each case is defined as the quotient of the dc power and the average power of the fluctuating component.

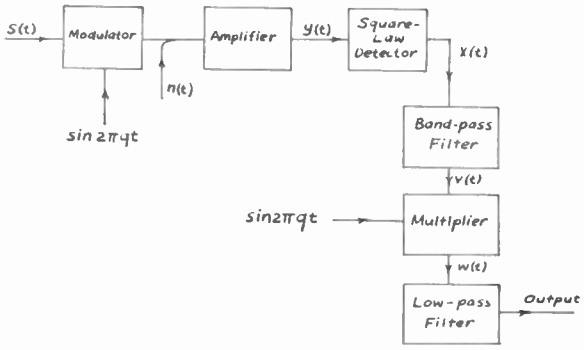

Fig. 1—Model of the Dicke radiometer.

Analysis of the Dicke Radiometer

The following assumptions are made:

1. Signal, $s(t)$, and noise, $n(t)$, have independent, stationary Gaussian amplitude distributions, with zero means and average powers σ_s^2 and σ_n^2, respectively.[5]
2. Signal and noise have uniform spectral densities over the range $f_1-\alpha/2$ to $f_1+\alpha/2$ cps, and are zero elsewhere.
3. The modulator produces 100 per cent amplitude modulation of the signal at a frequency of q cps and does not affect the noise.
4. The band-pass filter has uniform response over the range $q-\beta/2$ to $q+\beta/2$ cps and zero response elsewhere.
5. The low-pass filter has uniform response from zero to γ cps, and rejects all other frequencies.
6. The amplifier is linear, having constant gain over the signal spectrum. The complication of a superheterodyne receiver is omitted.
7. The output voltage of the detector, $x(t)$, is related to the input voltage, $y(t)$, by the equation: $x(t)=ky^2(t)$.
8. The output voltage of the multiplying circuit, $w(t)$, is given by $w(t)=v(t)\sin 2\pi qt$, where $v(t)$ is the output of the band-pass filter. (Fig. 1 above.)

[5] The units of each σ^2 is voltage squared, a one mho impedance level being understood.

The input voltage to the square-law detector has the form

$$y(t) = \tfrac{1}{2}s(t)[1+\sin 2\pi qt] + n(t).$$

The output voltage is

$$x(t)=k\{\tfrac{1}{4}s^2(t)[1+\sin 2\pi qt]^2+s(t)n(t)[1+\sin 2\pi qt]+n^2(t)\}.$$

The auto-correlation function of $x(t)$ is

$$\begin{aligned}R_1(\tau)=\overline{x(t)x(t+\tau)}=k\Big[&\overline{s^2(t)s^2(t+\tau)}\\ &\cdot\left(\frac{9}{64}+\frac{1}{8}\cos 2\pi q\tau+\frac{1}{128}\cos 4\pi q\tau\right)\\ &+\overline{s(t)s(t+\tau)}\;\;\overline{n(t)n(t+\tau)}\left(1+\frac{1}{2}\cos 2\pi q\tau\right)\\ &+\overline{n^2(t)n^2(t+\tau)}+\frac{3}{4}\,\overline{n^2(t)}\;\;\overline{s^2(t)}\Big].\end{aligned}$$

The quantities $\overline{s^2(t)s^2(t+\tau)}$ and $\overline{n^2(t)n^2(t+\tau)}$ are evaluated from a double integration over the joint bivariate normal distribution

$$\overline{s^2(t)s^2(t+\tau)} = \sigma_s^4 + 2[\overline{s(t)s(t+\tau)}]^2$$
$$\overline{n^2(t)n^2(t+\tau)} = \sigma_n^4 + 2[\overline{n(k)n(t+\tau)}]^2.$$

Auto-correlation functions $\overline{s(t)s(t+\tau)}$ and $\overline{n(t)n(t+\tau)}$ are found by taking the Fourier transforms of the assumed spectral densities of $s(t)$ and $n(t)$. Thus

$$\overline{s(t)s(t+\tau)} = \frac{\sigma_s^2\cos 2\pi f_1\tau\sin\pi\alpha\tau}{\pi\alpha\tau}$$

$$\overline{n(t)n(t+\tau)} = \frac{\sigma_n^2\cos 2\pi f_1\tau\sin\pi\alpha\tau}{\pi\alpha\tau}.$$

Substituting these relations in the expression for $R_1(T)$, and omitting periodic terms of frequencies $2q$ and $2f_1$, gives

$$\begin{aligned}R_1(\tau)=k^2\Big\{&\frac{\sigma_s^4}{8}\cos 2\pi q\tau+\left(\frac{9}{64}\sigma_s^4+\frac{3}{4}\sigma_s^2\sigma_n^2+\sigma_n^4\right)\\ &+\left(\frac{9}{64}\sigma_s^4+\frac{1}{2}\sigma_s^2\sigma_n^2+\sigma_n^4\right)\frac{\sin^2\pi\alpha\tau}{\pi^2\alpha^2\tau^2}\\ &+\frac{1}{4}\left(\frac{1}{2}\sigma_s^4+\sigma_n^2\sigma_s^2\right)\frac{\sin^2\pi\alpha\tau\cos 2\pi q\tau}{\pi^2\alpha^2\tau^2}\Big\}.\end{aligned}$$

The spectral density of the detector output, the inverse Fourier transform of $R_1(\tau)$, is divided into four parts, corresponding to the four terms of $R_1(\tau)$. That is

$$\begin{aligned}G_1(f) &= 4\int_0^\infty R_1(\tau)\cos 2\pi f\tau d\tau\\ &= G_{11}(f)+G_{12}(f)+G_{13}(f)+G_{14}(f).\end{aligned}$$

Carrying out the integration, the components are found to be

$$G_{11}(f)=\frac{k^2}{8}\,\sigma_s^4\delta(f-q)$$

$$G_{12}(f)=k^2\left(\frac{9}{64}\,\sigma_s^4+\frac{3}{4}\,\sigma_s^2\sigma_n^2+\sigma_n^4\right)\delta(f)$$

$$G_{13}(f)=2k^2\left(\frac{9}{64}\,\sigma_s^4+\frac{1}{2}\,\sigma_s^2\sigma_n^2+\sigma_n^4\right)\frac{\alpha-f}{\alpha^2},\quad 0<f<\alpha$$

$$G_{14}(f)=\frac{k^2}{2}\left(\frac{1}{2}\,\sigma_s^4+\sigma_n^2\sigma_s^2\right)\frac{\alpha-q}{\alpha^2},\quad 0<f<q$$

$$=\frac{k^2}{2}\left(\frac{1}{2}\,\sigma_s^4+\sigma_n^2\sigma_s^2\right)\frac{\alpha-f}{\alpha^2},\quad q<f<\alpha-q$$

$$=\frac{k^2}{4}\left(\frac{1}{2}\,\sigma_s^4+\sigma_n^2\sigma_s^2\right)\frac{\alpha+q-f}{\alpha^2},\quad \alpha-q<f<\alpha+q.$$

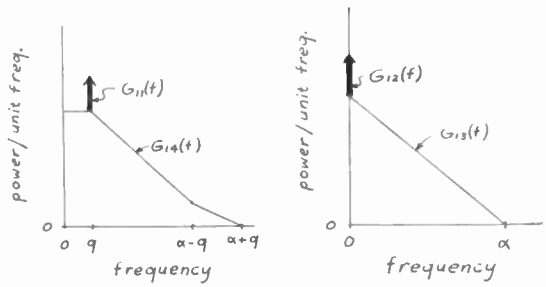

Fig. 2—Components of the spectral density of the detector output.

$G_{11}(f)$ represents the signal, while $G_{12}(f)$ represents dc that will not be transmitted by the band-pass filter (Fig. 2 above). The noise power at the output of the band-pass filter, P_2, is given by

$$P_2=\int_{q-(\beta-2)}^{q+\beta/2}[G_{13}(f)+G_{14}(f)]df.$$

Since $\alpha\gg\beta$, this can be approximated by

$$P_2=[G_{13}(q)+G_{14}(q)]\beta.$$

Substituting the expression for $G_{13}(f)$ and $G_{14}(f)$ and assuming that $\alpha\gg q$ yields

$$P_2=k^2\left[\frac{17}{32}\,\sigma_s^4+\frac{3}{2}\,\sigma_s^2\sigma_n^2+2\sigma_n^4\right]\frac{\beta}{\alpha}.$$

The spectral density of the noise changes slowly in the pass band of the filter because $\alpha\gg\beta$. Assuming that it is constant in the pass band leads to the following expression for the auto-correlation function of $v(t)$:

$$R_2(\tau)=\frac{k^2}{8}\,\sigma_s^4\cos 2\pi q\tau$$
$$+\frac{k^2}{\alpha}\left[\frac{17}{32}\,\sigma_s^4+\frac{3}{2}\,\sigma_s^2\sigma_n^2+2\sigma_n^4\right]\frac{\cos 2\pi q\tau\sin\beta\pi\tau}{\pi\tau}.$$

$v(t)$ can also be written

$$v(t)=[A+Bm(t)]\sin 2\pi qt$$

where $m(t)$ is a random voltage, and A and B are constants. The output of the multiplier is

$$w(t)=[A+Bm(t)]\sin^2 2\pi qt.$$

The auto-correlation function of $w(t)$ neglecting terms that are removed by the low-pass filter is

$$R_3(T)=\frac{k^2}{16}\,\sigma_s^4+\frac{k^2}{2\alpha}\left[\frac{17}{32}\,\sigma_s^4+\frac{3}{2}\,\sigma_s^2\sigma_n^2+2\sigma_n^4\right]\frac{\sin\pi\beta\tau}{\pi\tau}.$$

The spectral density at this point, consisting of a signal term $G_{31}(f)$ and a noise term $G_{32}(f)$ is expressed by

$$G_3=4\int_0^\infty R_3(\tau)\cos 2\pi f\tau d\tau=G_{31}(f)+G_{32}(f)$$

where

$$G_{31}(f)=\frac{k^2}{16}\,\sigma_s^4\delta(f)$$

and

$$G_{32}(f)=\frac{k^2}{\alpha}\left[\frac{17}{32}\,\sigma_s^4+\frac{3}{2}\,\sigma_s^2\sigma_n^2+2\sigma_n^4\right],\quad 0<f<\frac{\beta}{2}.$$

The signal power at the output of the low-pass filter is $k^2/16\sigma_s^4$, while the noise power is $G_{32}(0)\gamma$. Thus, the ratio of signal to noise is given by

$$\left(\frac{s}{n}\right)_0=\frac{\frac{1}{16}\,\sigma_s^4}{\frac{17}{32}\,\sigma_s^4+\frac{3}{2}\,\sigma_s^2\sigma_n^2+2\sigma_n^4}\left(\frac{\alpha}{\gamma}\right).$$

For weak signals the denominator is dominated by σ_n^4, so for this case the following simplification is made

$$\left(\frac{s}{n}\right)_0=\frac{1}{32}\,\frac{\sigma_s^4}{\sigma_n^4}\,\frac{\alpha}{\gamma}.$$

If an output signal-to-noise ratio of unity is required, the least detectable signal power in the input of a Dicke radiometer is

$$\sigma_{ld}^2=4\sqrt{2}\sigma_n^2\sqrt{\frac{\gamma}{\alpha}}.$$

The modulator wheel can be designed to cause square-wave modulation at q cps instead of the sine-wave type assumed. If this change is made and the sine-wave input to the multiplier retained, the analysis is complicated by the additional harmonics of q. But for weak signals the only significant effect of changing to a square-wave modulator is to increase the signal power by the factor $16/\pi^2$, this being the ratio of the power in the fundamental component of a square wave to that of a sine wave of the same peak amplitude. The minimum detectable signal power for the radiometer, when equipped with a square-wave modulator wheel, becomes[6]

$$\boxed{\sigma_{ld}^2=\frac{\sqrt{2}\Pi^2\sigma_n^2}{4}\sqrt{\frac{\gamma}{\alpha}}}.$$

[6] As pointed out by one of the reviewers, a square-wave input to the multiplier would increase the signal-to-noise ratio by the factor $\pi/\sqrt{8}$ if β is large enough to pass the harmonics of q.

Analysis of the Two-Receiver Radiometer[7]

The assumptions follow:

1. Signal, $s(t)$, noise in first receiver, $n_1(t)$, and noise in second receiver, $n_2(t)$, have independent, stationary, Gaussian amplitude distributions with zero means, and average powers σ_s^2, σ_{n1}^2, and σ_{n2}^2, respectively.
2. The signal and noise have flat spectral densities over the range $f_1-\alpha/2$ to $f_1+\alpha/2$ cps and are zero elsewhere.
3. The multiplier circuit obeys the equation $y(t)=kx_1(t)x_2(t)$, where $x_1(t)$ is the output of the first receiver and $x_2(t)$ that of the second.
4. The low-pass filter has uniform response from zero to γ cps, and no response elsewhere. (Fig. 3.)

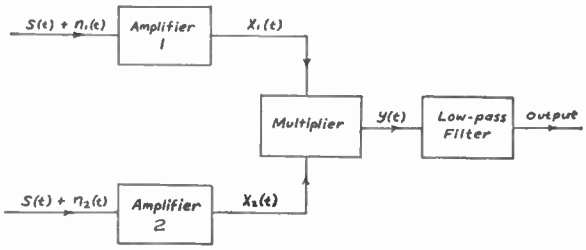

Fig. 3—Model of the two-receiver radiometer.

The voltage output of the multiplier is given by

$$y(t) = k\{s^2(t) + s(t)[n_1(t) + n_2(t)] + n_1(t)n_2(t)\}.$$

The auto-correlation function of $y(t)$ is

$$R_1(T) = k^2\{\overline{s^2(t)s^2(t+\tau)} + \overline{s(t)s(t+\tau)}\,[\overline{n_1(t)n_1(t+\tau)} + \overline{n_2(t)n_2(t+\tau)}] + \overline{n_1(t)n_1(t+\tau)}\;\overline{n_2(t)n_2(t+\tau)}\},$$

but

$$\overline{s^2(t)s^2(t+\tau)} = \sigma_s^4 + 2(\overline{s(t)s(t+\tau)})^2$$

$$\overline{s(t)s(t+\tau)} = \frac{\sigma_s^2 \cos 2\pi f_1\tau \sin \pi\alpha\tau}{\pi\alpha\tau}$$

$$\overline{n_1(t)n_1(t+\tau)} = \frac{\sigma_{n1}^2 \cos 2\pi f_1\tau \sin \pi\alpha\tau}{\pi\alpha\tau}$$

$$\overline{n_2(t)n_2(t+\tau)} = \frac{\sigma_{n2}^2 \cos 2\pi f_1\tau \sin \pi\alpha\tau}{\pi\alpha\tau}.$$

Substituting these relations, and omitting terms of frequency $2f_1$ yields

$$R_1(\tau) = k^2\left\{\sigma_s^4 + \frac{1}{2}[2\sigma_s^4 + \sigma_s^2(\sigma_{n1}^2 + \sigma_{n2}^2) + \sigma_{n1}^2\sigma_{n2}^2]\frac{\sin^2 \pi\alpha\tau}{\pi^2\alpha^2\tau^2}\right\}.$$

The first term, $R_{11}(\tau)=k^2\sigma_n^4$, describes the signal. The other term, $R_{12}(\tau)$, is noise. Noise power output of low-pass filter is approximated by $P=G_{12}(0)\gamma$, where $G_{12}(f)$ is the inverse Fourier transform of $R_{12}(\tau)$. Thus,

$$P = 4\gamma\int_0^\infty R_{12}(\tau)d\tau$$
$$= [2\sigma_s^4 + \sigma_s^2(\sigma_{n1}^2 + \sigma_{n2}^2) + \sigma_{n1}^2\sigma_{n2}^2]k^2\frac{\gamma}{\alpha}.$$

Since the output signal power is $k^2\sigma_s^4$, the ratio is

$$\left(\frac{s}{n}\right)_0 = \frac{\sigma_s^4}{2\sigma_s^4 + \sigma_s^2(\sigma_{n1}^2 + \sigma_{n2}^2) + \sigma_{n1}^2\sigma_{n2}^2}\left(\frac{\alpha}{\gamma}\right).$$

For the case where $\sigma_{n1}^2=\sigma_{n2}^2=\sigma_n^2$ and $\sigma_n^2 \gg \sigma_s^2$, the expression becomes

$$\left(\frac{s}{n}\right)_0 = \frac{\sigma_s^4}{\sigma_n^4}\frac{\alpha}{\gamma}.$$

A required output signal-to-noise ratio of unity results in this formula for the least-detectable signal power

$$\boxed{\sigma_{ld}^2 = \sigma_n^2\sqrt{\frac{\gamma}{\alpha}}}.$$

Conclusions

The minimum detectable signal power for the two-receiver radiometer is lower by a factor of 3.48. This can be attributed in part to the fact that the Dicke radiometer does not utilize the signal all of the time.

The engineering problems involved in the two devices are quite different. The two-receiver radiometer will ordinarily need a high degree of isolation between the two inputs, so that separate sources of the signal will be used. However, it is conceivable that the noise voltages in the two receivers can be made uncorrelated, if not independent. That is $n_1(t)$ and $n_2(t)$ need not be independent if their sine-wave components were always at a ninety-degree phase difference. But this situation seems difficult to obtain in practice.

Phase stability of the receivers is of great importance, since a 90-degree phase difference between them causes the signal to vanish. The multiplier or balanced modulator must be well-balanced and function over a wide bandwidth. A principal problem of radiometer circuits is that of gain-variation noise. It can be solved in the two-receiver circuit by the simple expedient of separate automatic gain controls on the receivers.

The modulator wheel of the Dicke radiometer must present a precise impedance match to the mixer, to avoid modulating the noise as well as the signal. Gain-variation noise is also eliminated by automatic gain control. The response time of the gain control must not be too short or the signal will be removed.

Although there is an appreciable difference in sensitivity between the two radiometers, the difference in input circuits will be more important in determining which should be employed for a given purpose.

Acknowledgment

The author wishes to acknowledge many helpful suggestions from Prof. W. Harman of Stanford University.

[7] A somewhat similar analysis can be found in R. M. Fano, "Signal to Noise Ratio in Correlation Detectors," *M.I.T. Res. Lab. Elec. Tech.* Rep. 186; 1951.

Correspondence

Optimizing the Design Characteristics of Triodes for Maximum Gain into a Fixed Load Impedance*

The question of optimizing the design of a triode was investigated, when operating with a small signal into an ac load impedance of a predetermined value R_L. An "ideal" triode, following the 3/2 power law, was assumed. As a further assumption, a fixed value of perveance P was assumed. In practical cases, the perveance is limited by cathode size, meaning heater wattage, and by the cathode to grid spacing, which is mostly a question of economics. Therefore, the remaining variable is the μ of the triode, which we will attempt to optimize.

With conventional terminology we write gain

$$G = g_m \frac{R_p R_L}{R_p + R_L} = \frac{\mu R_L}{R_p + R_L}.$$

To study the effect of tube variations on the gain we differentiate with respect to μ and equate to 0 for the point of maximum gain.

$$(R_p + R_L)^2 \frac{\partial G}{\partial \mu} = R_L(R_p + R_L) - \mu R_L \frac{\partial R_p}{\partial \mu} = 0.$$

Therefore

$$\mu \frac{\partial R_p}{\partial \mu} = R_p + R_L. \tag{1}$$

Now we describe the tube characteristics by:

$$I_p = P\left(E_g + \frac{E_p}{\mu}\right)^{3/2} \tag{2}$$

$$g_m = \frac{3P}{2}\left(E_g + \frac{E_p}{\mu}\right)^{1/2} \tag{3}$$

$$R_p = \frac{2\mu}{3P}\left(E_g + \frac{E_p}{\mu}\right)^{-1/2}. \tag{4}$$

We derive

$$\frac{\partial R_p}{\partial \mu} = \frac{2}{3P}\left(E_g + \frac{E_p}{\mu}\right)^{-1/2} + \frac{2\mu}{3P}(-1/2)\left(E_g + \frac{E_p}{\mu}\right)^{-3/2}\left(-\frac{E_p}{\mu^2}\right) = \frac{R_p}{\mu} + \frac{E_p}{3\mu I_p}$$

from (2) and (4). Substituting this into (1),

$$R_p + R_L = R_p + \frac{E_p}{3I_p};$$

thus

$$R_L = \frac{E_p}{3I_p} \quad \text{or} \quad I_p = \frac{E_p}{3R_L}. \tag{5}$$

This relation (5) expresses the conditions for maximum gain in terms of plate current, plate voltage and load resistance. It is interesting to note that no other parameters enter into this relation.

To evaluate μ, we introduce (2) into (5) and obtain

$$\mu_{opt} = \frac{E_p}{\left(\frac{E_p}{3PR_L}\right)^{2/3} - E_g}. \tag{5a}$$

To evaluate gain we write

$$G = \frac{g_m R_L}{1 + \frac{R_L}{R_p}},$$

and introduce (2), (4) and (5):

$$G = \frac{g_m R_L}{1 + \frac{R_L I_p}{\frac{2}{3}\mu\left(E_g + \frac{E_p}{\mu}\right)}} = \frac{g_m R_L}{1 + \frac{E_p}{2(\mu E_g + E_p)}}$$

$$\cdot G = \frac{g_m R_L}{1 + \frac{1}{2\left(1 + \frac{\mu E_g}{E_p}\right)}}. \tag{6}$$

Since $\mu E_g/E_p$ can only vary between 0 at 0 grid bias and -1 at cutoff, it can be shown the maximum value of gain is achieved at $E_g = 0$. This maximum gain is

$$G_{max} = \tfrac{2}{3} g_m R_L.$$

It is observed that this maximum gain is identical to what would be obtained if one made a pentode of high plate resistance with the same cathode-control grid structure, if the screen grid draws $\frac{1}{3}$ the cathode current.

In practical cases it will be advantageous to make a tube with closer spacing than the "ideal" triode, allowing some island formation. It can be assumed that maximum gain then will be obtained with a somewhat lower plate current than given by the above relation. However, it remains as a useful and simple rule of thumb.

MAX BARFISS
Tung-Sol Electric Inc.
Bloomfield, N. J.

* Received by the IRE, May 2, 1955; revised manuscript received, June 22, 1955.

Influence of the Order of Overtone on the Temperature Coefficient of Frequency of AT-Type Quartz Resonators*

It is well known that the temperature coefficient of frequency of AT-type quartz resonators depends on the order of overtone. In particular the angle giving the zero temperature coefficient of frequency is different for the fundamental and overtones. For example, the zero angles measured under certain conditions for the plate[1] are, for the fundamental mode 35°10′, for the third mode 35°18′, and for the fifth mode 35°20′. In the following, a theoretical explanation for this effect is given.

The frequency equation for the nth order of the thickness shear mode of a plate[2] is expressed by

$$f_n = \frac{n}{2t}\sqrt{\frac{c_\theta^D}{\rho}}\left(1 - \frac{1}{n^2}\frac{16e_\theta^2}{\pi\epsilon_\theta c_\theta^D}\frac{t}{t_0}\right), \tag{1}$$

where n is the order of the mode, c_θ^D the resulting elastic stiffness at constant normal displacement, e_θ the resulting piezoelectric stress constant, ϵ_θ the dielectric constant, t the thickness of the plate, $t_0 = t + \epsilon_\theta\Delta$ with Δ being the total electrode gap, and ρ the density. The subscript θ indicates the angle of orientation of the plate. For the temperature coefficient of frequency, considering only the terms of first order from (1), it follows that

$$Tf_n = \tfrac{1}{2}Tc_\theta^D + (\alpha_x - \alpha_z)\sin^2\theta + \tfrac{1}{2}\alpha_z - [2Te_\theta - Tc_\theta^D - T\epsilon_\theta]\frac{16e_\theta^2}{n^2\pi\epsilon_\theta c_\theta^D}\frac{t}{t_0}, \tag{2}$$

where α_x and α_z are the linear coefficients of expansion perpendicular and parallel to the axis. The last term in (2) becomes zero for infinitely large electrode gap $\Delta \to \infty$ ($t_0 \to \infty$) or for very high order of n. The difference between the temperature coefficient of frequency for the fundamental mode ($n = 1$) and the mode of the order n assuming a zero electrode gap ($t_0 = t$) is, according to (2),

$$Tf_n - Tf_1 = [2Te_\theta - Tc_\theta^D - T\epsilon_\theta] \cdot \frac{16e_\theta^2}{\pi\epsilon_\theta c_\theta^D}\left(1 - \frac{1}{n^2}\right). \tag{3}$$

As an example the AT-type quartz resonator may be considered. The values for $\theta = 35°10'$ are

$c_\theta^D = 29.26 \cdot 10^{10}$ dyn·cm^{-2} $\quad Tc_\theta = -6 \cdot 10^{-6}$/°C
$e_\theta = 2.88 \cdot 10^4$ ESU·cm^{-2} $\quad Te_\theta = 1.0 \cdot 10^{-4}$/°C
$\epsilon_\theta = 4.53$ $\quad T\epsilon_\theta = 0.$[3]

Accurate values for $T\epsilon$ are not yet known; however, the temperature change of ϵ in the temperature range considered is very small (see ref. 3). Using these values, the difference between the temperature coefficient of frequency for the fundamental mode Tf_1 and the mode of infinitely high order Tf_∞, assuming zero electrode gap, is

$$Tf_\infty - Tf_1 = [2Te_\theta - Tc_\theta^D - T\epsilon_\theta]\frac{16e_\theta^2}{\pi\epsilon_\theta c_\theta^D} = 0.66 \cdot 10^{-6}/°\text{C}. \tag{4}$$

* Received by the IRE, August 8, 1955.

[1] R. Bechmann, "Frequency-Temperature Behavior of Resonators of Natural and Synthetic Quartz," paper presented at the Ninth Annual Frequency Control Symposium of the U. S. Signal Corps, Components Division, Frequency Control Branch, Fort Monmouth, N. J.; May 26, 1955.
[2] R. Beckmann, "Thickness vibrations of piezoelectric crystal plates," *Arch. elekt. Übertragung*, vol. 6, pp. 361–368; 1952.
[3] A. Pavlovic, and R. Pepinsky, "Re-examination of low-temperature properties of crystalline quartz," *Jour. Appl. Phys.*, vol. 25, pp. 1344–1345; October, 1954.

Using the value $-5.15 \cdot 10^{-6}/°C$ for the change of the first-order temperature coefficient of frequency[1] with the angle of orientation θ, the zero angle of the temperature coefficient of frequency for the mode of infinitely high order is shifted about 7.7′ in arc in comparison with the fundamental mode—for the third mode the shift is about 6.8′. These values for the differences of the zero angles for the temperature coefficients of frequency are in good agreement with the experimental values given above. The calculated differences in the angles are somewhat smaller than the observed values. However, small uncertainties in these values are involved due to the omission of the unknown temperature coefficient of the dielectric constant T_{ϵ_θ}.

Similarly, the properties of BT-type quartz resonators and of thickness shear mode resonators made from other materials having zero temperature coefficients of frequency, for example EDT and DKT, can be calculated.

R. Bechmann
Brush Labs. Co., Div. Clevite Corp.
Cleveland, Ohio

Optimum Tube Utilization in Cascaded Distributed Amplifiers*

In the paper "Distributed Amplification"[1] a derivation is given for the minimum number of tubes required to produce a given gain, showing that a minimum of tubes is obtained when the individual stage gain is $e(=2.718)$. The derivation ignores the fact that in the usual practical situation both a gain and 3-db bandwidth are specified. This requires the evaluation of a bandwidth-narrowing factor which is introduced when stages are cascaded. This factor which depends on the type of transmission line and its design parameters will be evaluated for a design using constant-resistance bridged-T-lines (i.e., $Z_{0p}=Z_{0g}=R$).

The single-stage transfer function in this case is given by

$$\frac{|e_0|}{|e_{in}|} = \frac{ng_mR}{2[(1-x^2)^2+m^2x^2]}, \qquad (1)$$

where

x = normalized frequency (f/f_c),
n = number of tubes per stage,
$m^2 = L/(L-4M)$,
g_m = tube transconductance,
L = inductance of center-tapped coil, and
f_c = line cutoff frequency.

Eq. (1) is essentially equivalent to that derived in the referenced article.[2] The time delay per stage (τ) is a function of frequency given by

$$\tau = \frac{nm(1+x^2)}{\pi f_c[(1-x^2)^2+m^2x^2]}. \qquad (2)$$

Inspection of (1) shows that the steady-state frequency response is maximally flat for $m=\sqrt{2}$ and inspection of (2) shows that the time-delay vs frequency characteristic is maximally flat for $m=\sqrt{3}$. In the design of a pulse amplifier the steady-state amplitude response and the time-delay (or phase) response vs frequency can be considered of equal importance. This suggests using a compromise value for m, between the $\sqrt{2}$ and $\sqrt{3}$, in a practical design.

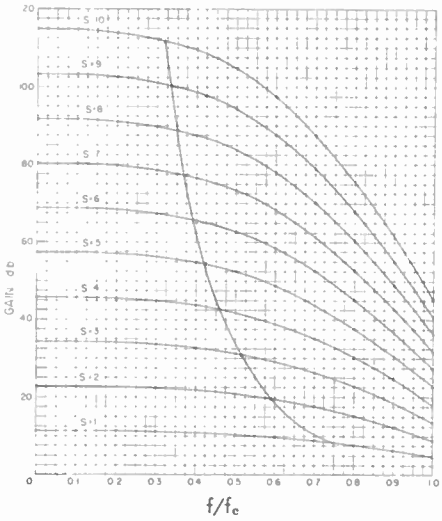

Fig. 1—Cascaded amplifier gain vs normalized frequency.

Fig. 1 is a graph of gain[3] vs normalized frequency as successive stages are cascaded with $m=1.5$. The 3-db points on each characteristic are shown connected by a smooth curve. In Fig. 2 these points have been replotted to show the cascaded resultant bandwidth (B) as a function of the number of cascaded stages (S). Fig. 3 is the same plot on a log/log scale. The points can now be connected by a straight line with reasonable accuracy and the empirical relation

$$B = 0.75f_cS^{-0.365} \qquad (3)$$

can be derived from Fig. 3.

With (3) now available the development is similar to that of the above mentioned paper:

$$N \text{ (total tube complement)} = nS. \qquad (4)$$

Before (4) can be differentiated, an additional relationship is needed between n and S. From (1), the zero frequency cascaded gain G is

$$G = \left[\frac{ng_mR}{2}\right]^S. \qquad (5)$$

For both constant-resistance bridged-T lines and m-derived lines,[4]

$$R = \frac{m}{\pi f_cC} = \frac{1.5}{\pi f_cC}, \qquad (6)$$

where C is kept to the minimum value dictated by the tube input capacity plus the stray wiring capacity. Substituting f_c from (3) in (6) and then substituting resultant expression for R in (5) and solving for n:

$$n = \frac{8\pi BCG^{1/S}S^{0.365}}{4.5g_m}. \qquad (7)$$

Eq. (7) is the additional relationship required. The parameters G and B are the specified gain and over-all bandwidth, and C and g_m are determined by the tube selected. The variables left to our control are the number of stages and the number of tubes per stage. Under the assumptions

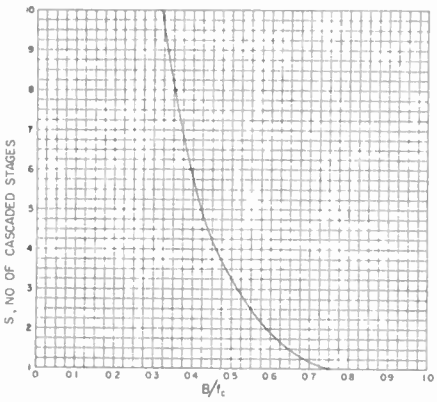

Fig. 2—Number of cascaded stages vs. normalized bandwidth.

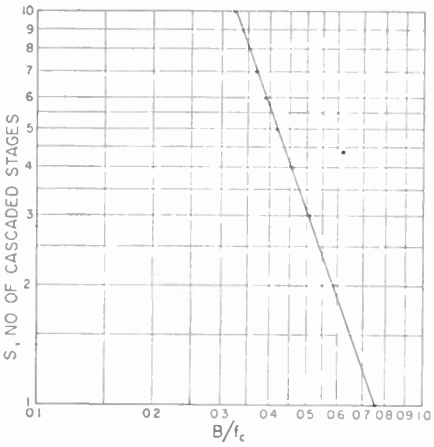

Fig. 3—Number of cascaded stages vs normalized bandwidth (log/log scale).

$$G = 10^4 \qquad B = 50 \text{ mc}$$
$$g_m = 5000 \text{ umhos} \qquad C = 7 \text{ uuf}$$

we have

$$n = 0.391(G)^{1/S}S^{0.365} \qquad (8)$$

and

$$N = 0.391(G)^{1/S}S^{1.365}. \qquad (9)$$

Finding dN/dS from (9) and letting the derivative equal zero:

$$1.365S - \ln G = 0, \qquad (10)$$

and for $G=10^4$:

S = 6.75 stages
N = 20.6 tubes
n = 3.14 tubes/stage
stage gain = 11.85 db (voltage gain of 3.92).

The best approximation to these figures for a practical amplifier would be seven stages of three tubes each.

The line cutoff frequency (f_c) can be calculated from (3) and the line impedance from (6) with the results.

$$f_c = 136 \text{ mc}$$
$$R = 500 \text{ ohms}.$$

Fig. 4 is a photograph of a distributed amplifier with design parameters reasonably close to the above. The tube comple-

* Received by the IRE, August 3, 1955.

[1] E. L. Ginzton, W. R. Hewlett, J. H. Jasberg and J. D. Noe, Proc. IRE, vol. 36, pp. 956–969; August 1948.

[2] *Loc. cit.*, p. 969, eq. (71).

[3] The gain scale (db) is actually arbitrary, the numbers shown were inserted after the final design was determined.

[4] Note similarity to reference 2, eqs. (11) and (20).

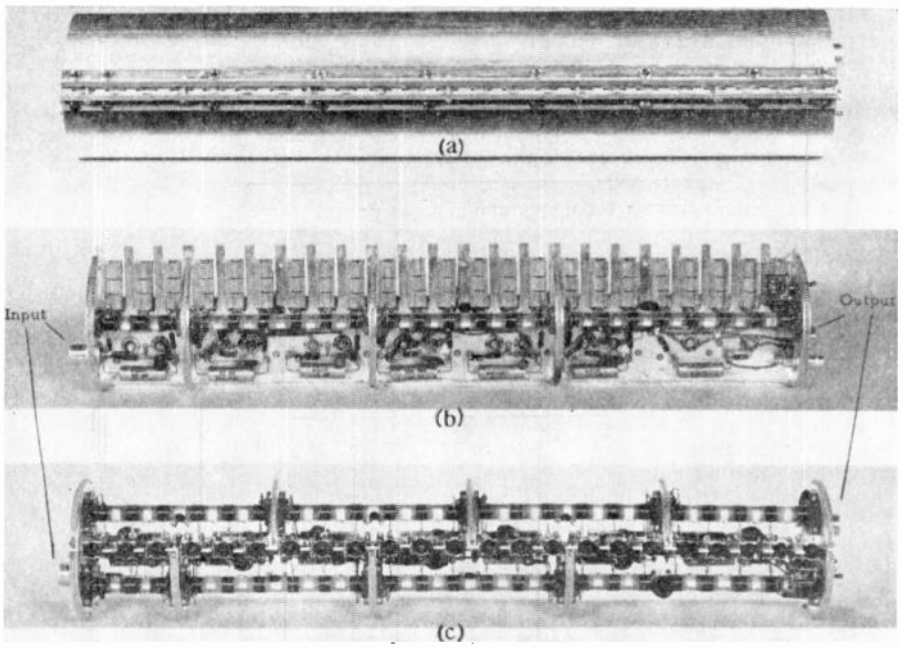

Fig. 4—80-db distributed amplifier. (a) amplifier enclosed in cylindrical jacket. (b) side view, jacket removed. (c) Top view, jacket removed.

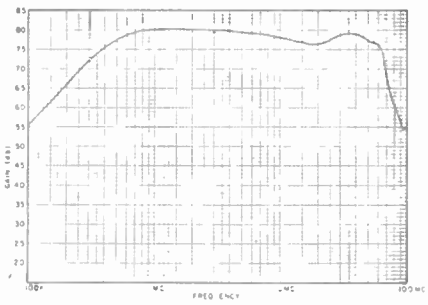

Fig. 5—Distributed amplifier frequency response.

ment is twenty-three 5840's, there being 5 tubes in the seventh (output) stage to obtain a greater output voltage swing than is available from the 3 tube stages. Fig. 5 shows the amplifier gain in db as a function of frequency for a total $B+$ current of 230 ma. The upper 3-db cutoff is at 55 mc.

A. I. Talkin
J. V. Cuneo
Diamond Ordnance Fuze Lab.
Washington 25, D. C.

Self-Bias Cutoff Effect in Power Transistors*

In a recent article[1] the author pointed out that the majority carrier current flowing through the base region of a transistor towards the base connection causes an ohmic voltage drop which is in such a direction as to reduce the forward bias on parts of the emitter distant from the base lead. In power transistors this effect is serious and substantially all the emitter current is carried by a small area of the emitter near to the base contact. In that article an expression was derived for this effect at moderate current densities, which, when the emitter efficiency term is included, can be written, for a p-n-p transistor,

$$j(x) \approx j(0)\left[1 + x\sqrt{\frac{1}{2W\sigma_b}\left(\frac{\sigma_b W}{\sigma_e L_e} + \frac{1}{2}\frac{W^2}{L_b^2}\right)\frac{q}{kT}j(0)}\right]^{-2}, \quad (1)$$

where $j(x)$ is the emitter current density at a distance x from the base connection (see Fig. 1), W is the base width, σ_e the conductivity, L_e the diffusion length of minority carriers in the emitter region, and σ_b the conductivity of the base region.

It has been pointed out to me by Mr. N. Golden of Transistor Products and Dr. R. N. Hall of the General Electric Company that the case of most practical interest occurs at injection levels much higher than those discussed. A more general solution for the high level case is presented below.

Webster[2] has derived an expression for α as a function of emitter current. If we omit surface terms and consider the semi-infinite transistor in Fig. 1, then for the p-n-p case,

$$1 - \bar{\alpha}(x) \approx \left[\frac{\sigma_b W}{\sigma_e L_e} + \frac{1}{2}\frac{W^2}{L_b^2}\right]\left[1 + \frac{z}{2}\right], \quad (2)$$

where

$$z = \frac{W\mu_e}{D_p\sigma_b}j(x), \qquad \bar{\alpha} = \frac{1}{j}\int_0^j \alpha\, dj. \quad (3)$$

If $\bar{\sigma}_b(x)$ is the average base conductivity "seen" by the base current at x, then

$$\bar{\sigma}_b(x) = h\sigma_b\left(1 + \frac{z}{2}\right), \quad (4)$$

where h is a weighting factor, approximately equal to $\frac{1}{2}$ for high currents.

If $i_b(x)$ is the base current at x, then

$$\frac{di_b}{dx} = -(1 - \bar{\alpha})j(x), \quad (5)$$

and if $V(x)$ is the forward bias voltage of the emitter relative to the base at x,

$$i_b(x) = -W\bar{\sigma}_b\frac{dV}{dx} - \frac{kT}{q}\frac{d\sigma_b}{dx}W, \quad (6)$$

where the second term on the right takes account of the flow of electrons through the base by diffusion.

These two equations are now treated by the method of reference 1, but taking into account the dependence of σ_b on x given by (4). We also assume that we can write

$$j(x) = j_0 e^{qv/kT}, \quad (7)$$

where j_0 is a constant. The equations can now be solved but the result is a complicated implicit expression for $j(x)$. To obtain an explicit expression we assume

$$z = \frac{W\mu_e}{D_p\sigma_b}j(x) \gg 1 \quad (8)$$

for all x less than the value in which we are interested. This restricts our discussion to values of $j(x)$ greater than about 20 amperes per square centimeter in typical cases.

Essentially, (8) implies that the conductivity of the base region is due principally to the electrons accompanying the injected holes, rather than to the original base material conductivity.

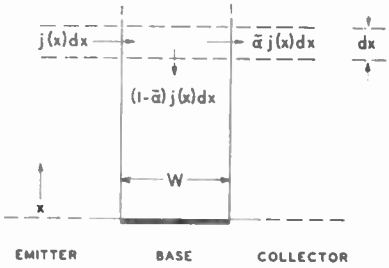

Fig. 1

With this restriction we find

$$j(x) \approx j(0)\left[1 + x\sqrt{\frac{1}{6W\sigma_b}\left(\frac{\sigma_b W}{\sigma_e L_e} + \frac{1}{2}\frac{W^2}{L_b^2}\right)\frac{q}{kT}j(0)}\right]^{-2}, \quad (9)$$

which then gives the fall-off of emitter current density with distance from the base connection (or the edge of the emitter in more complicated geometries). Eq. (9) differs from low level case only by factor $\sqrt{1/3}$ in coefficient x. Of this factor $1/\sqrt{2}$ is due to inclusion of diffusion term[3]; $\sqrt{2/3}$ to modulation of the base conductivity.

I should like to express my thanks to Dr. Hall and Mr. Golden for their interest and for many helpful suggestions.

N. H. Fletcher
Transistor Products, Inc.
Waltham, Massachusetts
(On leave from Div. of Radiophysics, C.S.I.R.O., Sydney, Australia)

* Received by the IRE, August 2, 1955.

[1] N. H. Fletcher, "Some aspects of the design of power transistors," Proc. IRE, vol. 43, pp. 551–559; May, 1955.

[2] W. M. Webster, "On the variation of junction transistor current amplification factor with emitter current," Proc. IRE, vol. 42, pp. 914–920; June, 1954

[3] R. N. Hall has treated the effects of diffusion and independently arrived at this same result. (Private communication.)

A Note on the Transfer Voltage Ratio of Resistive Networks with Positive Elements*

In a recent note[1] Reza and Lewis state the transfer voltage theorem,[1] "The magnitude of the voltage transfer ratio $A(s)$ of a passive RLC network containing no transformers is not greater than one for positive real values of s."

Their proof is based on the fact that the voltage transfer ratio for a purely resistive network (without ideal transformers) cannot exceed unity. A discussion at the Symposium on Circuit Analysis held at the University of Illinois in May, 1955 indicated that a simple proof of this (intuitively obvious) fact is not generally known. Such a proof is therefore given below.

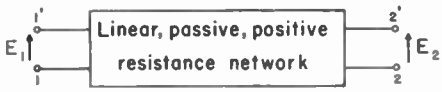

Fig. 1—Notation used (following Reza and Lewis).

Assume that a voltage $E_1 = V_1' - V_1$ is applied to the input terminals $1'-1$ of the network (Fig. 1). V_k denotes the potential of node k with respect to some reference point. For convenience, terminals $1'$ and $2'$ are taken to have potentials higher than (or equal to) terminals 1 and 2, respectively. Suppose that some node n different from node $1'$ has the maximum potential V_{max} of the network. Then all currents flowing through branches connecting n and its neighboring nodes are directed away from node n if all resistances are positive. In view of Kirchhoff's node current law, all these currents must be zero, and thus the potentials of all nodes connected to n must equal V_{max}. The argument may be repeated for any one of the nodes, say node m, connected to n, then for any one of the nodes connected to m, and so forth until node $1'$ appears connected to one of the nodes at potential V_{max}. Hence V_{max} must equal V_1', and the potential of no node of the network, including the output node $2'$, can exceed V_1'. Similarly, by considering a node k with the lowest potential V_{min}, it is seen that no node, including node 2, can have a potential lower than that of node 1. Thus the output voltage magnitude $|E_2| = |V_2' - V_2|$ cannot exceed the input voltage magnitude $|E_1| = |V_1' - V_1|$, and the voltage transfer ratio E_2/E_1 cannot exceed unity.

The proof given makes use of the fact that all elements are positive. The theorem is clearly not true, for example, for the passive network with negative elements shown in Fig. 2.[2]

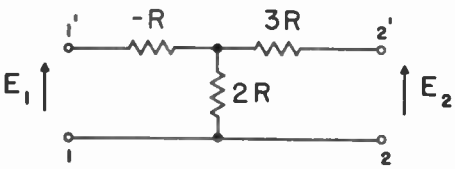

Fig. 2—A passive network for which the voltage transfer ratio exceeds unity.

The proof of Corollary I given by Reza and Lewis begins with, and rests on, the statement, "Since, for s real and positive, all elements act as resistors, then if $|E_1| = |E_2|$, terminals 2 and $2'$ must coincide with 1 and $1'$; that is, there must be zero resistance paths through the network between corresponding terminals." This statement may be proved as follows, except for the special Case II noted.

Case I—Finite Resistance between terminals 2 and $2'$ (Fig. 3). In this case ($E_2 \neq 0$), current flows from node $2'$ toward node 2. Hence, current must flow toward node $2'$ from at least one other node, say node 3. If $|E_2| = |E_1|$, then $V_2' = V_1'$ cannot be exceeded by any other node potential as shown above. Hence $V_3 = V_2'$ and the resistance between nodes 3 and $2'$ must be zero. By repeating this argument, it is seen that a zero resistance path must link nodes $2'$ and $1'$. Similarly, a zero resistance path must exist between nodes 2 and 1.

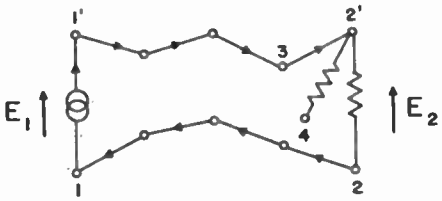

Fig. 3—Conditions existing when $|E_1| = |E_2|$, finite resistance between 2 and $2'$.

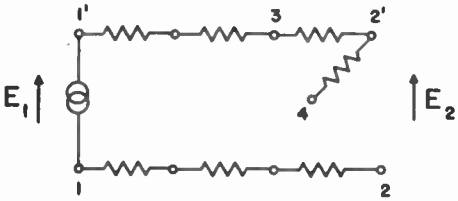

Fig. 4—Conditions existing when $|E_1| = |E_2|$, infinite resistance between 2 and $2'$.

Case II—Infinite resistance between terminals 2 and $2'$ (Fig. 4).[3] In this open circuit case no current can flow from node $2'$ toward node 2, and hence no current can flow toward node $2'$; hence the output and input nodes may be linked by resistance paths which carry no current.

R. J. Schwarz
Dep't, of Elec. Engrg.
Columbia University
New York 27, N.Y.

* Received by the IRE, July 22, 1955.

[1] F. M. Reza and P. M. Lewis II, "A note on the transfer voltage ratio of passive RLC networks," Proc. IRE, vol. 42, p. 1452; September, 1954.

[2] A passive network is defined as one whose total energy input is non-negative.

[3] This special case was pointed out by Dr. S. Darington.

Two Problems in Geometrical Optics and Application of the Results in Electron Trajectory Calculations*

Sometime back the author came across the two following two-dimensional problems:

1. Given a number of refracting media with circular cylindrical symmetry, that is, refracting surfaces disposed coaxially and the index of refraction a function of only the radius r (see Fig. 1), what can we say about the angles of incidence and/or refraction in the media for any given initial angle of incidence?

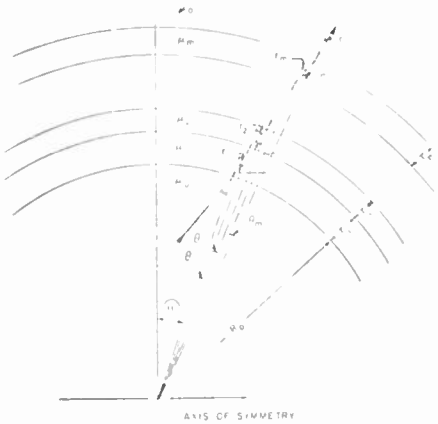

Fig. 1—Disposition of refracting surfaces (circular symmetry).

2. Given a number of refracting media whose disposition is as shown in Fig. 2,

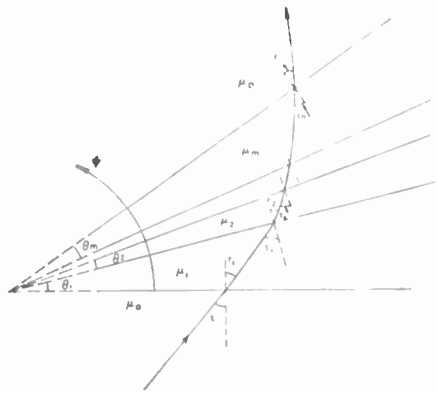

Fig. 2—Disposition of refracting surfaces (index of refraction function of polar angle ψ only).

where the refractive index is a function of only the polar angle ψ, what can we conclude about the angles of incidence and/or refraction in the media for any given initial angle of incidence?

As these problems are not treated in existing books[1] on geometrical and/or electron optics and since the solutions of the above problems are applicable to some interesting and practical problems, it was thought desirable to treat them here.

1. Let there be m media of refractive indices $\mu_1, \mu_2 \cdots, \mu_m$ (see Fig. 1). Let the initial angle of incidence and the final angle of refraction be denoted by i and r respectively. (For notation regarding other angles, see Fig. 1.) Let τ_j be the radial thickness of the jth medium. Then by the application of Snell's law and elementary trigonometry, we have

* Received by the IRE, August 3, 1955. Work carried out while the author was associated with the Electronics Lab., General Electric Co., Syracuse, N. Y.

[1] M. Born, "Optik," Springer, Berlin; 1933. J. L. Synge "Geometrical Optics," Cambridge University Math. Tract., 1937; W. Glaser, "Grundlagen der Elektronenoptik," Springer-Verlag, Wien; 1952.

$$\frac{\sin i}{\sin r_1} = \mu_1/\mu_0$$
$$\frac{\sin i_1}{\sin r_2} = \mu_2/\mu_1 \qquad (1)$$
$$\vdots$$
$$\frac{\sin i_m}{\sin r} = \mu_0/\mu_m,$$

and

$$\underline{/r_j} = \underline{/i_j} + \theta_j; \qquad j = 1, 2, \cdots m. \qquad (2)$$

Before we proceed with the case of an arbitrary value for m, consider first of all the case $m=1$. By the application of (1) and (2) we have

$$\frac{\sin i}{\sin r_1} \cdot \frac{\sin i_1}{\sin r} = 1,$$

and from trigonometry

$$\frac{R_0 + \tau_1}{\sin r_1} = \frac{R_0}{\sin i_1}.$$

Hence, the simple desired result[2]

$$\sin i = (1 + \tau_{1/R_0}) \sin r. \qquad (3)$$

Next, letting $m=2$, by a similar procedure as indicated above we obtain

$$\frac{\sin i}{\sin r} = (1 + \tau_{1/R_0})(1 + \tau_{2/R_0+\tau_1}). \qquad (4)$$

Finally, we can proceed to write the expressions for any general value of m, and these are

$$\frac{\sin i}{\sin r} = \prod_{k=1}^{m} \left\{ 1 + \frac{\tau_k}{R_0 + \sum_{j=1}^{k-1} \tau_{k-j}} \right\}, \qquad (5)$$

and

$$\frac{\sin i}{\sin i_m} = \frac{\mu_m}{\mu_0} \prod_{k=1}^{m} \left\{ 1 + \frac{\tau_k}{R_0 + \sum_{j=1}^{k-1} \tau_{k-j}} \right\}. \qquad (6)$$

[2] We note that if we have parallel plane symmetry a relation analogous to (3) would be of the form $\sin i = \sin r$.

Writing $\tau_{j/R_0} = \epsilon_j$, we can simplify (5) and (6) as follows.[3]

$$\frac{\sin i}{\sin r} = \prod_{k=1}^{m} \left\{ 1 + \frac{\epsilon_k}{1 + \sum_{j=1}^{k-1} \epsilon_{k-j}} \right\}$$
$$= \left\{ (1 + \epsilon_1) \frac{1 + \epsilon_1 + \epsilon_2}{1 + \epsilon_1} \cdots \cdot \frac{(1 + \epsilon_1 + \epsilon_2 \cdots + \epsilon_m)}{(1 + \epsilon_1 + \cdots + \epsilon_{m-1})} \right\}$$

i.e.,

$$\frac{\sin i}{\sin r} = \left(1 + \sum_{j=1}^{m} \epsilon_j\right) = (1 + \epsilon), \qquad (7)$$

and

$$\frac{\sin i}{\sin i_m} = \frac{\mu_m}{\mu_0}(1 + \epsilon), \qquad (8)$$

where

$$\epsilon = \sum_{j=1}^{m} \epsilon_j.$$

We can write similar expressions for $\theta_1, \theta_2, \cdots, \theta_m$. Recall that in geometrical optics when we say a medium has a refractive index $\mu > 1$ we mean light travels slower in that medium than in free space; in electron optics, electron travels faster in a medium of higher refractive index.

The above solution has been successfully used by the author in calculation of electron trajectories in region between mask and screen of a color television tube (see Fig. 3) where mask was replaced by conducting membrane permeable to electrons.

2. Again assume that we have m media (for details of notation regarding angles, see Fig. 2). By a repeated application of Snell's law and employing elementary trigonometry, we obtain the following relations analogous to (6) and (7).

$$\frac{\sin i}{\sin r} = \frac{\prod_{j=1}^{m} \sin r_j}{\prod_{j=1}^{m} \sin (r_j + \theta_j)} \qquad (9)$$

and,

$$\frac{\sin i}{\sin i_m} = \frac{\mu_m}{\mu_0} \frac{\prod_{j=1}^{m} (\sin r_j)}{\prod_{j=1}^{m} \sin (r_j + \theta_j)}. \qquad (10)$$

Eqs. (9) and (10) are useful for a step by step calculation. [It does not appear possible to write (9) and (10) in simpler forms unless some drastic assumptions are made.]

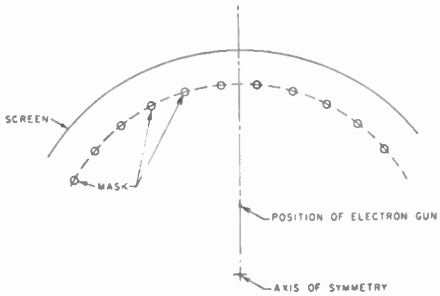

Fig. 3—Disposition of mask and screen in a color television tube.

The above relations can be employed for the calculation of electron trajectories in the region between two conducting plates at different potentials inclined at an angle. Such structures occur in present day cathode ray tubes. Other applications to the above results can be easily thought of.

S. V. Yadavalli
General Electric Microwave Lab. at Stanford
Palo Alto, Calif.

[3] This simplification was brought to the attention of the author by Dr. H. Ahlburg of The Electronics Laboratory, General Electric Co., Syracuse, N. Y.

Contributors

J. M. Barstow received the B.S. degree in physics from Washburn University in 1923, and the M.S. degree in physics from the University of Kansas in 1924.

J. M. Barstow

He was associated with the Southwestern Bell Telephone Co. until 1926, when he joined the Bell System. In 1927, he was a member of the AT&T development and research department. He was concerned in his early work with the development of circuit noise and room noise meters, and standards for room noise measurements. He also studied coordination problems for a joint project with Edison Electrical Institute.

During World War II, he was engaged in several military projects here and abroad. Since then, he has worked on the development of power-line carrier telephone systems and various problems associated with television and long-distance telephone transmission.

Mr. Barstow is Vice-Chairman of Panel 17 of the National Television System Commission and has participated in studies and tests which have led to the formulation of NTSC color-signal specifications. He is a member of Sigma Xi, the American Institute of Electrical Engineers, the Statistical Society of America, and the Society of Motion Picture and Television Engineers

❖

A. D. Berk was born on April 28, 1925, in Istanbul, Turkey, where he received the B.S. degree in E.E. from Robert College in 1947. He continued his studies here in America at the Rensselaer Polytechnic Institute and served as an instructor in the department of electrical engineering of the same institution. After receiving the M.S. degree from R.P.I. in 1951, he resumed his studies at M. I. T. while serving as a research assistant at the Research Laboratory of Electronics. He received the degree of Doctor of Science from M.I.T. in September, 1954.

A. D. Berk

Dr. Berk specializes in problems of electromagnetic theory. Since 1954 he has been a member of the technical staff of the Research Laboratories, Hughes Aircraft Company, Culver City, California. He is a member of Sigma Xi.

❖

C. E. Blakely was born October 25, 1927 in Trenton, Tenn. After serving three years in the Marine Corps as an electronics technician, he entered the University of Tennessee and received the B.S.E.E. degree in 1953.

C. E. Blakely

Since 1953 he has been a research assistant at the University of Tennessee, engaged primarily in electronics and electromagnetic radiation research. At the same time, he studied for his M.S., receiving this degree from this university in 1955.

Mr. Blakely, in addition to being a member of the IRE, is a member of Tau Beta Pi, Eta Kappa Nu, and Phi Kappa Phi.

❖

For a biography and photograph of M. R. Currie, see page 1533 of the October, 1955 issue of PROCEEDINGS OF THE IRE.

❖

L. O. Dolanský (SM'53) was born in Vienna, Austria, on May 6, 1919. He received the Ing. degree in electrical engineering from the Institute of Technology in Prague, Czechoslovakia in 1946, and the M.S. and E.E. degrees in electrical communications from the Massachusetts Institute of Technology in 1949 and 1952, respectively.

L. O. Dolanský

From 1942 to 1945, he worked with Radiotechna, a.s., a subsidiary of Siemens and Halske in Prělouč, Czechoslovakia. In 1945, he joined the teaching staff of the Institute of Technology in Prague, Czechoslovakia. He was associated with the Research Laboratory of Electronics at M.I.T., working on research problems in magnetic tape recording, pulse code modulation, frequency modulation, and television, from 1947 to 1952.

Since 1952 he has been working with the Electronics Research Project at Northeastern University on problems related to visual message presentation, speech analysis, and speech compression. At present, he is associate professor of research in communications at Northeastern. He has been teaching various undergraduate and graduate subjects in electrical engineering during the last three years.

Mr. Dolanský is a member of Tau Beta Pi, Sigma Xi, the American Society for Engineering Education, and the Massachusetts Society of Professional Engineers.

❖

E. E. Eldredge received the B.S. degree in electrical engineering from Brown University in 1927. He has had experience in all phases of radio communications, including antenna development, transmitter design, marine equipment, and instrumentation and pulse techniques.

E. E. Eldredge

He was chief engineer of Press Wireless Manufacturing Co. and Erco Radio Laboratory. Later, he became an engineering specialist in the systems engineering and techniques section of the Physics Laboratories of Sylvania Electric Products, Inc. at Bayside, N. Y.

Mr. Eldredge is presently manager of the equipment fabrication branch of Sylvania's Electronic Defense Laboratory at Mountain View, Calif.

❖

S. J. Goldstein, Jr. was born on June 23, 1925, in Indianapolis, Ind. He served as a radio technician in the Signal Corps from 1943 to 1946.

S. J. Goldstein, Jr.

In 1948, he received the B.S. in E.E. degree from Purdue University. He was employed by the Glenn L. Martin Co. for one year, and from 1949 to 1951 was associated with the Industrial Development Engineering Associates of Indianapolis.

From 1951 to 1953, Mr. Goldstein worked in the Jet Propulsion Laboratory of the California Institute of Technology. He received the M.S. degree from Stanford University in June, 1954, and is continuing graduate studies at Harvard College Observatory.

Mr. Goldstein is a member of Eta Kappa Nu, Tau Beta Pi, and Sigma Xi.

❖

H. Greenberg (A'52) was born on January 3, 1928, in New York, N. Y. He received the B.A. degree in physics from Brooklyn College in 1949. During 1950, he was a graduate assistant in the mathematics department of the University of Miami.

H. Greenberg

In 1949, Mr. Greenberg was a physicist with the Navy Department, where he was engaged in research on underwater sound. Since 1951, he has been with Sylvania Electric Products, Inc. in Bayside, N. Y. He has been concerned primarily with

the analysis of weapons systems and in research on traveling wave tubes.

Mr. Greenberg is a member of Pi Mu Epsilon, RESA, and the Operations Research Society of America.

❖

C. C. Hsu was born in Shanghai, China, on June 30, 1923. He received the B.S.E.E. degree from the Chiao-Tung University, Shanghai, in June, 1945. After coming to the United States in 1948, he was awarded the M.S. degree in engineering by the University of Michigan in 1949, and the Ph.D. degree in electrical engineering from Ohio State University in 1951.

C. C. Hsu

From 1945 to 1947, he worked as a junior engineer in China. From 1950 to 1951, he was appointed as a graduate assistant in the department of electrical engineering of Ohio State, and was an assistant professor in electrical engineering at the Michigan College of Mining and Technology, Houghton, Mich., in 1952. At present, he is employed by the Bendix Radio Division, Baltimore, Md.

Dr. Hsu is an associate member of Sigma Xi, and a member of Pi Mu Epsilon.

❖

D. B. Jordan (A'45) was born in Aberdeen, N.C. on June 9, 1923. He received the B.A. degree from Hofstra College in 1949, and the M.S. degree in applied mathematics from the Polytechnic Institute of Brooklyn in 1952.

D. B. Jordan

From 1949 to 1951, Mr. Jordan held a teaching fellowship at the Polytechnic Institute of Brooklyn. From 1951 to 1955, he was employed in the Physics Laboratories of the Sylvania Electric Products, Inc., where he worked on the theoretical analysis of communication systems. He also worked in the Missile Systems Laboratory on the design of analog and digital data reduction systems. In April, 1955, he joined the Guided Missile Division of Republic Aviation Corp. as senior systems engineer.

Mr. Jordan is a member of RESA, Kappa Mu Episilon, and Sigma Pi Sigma.

❖

B. A. Lengyel was born on October 5, 1910, in Budapest, Hungary. He attended the Polytechnic Institute and received the Ph.D. degree from Pázmány University of Budapest in 1935. In the fall of 1935, he came to the United States as a research fellow in mathematics at Harvard University.

Dr. Lengyel taught mathematics at the Polytechnic Institute in Budapest from 1931 to 1934, and at Rensselaer Polytechnic Institute from 1939 to 1942. After one year in the physics department of the College of the City of New York in 1943, he became an assistant professor of physics at the University of Rochester.

From 1946 to 1950 he was a staff member of the Naval Research Laboratory where he specialized in research in microwaves. After two years of service in the Office of Naval Research as a staff physicist he joined the research laboratories of the Hughes Aircraft Company in 1952. He is now the head of the Research Section of the Microwave Electronics Department.

Dr. Lengyel is a member of the American Mathematical Society, the Physical Society, and Sigma Xi.

❖

D. J. LeVine (S'43–A'44–M'49) was born in New York, N. Y., on October 10, 1921, He received the B.E.E. degree from the School of Technology, College of the City of New York in 1943, and the M.E.E. degree in 1952 from the Polytechnic Institute of Brooklyn.

D. J. LeVine

From 1943 to 1946, he served in the Signal Corps working with radar and PTM microwave relay communications equipment in the United States and Europe. From 1946 to 1948, he was with the Microwave Research Institute, Polytechnic Institute of Brooklyn, working primarily on microwave power measuring devices. Mr. LeVine joined the Federal Telecommunication Laboratories, Inc. in 1948, and at present he is working on microwave antennas, switching devices, and associated microwave components.

Mr. LeVine is an executive engineer in the Radio Communication Laboratory. He is an associate of the American Institute of Electrical Engineers.

❖

For a photograph and biography of J. G. Linvill, see page 882 of the July, 1955 issue of the Proceedings of the IRE.

❖

R. H. Mattson was born in Chisholm, Minn., in 1900. He served with the U. S, Navy from 1946 to 1947, and after completing the Navy electronics course, worked on airborne electronic equipment.

He received the B.E.E. degree with distinction from the University of Minnesota in 1951. In 1952 he received the M.S. degree in electrical engineering from the same university. Mr. Mattson joined the technical staff of Bell Telephone Laboratories in 1952 and since that time has specialized in transistor circuit design work. Most of this work has been with junction-type transistors in switching or large signal applications.

R. H. Mattson

Mr. Mattson is a member of Eta Kappa Nu and Tau Beta Pi.

❖

W. T. Patton was born on April 20, 1930, in Schenectady, N. Y. He received the B.S.E.E. degree from the University of Tennessee in 1952. He joined the department of electrical engineering of the University of Tennessee in March, 1952, and worked on the research staff of its engineering experiment station.

W. T. Patton

In May, 1953, he was called to active duty in the Navy. He is presently stationed at the Boston Naval Shipyard in Boston, Mass., where he is supervising the conversion of two destroyer escort radar picket ships.

Mr. Patton is a member of Eta Kappa Nu and Tau Beta Pi.

❖

F. V. Schultz (A'32–SM'45) was born on November 7, 1910, in Petersburg, Mich. He received the B.S.E.E. degree in 1932, the M.S.E.E. degree in 1939, and the Ph.D. degree in 1950, all from the University of Michigan. After five years in industry, primarily as a radio receiver development engineer he joined the Department of Electrical Engineering of Michigan State College, where he remained from 1937 until 1941.

F. V. Schultz

During World War II Dr. Schultz was a group leader in the Radar Laboratory of the Wright Air Development Center, where he

was concerned with the development of antennas and radar beacons. From 1946 to 1950 he was a research Engineer in the Engineering Research Institute of the University of Michigan. During this time Dr. Schultz was engaged in research studies on missile guidance systems and on electromagnetic wave scattering problems.

Since 1950 he has been professor of electrical engineering at the University of Tennessee, in charge of instruction and research in electronics.

He is a member of Sigma Xi, Tau Beta Pi, Phi Kappa Phi, Eta Kappa Nu, the American Physical Society and the American Society for Engineering Education.

❖

W. Serniuk (S'41–A'43–M'46–SM'50) was born on December 4, 1919, in Elizabeth, N. J. He received the B.S. degree in engineering physics from the University of Michigan in 1942, and the M.S.E.E. degree from the Polytechnic Institute of Brooklyn in 1953.

W. Serniuk

He joined Sylvania Electric Products, Inc., as an engineer in 1942. During World War II, he worked on the development of proximity fuzes at Sylvania's Appliance Division in Ipswich, Mass.

In 1945, he was transferred to the Physics Laboratories at Bayside, N. Y. where he was head of the Systems Engineering and Techniques Section. He joined the staff of the Electronic Defense Laboratory at Mountain View, Calif. in 1953, and is now manager at the equipment branch.

Mr. Serniuk is a member of Tau Beta Pi, Sigma Xi, and Phi Kappa Phi.

❖

W. Sichak (M'46) was born on January 7, 1916, in Lyndora, Pa. He received the B.A. degree in physics from Allegheny College in 1942.

W. Sichak

From 1942 to 1945, he was engaged in developing microwave radar antennas at the Radiation Laboratory of Massachusetts Institute of Technology. Since then, he has been with Federal Telecommunication Laboratories, working on microwave antennas and allied equipment.

Mr. Sichak is an associate director of the Radio Communication Laboratory. He is a member of the American Physical Society.

❖

J. D. Tillman (M'53) was born in July, 1921, in Evansville, Ind. He attended Evansville College and the University of Tennessee, and received the B.S.E.E. degree in 1947. In 1950, he received the M.S. degree from the same university. He has been on the staff of the electrical engineering department there since 1947, and is now an assistant professor.

J. D. Tillman

Mr. Tillman has been engaged mainly in antenna research since 1951. He is a member of Tau Beta Pi, Eta Kappa Nu, Phi Kappa Phi, the American Institute of Electrical Engineers, the Audio Engineering Society, and the American Society for Engineering Education.

❖

A van der Ziel (SM'49) was born at Zandeweer, The Netherlands, on December 12, 1910. From 1928 to 1934 he studied physics at the University of Groningen, The Netherlands, where he received his Ph.D. in 1934.

A. van der Ziel

He was a member of the research staff of the Physics Laboratory of N. V. Philips' Gloeilampenfabrieken, Eindhoven, The Netherlands, from 1934 to 1947. From 1947 to he was an associate professor at the University of British Columbia, Vancouver, Canada, and has been professor of electrical engineering at the University of Minnesota since 1950.

He is a member of the American Physical Society and Sigma Xi.

❖

For a photograph and biography of J. R Whinnery, see page 106 of the January 1955 issue of the PROCEEDINGS OF THE IRE

IRE News and Radio Notes

San Francisco to Be Site for Semiconductor Symposium

The Fourth Annual Semiconductor Symposium of the Electrochemical Society will be held at the Mark Hopkins Hotel, San Francisco, Calif., April 29–May 3.

Two half-day sessions on semiconducting materials (elemental, alloys, and compounds), one half-day session on surface controlled phenomena, and one half-day session on chemical process technology are planned. In each area there will be, one review paper on the state of the field, presentations of new information, and "late news" presentations.

Persons wishing to offer papers at the symposium should notify the General Chairman of the titles of their proposed papers no later than November 15. A 75-word abstract, which will be printed in the meeting program, should be submitted no later than January 15. An additional 1,000-word extended abstract, including brief pertinent data, illustrations, and curves, should be submitted before February 1. This second abstract will be printed in a booklet, *Enlarged Abstracts of Papers Presented by the Electronics Division*, which will be available at cost at the symposium.

Persons wishing to make ten-minute, "late news" presentations should send word of either the title or subject to the General Chairman as soon as possible. The deadline for 75-word abstracts on these papers is April 8. These titles and abstracts will not be included in the meeting program nor the *Enlarged Abstracts*, but mimeographed copies will be available prior to the meeting.

All material intended for presentation at the symposium should be submitted to the General Chairman, J. W. Faust, Jr., Westinghouse Research Labs., Beulah Road, Churchill Borough, Pittsburgh 35, Pa.

Joint Computer Conference Proceedings Now Available

The 1955 Proceedings of the Western Joint Computer Conference is now available at IRE headquarters at $3.00 per copy. These *Proceedings* include the papers presented at the conference in Los Angeles, March 1–3. The conference was jointly sponsored by the IRE, AIEE, and the Association for Computing Machinery.

IRE Will Present Hogan, Bullington and Hinman with 1956 Awards at National Convention Next March

The Institute of Radio Engineers has made John V. L. Hogan, President of Hogan Laboratories and founder of station WQXR, the recipient of the IRE Medal of Honor, highest technical award in the radio engineering profession. The award, given "for his contributions to the electronic field as a founder and builder of The Institute of Radio Engineers, for the long sequence of his inventions, and for his continuing activity in the development of devices and systems useful in the communications art," will be presented during the IRE National Convention in New York City next March.

J. V. L. Hogan

Mr. Hogan began his career in 1906 as a laboratory assistant to Lee De Forest. From 1910 to 1921 he held posts with the National Electric Signaling Company and the International Radio Telegraph Company. He then became a consulting engineer in New York City. He is responsible for many inventions in radio, television, and facsimile fields, and was founder and owner of station WQXR, until it was acquired by *The New York Times*. Mr. Hogan is president of Hogan Laboratories, Inc., New York City. In 1912 he helped found the Institute of Radio Engineers, served as Vice-President from 1916 to 1919, and President in 1920. He has served frequently on the Board of Directors as well as on many IRE committees.

The Morris Liebmann Memorial Prize, awarded annually for a recent, important contribution to radio engineering was given to Kenneth Bullington, Bell Telephone Laboratories, "for his contributions to the knowledge of tropospheric transmission beyond the horizon, and to the application of the principles of such transmission to practical communications systems."

K. Bullington

Mr. Bullington joined Bell Telephone Laboratories in 1937 and since that time has been engaged almost entirely in studies relating to the propagation of radio waves. His work on scatter propagation has been a major factor in extending the range of military communications systems.

Wilbur S. Hinman, Jr., Director of the Diamond Ordnance Fuze Laboratories, has been awarded the Harry Diamond Memorial Award, given to persons in government service for outstanding work in radio and electronics. It was presented "for his contributions to the electronic art in the fields of meteorology and proximity fuzes."

W. S. Hinman

Mr. Hinman has contributed to aircraft navigation aids, radiosondes for obtaining information on upper-air weather, and the proximity fuze.

Calendar of Coming Events

IRE East Coast Conference on Aeronautical and Navigational Electronics, Lord Baltimore Hotel, Baltimore, Md., Oct. 31–Nov. 1

Symposium on Applied Solar Energy, Westward Ho Hotel, Phoenix, Ariz., Nov. 1–5

Kansas City Section Electronics Conference, Kansas City, Kansas, Nov. 3–4

IRE-AIEE-ACM Eastern Joint Computer Conference, Hotel Statler, Boston, Nov. 7–9

IRE-AIEE-ISA Electrical Techniques in Medicine and Biology, Shoreham Hotel, Washington, D. C., Nov. 14–16

Second International Automation Exposition, Chicago Navy Pier, Chicago, Illinois, November 14–17

American Society for Quality Control, Tenth Mid-West Conference, Schroeder Hotel, Milwaukee, Wisconsin, November 17–18

IRE-PGCS Symposium on Aeronautical Communications—Civil and Military; Utica, New York, Nov. 21–22

PGI and Atlanta Section Data Processing Symposium, Hotel Biltmore, Atlanta, Ga., Nov. 28–30

EJC Nuclear Science and Engineering Congress, Cleveland, Ohio, December 12–16

IRE Second National Symposium on Reliability and Quality Control, Hotel Statler, Washington, D. C., January 9–10

PGEC Dallas-Ft. Worth Chapter Simulation Symposium, Dallas, Texas, Jan. 19–21

IRE-AIEE-U. of Pa. Conference on Transistor Circuits, University of Pennsylvania, Philadelphia, Pa., Feb. 16–17

IRE National Convention, New York, March 19–22

BPI Symposium on Nonlinear Circuit Analysis, II, Engineering Societies Building, New York, April 25–27

Electrochemical Society Semiconductor Symposium, Mark Hopkins Hotel, San Francisco, Calif., April 29–May 3

IRE-AIEE-RETMA WCEMA Electronics Components Conference, Washington, D. C., May 1–3

IRE National Aeronautical and Navigational Electronics Conference, Biltmore Hotel, Dayton, Ohio, May 14–16

IRE-AIEE-IAS-ISA National Telemetering Conference, Statler Hotel, Los Angeles, California, August 21–25

Two Foreign Sections Added

At its September meeting, the IRE Board of Directors approved the establishment of two foreign Sections, the Newfoundland Section and the Egypt Section. Newfoundland thus becomes the tenth Section to be located in Canada. The other Canadian Sections are Alberta, Bay of Quinte, Hamilton, London, Montreal, Ottawa, Toronto, Vancouver, and Winnipeg. Egypt joins the Israel Section in the Near East area. Other links in the expanding chain of international IRE activity are foreign Sections located in Buenos Aires and Hawaii. Sixty-four additional Sections exist within the continental United States.

Previously on May 4, the Westchester County Subsection of the New York Section had been established. The establishment of the Piedmont Subsection in the North Carolina-Virginia Section followed at the September meeting.

Advisory Board Chosen for Washington Symposium on Reliability and Quality Control

The Advisory Board for the Symposium on Reliability and Quality Control in Electronics, to be held January 9 and 10 in Washington, has been chosen recently. The function of the board will be to prepare a program of interest and value to IRE members. A cross section of military, government, commercial, and industrial activities are represented by the members of the board. The members will review papers, recommend general subjects, and moderate some of the symposium sessions.

The Advisory Board is made up of: *Max Batsel*, RCA; *Capt. Rawson Bennett*, USN; *Capt. Henry Bernstein*, USN; *M. Barry Carlton*, Magnavox; *Brig. Gen. William P. Farnsworth*, USAF; *Dr. Robert D. Huntoon*, Nat. Bureau of Stds.; *L. A. Hyland*, Hughes Aircraft Co.; *John Keto*, Wright Air Development Center; *W. H. Martin*, Dep. Ass. Secretary of Defense; *Dr. J. W. McRae*, Sandia Corporation; *D. E. Noble*, Motorola, Inc.; *Dr. Louis Ridenour*, Lockheed Aircraft Corp.; *Dr. A. L. Samuel*, IBM Corp.; *Major Gen. Leslie E. Simon*, U. S. Army; *Julian K. Sprague*, Sprague Electric Co.

Communications Engineering Society Formed in Germany

The Association of German Electrical Engineers (VDE), Frankfort/Main, recently founded a new subdivision, the Society of Communications Engineers (Nachrichtentechnische Gesellschaft, NTG). The society is subdivided into twenty sections covering all fields of communications engineering. Darmstadt is the headquarters for this new, nation-wide, nonprofit organization. The present membership of 1,000 is headed by Hans Busch of the Technological Institute, Darmstadt, President; and Hans Jakob Piloty of the Technological Institute, Munich, Vice-President.

Canadian IRE Convention Set for Toronto October 1–3, 1956

C. A. Norris, General Chairman, will head the Convention Committee for the Canadian IRE Convention and Show in Toronto, October 1–3, 1956.

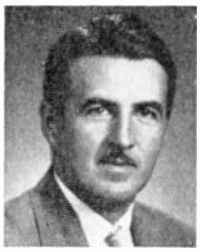

C. A. Norris

The convention, featuring more than 200 engineering exhibits, will meet in a new building to be erected at the Canadian National Exhibition. It will be the first held in this building, which houses an auditorium, theater, committee rooms, and restaurant facilities.

Other committee chairmen include: E. O. Swan, *Exhibits and Registration;* E. L. Palin, *Social Activities;* R. C. Poulter, *Advertising, Publicity and Program;* G. Sinclair, *Technical Program;* C. H. Hathaway, *Finances;* C. Eastwood, *Recording Secretary;* C. Simmonds, *Corresponding Secretary;* and F. H. R. Pounsett, *Liaison with IRE Region Eight.* A. P. H. Barclay, *Chairman of the Toronto Section*, is an *ex-officio* member of the committee.

Further information may be obtained from: R. C. Poulter, Canadian IRE Convention, Radio College of Canada, 86 Bathurst Street, Toronto 2B, Ontario.

Gaudreau to Direct Conveyor Automation Clinic Sessions

Armand T. Gaudreau, Management Consultant, will direct the Conveyor Automation Clinic sessions at the Second International Automation Exposition, Chicago Navy Pier, November 14–17. Each lecture will be focused on a phase of the application of conveyors in supplying the prime mechanism to automation: work positioning at the machines, inter-machine transfers of materials, inter-flow handling of materials, inter-building transportation of materials, automatic handling from assembly to storage, integrating material flows through production.

The following conveyor manufacturer exhibitors are participating in the Conveyor Clinic: Chainveyor Corp., Mechanical Handling Systems, Inc., Jervis B. Webb Co.

The Electronic Computer Clinic will be repeated this year but will be twice as large. The clinic will again be under the direction of Milton Aronson, Editor of *Instruments and Automation*. The following exhibitors will make up the Computer Clinic: Austin Co., Special Devices Division; Bendix Computer Division; Berkeley Division, Beckman Instrument Co.; Clevite-Brush Development Co.; Electronic Associates, Inc.; Goodyear Aircraft Corp.; International Business Machines Co.; Librascope, Inc.; Teleregister Corp.

Standard Acoustical Terminology to Be Revised in June

American Standard Acoustical Terminology Z24.1–1951 is being revised to correct errors and to add definitions needed in the widening field of acoustics. A draft will be submitted to the American Standard Sectional Committee Z24 in June, 1956. The revision is being based largely on comments already received on the existing standard.

Suggested revisions should be sent immediately to the Chairman of Writing Group Z24-W-5, Robert W. Young, U. S. Navy Electronics Laboratory, San Diego 52, California.

P.G. on Communications Systems Holds Symposium this Month

The Professional Group on Communications Systems has announced that the first Aeronautical Communications Symposium will be held at the Hotel Utica, Utica, N. Y., November 21–22.

Many engineering concerns in the United States will exhibit their products, and a variety of technical papers, covering both military and civilian aspects of aeronautical communications systems will be presented by proponents. The symposium will stress both ground-to-ground and ground-to-air communications systems used to support present-day aeronautical activities.

Several social events are also planned for those attending the symposium, and the $2.00 registration fee to members and nonmembers permits full participation in the symposium.

Professional Group News

Three New Chapters Approved

On September 7, the Executive Committee approved the establishment of three new Professional Group Chapters: Denver Chapter, PG on Antennas and Propagation; San Francisco Chapter, PG on Production Techniques; Los Angeles Chapter, PG on Microwave Theory and Techniques.

Obituary

Edward L. Nelson (A'19–M'25–F'38), former radio and military development engineer at Bell Telephone Laboratories, at Whippany, N. J., died recently.

A veteran of more than thirty-four years with the Bell System when he retired in 1951, Mr. Nelson had specialized in the development of radio-telephone systems and radio transmitters and receivers during the greater part of his career with Bell Laboratories.

During World War II, he was in charge of a group of engineers in the development of radar sets for aircraft and ships. Upon his retirement, he became technical director of the Signal Corps Engineering Laboratory at Fort Monmouth, N. J. He was named chief scientist of the Signal Corps' research and development division in Washington about a year ago.

Born in Warsaw, Indiana in 1891, Mr. Nelson received the B.S. degree in electrical engineering from Armour Institute of Technology in 1914. Joining the IRE in 1919 he became a Fellow in 1938. He had served as an IRE Representative, a member of the Board of Editors, and as Chairman of the Broadcasting Committee.

Technical Committee Notes

The **Electronic Computers** Committee met at IRE Headquarters on August 9 with Chairman Robert Serrell presiding. The entire meeting was devoted to discussing and amending the *Proposed Standards on Electronic Computers: Definitions of Electronic Computer Terms.*

J. E. Eiselein presided at a meeting of the **Industrial Electronics** Committee on September 7 at IRE Headquarters. A request was made to the committee to actively assist in the immediate future in the procurement of papers for the annual sessions in March of 1956. It is the intent of the committee to offer any papers made available particularly to the Professional Group on Industrial Electronics or the Professional Group on Production Techniques.

The committee reviewed the subcommittee personnel and announced the addition of Subcommittee 10.3 on Industrial Electronics Instrumentation and Control with E. Mittelmann as chairman. The overall program for expansion in the Industrial Electronics Committee both in membership and activity has dictated the need for this new subcommittee. Two basic areas of work are planned for the immediate future: a detailed compilation of transducer categories, the solder problem in general with particular attention to the problems of automation.

The **Recording and Reproducing** Committee met on September 7 at IRE Headquarters with A. W. Friend presiding. A major portion of the meeting was devoted to the discussion of high fidelity standards in connection with an editorial entitled "High Fidelity at the Crossroads" from the June issue of *Tele-Tech.* This editorial was brought to the attention of the committee by B. B. Bauer, Secretary-Treasurer of the Professional Group on Audio. The following recommendation was decided upon by the committee: "The Recording and Reproducing Committee recommends that the Chairmen of the Audio Techniques Committee, IRE 3, the Electroacoustics Committee, IRE 6, and the Recording and Reproducing Committee, IRE 19, jointly prepare a letter to Mr. Bauer in answer to his letter of June 17 concerning standards on high fidelity. The committee is sympathetic to the needs of the growing industry and wishes to cooperate in any permissible way. In this regard, a list of all pertinent existing standards of the professional and trade organizations is in preparation. This list will be made available to all interested groups. This letter should include (1) that it is not within the scope of their operation to set up a dividing line between high fidelity and non high fidelity; (2) insofar as standardization of measurement techniques is concerned, the IRE is already engaged in such standardization; and (3) any standards on techniques of measurement that apply to equipment in general, also apply to high fidelity."

Books

Basic Theory in Electrical Engineering by R. G. Kloeffler and E. L. Sitz

Published (1955) by Macmillan Co., 605 Fifth Ave., New York 11, N.Y. 321 pages+4 page index +viii pages. Illustrated. 5¾×8½. $5.50.

This book is written as a text for sophomore college students majoring in electronics, communications or electric power. It covers dc circuits and steady-state fields while laying the groundwork for ac circuits and fields. Although it is somewhat shorter than many other well-known texts, the authors have done an exceptionally fine piece of work in retaining the more fundamental material so that the book does not suffer from omission of vital information and training. The chapter on solution of electric circuits is well done, including presentation of both mesh and nodal methods of solution as well as Thevenin's and Norton's theorem. A wealth of problems throughout the book gives the instructor a wide choice of material to assign the student.

On the other hand, there seems little other than the excellent organization in this book which is new compared to older texts. As in most books, for example, a true vector notation is not used in the treatment of magnetic and electric fields. The authors state in the chapter on the magnetic circuit that H and B are vectors, symbolize them by bold-face type, yet treat them as scalars in most of the equations. They have added a final chapter, "Introduction to Electromagnetic Waves," in which they include the concept of dot products, but even here their symbology does not conform to the latest standards established by IRE and other cooperating organizations.

On the whole, the book should prove quite satisfactory as a text for sophomore students and is a creditable contribution to the literature in this field.

Austin V. Eastman
University of Washington
Seattle, Washington

Amplitude-Frequency Characteristics of Ladder Networks by E. Green

Published (1955) by Marconi's Wireless Telegraph Co., Ltd., Marconi House, Chelmsford, Essex, England 117 pages+iii pages+38 appendices. 88 Figures. 10×7½. 25 s.

This book deals with the analysis and synthesis of ladder networks and is directed toward the design engineer who is working in the rf power field or small signal field.

The book covers filter characteristics of ladder networks. Three types of responses included in this treatment are undercoupled, maximally flat, and equal ripple (Tchebysheff). The attack is from a low pass filter to a band pass, high pass or a band elimination response. The transformations necessary to go from the low pass filter are quite simple.

There is a section on application which includes the design of networks using vacuum tubes in which a power bandwidth figure of merit or gain bandwidth figures of merit are used. These are utilized to obtain the optimum performance of such circuits. One of the gain bandwidth figures of merit depends upon there being equal terminal capacities and the other depends upon there being equal terminal volts.

The volume is divided into about a dozen parts. Among them is a good section on broadband matching of reactive loads. The reflection coefficient was rather easily handled. Also, in a section called filters, the attenuation characteristics outside of the primary response region is mentioned. In addition, there is a small section on the input impedance or admittance of maximally flat and equal ripple filters.

Green's book contains many helpful and important tables. There are numerous function plots and comparisons between maximally flat and equal ripple type filters, a few well chosen examples illustrate certain basic operations leading to the synthesis of filters.

This work is an outstanding contribution in its field, although the style of presentation leaves much to be desired. The very abbreviated style depends heavily upon the list of symbols and much is left to the imagination. The author only hints at certain conclusions and how they fit into the picture. Ideas are often lightly sketched. Clear thinking and directed endeavor are required to follow the book closely. For some purposes this style of presentation would be desirable since it is thought-provoking.

This book could be used by anyone with filter problems. Its most fruitful targets, however, are those people who are already familiar with filter problems and their solutions.

William E. Richeson, Jr.
Stanford Research Institute
Menlo Park, California

Elements of Servomechanism by George J. Thaler

Published (1955) by McGraw-Hill Book Co., Inc., 330 West 42 St., New York 36, N. Y. 264 pages+4 page index+x pages. Illustrated. 9¼×6¼. $7.50.

As stated in the preface, "The material in this text is intended for a one-semester senior undergraduate course." The book fulfills its intentions well, and does not contain any advanced analysis or synthesis methods which might interest an advanced student or an engineer experienced in the field.

The book itself is brief but well organized. There is a complete introduction and summary for each chapter, and each chapter contains a different topic which developes logically and naturally from the preceding chapters and topics. Reference is frequently made to practical considerations. This is particularly interesting and helpful in an introductory book. The discussions in the early chapter concerning system performance and definitions are brief but complete and serve to acquaint the reader with the function of a feedback control system, its

purpose, and its design problems. The actual system components, their use and construction are adequately discussed in the second appendix.

The illustrations, are plentiful, clear, and exceptionally complete, especially where system transient responses are described. In fact, the figures showing system transient responses for various non-linearities make a valuable reference.

This book is unique in that transfer functions and stability criteria are developed without recourse to the Laplace Transform in the text. However, an introduction to the Laplace Transform is given in an appendix. The reader is also introduced to advanced linear analysis in one chapter and to non-linear analysis in the last chapter. These chapters serve as incentives for further study.

Perhaps the chief detriment to the book may be found in its brevity. Frequently, short statements are made about system performance and methods of analysis as if they were definite rules. These statements may prove misleading to the uninitiated. For instance, in a transient response discussion in Chapter Two, a quadratic system is referred to, and it is implied from its responses that any system with an overshoot always has a frequency of oscillation from which the performance of the system may be estimated. However, stable servomechanisms with two integrations may be designed with a large overshoot, but without apparent oscillations. In another case it is stated that "Block diagrams . . . aid in setting up equations for systems." Actually, it is more fundamental and correct to set up block diagrams from system equations. Of course, when used as a textbook in college, it could be supplemented with more detailed information from an instructor.

Although brief, this book is a well written introduction to the elements of servomechanisms through the particular medium of the frequency response.

GEORGE S. AXELBY
Westinghouse Electric Corp.
Baltimore, Maryland

Networks, Lines, and Fields by John D. Ryder

Published (1955) by Prentice-Hall, 705 Fifth Ave., New York, N.Y. 564 pages+7 page index+xi pages. Illustrated. 5¾×8¾ $7.65.

This book, a slightly modified and somewhat expanded revision, is the second edition of Dean Ryder's earlier text, which was favorably received when it first appeared in 1949. Several new chapters have been added, the chapter titles now read as follows: "Net work Transformations," "Resonance," "Impedance Transformation and Coupled Circuits," "Filters," "Transmission Line Parameters," "Transmission Line Theory," "The Line at Radio Frequencies," "The Line at Power Frequencies," "Equations of the Electromagnetic Field, Radiation," "Transmission and Reflection of Plane Waves at Boundaries," "Guided Waves between Parallel Planes," "Wave Guides," "Radiation into Space."

The book seems to divide itself into three major sections. The first part, comprising four chapters, is largely one of general network analysis. It begins with a study of most of the important topics of network analysis, with a reasonably adequate discussion of the loop analysis, the node analysis, and the important network theorems. Frequency selective networks are discussed, and an account is given of the Foster Reactance theorem. A fairly good description is given of magnetically coupled circuits. A reasonably standard treatment of filters of type-K and the m-derived types is available.

The second important division, also consisting of four chapters, is devoted largely to transmission line phenomena. A complete treatment is given of the determination of the parameters of transmission lines: the single line, and multiple conductors with various conductor arrangements, symmetrical and unsymmetrical. Transmission line theory is presented largely in terms of the exponential factors and reflection factors in order to stress the wave character of the transmission. The line at radio frequencies is presented in a manner to stress the problem of standing waves, and also to show the impedance transforming properties of rf line devices. The rectangular impedance chart and the Smith chart are introduced, and a number of problems are studied with their use. A discussion is included of the line at power frequencies.

The last five chapters constitute the final part of the book and concern themselves with guided and radiated electromagnetic fields. A chapter is included on the essential aspects of the electromagnetic field equations, the plane wave, and the Poynting theorem. A complete account is given of the transmission and reflection of plane waves at boundaries. This is followed by a discussion of guided waves between parallel planes. The region of propagation is then confined by added boundaries thereby leading to the study of wave guides. An introduction to the essentials of radiation into space, the elements of antenna theory, and the radiation properties of several selected radiators, completes the text.

On the whole the writing is lucid, and the explanations good. Issue can be taken with the author on a number of occasions, but in most cases these are small matters. For example, the reference positive polarity has not been indicated in all cases, although these have been included where specifically required. A consistent policy of reference positive polarity markings would have been desirable, the use of e and V for potential difference serves only to complicate a network analysis development; the discussion in Section 1–17 of the Parallel-T network proceeds much more directly by a node analysis. On page 42, for the sake of generality, the expansion of a determinant in terms of minors or cofactors should have been included, the discussion of the Foster reactance theorem is largely extraneous in its present environment. It is only one of many synthesis techniques, and as the general synthesis problem is not examined, this might well have been omitted. A number of other similar points can be raised throughout the text.

It is anticipated that the book will be accorded a favorable reception, as it does provide the student and the practicing engineer with the essential background and analytical techniques for handling a large group of important network configurations under steady state excitation.

SAMUEL SEELY
Syracuse University
Syracuse, New York

Experiments in Electronics and Communication Engineering by E. H. Schulz, L. T. Anderson, R. M. Leger.

Published (1955) by Harpers and Bros., 49 E. 33 St., New York 16, N. Y. 339 pages+3 page index+viii pages. Illus. 9¼×6¼. $6.00.

This is a second edition of a laboratory manual, published in 1943, designed to serve the needs of war training programs of college grade in World War II. This second edition embodies a thorough revision of the material to bring it up to date, and is intended primarily for college courses in conjunction with the theoretical courses in communications engineering.

Ninety-three experiments are presented, giving a very complete coverage of communications networks, electronics, and the applications of vacuum tubes. It is not intended that the experiments be performed in any fixed order. For example, the experiment on the cathode-ray oscillograph and its uses as a measuring instrument would naturally precede experiments where it is used as an auxiliary equipment.

A notable feature of the book is the able presentation of the theory of each experiment which precedes suggestions for the apparatus to be used and the general nature of the measurements which are to be made. Except in the case of some of the more elaborate setups, the theory given is sufficient. In certain cases, further reading is desirable. This would naturally be available if the experimental work is kept reasonably in step with the theoretical courses.

The authors suggest, in the chapter on laboratory technique, their belief that laboratory directions should be general, rather than detailed, so as to develop initiative in the student. In the judgment of this reviewer, this purpose will be served if the laboratory work be so assigned and supervised as to give it effectiveness as demonstration material for the theoretical part of the course. This manual should be found valuable for such an integrated course.

FREDERICK W. GROVER
Union College
Schenectady, N. Y.

Second Thoughts on Radio Theory by "Cathode Ray"

Published (1955) by Iliffe and Sons Ltd., Dorset House, Stamford St., London, England. 403 pages+6 page index. Illus. 8¾×5¾. 25 s.

The "second thoughts" contained in this book might well have been called a "fresh look" at basic radio-frequency concepts. They are a lively exploration of the fundamentals of radio circuits, transmission, techniques and mathematics. Readers of *Wireless World* will be pleased to find here a collection of some forty of the articles by "Cathode Ray" which have previously been published in that magazine. Other readers will learn that even radio mathematics can be intelligible, interesting, and sometimes even humorous.

In its utility to the student and worker in radio, the book reminds the reviewer of the *Wireless Telegraphist's Pocket Book of Notes, Formulae and Calculations* by Professor J. A. Fleming, which was published in England in 1915, and which continued to be a classic reference book for many years.

The forty-four chapters are arranged in four groups: Basic Ideas, Circuit Elements and Techniques, Circuit Calculations, and In Lighter Mood. Illustrative of the author's treatment of the subjects is Chapter Nine on "Phase." Here, after citing a lecture in which the famous Dutch professor, Dr. Balth van der Pol referred to the large variety of definitions which have appeared in books and then gave his own choice, this author sets forth a straightforward and quite informal discussion of what to many is the rather abstruse concept of "phase." He makes it far from abstruse. After describing its existence "in an operation which occurs periodically" as "the stage or state to which the operation has proceeded," he illustrates "phase" in terms of the mass production of a radio receiver and then in terms of the pulses radiated by a radar transmitter. The appealing manner of the author's presentation is indicated by the titles of the successive sections of this chapter. They are: "What Kind of Thing Is It?" "A More Precise Definition," "Phase Difference," "Some Wrong Ideas," "Constant and Variable Phase Difference," "Phase and Waveform," "Phase Angle," and "Summary."

This is a book of contrasts in moods, but of great consistency in readability. It is a book which one likes to have on his table for technical browsing. One wishes that the author had not chosen to hide his identity behind a nom de plume.

The usefullness of the book is enhanced by a six-page index. At the end there are presented, with some humorous overtones, the answers to a dozen problems which are, here and there, posed for the reader.

LAURENS E. WHITTEMORE
American Telephone and Telegraph Co.
New York, N. Y.

Report of the Physical Society Conference on the Physics of the Ionosphere

Published (1955) by The Physical Society, 1 Lowther Gardens, Prince Consort Rd., London S.W. England. 406 pages. Illus. 10¼×7. 40 s.

This is a book primarily intended for the serious student of ionospheric physics. It contains a series of fifty papers on the physics of the ionosphere in relation to radio wave propagation. These papers were submitted in connection with a scientific conference held in September 1954 at Cambridge University. While most of the contributions are concerned with current research there are four survey papers dealing with: the lowest ionosphere, A. H. Waymick; irregularities and movements in the ionosphere, J. A. Ratcliffe, the ionospheric F-2 layer, D. F. Martyn; and the mathematics of wave propagation through the ionosphere, K. G. Budden.

A feature of the conference was a presentation by D. K. Bailey of the hitherto classified work that has been done in recent years by the Bureau of Standards on long distance ionospheric scatter-transmission at VHF. It is unfortunate that the account of this work included in the book is only a summary written from notes taken at the conference. Readers may like to compare this summary (paper 12) with a contribution by W. Dieminger on short wave echoes from the lower ionosphere (paper 5). The two papers describe what are at first sight two different phenomena, but in discussion at the conference it seemed quite likely that the two phenomena are in reality the same.

HENRY G. BOOKER
Cornell University
Ithaca, N. Y.

Principles of Communication Systems by W. D. Hershberger

Published (1955) by Prentice-Hall, Inc., 70 Fifth Avenue, New York 11, N. Y. 244 pages+5 page index+xiii pages. Illus. 8½×5½. $6.65.

There is a great need in the field of communications for a book like this one where, as the cover blurb states, emphasis is not placed on the "hardware" of any particular system, but on topics such as signals and their spectra, information theory, and detection. It states that after considering the characteristics of channels useful in communication—radio and transmission lines, in particular—the author examines human and other factors which determine the design and limit the performance of any given system.

The author faithfully follows the blurb in his chapter outline: first a chapter discussing the makeup of a communication system, then signals and their spectra, followed by a chapter on information and rate of transmission of information. Next the contents calls for a chapter on noise, one on modulation and detection, another on transmission lines, and then the background is concluded by a chapter on characteristics of radio waves. The last hundred pages deals with systems, including chapters on audio frequency systems, radar systems, television, and the design of communication systems.

Unfortunately the outline is the best part of the book because the contents are just not there. Important equations are given without background or derivation—the Hartley-Shannon equation, the autocorrelation function, and others—while unimportant equations for this study such as the transmission line equations are derived in detail. Most of the book is taken up with discussions of material that should have been covered in elementary and intermediate radio courses and very little is presented on the relationship of system concepts to information theory, noise, modulation, and detection. The chapter on the design of communication systems is eight pages long. However, the book would make an interesting few hours reading for someone wanting an elementary survey of communication systems.

NATHAN MARCHAND
Marchand Electronic Laboratories
Bryam, Connecticut

RECENT BOOKS

Buchsbaum, Walter H., *Color TV Servicing*. Prentice-Hall, Inc., 70 Fifth Ave., New York 11, N.Y. $6.35.

Halliday, David, *Introductory Nuclear Physics*. John Wiley and Sons, Inc., 440 Fourth Ave., New York 16, N. Y. $7.50.

Infrared: A Library of Congress Bibliography. PB 111643. Office of Technical Services, U. S. Dept. of Commerce, Washington, D. C. $3.00.

Ireson, W. G., and Grant, E. L., *Handbook of Industrial Engineering and Management*. Prentice-Hall, Inc., 70 Fifth Ave., N. Y. 11, N. Y. $16.00.

June, Stephen A., Bardis, J. D., Lurio, L. H., Polaner, L. S., Sagedahl, O., Skleanr, H. A., Yenken, B. K., *The Automatic Factor*. Instruments Pub. Co., 845 Ridge Ave., Pittsburgh 12, Pa. $1.50.

Mobile Manual for Radio Amateurs. American Radio Relay League, West Hartford, Connecticut. $2.50.

Proceedings on the Eighth Annual Conference on the Administration of Research. New York University Press, Washington Square, New York 3, N. Y. $4.00.

Proceedings of the Mixed Commission on the Ionosphere. General Secretariat of U.R.S.I., 42 Rue des Minimes, Brussels, Belgium, $6.00.

Spreadbury, E. A. W., *Television Receiver Servicing*. Iliffe and Sons, Ltd., Dorset House, Stamford Street, London, England. 21 s.

U.R.S.I. Proceedings of the XI General Assembly: Vol. Ten, Part Four. General Secretariat of U.R.S.I., 42 Rue des Minimes, Brussels, Belgium. $1.20.

Professional Groups†

Aeronautical & Navigational Electronics—Edgar A. Post, Navigational Aides, United Air Lines, Operations Base, Stapleton Field, Denver 7, Colo.

Antennas & Propagation—Delmer C. Ports, Jansky & Bailey, 1339 Wisconsin Ave., N.W., Washington 7, D. C.

Audio—*Chairman*, W. E. Kock, Bell Tel. Labs., Murray Hill, N. J.

Automatic Control—Robert B. Wilcox, Raytheon Manufacturing Co., 148 California St., Newton 58, Mass.

Broadcast & Television Receivers—W. P. Boothroyd, Philco Corp., Philadelphia Pa.

Broadcast Transmission Systems—O. W. B. Reed, Jr., Jansky & Bailey, 1735 DeSales St., N.W., Washington, D. C.

Circuit Theory—J. Carlin, Microwave Res. Inst., Polytechnic Inst. of Brooklyn, 55 Johnson St., Brooklyn 1, N. Y.

Communications Systems—A. C. Peterson, Jr., Bell Labs., 463 West St., New York 14, N. Y.

Component Parts—A. W. Rogers, Comp. & Materials Branch, Squier Signal Lab., Ft. Monmouth, N. J.

Electron Devices—J. S. Saby, Electronics Laboratory, G.E. Co., Syracuse, N. Y.

Electronic Computers—J. H. Felker, Bell Labs., Whippany, N. J.

Engineering Management—Max Batsel, Engineering Products Dept., RCA Victor Div.—Bldg. 10-7, Camden, N. J.

Industrial Electronics—George P. Bosomworth, Engrg. Lab., Firestone Tire & Rubber Co., Akron 17, Ohio

Information Theory—Louis A. DeRosa, Federal Telecommunications Lab., Inc., 500 Washington Avenue, Nutley, N. J.

Instrumentation—F. G. Marble, Boonton Radio Corp., Intervale Rd., Boonton, N. J.

Medical Electronics—V. K. Zworykin, RCA Labs., Princeton, N. J.

Microwave Theory and Techniques—A. C. Beck, Box 107, Red Bank, N. J.

Nuclear Science—M. A. Schultz, Westinghouse Automatic Power Division, Bettis Field, Pittsburgh 30, Pa.

Reliability and Quality Control—Victor Wouk, Beta Electric Corp., 333 E. 103rd St., New York 29, N. Y.

Production Techniques—R. R. Batcher, 240-02—42nd Ave., Douglaston, L. I., N. Y.

Telemetry and Remote Control—C. H. Hoeppner, Stavid Engineering, Plainfield, N. J.

Ultrasonics Engineering—M. D. Fagen, Bell Labs., Whippany, N. J.

Vehicular Communication—Newton Monk, Bell Labs., 463 West St., N. Y., N. Y.

† Names listed are Group Chairmen.

Sections*

Akron (4)—H. L. Flowers, 2029 19 St., Cuyahoga Falls, Ohio; H. F. Lanier, 49 W. Lowell St., Akron, Ohio

Alberta (8)—J. W. Porteous, Alberta Univ., Edmonton, Alta., Canada; J. G. Leitch, 13024—123A Ave., Edmonton, Alta., Canada.

Albuquerque-Los Alamos (7)—C. A. Fowler, 3333 49 Loop, Sandia Base, Albuquerque, N. Mex.; T. G. Banks, Jr., 1124 Monroe St., S.E., Albuquerque, N. Mex.

Atlanta (3)—D. L. Finn, School of Elec. Engr'g., Georgia Inst. of Tech., Atlanta, Ga.; P. C. Toole, 605 Morningside Dr., Marietta, Ga.

Baltimore (3)—C. D. Pierson, Jr., Broadview Apts. 1126, 116 West University Pkwy., Baltimore 10, Md.; M. I. Jacob, 1505 Tredegar Ave., Catonsville 28, Md.

Bay of Quinte (8)—J. C. R. Punchard, Elec. Div., Northern Elec. Co. Ltd., Sydney St., Belleville, Ont., Canada; M. J. Waller, R.R. 1, Foxboro, Ont., Canada

Beaumont-Port Arthur (6)—L. C. Stockard, 1390 Lucas Dr., Beaumont, Texas; John Petkovsek, Jr., 4390 El Paso Ave., Beaumont, Texas

Binghamton (4)—O. T. Ling, 100 Henry Street, Binghamton, N. Y.; Arthur Hamburgen, 926 Glendale Dr., Endicott, N. Y.

Boston (1)—T. P. Cheatham, Jr., Hosmer St., Marlborough, Mass.; R. A. Waters, IRE Boston Section Office, 73 Tremont St., Room 1006, Boston 8, Mass.

Buenos Aires—J. M. Rubio, Ayacucho 1147, Buenos Aires, Argentina; J. L. Blon, Transradio Internactional, San Martin 379, Buenos Aires, Argentina

Buffalo-Niagara (1)—D. P. Welch, 859 Highland Ave., Buffalo 23, N. Y.; William S. Holmes, 1861 Ellicot Rd., West Falls, N. Y.

Cedar Rapids (5)—Ernest Pappenfus, 1101 30 Street Dr., S.E., Cedar Rapids, Iowa; E. L. Martin, 1119 23 St., S.E., Cedar Rapids, Iowa

Central Florida (3)—Hans Scharla-Nielsen, Radiation Inc., P.O. Drawer 'Q', Melbourne, Fla.; G. F. Anderson, Radiation Inc., P.O. Box 'Q', Melbourne, Fla.

Chicago (5)—J. J. Gershon, De Vry Tech. Inst., 4141 Belmont Ave., Chicago 41, Ill.; J. S. Brown, 9829 S. Hoyne Ave., Chicago 43, Ill.

Cincinnati (4)—R. A. Maher, 6133 Sunridge Drive, Cincinnati 24, Ohio; W. S. Alberts, 6533 Elwynne Dr., Silverton, Cincinnati 36, Ohio

Cleveland (4)—H. R. Mull, 4558 Silverdale Ave., North Olmsted, Ohio; W. G. Piwonka, 3121 Huntington Rd., Cleveland 20, Ohio

Columbus (4)—W. E. Rife, 6762 Rings Rd., Amlin, Ohio; R. L. Cosgriff, 2200 Homestead Dr., Columbus, Ohio.

Connecticut Valley (1)—H. E. Rohloff, The Southern New England Tel. Co., 227 Church St., New Haven, Conn.; B. R. Kamens, 45 Brooklyn Circle, New Haven 15, Conn.

Dallas-Fort Worth (6)—A. R. Teasdale, Jr., 3925 Potomac Ave., Ft. Worth 7, Tex.; C. F. Seay, Jr., Collins Radio Co., 1930 Hi-Line Dr., Dallas, Tex.

Dayton (5)—A. B. Henderson, 801 Hathaway Rd., Dayton 9, Ohio; N. A. Nelson, 310 Lewiston Rd., Dayton 9, Ohio

Denver (6)—R. E. Swanson, 1777 Kipling St., Denver 15, Colo.; S. M. Bedford, Jr., Mountain States Tel. & Tel., Room 802, Denver, Colo.

Des Moines-Ames (5)—A. A. Read, 511 Northwestern Ave., Ames, Iowa; W. L. Hughes, E. E. Dept., Iowa State College, Ames, Iowa

Detroit (4)—N. D. Saigeon, 1544 Grant, Lincoln Park 25, Mich.; A. L. Coates, 1022 E. Sixth St., Royal Oak, Mich.

Egypt—Officers to be elected.

Elmira-Corning (1)—R. A. White, 920 Grand Central Ave., Horseheads, N. Y.; R. G. Larson, 220 Lynhurst Ave., Windsor Gardens, Horseheads, N. Y.

El Paso (6)—J. F. Stuart, Box 991, El Paso, Texas; W. T. McGill, 7509 Mazatlan Rd., El Paso, Texas

Emporium (4)—E. H. Boden, R.D. 1, Emporium, Pa.; H. S. Hench, Jr., R.D. 2, Emporium, Pa.

Evansville-Owensboro (5)—E. C. Gregory, 1120 S.E. First St., Apt. B-2, Evansville, Ind.; A. K. Miegl, 904 Kelsey Ave., Evansville, Ind.

Fort Wayne (5)—J. J. Iffland, 2603 Merivale St., Kirkwood Park, Ft. Wayne 8, Inc.; T. L. Slater, 1916 Eileen Dr., Waynedale, Ind.

Hamilton (8)—G. M. Cox, 154 Victoria St., S., Kitchener, Ont., Canada; A. L. Fromanger, Box 507, Ancaster, Ont., Canada

Hawaii (7)—G. W. Clark, Box 193, Lanikai, Oahu, T. H.; J. R. Sanders, c/o Matson Navigation Co., Box 899, Honolulu, T. H.

Houston (6)—L. W. Erath, 2831 Post Oak Rd., Houston, Tex.; R. W. Olson, 267 Pine Hollow Lane, Houston 19, Tex.

Huntsville (3)—A. L. Bratcher, 308 East Holmes St., Huntsville, Ala.; W. J. Millsap, 518 Woodmont, Huntsville, Ala.

Indianapolis (5)—J. T. Watson, 407 N. Penn. 508, Indianapolis 4, Ind.; M. J. Arvin, 4329 Fletcher Ave., Indianapolis 3, Ind.

Inyokern (7)—G. D. Warr, 213-A Wasp Rd., China Lake, Calif; B. B. Jackson, 54-B Rowe St., China Lake, Calif.

Israel—Franz Ollendorf, Box 910, Hebrew Inst. of Tech., Haifa, Israel; J. H. Halberstein, P.O.B. 1, Kiriath Mozkin, Israel

Ithaca (1)—Ben Warriner, General Electric Co., Advanced Electronics Ctr., Cornell University, Ithaca, N. Y.; R. L. Wooley, 110 Cascadilla St., Ithaca, N. Y.

(*Cont'd on next page*)

* Numerals in parentheses following Section designate Region number. First name designates Chairman, second name, Secretary.

(*Sections cont'd*)

Kansas City (6)—Richard W. Fetter, 8111 W. 87 St., Overland Park, Kan.; Mrs. G. L. Curtis, Radio Industries, Inc., 1307 Central Ave., Kansas City 2, Kan.

Little Rock (6)—J. E. Wylie, 2701 N. Pierce, Little Rock, Ark.; Jim Spilman, A. R. & T. Electronics, P.O. Box 370, North Little Rock, Ark.

London (8)—C. F. MacDonald, 328 St. James St., London, Ont., Canada; J. D. B. Moore, 27 McClary Ave., London, Ont., Canada

Long Island (2)—Paul G. Hansel, Addison Lane, Greenvale, L. I., N. Y.; W. P. Frantz, Sperry Gyroscope Co., Great Neck, L. I., N. Y.

Los Angeles (7)—Walter E. Peterson, 4016 Via Cardelina, Palos Verdes Estates, Calif.; John K. Gossland, 318 E. Calaveras St., Altadena, Calif.

Louisville (5)—R. W. Mills, 1017 Eastern Pkway, Louisville 4, Ky.; L. A. Miller, 314 Republic Bldg., Louisville 2, Ky.

Lubbock (6)—R.B. Spear, 510 E. Hill St., Brownfield, Texas; J. B. Joiner, 2621 30 St., Lubbock, Texas

Miami (3)—C. S. Clemans, Station WSWN, Belle Glade, Fla.; H. F. Bernard, 3670 S.W. Ninth Terrace, Miami 34, Fla.

Milwaukee (5)—Alex Paalu, 1334 N. 29 St., Milwaukee 8, Wis.; J. E. Jacobs, 6230 S. 116 St., Hales Corner, Wis.

Montreal (8)—R. W. Cooke, Box 630, Sta. 'O', Ville St. Laurent, Que., Can., F. H. Margolick, Canadian Marconi Co., 2442 Trenton Ave., Montreal, Que., Can.

Newfoundland Section—(Officers to be elected).

New Orleans (6)—L. J. N. Du Treil, 202 Homedale Ave., New Orleans 24, La.; J. A. Cronvich, Dept. Elec. Eng'g., Tulane University, New Orleans 18, La.

New York (2)—A. C. Beck, Box 107, Red Bank, N. J.; J. S. Smith, Elec. Eng'g. Dept., New York Univ., University Heights, New York 53, N. Y.

North-Carolina-Virginia (3)—J. C. Mace, 1616 Jefferson Park Ave., Charlottesville, Va.; Allen L. Comstock, 1404 Hampton Drive, Newport News, Va.

Northern New Jersey (2)—P. S. Christaldi, Box 111, Clifton, N. J.; R. J. Kircher, 145 Maple St., Summit, N. J.

Northwest Florida (3)—K. L. Huntley, Mary Esther, Fla.; G. C. Jones, 12 N. Okaloosa Rd., Fort Walton Beach, Fla.

Oklahoma City (6)—G. W. Holt, 4420 N.W. 19 Blvd., Oklahoma City 7, Okla.; W. E. Lucey, 1348 Kinkaid Ave., Oklahoma City 9, Okla.

Omaha-Lincoln (5)—M. L. McGowan, 5544 Mason St., Omaha 6, Neb.; C. W. Rook, Dept. Elec. Eng., Univ. of Nebraska, Lincon 8, Neb.

Ottawa (8)—George Glinski, 14 Dunvegan Rd., Ottawa, Ont., Canada; C. F. Pattenson, 3 Braemar, Ottawa 2, Ont., Canada

Philadelphia (3)—C. R. Kraus, Bell Telephone Co. of Pa., 1835 Arch St., 16 Floor, Philadelphia 3, Pa.; Nels Johnson, Philco Corp., 4700 Wissahickon Ave., Philadelphia 44, Pa.

Phoenix (7)—William R. Saxon, 641 E. Missouri, Phoenix, Ariz.; G. L. McClanathan, 509 East San Juan Cove, Phoenix, Ariz.

Pittsburgh (4)—F. C. Alexander, 2824 Mt. Royal Blvd. & Sutter Rd., Glenshaw, Pa.; K. A. Taylor, Bell Tel. Co. of Pa., 416 Seventh Ave., Pittsburgh 19, Pa.

Portland (7)—Howard Vollum, 1000 N.W. Skyline Blvd., Portland, Ore.; R. R. Pooley, Radio Station KPOJ, Box 31, Portland 7, Ore.

Princeton (2)—G. C. Sziklai, Box 3, Princeton, N. J.; L. L. Burns, Jr., R.C.A. Labs., Princeton, N. J.

Rochester (1)—G. H. Haupt, 48 Van Voorhis Ave., Rochester 17, N. Y.; B. L. McArdle, Box 54, Brighton Sta., Rochester 10, N. Y.

Rome-Utica (1)—H. F. Mayer, 60 Fountain St., Clinton, N. Y.; R. S. Grisetti, 67 Route St., New Hartford, N. Y.

Sacramento (7)—R. C. Bennett, 2239 Marconi Ave., Sacramento 21, Calif.; R. A. Paucher, 3021 Mountain View Ave., Sacramento 21, Calif.

St. Louis (6)—F. A. Fillmore, 5758 Itaska St., St. Louis 9, Mo.; Christopher Efthim, 1016 Louisville Ave., St. Louis 10, Mo.

Salt Lake City (7)—A. L. Gunderson, 3906 Parkview Dr., Salt Lake City, Utah; S. B. Hammond, Engineering Hall, Univ. of Utah, Salt Lake City 1, Utah.

San Antonio (6)—C. M. Crain, Engineering Bldg. 149, University of Texas, Austin 12, Texas; W. H. Hartwig, Dept. of Elec. Engr., University of Texas, Austin 12, Texas

San Diego (7)—F. X. Brynes, 1759 Beryl St., San Diego 9, Calif.; R. T. Silberman, 4274 Middlesex Dr., San Diego, Calif.

San Francisco (7)—A. J. Morris, 1827 Cordilleras Rd., Redwood City, Calif.; J. S. McCullough, 1781 Willow St., San Jose 25, Calif.

Schenectady (1)—C. C. Allen, 2064 Baker Ave., Schenectady 9, N. Y.; A. E. Rankin, 833 Whitney Dr., Schenectady, N. Y.

Seattle (7)—A. E. Harrison, Elect. Engr'g. Dept., Univ. of Washington, Seattle 5, Wash.; R. H. Hoglund, 1825 E. Lynn St., Seattle 2, Wash.

Syracuse (1)—W. H. Hall, General Electric Co., Syracuse, N. Y.; Major A. Johnson, R.D. 1, Totman Rd., East Syracuse, N. Y.

Toledo (4)—L. S. Rynder, 140 Rockingham St., Toledo 10, Ohio; L. R. Klopfenstein, Portage, Ohio

Toronto (8)—A. P. H. Barclay, 2 Pine Ridge Dr., Toronto 13, Ont., Canada; H. W. Jackson, 352 Laird Dr., Toronto 17, Ont., Canada

Tulsa (6)—Glen Peterson S. 83 East Ave., Tulsa, Okla.; D. G. Egan, Research Lab., Carter Oil Co., Box 801, Tulsa 2, Okla.

Twin Cities (5)—F. S. Hird, Northwestern Bell Tel. Co., 224 S. Fifth St., Minneapolis, Minn.; J. L. Hill, 25 17 Ave., N.E., North St. Paul 9, Minn.

Vancouver (8)—Miles Green, North-West Tel Co., 2226 W. Tenth Ave., Vancouver, B. C., Canada; J. S. Gray, 4069 W. 13 Ave., Vancouver, B. C., Canada

Washington (3)—T. B. Jacocks, General Electric Co., 777 14 St., N.W., Washington, D. C.; R. I. Cole, 2208 Valley Circle, Alexandria, Va.

Williamsport (4)—George Amey, 968 N. Market St., Williamsport, Pa.; W. H. Brebee, 818 Park Ave., Williamsport, Pa.

Winnipeg (8)—R. M. Simister, 179 Renfrew St., Winnipeg, Man., Canada; G. R. Wallace, 400 Smithfield Ave., Winnipeg, Man., Canada

Subsections

Berkshire County (1)—S. C. Leonard, Cheshire, Mass.; W. E. Neubert, 21 Highlawn Dr., Pittsfield, Mass.

Buenaventura (7)—W. O. Bradford, 301 East Elm St., Oxnard, Calif.; M. H. Fields, 430 Roderick St., Oxnard, Calif.

Centre County (4)—W. J. Leiss, 1173 S. Atherton St., State College, Pa.

Charleston (3)—W. L. Schachte, 152 Grove St., Charleston, S. C.; Arthur Jones, 21 Madden Dr., Charleston Heights, S. C.

East Bay (7)—J. M. Rosenberg, 1134 Norwood Ave., Oakland 10, Cal.; C. W. Park, 6035 Chabolyn Terrace, Oakland, Cal.

Erie (1)—R. S. Page, 1224 Idaho Ave., Erie 10, Pa.; R. H. Tuznik, 905 E. 25 St., Erie, Pa.

Fort Huachuca (2)—Officers to be elected.

Lancaster (3)—G. W. Scott, Armstrong Cork Co., Lancaster, Pa.; G. E. Mandell, 522 E. King St., Lancaster, Pa.

Mid-Hudson (2)—E. J. Breiding, 54 S. Grand Ave., Poughkeepsie, N. Y.; E. S. Wilson, I.B.M., Poughkeepsie, N. Y.

Monmouth (2)—G. F. Senn, 81 Garden Rd., Little Silver, N. J.; C. A. Borgeson, 82 Garden Rd., Little Silver, N. J.

Orange Belt (7)—B. F. Husten, Naval Ord. Lab., Corona, Calif.; T. A. Mayeda, 3120 Locust St., Riverside, Calif.

Palo Alto (7)—John V. N. Granger, 320 Encinal Ave., Menlo Park, Calif.; W. B. Wholey, 342 Verano Dr., Los Altos, Calif.

Pasadena (7)—P. H. Reedy, 1742 Grevelia St., Apt. E, South Pasadena, Calif.; Jennings David, 585 Rim Rd., Pasadena 8, Calif.

Piedmont—Officers to be elected.

Richland (7)—R. G. Clark, 1732 Howell, Richland, Washington; R. E. Connally, 515 Cottonwood Dr., Richland, Wis.

Tucson (7)—R. C. Eddy, 1511 E. 20 St., Tucson Ariz.; P. E. Russell, Elect. Eng. Dept., Univ. Ariz., Tucson, Ariz.

USAFIT (5)—L. A. Yarbrough, Box 3001, USAFIT, Wright-Patterson AFB, Ohio; J. J. Gallagher, Box 3482 USAFIT, Wright Patterson AFB, Ohio

Weschester County (2)—Joseph Reed, 52 Hillcrest Ave., New Rochelle, N. Y.; D. S. Kellogg, 9 Bradley Farms, Chappaqua, N. Y.

Wichita (6)—H. G. Swift, 1642 South Main, Wichita, Kan.; Vernon N. Johnson, 1652 S. Edgemoor, Wichita 17, Kan.

IRE INSTRUMENTATION CONFERENCE AND EXHIBIT

SPONSORED BY THE PROFESSIONAL GROUP ON INSTRUMENTATION AND THE ATLANTA SECTION

NOVEMBER 28–30, ATLANTA, BILTMORE HOTEL

MONDAY, NOVEMBER 28

8:00 A.M.—Registration

9:00 A.M. to 10:00 P.M.—Exhibits

10:30 A.M.—OPENING SESSION

Chairman: B. J. Dasher, Georgia Institute of Technology.

"Welcome," B. J. Dasher, Conference Manager.

"Control and Power Supply Problems of Unmanned Satellites," Ernst Stuhlinger, Redstone Arsenal.

2:30 P.M.—RECORDING AND DATA UTILIZATION

Chairman: E. K. Ritter, Georgia Institute of Technology.

"A Twenty-four Channel Cathode Ray Oscilloscope for Monitoring Magnetic Tape Records," Frank C. Smith, Jr. and Robert R. Pittman, Southwestern Industrial Electronics Co.

"Simplified Automatic Data Plotter for Telemetering Systems (SADAP)," H. P. Riblet, Johns Hopkins University.

"New Airborne Recorder Design Techniques," Armand L. Klein, Ampex Corp.

"A High-Speed Reader for Perforated Tape," R. J. Bianco, Aberdeen Proving Ground.

"Permanent Digital Function Storage Using Neon Tubes," M. S. Raphael and A. S. Robinson, Columbia University.

"A Survey of Navigational Measurements Methods for Missile Guidance Systems," S. L. Johnston, Redstone Arsenal.

TUESDAY, NOVEMBER 29

9:00 A.M. to 6:00 P.M.—Exhibits

9:30 A.M.—DATA HANDLING SYSTEMS

Chairman: Thomas L. Greenwood, Redstone Arsenal.

"A Central Facility for Processing Engineering Test Data," Edward C. Allmond, Air Force Armament Center.

"Requirements of Data Processing Facilities," I. R. Heimlich, McDonnel Aircraft Co.

"A Digital Data Gathering System," C. Fanwick, J. S. Lanza and J. Ottobre, Stavid Engineering, Inc.

"Digital Solutions to Instrumentation and Automatic Control Problems," Benjamin Kessel and Robert W. Brooks, Computer Control Co.

"The Analog Computer as an Operational Test Instrument for Jet Engine Testing," L. F. Burns, W. K. McGregor, Aro Inc.

"An Analog Data Handling System," J. M. Googe, Aro Inc.

2:30 P.M.—PROCESSING TECHNIQUES

Chairman: George B. Hoadley, North Carolina State College.

"A General Purpose Electronic Multiplier," Robert A. Meyers, David Taylor Model Basin.

"The Application of Analogue Techniques to a Continuously Rotating Magnetic Drum," J. L. Douce and J. C. West, University of Manchester, Manchester, Eng.

"Rapid Automatic Digitization and Sorting of Random Graphical Data," Victor S. Carson, North Carolina State College.

"A Phase Filter Applied to Spectral Phonocardiography," F. H. Middleton, G. B. Gilbert and W. H. Huggins, Johns Hopkins University, and G. N. Webb, Johns Hopkins Hospital.

"The ORDRAT—Ordnance Dial Reader and Translator," P. M. Kintner, Ballistics Research Lab., R. E. Howard, S. B. Peterson, and R. C. Webb, Denver Research Inst.

"The Doppler Data Translator," Paul M. Kintner, Ballistics Research Laboratory, and E. J. Armotta, Potter Instrument Co.

Tuesday Evening

Cocktail Party and Banquet

Speaker: John D. Ryder, President IRE, "Engineering Is Science."

WEDNESDAY, NOVEMBER 30

9:00 A.M. to 6:00 P.M.—Exhibits

9:30 A.M.—ANALOG TO DIGITAL CONVERSION

Chairman: R. L. Sink, Consolidated Engineering Corporation.

"High-Speed Analog-Digital Convertors," Martin L. Klein, No. Am. Aviation, Inc.

"An Unusual Electronic Analog-Digital Conversion Method," Blanchard D. Smith, Jr., Melpar, Inc.

"Sine-Cosine Angular Position Encoders," Carl P. Spaulding, Datex Division, G. M. Giannini and Co., Inc.

"Precision Direct-Reading, Binary-Position Encoders," W. I. Frank and A. B. White, Electronics Corporation of America.

"Digitization of Carrier Excited Transducers Using a Programmed Attenuator," John R. Zweizig, Cal. Inst. Tech.

2:30 P.M.—TRANSDUCERS

Chairman: R. D. Hurlbert, Rich's, Inc.

"Mathematical Definitions for Transducer Measure Criteria," L. J. Fogel, Stavid Engineering, Inc.

"New Multi-Purpose Industrial Transducers," Wm. F. Newbold, John V. Werme, Minneapolis-Honeywell Regulator Co.

"A Digital Sine-Cosine Transducer," W. Henn, A. S. Robinson, Columbia Univ.

"A New DC Voltage Discriminator with Independent Control of Threshold Voltage and Voltage Differential," N. Paul Stucky, Minneapolis-Honeywell Regulator Co.

"A Binary Coded Decimal Convertor," Martin Ziserman, The Norden Laboratories.

EIGHTH ANNUAL CONFERENCE ON ELECTRICAL TECHNIQUES IN MEDICINE AND BIOLOGY

SPONSORED BY IRE, AIEE, AND ISA, SHOREHAM HOTEL, WASHINGTON, D. C., NOVEMBER 14–16

Morning, November 14

RECENT ADVANCES IN ANGIOCARDIOGRAPHY

Chairman: Theodore F. Hilbish, M.D. M.P.H., Chief, Diagnostic Radiological Service, Nat. Inst. Health, Bethesda, Md.

Four papers will be presented.

Afternoon, November 14

Inspection trip to the National Institutes of Health, Bethesda, Maryland.

Morning, November 15

AUDIOLOGY AND INSTRUMENTATION FOR HEARING

Chairman: Dr. Scott Reger, Department of Otolaryngology, University of Iowa Hospital, Iowa City, Iowa.

Four papers will be presented.

Afternoon, November 15

Inspection trip to Naval Medical Research Institute, Bethesda, Maryland.

Morning, November 16

INSTRUMENTATION IN MEDICINE AND BIOLOGY

Chairman: W. A. Wildhack, Chief of Office of Basic Instrumentation, National Bureau of Standards, Washington, D. C.

Six papers will be presented.

Afternoon, November 16

Inspection trip to National Bureau of Standards, Washington, D. C.

Abstracts of IRE Transactions

The following issues of "Transactions" have recently been published, and are now available from the Institute of Radio Engineers, Inc., 1 East 79th Street, New York 21, N. Y. at the following prices. The contents of each issue and, where available, abstracts of technical papers are given below.

Sponsoring Group	Publication	Group Members	IRE Members	Non-Members*
Aeronautical and Navigational Electronics	Vol. ANE-2, No. 3	$0.95	$1.45	$2.85
Audio	Vol. AU-3, No. 4	$1.15	$1.75	$3.45

* Public libraries and colleges may purchase copies at IRE Member rates.

Aeronautical and Navigational Electronics

Vol. ANE-2, No. 3, September, 1955

Lewis M. Hull, Pioneer in Aeronautical Electronics Award

RTCA-IRE West Coast Meeting—The Editor

What Is RTCA, Its Philosophy, and Its Relationship to IRE and Other Professional Societies?—J. H. Dellinger

Improving Air-Ground Communications—E. W. Pappenfus

Instrumentation Requirements for All-Weather Helicopter Flight—R. F. Bohling

Combining the Automatic Pilot and the Flight Director—E. H. Fritze and J. D. Rector

Aircraft Antenna System Lightning Protection—R. F. Huber, M. M. Newman, and J. D. Robb

A Miniature Airborne Pictorial Plotter—S. Romano

IRE-RTCA Symposium

Contributors in This Issue

Audio

Vol. AU-3, No. 4, July–August, 1955

PGA Comes of Age

PGA Chapter News

A Multi-Loop, Self-Balancing Power Amplifier—J.R. Macdonald

A multi-loop, push-pull power amplifier of exceptional characteristics is described. It employs special circuits to maintain accurate push-pull signal balance throughout and to hold the static or steady-state dc cathode currents of the output tubes equal. A pair of 807 tubes are used in class AB_2 to yield 65 w average power output at less than 1 per cent intermodulation distortion with 30 db of over-a negative feedback. Using local positive voltage feedback in addition, the intermodulation distortion is 0.1 per cent at 45 w and less than 0.2 per cent at 60 w. At full power output, the −0.5 db points occur at 19.8 cps and 22.4 kcps. The rise time of the amplifier is 3 μs, and its transient response and recovery from overload approach the ideal. There are no peaks at the ends of the response curve. A noise level of −106 db referred to 60 w output is attained. Extensive measurements of amplifier characteristics under various conditions are described.

Properties of Junction Transistors—R. J. Kircher

The motion of electrons and holes is considered in relation to the PN junction and it in turn is considered in relation to the junction transistor. Electrical properties, equivalent circuit diagrams, and limiting conditions of operation of junction transistors are discussed. Special equations and features of the common base, common emitter, and common collector configurations are developed and tabulated.

Low Distortion Operation of Some Miniature Dual Triodes—J. Z. Knapp

The variation of distortion with available parameters for low level rc-coupled triode stages is investigated and, the possibility of minimizing second harmonic distortion utilizing signal-source impedance and the nonlinear, noninfinite dynamic grid resistance as an amplitude-correcting device, is explored and found to warrant further consideration. Some data on distortion-level reproducibility for randomly-selected tubes is presented and the limitation of local feedback as a distortion reduction scheme is pointed out. Variation of distortion with signal level is discussed and demonstrated.

Contributors

Abstracts and References

Compiled by the Radio Research Organization of the Department of Scientific and Industrial Research, London, England, and Published by Arrangement with that Department and the *Wireless Engineer*, London, England

NOTE: The Institute of Radio Engineers does not have available copies of the publications mentioned in these pages, nor does it have reprints of the articles abstracted. Correspondence regarding these articles and requests for their procurement should be addressed to the individual publications, not to the IRE.

Acoustics and Audio Frequencies..... 1684
Antennas and Transmission Lines..... 1685
Automatic Computers..... 1685
Circuits and Circuit Elements..... 1686
General Physics..... 1688
Geophysical and Extraterrestrial Phenomena..... 1689
Location and Aids to Navigation..... 1691
Materials and Subsidiary Techniques... 1691
Mathematics..... 1694
Measurements and Test Gear..... 1694
Other Applications of Radio and Electronics..... 1695
Propagation of Waves..... 1695
Reception..... 1696
Stations and Communication Systems... 1696
Subsidiary Apparatus..... 1697
Television and Phototelegraphy..... 1697
Tubes and Thermionics..... 1697
Miscellaneous..... 1698

The number in heavy type at the upper left of each Abstract is its Universal Decimal Classification number and is not to be confused with the Decimal Classification used by the United States National Bureau of Standards. The number in heavy type at the top right is the serial number of the Abstract. DC numbers marked with a dagger (†) must be regarded as provisional.

The Index to the Abstracts and References published in the PROC. IRE from February, 1954 through January, 1955 is published by the PROC. IRE, April, 1955, Part II. It is also published by *Wireless Engineer* and included in the March, 1955 issue of that journal. Included with the Index is a selected list of journals scanned for abstracting with publishers' addresses.

ACOUSTICS AND AUDIO FREQUENCIES

534.2–8 2809
Absorption and Velocity of Ultrasonic Waves of Finite Amplitude in Liquids—D. M. Towle and R. B. Lindsay. (*Jour. Acous. Soc. Amer.*, vol. 27, pp. 530–533; May, 1955.) Measurements have been made of the absorption and velocity as a function of the intensity. Results are reported for propagation in distilled water and dilute solutions of acetic acid and sodium acetate and for glycerine, using frequencies from 4 to 9 mc. Absorption was observed to vary but velocity remained unchanged.

534.2–8 2810
Phase Velocity and Absorption Measurements in Water containing Air Bubbles—F. E. Fox, S. R. Curley and G. S. Larson. (*Jour. Acous. Soc. Amer.*, vol. 27, pp. 534–539; May, 1955.) Measurements were made of the phase velocity and absorption at frequencies from 10 kc to 1 mc. Phase velocity varied from 500 m/s to 2,500 m/s and peak absorption was >30 db/cm with the bubbles constituting 0.02 per cent of the volume.

534.2–8 2811
Attenuation of Ultrasound in Aqueous Suspensions—V. J. Stakutis, R. W. Morse, M. Dill and R. T. Beyer. (*Jour. Acous. Soc. Amer.*, vol. 27, pp. 539–546; May, 1955.) Measurements were made using ultrasonic pulses of frequency between 15 and 30 mc in suspensions of lycopodium spores and of a quartz sand at various concentrations. The attenuation constant varies linearly with the concentration over the range investigated.

534.232+538.566 2812
Relation between the Intensity Distributions over Radiating Systems and their Directivity Characteristics—Eckart. (See 2923.)

534.232–8 2813
Design of Large Variable Resonant Frequency Transducers—F. J. Fry, F. Dunn and W. J. Fry. (*Jour. Acous. Soc. Amer.*, vol. 27, pp. 570–575; May, 1955.) A transducer is described comprising a plane array of piezoelectric elements coupled to a mercury column of variable length. The system is enclosed in a steel tank with a rubber window for underwater use; it is capable of providing high acoustic power over a wide frequency range. See also 2319 of 1951 (Hall and Fry).

534.24:551.596.1 2814
Echoes in Forests—N. V. Ivashchenko. (*Priroda, Moscow*, vol. 44, pp. 117–118; March, 1955.) The duct effect and sound echoes observed in woods are probably due to reflections at a layer of warmer air above and around the wood; such a layer would be produced by the sun, in the absence of high winds.

534.414 2815
Theory of Arbitrary Systems of Weakly Coupled Acoustic Resonators—E. Christian (*Acustica*, vol. 5, pp. 119–130; 1955. In German.) First-order perturbation theory is used. The frequency splitting caused by volume deformation is calculated as well as that resulting from detuning due to the coupling spaces. The coupling frequencies are found as solutions of a secular determinant whose elements are composed of energy terms.

534.61:534.79 2816
Testing and Calibration of Commercial Phonmeters with Particular Reference to Measurements of Traffic Noise—S. Kitsopoulos. (*Bull. Schweiz. elektrotech. Ver.*, vol. 46, pp. 372–376, 389; April 16, 1955.)

534.614–8 2817
Dispersion of Ultrasonic Pulse Velocity in Cylindrical Rods—L. Y. Tu, J. N. Brennan and J. A. Sauer. (*Jour. Acous. Soc. Amer.*, vol. 27, pp. 550–555; May, 1955.) Measurements were made of the velocity of compression and shear waves in rods of Al alloy, brass, Cu and steel with diameters from 1/8 to 1 inch, using pulses with carrier frequencies of 200, 400, 1,000 and 2,500 kc. With compression waves the velocity depends on the ratio between rod radius a and λ, its value practically reaching that appropriate to the bulk material when $a/\lambda = 2.5$. No such dispersion is observed with shear waves.

534.75 2818
The Reception of Repeated and Overlapping Speech Patterns—J. W. Black. (*Jour. Acous. Soc. Amer.*, vol. 27, pp. 494–496; May, 1955.) Experiments are reported on the effect on intelligibility of presenting speech syllables almost simultaneously via a direct channel and via a variable-delay channel. With the delay varied by 0.03-sec steps up to 0.33 sec, intelligibility was in all cases lower than for the direct signal alone.

534.75 2819
Statistical Study of Differential Auditory Sensitivity in relation to Intensity—R. Chocholle. (*Acustica*, vol. 5, pp. 134–141; 1955. In French.)

534.78 2820
Development of a Quantitative Description of Vowel Articulation—K. N. Stevens and A. S. House. (*Jour. Acous. Soc. Amer.*, vol. 27, pp. 484–493; May, 1955.)

534.78:534.4 2821
A Difference Limen for Vowel Formant Frequency—J. L. Flanagan. (*Jour. Acous. Soc. Amer.*, vol. 27, pp. 613–617; May, 1955.)

534.851:681.85 2822
Calibration of Test Records by Interference Patterns—B. B. Bauer. (*J. acoust. Soc. Amer.*, vol. 27, pp. 586–594, May, 1955.)

534.86:621.395.625.3:621.318.13 2823
Alloy improves Magnetic Recording—C. W. Lufcy and W. T. Heath. (*Electronics*, vol. 28, pp. 137–139; June, 1955.) Recording and reproducing heads made from cold-rolled alfenol [2456 of 1954 (Nachman and Buehler)] have been investigated; they have high wear resistance and resolution and low losses, all important advantages for handling video signals.

534.862.4:621.395.625.3 2824
Survey of Flux-Responsive Magnetic Reproducing Heads—O. Kornei. (*Jour. Acous. Soc. Amer.*, vol. 27, pp. 575–580; May, 1955.)

621.395.623.743 2825
Wide-Range Electrostatic Loudspeakers—P. J. Walker. (*Wireless World*, vol. 61, pp. 208–211, 265–269, 381–384; May/June/August, 1955. Correction, *ibid.*, vol. 61, p. 346; July, 1955.) By reducing the acoustical efficiency of the es loudspeaker to a level comparable with that of moving-coil loudspeakers it is possible to obtain linear response over 4–5 octaves anywhere in the audible range. Methods of coupling the diaphragm to the air are discussed and compared with moving-coil practice. The advantages of a strip diaphragm of length great compared with $\lambda/3$ at the lowest frequency to be reproduced, and width small compared with λ at the highest frequency, are enumerated. The acoustical problem is discussed with reference to equivalent networks. Efficiency in converting electrical power into sound is best achieved by the use of several units each covering a restricted bandwidth (>2 octaves) and fed through crossover networks. The acoustical relations between the

loudspeaker and the room in which it is used are discussed; the characteristics of small corner-mounted diaphragms are compared with those of large diaphragms radiating on both sides

621.395.625.2+621.395.616 2826
Capacitive Transducer has Low Impedance—H. P. Kalmus. (*Electronics*, vol. 28, pp. 161–163; June, 1955.) A peak-rectifier circuit is used with the transducer, comprising a pair of metal plates and a stylus between them, arranged in series with the rectifier diode. For typical stated operating conditions the device is equivalent to an audio generator with open-circuit voltage of 250 mv and internal impedance 5 kΩ. Use of the principle in the design of a gramophone pickup and a capacitor microphone is discussed briefly.

ANTENNAS AND TRANSMISSION LINES

621.315.212 2827
Investigation of a Production Length of Cable by Terminal-Impedance Measurements—M. Cotte. (*Câbles & Transm.*, vol. 9, pp. 161–171; April, 1955.) Local impedance variations of coaxial cable are determined by constructing a Fourier series based on terminal-impedance measurements. Both negligible and appreciable line attenuations are considered. The results agree well with those obtained by other methods.

621.315.212+621.372.8]:621.317.3 2828
Measurement of Weak Reflections in Coaxial-Line and Waveguide Systems—Epprecht and Stäger. (See 3037.)

621.372 2829
Propagation of a Fundamental Wave between Parallel Surfaces—E. Burshtein and L. Solov'ev. (*C.R. Acad. Sci. U.R.S.S.*, vol. 101, pp. 465–468; March 21, 1955. In Russian.) The fundamental wave is considered to be one which, in the limiting case of plane boundary surfaces, becomes a homogeneous plane wave. The phase velocity midway between the boundary surfaces, which may be slightly curved, is calculated and the phase distribution on the midway surface and the normals to the lines of constant phase; i.e., the wave "rays," are hence determined.

621.372.2 2830
The Uniform-Structure Electromagnetic Delay Line—P. M. Prache. (*Câbles & Transm.*, vol. 9, pp. 112–143; April, 1955.) Complete theory of a system constituted by a copper coil wound on a cylindrical insulating former and connected to a straight return wire through uniformly distributed capacitances. Calculated values of delay, characteristic impedance and attenuation for both screened and unscreened lines are in good agreement with experimental results. Optimum dimensions for obtaining given characteristics are deduced.

621.372.2:517 2831
The Electromagnetic Delay Line, Source of Relations between Bessel Functions and Elliptic Integrals—P. M. Prache. (*Ann. Télécommun.*, vol. 10, pp. 82–86; April, 1955.) Expressions for the delay-line vector magnetic potential and field are derived in terms of Bessel functions and quoted from standard electromagnetic theory in terms of elliptical integrals. By comparing the two sets of expressions, infinite integrals of products of Bessel functions can be reduced to elliptic integrals which can be calculated easily from tables.

621.372.8 2832
On the Theory of Circularly Symmetric TM Waves in Infinite Iris-Loaded Guides—C. C. Grosjean. (*Nuovo Cim.*, vol. 1, pp. 427–438; March 1, 1955. In English.) Exact theory is developed, making use of the Floquet theorem. The final equations form an infinite linear system which can be transformed in several ways to derive new formulas, but which has not yet been solved explicitly.

621.372.8 2833
Mathematical Transformation of a System of Equations appearing in the Theory of TM Wave Propagation in Corrugated Guides—C. C. Grosjean. (*Nuovo Cim.*, vol. 1, pp. 439–446; March 1, 1955. In English.)

621.372.8 2834
On the (β_0, k) Diagrams for Circularly Symmetric TM Waves in Infinite Iris-Loaded Waveguides—V. J. Vanhuyse. (*Nuovo Cim.*, vol. 1, pp. 447–452; March 1, 1955. In English.) For the case of infinitely thin irises, the equations derived by Grosjean (2833 above) are simplified to give results directly related to the pass bands in the frequency/propagation-constant characteristics.

621.372.8 2835
Calculations for Ridge Waveguides—H. G. Unger. (*Arch. elekt. Übertragung*, vol. 9, pp. 157–161; April, 1955.) Design formulas are derived for ridge waveguides of arbitrary cross section. Numerical examples are discussed. Results are compared with calculations for given cross sections made by other workers.

621.372.8 2836
On the Proper Frequencies of Terminated Corrugated Waveguides—V. J. Vanhuyse. (*Physica*, vol. 21, pp. 269–280; April, 1955; ibid., vol. 32, p. 603; July, 1955.) Starting from Maxwell's equations, analysis is given for circularly symmetrical TM waves propagated in an iris-loaded guide terminated at each end by a half-length section. The theory is extended to cases where the diameters of the sections are not all equal. Measurements were made on waveguides with one, three and five whole sections plus the terminating half-sections; the results are in good agreement with those predicted by theory.

621.396.67 2837
Radiation from Aerials—G. Barzilai. (*Wireless Engr.*, vol. 32, pp. 223–225; August, 1955; Correction, ibid., vol. 32, p. 258; September, 1955.) "A formal expression for the complex power radiated by a thin, centre-driven aerial is derived in terms of the vector potential on the surface of the conductor, making no assumption on the distribution of current. A similar expression is then obtained for the complex power radiated by the same aerial, on the assumption of sinusoidal-current distribution. By letting the radius of the conductor approach zero, the asymptotic forms of the two aforesaid expressions are compared."

621.396.67 2838
Multipoles and Asymmetrical Schelkunoff Waves—L. Ferrari. (*R.C. Acad. naz. Lincei*, vol. 18, pp. 304–308; March, 1955.) Extension of analysis presented previously (27 of January).

621.396.676.029.53 2839
How to design Sailboat Antennas—E. Robberson. (*Electronics*, vol. 28, pp. 140–143; June, 1955.) The special problems relating to the design of mf antennas for use on vessels with an extensive superstructure are discussed.

621.396.677.029.64 2840
Study of Multiple-Horn Aerials—J. Salomon and B. Brunet. (*Rev. tech. Comp. franç. Thomson-Houston*, no. 19, pp. 75–100; April, 1955.) Theoretical and experimental investigations are reported of parabolic reflectors fed by several primary radiators. The advantages and limitations of defocusing are discussed. Various coupling arrangements of the primary radiators are considered. See also 2841 below.

621.396.677.029.64:621.396.96 2841
Design and Construction of Radar Aerials for the 10-cm Band—P. E. Vincelet. (*Rev. tech. Comp. franç. Thomson-Houston*, No. 19, pp. 59–74; April, 1955.) Design problems are considered in relation to the radiation pattern required; range, gain, number of radiating elements and reflector dimensions are considered. The characteristics of the rotating joints are discussed. Details are given of an antenna with five pyramidal horns; test methods are indicated.

621.396.677.3 2842
Optimum Design of Directive Antenna Arrays Subject to Random Variations—E. N. Gilbert and S. P. Morgan. (*Bell Syst. Tech. Jour.*, vol. 34, pp. 637–663; May, 1955.) A statistical expression is derived for the radiation pattern of an arbitrary array with random variations of the position and excitation of the elements. When the element positions are either fixed or subject to displacements with a spherically symmetrical distribution, the pattern is given by that of the undisturbed array together with a "background" component having the same directivity as the pattern of a single element. The design of superdirective arrays is discussed with emphasis on the need to maintain this background component constant while maximizing the gain of the array. Numerical examples are given.

621.396.677.3:523.16:53.088.22 2843
Correcting for Gaussian Aerial Smoothing—R. N. Bracewell. (*Aust. J. Phys.*, vol. 8, pp. 54–60; March, 1955.) If the values established in a two-dimensional radio-astronomy survey with a Gaussian antenna beam are at intervals of $\sqrt{2}$ standard deviations, then the correction for antenna smoothing is simply calculated as the difference between the value to be corrected and the mean of the neighboring four values.

621.396.677.31 2844
The Effect of the Source Distribution on Antenna Patterns—S. Matt and J. D. Kraus. (Proc. IRE, vol. 43, pp. 821–825; July, 1955.) An examination is made of the effect on the observed polar diagram of a receiving antenna of appreciable extension of the radiation source. The problem is discussed in relation to the Ohio State University radiotelescope antenna, which comprises 96 helical antennas in a broadside array of length about 40λ and width about 5.6 λ when operating at a frequency of 250 mc. The extension of sources is deduced approximately from observed patterns; an analytical method of determining source extension is also discussed.

AUTOMATIC COMPUTERS

681.142 2845
Electronic Computers for the Businessman—J. M. Carroll. (*Electronics*, vol. 28, pp. 122–131; June, 1955.) A survey covering 38 commercially available digital computers. Important characteristics are tabulated.

681.142 2846
Storage Devices for High Speed Calculators—A. D. Booth. (*Research, (London)*, vol. 8, pp. 130–140; April, 1955.) A survey covering thermal, optical, sonic-delay, electrochemical, cr tube, ferroelectric, capacitor, magnetic-drum, magnetostriction and magnetic-core devices.

681.142 2847
A Proposed Modification to the C.S.I.R.O. Mark I Computer—B. E. Swire. (*Aust. J. Phys.*, vol. 8, pp. 184–186; March, 1955.) The suggestion is put forward that a facility be built into the machine for distinguishing between machine commands and interpretive or "hyper" commands so that the former are

performed directly while on receipt of one of the latter control is directed to the head of the interpretation routine with simultaneous storage of the link datum to enable return of control to the next program command after performance of the hyperfunction. This would result in a considerable gain in speed. See also 640 and 641 of 1954 (Pearcey and Hill).

681.142:511.142 2848
Automatic Square Rooting—E. H. Lenaerts. (*Electronic Engng.*, vol. 27, pp. 287–289; July, 1955.) A computation method is described, with examples, and an indication is given of the type of additional circuit required in computers of the LEO type [3473 of 1954 (Pinkerton *et al.*)]. The square root of a 40-digit number is obtained in 6.4 ms.

681.142:538.221 2849
Multiple-Coincidence Magnetic Storage Systems—R. C. Minnick and R. L. Ashenhurst. (*Jour. Appl. Phys.*, vol. 26, pp. 575–579; May, 1955.) "In existing magnetic matrix storage systems a given location is selected by applying to two intersecting wires a current equivalent to one-half of the selecting field. This situation is generalized so that any core is selected by energizing p wires each with a current equivalent to $1/p$ of the selecting field. The advantages gained are in the correspondingly smaller fields applied to the non-selected cores, or alternatively, in the faster switching times obtainable by applying a total field greater than the coercive force to the selected core . . . Specifically, a storage matrix is illustrated in which the cores are toroids etched from a continuous sheet of magnetic material."

681.142:621.384.622 2850
A Computer for solving some Problems in connection with Travelling-Wave Particle Accelerators—Crowley-Milling. (See 3061.)

681.142.002.2 2851
Digital Computer Plug-In Units and Associated Equipment—J. N. Harris and F. L. McNamara. (*Elect. Engng, N. Y.*, vol. 74, pp. 326–329; April, 1955.) Basic circuits etched on small boards are plugged into standard 32-contact receptacles, 15 of which are combined in a sub-rack assembly complete with power wiring.

CIRCUITS AND CIRCUIT ELEMENTS

621.3.018.7 2852
The Unit Step, the Unit Pulse, and the Dirac Operator—R. Cazenave. (*Ann. Télécommun.*, vol. 10, pp. 50–53; March, 1955.) The unit pulse is identified as the derivative of the unit step, and the identity between the unit pulse and the Dirac function is demonstrated by considering the establishment of a direct current in a circuit with finite inductance but vanishing capacitance.

621.3.049.75 2853
"Stamping" Metals by Etching—A. Coleman. (*Mater. & Meth.*, vol. 41, pp. 96–97; March, 1955.) The process briefly described consists of printing the pattern of the desired circuit or part on a flat metal sheet or strip with an acid-resistant ink and then etching away the unprotected metal. The printing can be performed by a photographic, lithographic or silk-screen process.

621.316.8:621.396.828 2854
Resistors for Radio-Interference Suppression in Otto-Cycle [internal-combustion] Engines—Henniger. (See 3083.)

621.318.57:621.314.7 2855
Directly Coupled Transistor Circuits—R. H. Beter, W. E. Bradley, R. B. Brown, and M. Rubinoff. (*Electronics*, vol. 28, pp. 132–136; June, 1955.) Switching circuits using surface-barrier and alloy-junction transistors are described. In many cases the only other circuit components required are resistors. Rise and fall times of about 0.08 μs and 0.10 μs respectively are obtained. Applications in digital computers are mentioned.

621.372 2856
Further Analysis of Transmission-Line Directional Couplers—R. C. Knechtli. (PROC. IRE, vol. 43, pp. 867–869; July, 1955.) The conditions for infinite directivity in transmission line directional couplers derived by Firestone (49 of January) are discussed; more general conditions are derived valid for any degree of coupling.

621.372.412:549.514.51 2857
Frequency Aging of High-Frequency Plated Crystal Units—A. W. Warner. (PROC. IRE, vol. 43, pp. 790–792; July, 1955.) The aging process is discussed in terms of contamination of the quartz crystal; the influence of various production methods is examined. Data obtained with units in metal and glass enclosures are presented graphically.

621.372.412:549.514.51 2858
The Effect of Temperature and Acoustic Impedance of Vapours on the Electrical Constants of Quartz—S. Parthasarathy and V. Narasimhan. (*Ann. Phys., Lpz.*, vol. 15, pp. 302–310; March 15, 1955. In English.) Measurements were made of the equivalent resistance of a crystal vibrating in vapors of various organic liquids. At a given temperature, the equivalent resistance depends on the pressure. As the temperature increases the equivalent resistance decreases, the rate of decrease depending on the particular vapor.

621.372.413 2859
Tunable Temperature-Compensated Reference Cavity—M. S. Wheeler. (*Wireless Engr.*, vol. 32, pp. 201–205; August, 1955.) A design is discussed based on separation of the tuning and temperature-compensation functions. Temperature compensation at fixed frequency is discussed first and the conditions for variable frequency are then deduced. Experiments indicate that a cavity with a double-nosed construction can be made satisfying the theoretical requirements over a 5 per cent or 10 per cent band. Analysis is presented with reference to an equivalent circuit.

621.372.5 2860
Active-Ladder-Network Analysis—H. D. Polishuk. (*Wireless Engr.*, vol. 32, pp. 215–220; August, 1955.) A computationally economical method is developed in which the voltage appearing across the final "rung" of the ladder is expressed as a function of the individual randomly distributed sources of emf by a reduction process involving successive applications of Thévenin's theorem to all the meshes. The method is illustrated by examples.

621.372.5 2861
Representation of the General Linear Four-Terminal Network and some of its Properties—C. G. Aurell. (*Ericsson Tech.*, vol. 11, pp. 155–179; 1955.) Nonreciprocal networks are considered. Equations are formulated in terms of power and impedance. A method of representation is developed based on introduction of a circuit element called the "antireciprocal transition" in series with a reciprocal network. Power attenuation and matching are investigated. A new criterion for classifying networks as passive or active is proposed. A grounded-emitter transistor amplifier is discussed as a particular application of the theory.

621.372.5 2862
The Design of Quadripoles—M. Skalicky. (*Elektrotech. u. Maschinenb.*, vol. 72, pp. 173–174; April 15, 1955.) In the case of symmetrical quadripoles, by writing $\sqrt{K/L}=p$ and $\sqrt{KL}=Z$, where K and L are the impedance parameters defined earlier (3030 of 1952), general expressions are derived by a matrix treatment for the current and voltage in a ladder network, in which the characteristic-impedance term Z occurs only in the first degree.

621.372.5 2863
Synthesis of Passive Quadripoles—F. Hott. (*Rev. gén. Élect.*, vol. 64, pp. 203–205; April, 1955.) It is shown that any passive quadripole can be constituted by combining a two-terminal network with a T or Π network, the whole comprising four two-terminal physically realizable networks with complex impedance.

621.372.5 2864
A New Method for investigating Linear Quadripoles—J. de Buhr. (*Fernmeldetech. Z.*, vol. 8, pp. 200–204; April, 1955.) A treatment based on representation of impedance transformations by displacements on the surface of a sphere; known graphical methods are made accessible to a purely geometric treatment by the method of projection. Problems of networks satisfying Kirchhoff's laws can be solved with compasses and ruler.

621.372.5 2865
Impossible Behavior of Nonlinear Networks—R. J. Duffin. (*Jour. Appl. Phys.*, vol. 26, pp. 603–605; May, 1955.) The following proposition is discussed: "An isothermal electromechanical system whose primary resistors are quasi-linear cannot convert direct current to alternating current." A resistor is said to be quasi-linear if the voltage drop across it is a function only of the current, and if the differential resistance is positive.

621.372.5 2866
Note on the Kramers-Kronig Relations—M. K. Brachman. (*Jour. Appl. Phys.*, vol. 26, pp. 497–498; May, 1955.) "The explicit form of the relationship between the real and imaginary parts of a physically realizable network function is correlated with the alternate conventions available for such problems. The transformation from a linear frequency scale to a logarithmic one is simply effected by considering the Mellin transforms of the appropriate functions."

621.372.5:621.375.13 2867
Some Gyrator and Impedance Inverter Circuits—B. P. Bogert. (PROC. IRE, vol. 43, pp. 793–796; July, 1955.) The design of feedback amplifiers to provide impedance inversion is considered. Negative-impedance elements may be included to compensate for the residual impedances in the inverter; when this is done the circuit exhibits gyrator properties. Measurements on a high-stability amplifier with a series resistance of −600Ω in the input lead indicated that accurate impedance inversion was obtained for load resistances from 40 Ω to 4,000 Ω.

621.372.5:621.396.822 2868
Nyquist's and Thevenin's Theorems generalized for Nonreciprocal Linear Networks—R. Q. Twiss. (*Jour. Appl. Phys.*, vol. 26, pp. 599–602; May, 1955.) Theory of nonreciprocal networks such as those including ferrites is developed taking account of internal noise sources. The system can be treated as the combination of a source-free network together with a set of correlated noise-current or noise-voltage generators. Modifications of the treatment are indicated for dealing with cases where the actual noise sources are at different temperatures, as in the problem of determining the noise correlation between two receiver channels connected to a gyrator fed by two coupled antennas.

621.372.5.012 2869
Determination of the Frequency and Phase Characteristics of a Network for a Given Attenuation Curve—H. Kaufmann. (*Arch. elekt. Übertragung*, vol. 9, pp. 192–198; April, 1955.) A modification of the graphical method developed by Baum (3040 of 1948) is described for deriving a realizable attenuation characteristic approximating to the given one.

621.372.54 2870
A Derivation Method for designing Two- and Three-Element Filter Structures—J. E. Colin. (*Câbles & Transm.*, vol. 9, pp. 81–111; April, 1955.) A summary of fundamental principles with specific examples of two- and three-element designs using loss-free elements with no mutual inductance. The H, N and associative derivations, and an extension of Zobel's *m* derivation are treated, also the *LC* derivation involving interchange of *L* and *C*. Application of Norton's transformation is illustrated.

621.372.542.21:621.396.822 2871
The Noise-Power Bandwidths of Iterated Low-Pass *RC* Filters—W. E. Smith. (*Aust. J. appl. Sci.*, vol. 6, pp. 7–12; March, 1955.) "The noise-power bandwidths of *n*-section low-pass *RC* filters are calculated exactly from the transfer function for $n=1$ to 6. An asymptotic expression is derived for the bandwidth when the number of sections is large, and then the bandwidth is inversely proportional to n^2."

621.373.4 2872
The Periodic Solutions of a Nonlinear Differential Equation of the Second Order with Unsymmetrical Non-Linear Damping, and a Forcing Term—A. W. Gillies. (*Quart. J. Mech. appl. Math.*, vol. 8, pp. 107–128; March, 1955.) The differential equation considered gives a closer approximation to the behavior of tube oscillators than the van der Pol equation, and demonstrates the frequency deviation associated with the presence of higher harmonics.

621.373.42:621.385.029.64:621.316.726 2873
Study of the Relative Frequency Fluctuations of Two Reflex Klystrons stabilized by Different Methods—L. Jampierre. (*Ann. Télécommun.*, vol. 10, pp. 65–78, 87–99; March /April, 1955.) In connection with projected experiments of the Michelson type, it was desired to ascertain whether a variation of 0.08 c/s due to modulation could be detected in the frequency of 10-kmc oscillations modulated at 0.5 c/s. A study was made of the inherent frequency fluctuations of klystron oscillators and of methods for limiting them, with particular reference to the stabilization of supply sources. Alternative electronic methods involving use of waveguides and cavity resonators were used to stabilize the frequency of the beat between the two klystron oscillations, one of which was modulated. Filters of bandwidth 0.5 c/s were used to improve this stability. Results are compared with those of Pound (1311 of 1948) and Essen (1085 of 1953); they indicate that it should be possible with present-day techniques to detect a frequency variation of the order of 1 part in 10^{11}.

621.373.42.029.64 2874
Phase Stabilization of Microwave Oscillators—M. Peter and M. W. P. Strandberg. (Proc. IRE, vol. 43, pp. 869–873; July, 1955.) Description of a circuit incorporating a single stable feedback loop, that has been used to stabilize the frequency of a Type-2K50 K-band klystron by locking it to a harmonic of a quartz-controlled oscillator. Any phase modulation in the klystron is detected in a phase discriminator, the resulting signal is amplified in a differential dc amplifier and applied to the klystron repeller electrode.

621.373.421.1:621.396.822 2875
Phase Fluctuations in a Valve Generator—I. S. Gonorovski. (*C. R. Acad. Sci. U.R.S.S.*, vol. 101, pp. 657–660; April 1, 1955. In Russian.) The effect of shot noise on an oscillator operating in the steady state is considered theoretically. The intensity and the statistical properties of the shot current are independent of the feedback circuit and can thus be represented by a separate noise-current generator in parallel with the oscillator; analysis is presented on the basis of such an equivalent circuit.

621.373.421.11 2876
Frequency Stable *LC* Oscillators—W. B. Bernard and J. K. Clapp. (Proc. IRE, vol. 43, pp. 875–876; July, 1955.) Critical comment on 3170 of 1954 and author's reply.

621.373.431.1 2877
Analysis of the Relaxation Period of a Multivibrator—D. C. Sarkar and R. Ahmed. (*Indian J. Phys.*, vol. 28, pp. 533–541; November, 1954.) The analysis takes account of positive grid swing and appreciable shunting capacitance. Comparison of values obtained from the theory with experimental results indicates that the method is satisfactory.

621.373.431.1:621.314.63 2878
A Semiconductor Diode Multivibrator—J. J. Suran and E. Keonjian. (Proc. IRE, vol. 43, pp. 814–820; July, 1955.) A circuit is described using one double-base diode [see e.g. 2535 of 1954 (Aldrich and Lesk)] together with one ordinary diode and only three resistors and one capacitor.

621.373.432 2879
Significance of the Mandelstam Condition in the Oscillations of a Neon Lamp—P. Jean. (*C. R. Acad. Sci.*, (*Paris*), vol. 240, pp. 2059–2061; May 23, 1955.) Theory presented previously (3502 of 1954) is generalized. For relaxation oscillations to occur, three conditions must be satisfied simultaneously, including the Mandelstam condition which requires that the energy of the system shall remain constant at the discontinuity. This condition can be satisfied using a *RC* circuit, but not using a *RL* circuit.

621.373.52 2880
Isocline Diagrams for Transistor Circuits—F. Oakes. (*Electronic Engng.*, vol. 27, pp. 312–317; July, 1955.) "The method described for the graphical analysis of transistor negative resistance oscillators is based on non-linear mechanics, and does not necessitate approximation of curved transistor characteristics by straight lines. Voltage and current trajectories can be obtained by a simple construction which also indicates the rate of change of the voltages and currents during the course of cyclic or transient phenomena."

621.374.32:621.318.57 2881
Nonsaturating Pulse Circuits using Two Junction Transistors—J. G. Linvill. (Proc. IRE, vol. 43, pp. 826–834; July, 1955.) Junction transistors are found to be fast enough for pulse applications if the collector voltage is prevented from reaching zero. Switching times $<1\ \mu s$ can be achieved with available types. The required limiting action is effected by introducing diodes which terminate the switching transients by their breakdown. A two-transistor binary counter is described.

621.374.4 2882
A Decade Frequency Divider—R. B. Mobsby. (*Electronic Engng.*, vol. 27, pp. 295–298; July, 1955.) A divider developed for use with a quartz-crystal clock consists basically of a chain of Eccles-Jordan binary pairs whose over-all division ratio has been reduced by means of feedback. A complete circuit diagram is given.

621.375.2.024 2883
Method of reducing Zero Error and Drift in Breaker Type D.C. Amplifiers—T. M. Dauphinee. (*Rev. sci. Instrum.*, vol. 26, pp. 401–402; April, 1955.) Thermal emf's in the input transformer are cancelled by using a double-pole double-throw input chopper and connecting a high-quality capacitor in series with the winding.

621.375.2.029.4 2884
Low-Frequency Decoupling of Cathode and Screen Grid of an Amplifier Valve—R. Dessoulavy. (*Tech. Mitt. schweiz. Telegr.-Teleph. Verw.*, vol. 33, pp. 137–143; April 1, 1955. In French.) A method is described for using the Smith chart to determine the falling off at the upper and lower ends of the af response curve due to the decoupling capacitors.

621.375.221 2885
Distortion and Power in Aperiodic Amplifiers using Ideal Screen-Grid Valves—P. Schiaffino. (*Ricerca sci.*, vol. 25, pp. 896–921; April, 1955.) Calculations are made for Class A, AB, B and C operation, assuming a parabolic or nearly parabolic tube characteristic. A determination is made of the input waveform required to give a pure sinusoidal output. The effect of negative feedback is studied. Operation with sawtooth or square pulses is discussed.

621.375.221.2 2886
The Band-Pass Distributed Amplifier—V. C. Rideout and T. P. Tung. (*J. Indian Inst., Sci.*, Section B, vol. 37, pp. 138–161; April, 1955.) General expressions are derived for the gain of a distributed amplifier with any number of tubes coupled by identical filter sections. The analysis indicates that reduction of band-edge peaks is more difficult for band-pass than for low-pass amplifiers. Choice of suitable filter networks for the band-pass case is discussed, and some experimental results are presented for a 4-tube amplifier with a pass band from 51 mc to 81.8 mc.

621.375.223 2887
Design of Wide-Band *RC* Amplifiers—E. Schuon. (*Fernmeldetech. Z.*, vol. 8, pp. 233–239; April, 1955.) Discussion of multistage amplifier with inductive equalization in the anode circuit. The effect of negative feedback in the cathode line is examined.

621.375.232.3 2888
Active-Error Feedback and its Application to a Specific Driver Circuit—J. R. Macdonald. (Proc. IRE, vol. 43, pp. 808–813; July, 1955.) Feedback amplifiers are discussed in which the feedback signal is nominally equal to the input; the difference, which is proportional to the distortion or error in the output, is amplified in a separate circuit and re-injected with the proper polarity to reduce the output error. Analysis is given for a cathode-follower circuit incorporating this principle; the arrangement is especially suitable for driving the grid of an output tube highly positive. Experimental results support the theory.

621.375.4+621.373.52+621.318.57]:621.314.7 2889
The Transistor: Part 6—Applications—H. G. Bassett. (*P.O. elect. Engrs' J.*, vol. 48, pp. 47–52; April, 1955.) Amplifier, oscillator and switching circuits are discussed. Part 5: 3109 below.

621.375.4:621.314.7 2890
Linear Properties of the Transistor—G. Ledig. (*Fernmeldetech. Z.*, vol. 8, pp. 221–228; April, 1955.) Formulas and charts for various transistor circuits are presented.

621.375.4:621.314.7 2891
Internal Feedback and Neutralization of Transistor Amplifiers—A. P. Stern, C. A.

Aldridge, and W. F. Chow. (PROC. IRE, vol. 43, pp. 838–847; July, 1955.)

621.375.43:621.314.7 2892
Tensor Analysis of Transistor Feedback Circuits—G. Ledig. (*Arch. elekt. Übertragung*, vol. 9, pp. 162–167; April, 1955.) Theory is presented for the grounded-base circuit. The coefficients of the impedance matrix for the back-coupled circuit are obtained by multiplyplying those for the original circuit by certain characteristic tensors derived from the relation between the currents in the original and in the back-coupled arrangements. Particular conditions examined include current feedback, positive and negative voltage feedback, and other arrangements involving two feedback paths. Applicability of the duality principle is discussed.

621.376.3:621.317.39 2893
A Linear Capacitance-Change Circuit—V. H. Attree. (*Electronic Engng.*, vol. 27, pp. 308–310; July, 1955.) Capacitance changes produced by mechanical displacement modulate the frequency of a 465-kc Franklin oscillator which drives a nonode fm discriminator. Sensitivity is 10 V/pF, and the output is linear between −40 and +40 V. About 30 references are given to measurements of mechanical and other quantities by means of a capacitance change.

621.376.32:621.314.63 2894
Crystal Diodes in Voltage Dividers, in particular for increasing the Linearity and Slope of Static and Dynamic Characteristics—H. Meinke and A. Rihaczek. (*Fernmeldetech. Z.*, vol. 8, pp. 273–276; May, 1955.) Hf voltage dividers are discussed comprising a diode in series with a passive element, the voltage division ratio being varied by suitably controlling the diode. Applications to reactance-tube fm circuits are described.

621.375.4.029.3:621.314.7 2895
Transistor Audio Amplifiers [Book Review]—R. F. Shea. Publishers: Chapman and Hall, London, 52 s. (*Wireless Engr.*, vol. 32, p. 226; August, 1955.) Only junction transistors are considered.

GENERAL PHYSICS

53.087/.088 2896
Sharpening of Observational Data in Two Dimensions—E. J. Burr. (*Aust. J. Phys.*, vol 8, pp. 30–53; March, 1955.) The problem considered is that of recovering true distributions from smoothed observed distributions; this involves the solution of a linear integral equation. Several methods of solving the equation are examined and a technique for the application of polynomial solutions is presented. The effect of random errors in the observational data is taken into account wherever possible.

534.015.1 2897
Representation of the Modes of Motion of an Undamped Linear Oscillating System with Two Degrees of Freedom—K. Auch and W. Braunbek. (*Ann. Phys., Lpz.*, vol. 15, pp. 255–267; March 15, 1955.) The general solution of the differential equations for a system comprising two coupled mass-points corresponds to the superposition of two natural oscillations, but a better idea of the phenomenon is obtained by considering the motion as a single oscillation modulated in phase and in amplitude. This approach is illustrated graphically.

535.376 2898
Polarization Effects on the Brightness Waves of Electroluminescence—F. Matossi. (*Phys. Rev.*, vol. 98, pp. 434–437; April 15, 1955.) The observed cyclical variation of brightness of electroluminescent systems excited by sinusoidal fields is shown to be related to polarization effects of the type discussed e.g. by Jaffé (2193 of 1952) in connection with semi-conductors.

535.377 2899
Theory of Thermoluminescence—Ch. B. Lushchik. (*C. R. Acad. Sci. U.R.S.S.*, vol. 101, pp. 641–644; April 1, 1955. In Russian.)

535.514:538.61 2900
Polarization of Light by Aspherical Ferromagnetic Particles in a Uniform Magnetic Field: Part 1—Experimental Investigations with a γ-Fe_2O_3 Smoke. Part 2—Theory—E. Fick. (*Z. Phys.*, vol. 138, pp. 183–189; July 10, 1954. vol. 140, pp. 308–339; March 21, 1955.)

537.122:530.145 2901
Calculation of the Elementary Electric Charge from the Energy Quantum Model—H. Zuhrt. (*Arch. elekt. Übertragung*, vol. 9, pp. 181–191; April, 1955.) By extending the theory developed previously (2252 of August and back references), a value of 5.17×10^{-10} esu is obtained for the elementary electric charge; this differs by 7.7 per cent from the established value for the electron, the difference being mostly due to the approximations used.

537.213:621.372:517.54 2902
Nets composed of Parts of Circles for the Approximate Solution of Field Problems—Tasny-Tschiassny. (See 3033.)

537.22 2903
Dielectric Layer with Spherical Cavity in Homogeneous Electrostatic Field—R. N. Kaufman. (*C. R. Acad. Sci., U.R.S.S.* vol. 101, pp. 633–636; April 1, 1955. In Russian.) The special case of a cavity with center equidistant from the two faces of the layer is considered mathematically; a method is indicated for solving the problem when the cavity is not centrally placed.

537.226 2904
Calculation of Internal Field in Relaxation Polarization in Polycrystalline Dipole-Type Dielectrics—G. I. Skanavi and A. N. Gubkin. (*Zh. eksp. teor. Fiz.*, vol. 28, pp. 85–95; January, 1955.)

537.311.62 2905
Skin Resistance of a Transmission-Line Conductor of Polygon Cross Section—H. A. Wheeler. (PROC. IRE vol. 43, pp. 805–808; July, 1955.) A theorem is presented according to which a conductor whose cross section is a polygon that can be circumscribed on a circle has the same skin resistance as a conductor of of the same material having the said circle as its cross section. See also 331 of 1943.

537.311.62 2906
Calculation of the A.C. Resistance of a Solid Conductor with Rectangular Cross-Section—L. Piglione. (*Electrotecnica*, vol. 41, pp. 221–224; April 25, 1954.) The Joule-effect losses are calculated, starting from Maxwell's equations and making assumptions corresponding to those for the case of a circular cross section. The results are compared with those obtained by investigating penetration depth.

537.5 2907
Statistical Description of Assemblies with Collective Interaction: Parts 1 and 2.—G. Ecker. (*Z. Phys.*, vol. 140, pp 274–307; March 21, 1955.) A critical review of literature on the subject is presented. Two types of assemblies of electrons and ions are distinguished: (*a*) those with a finite number of discrete beams with definite velocity, and (*b*) those with thermally disordered motion with or without superimposed beams. Investigation of the first type of assembly leads to satisfactory results; the difficulties encountered in dealing with assemblies of the second type are due to neglecting the limitations of the models used. The model of the dispersed charge-carrier assembly presented by Twiss (1316 of 1953) is then considered and the concepts of collision and the collision zone are discussed.

537.52:537.226 2908
Phenomenological Theory of Townsend Breakdown in Dielectrics—P. L. Auer. (*Phys. Rev.*, vol. 98, pp. 320–327; April 15, 1955.)

537.52:538.56.029.6 2909
High-Frequency Gas Discharge Plasma in Hydrogen—D. J. Rose and S. C. Brown. (*Phys. Rev.*, vol. 98, pp. 310–316; April 15, 1955.) The microwave field strength required to maintain a hydrogen plasma in the steady state is calculated from theory based on a solution of the Boltzmann transport equation. The results are in satisfactory agreement with measurements made in a resonant cavity at different values of pressure and plasma concentration.

537.525 2910
Theory of High-Frequency Discharge in Gases at Low Pressures. Calculation of Electron Distribution Function—J. Salmon. (*J. Phys. Radium*. vol. 16, pp. 210–218; March, 1955.) The electron distribution is obtained by resolving Boltzmann's equation by a method of successive approximations, considering both elastic and inelastic collisions. The electron temperature corresponding to a Maxwellian velocity distribution is derived and the general form of the equation of evolution of electronic density is given.

537.525 2911
Role of Positive Ions in High-Voltage Breakdown in Vacuum—H. C. Bourne, Jr., R. W. Cloud, and J. G. Trump. (*Jour. Appl. Phys.*, vol. 26, pp. 596–599; May, 1955.)

537.525:621.396.822.029.62/.63 2912
Microwave and Metre-Wave Radiation from the Positive Column of a Gas Discharge—L. W. Davies and E. Cowcher. (*Aust. J. Phys.*, vol. 8, pp. 108–128; March, 1955.) Radiation intensity measurements were made at 200 mc and 3 kmc on a Ne discharge by inserting the positive column in a resonant cavity and comparing the cavity output with that of a known noise source. The rf power per unit bandwidth is expressed in terms of kT', where k is Boltzmann's constant and T' is the equivalent noise temperature and is comparable with the temperature of the electrons in the discharge. The departure of T' from the value corresponding to a Maxwell or Druyvesteyn electron-velocity distribution is investigated.

537.533 2913
Resonance-Type Secondary-Electron Multiplication—K. Krebs and H. Meerbach. (*Ann. Phys., Lpz.*, vol. 15, pp. 189–206; January, 15, 1955.) Electron multiplication by means of an hf field applied between a pair of parallel plates with secondary-electron emission rate greater than unity is considered theoretically and a relation is derived between the hf amplitude, the length of field lines and the phase at impact required for "avalanche" multiplication. Expressions are also obtained for the starting and cut-off voltages. Calculated results are in good agreement with experimental results. See also 2629 of 1954 (Hatch and Williams) and 790 of 1951 (Krebs).

537.533.8+535.215 2914
Delayed Electron Emission in Metals—K. Seeger. (*Z. Phys.*, vol. 141, pp. 221–236; April 21, 1955.) Continuation of earlier work (3266 of 1953). Results of experiments on W indicate that delayed-emission centers are imperfections in the lattice of the oxide surface film. These imperfections act as traps which can be emptied by heating to about 600 degrees C and destroyed by heating to 1,000 degrees C.

537.56 2915
Kinetic Theory of Weakly Ionized Homogeneous Plasmas: Part 2—M. Bayet, J. L. Delcroix and J. F. Denisse. (*J. Phys. Radium*, vol. 16, pp. 274–280; April, 1955.) The second-order approximation to the electron-velocity-distribution function, relating to the energy exchanges between an applied electric field and the plasma in a Lorentz-type gas, is developed. The resulting expression contains a divergent term corresponding to a nonstationary state in which the electron gas continually heats up. The quality factor, Q, of the plasma is calculated. The derivation of certain formulas used in part 1 (1624 of June) is given in an appendix.

537.56:538.56 2916
Longitudinal Plasma Oscillations: Part 1—A. A. Luchina. (*Zh. eksp. teor. Fiz.*, vol. 28, pp. 17–27; January, 1955.) A theoretical investigation is presented in which the effect of motion of ions is taken into consideration.

537.56:538.56 2917
Longitudinal Plasma Oscillations: Part 2—G. Ya. Myakishev and A. A. Luchina. (*Zh. eksp. teor. Fiz.*, vol. 28, pp. 28–37; January, 1955.) The equations derived in Part 1 (2916 above) are applied to the investigation of the dispersive properties of the plasma for the case of (*a*) hf oscillations, (*b*) lf oscillations, and (*c*) high electron-drift velocities. Results show that in the propagation of longitudinal waves in discharge tubes the motion of ions is frequently of importance. Formulas are derived for the dependence of the space periodicity and the damping coefficient on the discharge parameters.

537.568 2918
Recombination between Electrons and Positive Ions—M. Bayet and D. Quemada. (*J. Phys. Radium*, vol. 16, pp. 334–338; April, 1955.) A bibliography of 59 references is critically examined. Nearly always, recombination takes place by an interaction involving at least two atoms; direct recombination of an electron and a positive ion in a plasma, involving the radiation of excess energy, is relatively rare.

538.1:538.569.4.029 6 2919
Theory of Apparatus for Observation of Nuclear Magnetic Resonance—H. Pfeifer. (*Ann. Phys., Lpz.*, vol. 15, pp. 311–324; March 15, 1955.)

538.3 2920
A Postulational Approach to Electromagnetism—P. Moon and D. E. Spencer. (*Jour. Franklin Inst.*, vol. 259, pp. 293–305; April, 1955.)

538.561:537.1 2921
Interaction of Moving Charges with Wave Circuits—J. R. Pierce. (*Jour. Appl. Phys.*, vol. 26, pp. 627–638; May, 1955.) "When a charge moves along a nondispersive transmission line it induces forward and backward wave components in the line. For unaccelerated motion there is no radiation unless the charge moves with the speed of an unforced wave. For small accelerations, both radiation to the line and electromagnetic inertial effects caused by changes in the energy of the fields will be observed. The electromagnetic mass at velocities greater than the wave velocity is negative. Large accelerations can be handled by numerical computation. In the case of dispersive circuits, the charge radiates at frequencies for which the phase velocity of the circuit is equal to the velocity of the charge. This radiation is identified with Cherenkov radiation. Similar radiation takes place when a charge moves through a plasma."

538.561:537.122 2922
Čerenkov Radiation of Electrons moving parallel to a Dielectric Boundary—J. G. Linhart. (*Jour. Appl. Phys.*, vol. 26, pp. 527–533; May, 1955.) Analysis is based on an eigenfunction expansion of the em field. The process may be interpreted as an excitation of surface waves.

538.566+534.232 2923
Relation between the Intensity Distributions over Radiating Systems and their Directivity Characteristics—G. Eckart. (*Arch. elekt. Übertragung*, vol. 9, pp. 177–180; April, 1955.) Fourier-transform analysis is used to show that, contrary to Fischer's result (1221 of 1953), the directivity characteristic of a linear or plane radiator of finite dimensions is uniquely related to the amplitude distribution over the radiator. The theory is extended to the consideration of propagation media with local inhomogeneities acting as secondary radiators, and an investigation is made of the relation between distribution of inhomogeneities and the directivity characteristic of the scattered radiation.

538.566:535.31 2924
Study of the Electromagnetic Field in the Vicinity of a Reflecting Surface—M. Bouix. (*C. R. Acad. Sci., (Paris)*, vol. 240, pp. 1763–1765; May 2, 1955.) Analysis is given for the general case of a plane incident wave with elliptical polarization. If the reflecting surface is an infinite plane, the reflected wave is also plane; modifications of the reflected wave by other types of reflecting surface are mentioned.

538.566:537.311.31:539.23 2925
Simultaneous Partial Absorption, Reflection and Transmission of a Nonuniform Plane Wave by a Thin Metal Film—M. Gourceaux. (*C. R. Acad. Sci., (Paris)*, vol. 240, pp. 1871–1872; May 9, 1955.) The theory developed for uniform waves (1960 of July) is extended to nonuniform waves such as those propagated in waveguides. Appropriately modified expressions for the energy components are obtained by taking account of the guided-wave phase velocity. Conditions with a set of parallel films are discussed. A film of thickness such as to absorb 4/9 of the incident energy can be made totally absorbing by setting up standing waves at the back surface.

538.566:537.533 2926
The Interaction between an Obliquely Incident Plane Electromagnetic Wave and an Electron Beam: Part 1—H. Wilhelmsson. (*Chalmers tek. Högsk. Handl.*, No. 155, 31 pp., 1954. In English.) The investigation reported is relevant to the operation of mm-wave generators and to phenomena occurring in the solar corona. Analysis is presented for (*a*) magnetic field vector, and (*b*) electric field vector of the incident wave perpendicular to the electron beam; the general solution for an arbitrarily polarized wave is obtained as the sum of the two separate solutions. When the axial phase velocity of the wave is equal to the beam velocity, the beam behaves like a metal reflector. Coupling between different modes in the scattered wave and in the wave inside the beam is taken into account; this coupling vanishes if the wave is incident normally or if the beam is in vacuum. Resonance occurs at certain values of beam velocity.

538.566:621.372.8 2927
Direct Measurement of the Ellipticity of the R. F. Cotton Effect by the Quarter-Wave Method—R. Servant, P. Loudette and A. Charru. (*C. R. Acad. Sci., (Paris)*, vol. 240, pp. 1978–1980; May 16, 1955.) Measurements were made using a circular waveguide of diameter 7 cm with an antenna at one end connected to a 9-cm-λ klystron and a rotatable probe at the other end. Two copper pins of lengths 60 mm and 40 mm respectively are fixed 62 mm apart in an axial insulator rod making angles of 65 degrees and 35 degrees respectively with the direction of the electric field. The variation with wavelength of the plane of polarization and of the degree of extinction obtainable are shown graphically. It is shown that the wave is elliptically polarized by inserting a quarter-wave unit to produce a linear polarization.

538.569.4 2928
Electron Spin Resonance Absorption in Metals: Part 1—Experimental—G. Feher and A. F. Kip. (*Phys. Rev.*, vol. 98, pp. 337–348; April 15, 1955.) Measurements were made on Li, Na, K, Be, Mg, Al, Pd and W over the temperature range 4–296 degrees K, using a cavity-resonator technique at frequencies of 300 mc and 9 kmc. The dimensions of the specimens were in some cases large and in others small compared with skin depth. The results are compared with those predicted by Dyson's theory (2929 below).

538.569.4 2929
Electron Spin Resonance Absorption in Metals: Part 2—Theory of Electron Diffusion and the Skin Effect—F. J. Dyson. (*Phys. Rev.*, vol. 98, pp. 349–359; April 15, 1955.) Part 1: 2928 above.

538.569.4:535.33 2930
Inversion Spectrum of Ammonia—T. Nishikawa and K. Shimoda. (*Jour. Phys. Soc. (Japan)*, vol. 10, pp. 89–92; February, 1955.) As a result of an investigation over the frequency range 12–20 kmc, 29 lines have been found and 33 lines re-measured.

538.569.4:621.372.029.64 2931
Theory of Molecular [-beam] Oscillator and Molecular [-beam] Power Amlifier—N. G. Basov and A. M. Prokhorov. (*C. R. Acad. Sci. U.R.S.S.*, vol. 101, pp. 47–49; March 1, 1955. In Russian.) Theory is given of a device similar to that described by Gordon et al. (100 of January). The condition for self-excitation is stated and expressions are given for the frequency, amplitude and maximum power output of the oscillators and for the power-amplification factor and the condition for linear amplification of the amplifier.

539.181.08:537.311.33 2932
A Conductivity-Type Molecular-Beam Detector—G. Fricke and H. Friedburg. (*Z. Phys.*, vol. 141, pp. 171–174; April 21, 1955.) An iodine molecular beam can be detected by observing the change in conductivity due to introduction of impurities in a Cu_2O-film detector. The detection threshold of this device, which is briefly described, is about 5×10^9 molecules/cm^2.

GEOPHYSICAL AND EXTRATERRESTRIAL PHENOMENA

523.16 2933
Observations of a Variable Radio Source associated with the Planet Jupiter—B. F. Burke and K. L. Franklin. (*Jour. geophys. Res.*, vol. 60, pp. 213–217; June, 1955.) A variable source of radiation on 22.2 mc was observed on 9 records out of a possible 31 obtained during the first quarter of 1955. The derived position of the source corresponds to that of the planet Jupiter.

523.16:523 72 2934
Monochromatic Character of Bursts of Solar R. F. Radiation—V. V. Vitkevich. (*C. R. Acad. Sci. U.R.S.S.*, vol. 101, pp. 229–231; March 11, 1955. In Russian.) Bursts of solar-radiation in the 200-mc region were recorded simultaneously by two receivers tuned to frequency bands about 4 mc apart. Analysis of the observations indicates that the average effective bandwidth of all bursts is about 6 mc and that of high-intensity bursts (i.e., with intensities more than 50 per cent above the average) is about 12.3 mc. A note on similar

work was published by E. Blum (*Ann. Univ. Paris*, vol. 23, p. 136; 1953).

523.16:53.088.22:621.396.677.3 2935
Correcting for Gaussian Aerial Smoothing—Bracewell. (*See* 2843).

523.16:621.396.822:523.755 2936
Results of Observations of Scattering of R.F. Waves by Electron [-density] Inhomogeneities of the Solar Corona—V. V. Vitkevich. (*C. R. Acad. Sci. U.R.S.S.*, vol. 101, pp. 429–432; March 21, 1955. In Russian.) Results similar to those reported by Machin and Smith (98 of 1953) were obtained in observations of the occulations of NGC 1952 in June, 1952, 1953, and 1954. The observations were made at wavelengths between 3.5 and 6 m. In 1954, interferometer base-lengths of 700 and 500 m were used at 5.8 m λ, giving beam widths of 28.5′ and 40′ respectively. Rapid amplitude changes were noticed; those associated with changes within a few seconds are believed to be due to the relativistic motion of electron inhomogeneities, those of the order of a few minutes to corpuscular streams.

523.2:538.3 2937
Of an Interplanetary Magnetic Field—A. Beiser. (*Jour. geophys. Res.*, vol. 60, pp. 155–159; June, 1955.) Arguments are presented for the existence of an interplanetary magnetic field of intensity not exceeding 5×10^{-8} G. Such a field would explain the observed cut-off in the primary cosmic-ray momentum spectrum and time delays in solar-terrestrial phenomena.

523.5:621.396.96 2938
Radio-Echo Observations of Meteors in the Southern Hemisphere—A. A. Weiss. (*Aust. J. Phys.*, vol. 8, pp. 148–166; March, 1955.) Results are presented of observations at Adelaide using apparatus similar to that described by Aspinall et al. (3003 of 1951), operating on a frequency of 67 mc, and by Robertson et al. (1424 of 1954), operating at 26.8 mc, for measurements of shower radiants and upper-atmosphere winds respectively.

523.72:621.396.822.029.6 2939
Solar R.F. Radiation at 10 cm Wavelength—B. Vauquois. (*C.R. Acad. Sci., Paris*, vol. 240, pp. 1862–1864; May 9, 1955.) The total emission at 10.7 cm λ depends on both total area and position of sunspots. The variation with distance of the sunspots from the center of the disk is expressed by a "darkening" factor whose value has been determined (*a*) directly, by observing the passage of groups of spots, and (*b*) by assigning trial values and comparing the resulting value of total emission with observations. Results by the two methods are in agreement. Consideration of absorption variations to be expected in consequence of variations of sunspot position indicates that the darkening must be partly due to the change of geometric form of the emitting areas.

523.746 2940
The Sunspot Cycle, 649 B.C. to A.D. 2000—D. J. Schove. (*Jour. geophys. Res.*, vol. 60, pp. 127–146; June, 1955.) Analysis of available records indicates that the mean period of the fundamental sunspot cycle is 11.1 years, the length of the cycle varying in the opposite sense to auroral activity; there is also a long-term cycle with a period of 77½–78 years.

523.75:550.385 2941
Solar Prominences and Geomagnetic Disturbance—W. O. Roberts and D. E. Trotter. (*Jour. Atmos. Terr. Phys.*, vol. 6, pp. 282–283; May, 1955.) An attempt, by statistical analysis of solar data, to identify the solar *M* regions with the large prominences observed at intermediate and high solar latitudes, gave negative results.

523.78 2942
Observations of the Infrared Radiation during the Solar Eclipse of 30th June 1954 in Tashkent—I. N. Yaroslavtsev. (*Bull. Acad. Sci. U.R.S.S., sér. géophys.*, pp. 185–186; March/April, 1955. In Russian.) Results presented graphically show the changes during the eclipse of the fraction of the total incident flux contained in the infrared band (curve 3).

550.385 2943
Time Relationship of Small Magnetic Disturbances in Arctic and Antarctic—S. J. Ahmed and W. E. Scott. (*Jour. geophys. Res.*, vol. 60, pp. 147–154; June, 1955.)

550.385:523.7:523.2:538.3 2944
Solar-Terrestrial Time Delays—A. Beiser (*Jour. geophys. Res.*, vol. 60, pp. 161–164; June, 1955.) The observed delay of about 24 hours between the meridian passage of a sunspot or flare and the onset of an associated magnetic storm or aurora is shown to originate in the deflection of the ion streams involved by either a solar magnetic dipole of moment $\not> 10^{29}$ G. cm³, or an interplanetary magnetic field of intensity $\not> 4\times10^{-8}$ G, or a combination of the two. See also 2937 above.

551.510.4/.5 2945
Seasonal Variations of the Intensity of Bands due to OH and O_2 Molecules in the Atmosphere in the Luminescence of the Night Sky—P. Berthier. (*C.R. Acad. Sci., Paris*, vol. 240, pp. 1796–1798; May 2, 1955.)

551.510.4/.5 2946
Post-Twilight and Nocturnal Variations of Intensity of OH and O_2 Bands in the Near Infrared—P. Berthier. (*C.R. Acad. Sci., Paris*, vol. 240, pp. 1919–1921; May 9, 1955.)

551.510.535 2947
First Investigation of Ambient Positive-Ion Composition to 219 km by Rocket-Borne Spectrometer—C. Y. Johnson and E. B. Meadows. (*Jour. geophys. Res.*, vol. 60, pp. 193–203; June, 1955.) Measurements were made in the range 8–49 atomic mass units (amu). The most prominent ion peaks found at altitudes between 93 and 124 km on the ascent were at 16, 26, 30 and 32 amu. From 124 to 219 km ions of 16 and 32 amu persisted.

551.510.535 2948
On the Analysis of Experimental Recombinance Data using a Nonuniform Recombinance Model proposed by Chapman—Chong Chol Kim and C. Dickerman. (*Jour. geophys. Res.*, vol. 60, pp. 229–230; June, 1955.) Experimental values given by Mitra and Jones (114 of January) have been used to check the validity of Chapman's formula (708 of March) for height variation of recombinance, $\alpha=\alpha_0(1+e^{-cz})$. The best fit is obtained for $c=1.2$, with the recombinance datum level at 98 km. The relation between log $[n_{em}(\chi)/n_{em}(0)]$ and log cos χ, where $n_{em}(\chi)$ is the maximum density of electrons for solar zenith angle χ, is approximately linear over most of the range of χ, for $c=1$. Corrections to Chapman's paper are notified.

551.510.535:523.746.5:621.396.11 2949
The Influence of the Sunspot Cycle on the (M 3000) F_2 Transmission Factor—E. Theissen (*Jour. Atmos. Terr. Phys.*, vol. 6, pp 243–249; May, 1955. In French.) An analysis of results obtained over a period of eight years by a number of stations north and south of the equator shows that the influence of the sunspot cycle on the height of the F_2 layer exhibits a seasonal and a diurnal variation, with a maximum effect in the afternoon. Noon and midnight values of the (M 3000) F_2 factor cannot be taken as representative of day and night.

551.510.535:523.78:621.396.81 2950
A Note on Radio Field Strength Observations made at Ahmedabad during the Total Solar Eclipse on 30 June 1954—Rastogi and Sheriff. (See 3077.)

551.510.535:621.3.087.4 2951
Instrumentation for the Continuous Measurement of Certain Ionospheric Echo Characteristics—R. W. Parkinson. (*Rev. Sci. Instrum.*, vol. 26, pp. 319–323; April, 1955.) Details are given of the receiving system associated with the equipment described by Jones (3599 of 1953). A crossed-loop antenna picks up both the direct and the reflected waves from the transmitter, about 5 km away. The elliptically polarized echo is resolved into components which are appropriately combined and displayed in succession on a cro. Examples are shown of continuous photographic records obtained. The resolution of split echoes is facilitated by suitably varying the cro beam intensity.

551.510.535:621.3.087.4 2952
A Panoramic Ionospheric Recorder for the Study of Travelling Disturbances in the Ionosphere—L. H. Heisler. (*Aust. J. appl., Sci.*, vol. 6, pp. 1–6; March, 1955.) A description is given of a recorder covering the frequency range 1–15 mc in 7½ or 15 seconds. This is achieved by heterodyning an oscillator which is continuously variable from 31 to 46 mc with a pulsed 30-mc oscillator and amplifying the resultant pulsed signal to provide the transmitter output. The same variable oscillator is used in the superheterodyne receiver. A block diagram of the recorder is given and typical *h'f* records are shown. Both single records on 16-mm film and continuous records on 35-mm film moving at 3/8 or 3/16 inch/min can be made, using cr tubes with long- and short-persistence screens respectively.

551.510.535:621.3.087.4 2953
Modern Ionosphere Sounding Equipment of the Netherlands PTT: Part 2—P. L. M. van Berkel. (*Tijdschr. ned. Radiogenoot.*, vol. 19, pp. 305–323; November, 1954. In English.) High-power slowsweep equipment is described. The tuning mechanism comprises a set of simultaneously and continuously variable coils and capacitors, covering the range 1.3–16 mc in one band. Sweep time is 100 s. Pulse output power is about 10 kw; pulse repetition frequency is usually 50 c/s. A special camera with continuous film transport is used. See also 2989 of 1953.

551.510.535:621.396.11.029.55/.62 2954
A Note on Factors affecting the Interpretion of Observations of Transient Echoes from the Ionosphere—Shain and Kerr. (*See* 3075.)

551.510.535:621.396.812.3:519.24 2955
Notes on Correlation Methods for Evaluating Ionospheric Winds from Radio Fading Records—D. G. Yerg. (*Jour. geophys. Res.*, vol. 60, pp. 173–185; June, 1955.) A method requiring only six values of the correlation coefficient, obtained from fading records at three receiver stations, is developed. The theory is extended to include elliptical constant-correlation contours in the horizontal plane. Data obtained during February, 1954 indicate that the correlation ellipse shows a preferred orientation and that fading associated with random changes in the ionosphere is as important as that associated with drift.

551.594.221 2956
Results of Lightning Measurements during the Years 1947–1954 on Monte San Salvatore—K. Berger. (*Bull. schweiz. elektrotech. Ver.*, vol 46. pp. 405–424; April 30, 1955.) Electrical, magnetic and optical measurements made with the equipment described previously (2618 of September) are reported and discussed.

551.594.223 2957
Nature of Ball Lightning—P. L. Kapitsa.

(*C.R. Acad. Sci. U.R.S.S.*, vol. 101, pp. 245–248; March 11, 1955. In Russian.) Energy considerations indicate that ball lightning can be sustained neither by a chemical process nor by a nuclear process. It is suggested that the luminous ball could be produced in a weakly ionized gas by a resonance process, the energy required to increase the ionization and then to maintain it inside a sphere of diameter d being supplied by rf waves with $\lambda = 3.65\ d$. The center of the sphere would coincide with a maximum of the wave interference field. The rf waves could be due to an oscillatory process in the ionized atmosphere excited by a lightning discharge. The proposed mechanism also explains bead lightning, the absence of influence of wind on the position of the luminous ball, and the waveguide effect of chimneys. Explosive and quiet types of decay are associated respectively with rapid and slow changes in the rf field strength at the end of the phenomenon. Observations in the decimeter-λ region ($d \approx 10$ to 20 cm) during thunderstorms and experiments on the artificial production of ball lightning are suggested.

551.594.5:621.396.11.029.62 2958
Radio Observations of the Aurora—N. C. Gerson. (*Jour. Atmos Terr. Phys.*, vol. 6, pp. 263–267; May, 1955.) Observations during the period 1949–1951 by means of transmissions over North America mainly at 50 mc indicate that the ionization aurora occurs with greatest frequency near the equinoxes, as does the visual aurora.

LOCATION AND AIDS TO NAVIGATION

621.396.933 2959
The Accuracy of the V.H.F. Omnirange System of Aircraft Navigation: a Statistical Study—W. G. Anderson. (*Trans. IRE*, vol. ANE-2, pp. 25–37; March, 1955.)

621.396.96+621 396.933 2960
New Navigational Aids—(*Wireless World*, vol. 61, pp. 375–377; August, 1955.) Radio and radar equipment at the 1955 Paris air show included apparatus for remote presentation of radar signals by television, incorporating a signal-storage cr tube at the radar site; a device for reducing cloud clutter in airborne collision-warning radar; and a blind-landing system operating on a single frequency.

621.396.96 2961
Some C.F.T.H. Radar Equipment for the 10-cm Band—P. Bouvier. (*Rev. tech. Comp. franç., Thomson-Houston*, No. 19, pp. 11–25; April, 1955.)

621.396.96 2962
Effect of Internal Fluctuations and Scanning on Clutter Attenuation in M.T.I. [moving-target-indication] Radar—R. S. Grisetti, M. M. Santa, and G. M. Kirkpatrick. (*Trans. IRE*, vol. ANE-2, pp. 37–41; March, 1955.) Charts are presented showing (*a*) the effect of fluctuations of the scatterers and (*b*) the improvement obtainable by scanning and by using antennas with specially shaped radiation patterns.

621.396.96 2963
Cumulative Probability of Radar Detection—T. J. Rooney, L. S. Rider, and B. H. Rudwick. (*Tele-Tech*, vol. 14, Section 1, pp. 70–72, 184; April, 1955.) The probability of detecting a target on two successive scans before it reaches a given range is a function of the number of times it has been scanned and of the probabilities that it is seen on each of these scans. Tables and curves are given for evaluating this function and for determining the optimum scan rate for given target velocities.

621.396.96:519.2 2964
Signal-to-Noise Improvement and the Statistics of Track Populations—N. Wax. (*Jour. Appl. Phys.*, vol. 26, pp. 586–595; May, 1955.) Tracking processes such as those involved in radar tracking and in scanning nuclear emulsions are studied. The equilibrium track population, the age distribution of the population at equilibrium, and a signal-to-noise improvement factor are obtained for each of the models considered. The equilibrium population can be kept to reasonably small values and the signal-to-noise ratio improved if effective methods are used to eliminate deteriorating tracks.

621.396.96:621.396.6 2965
Microwave Circuits for Radar Transmitter-Receivers—L. Milosevic. (*Rev. tech. Comp. franç. Thomson-Houston*, No. 19, pp. 27–57; April, 1955. A detailed and fully illustrated account of equipment of the type installed at the Orly airport in 1953.

621.396.963.3 2966
A Note on Trace-to-Trace Correlation in Visual Displays: Elementary Pattern Recognition—P. McGregor. (*Jour. Brit. IRE*, vol. 15, pp. 329–331; June, 1955.) Subjective tests made with chemical-recorder and cr-tube intensity-modulated displays show that over a range of input signal-noise ratio from −10 to 0 db, correlation of successive traces offers an improvement of detectability with increasing number of scans better than that theoretically obtained by "integration."

MATERIALS AND SUBSIDIARY TECHNIQUES

531.788:621.316.86:537.312.6 2967
Use of Thermistors as Vacuum Gauges—Y. Lortie. (*J. Phys. Radium*, vol. 16, pp. 317–320; April, 1955.) The conditions necessary to secure maximum reliability and sensitivity over a given pressure range are discussed, with special reference to the range $1\text{–}10^{-3}$ mm Hg.

535.215+537.533.8 2968
Effect of Electron Bombardment on Secondary and Photo-electron Emission of Cesium-Antimonide—K. Miyake. (*Jour. Phys. Soc. Japan*, vol. 10, pp. 164–165; February 1955.) Fatigue effects and modifications of the spectral photoelectric response are shown graphically.

535.215:537.311.33 2969
Temperature Dependence of the Width of the Band Gap in Several Photoconductors—R. H. Bube. (*Phys. Rev.*, vol. 98, pp. 431–433; April 15, 1955.) The temperature variation of the energy gap in CdS, CdSe, CdTe and ZnSe is determined from measurement of the photosensitivity/wavelength characteristic at various temperatures between 90 degrees and 400 degrees K. The observations for CdS and CdSe suggest the existence of double conduction or valence bands.

535.215:546.32 2970
Experimental Contribution to the Theory of the External Photoelectric Effect in Compact Alkali Metals—R. Suhrmann. (*Z. Naturf.*, vol. 9a, pp. 968–973; November, 1954.) The form of the observed spectral sensitivity curve for very pure K surfaces is discussed. A maximum is exhibited at 400 mμ; this is attributed to the variation with wavelength of the absorption coefficient and to the small depth from which the photoelectrons are emitted.

535.215:546.47–31 2971
Influence of Oxygen, Water Vapour and Organic Compounds on Photoelectric Processes in Zinc Oxide—E. K. Putseiko and A. N. Terenin. (*C. R. Acad. Sci. U.R.S.S.*, vol. 101 pp. 645–648; April 1, 1955.) In Russian.) Results of measurements of the change of photo-emf with short-period and with continuous illumination are presented graphically and are discussed. No effect was observed as being due to the different methods used in preparing the ZnO specimens.

535.215:546.482.21 2972
Intermittent-Illumination Measurements on Photoconducting CdS—E. A. Niekisch. (*Ann. Phys., Lpz.*, vol. 15, pp. 279–301; March 15, 1955.) The method discussed was described previously by Fassbender and Lehman (*ibid.* vol. 6, p. 215; 1949), and makes use of the possibility of varying the electron concentration of photoconductors independently of the mobility. The value found for the mobility by this method is not the "micromobility," but a quantity dependent on the trap distribution; if the micromobility is known, the trap distribution can hence be determined. Measurements are reported of the variation of the dc and ac components with temperature and with the intensity of the intermittent illumination. Interpretation of the results does not require the assumption of a marked temperature dependence of the recombination coefficient.

535.215:546.482.21:621.396.822 2973
Measurement of Shot Noise in CdS Crystals—C. I. Shulman. (*Phys. Rev.*, vol. 98, pp. 384–386; April 15, 1955.) "The noise power spectrum associated with photoconduction current in CdS crystals with indium electrodes is found to flatten off at low frequencies at a value that corresponds closely to the noise inherent in the photon absorption process itself plus that associated with the random nature of the carrier recombination process. It is found that the noise power is not a unique function of the photoconduction current, but varies as the square of the applied voltage, and linearly with light intensity, as suggested by a simple model not unlike that of the photomultiplier."

535.37 2974
Paramagnetic Resonance Spectrum of Some Doubly Activated Phosphors—W. Low. (*Phys Rev.*, vol. 98, pp. 426–431; April 15, 1955.) Investigations of SrS phosphors with various rare-earth activators are reported.

535.37 2975
Thermoluminescence of Alkali Halide Phosphors—H. N. Bose. (*Proc. Phys. Soc.*, vol. 68, pp. 249–252; April 1, 1955.)

535.37 2976
Determination of the Depths of Electron Traps by Thermoluminescence—G. Curie and D. Curie. (*Jour. Phys. Radium*, vol. 16, pp. 199–205; March, 1955.)

535.37 2977
ZnS (Ag) Phosphor Mixtures for Neutron Scintillation Counting—P. G. Koontz, G. R. Keepin and J. E. Ashley. (*Rev. sci. Instrum.*, vol. 26, pp. 352–356; April, 1955.)

535.37:532.11 2978
Some Investigations on the Effects of Pressure of the Luminescence of Solids—(*Bull. Res. Counc. Israel*, vol. 4, pp. 219–224; December, 1954.)
Part 1 (pp. 219–221).—E. A. Braun.
Part 2 (pp. 222–224).—E. A. Braun and A. Barouch.

535.37:537.311.33 2979
Decay of Phosphorescence with Activators and Traps arising from the same Impurity in Different Valency States—K. Lehovec. (*J. opt. Soc. Amer.*, vol. 45, pp. 219–222; March, 1955.)

535.376 2980
Radiation-Controlled Electroluminescence and Light Amplification in Phosphor Films—D. A. Cusano. (*Phys. Rev.*, vol. 98, pp. 546–547; April 15, 1955.) Preliminary report of effects observed when a voltage is applied to a nongranular layer of ZnS:Mn,Cl phosphor excited by ultraviolet or X rays.

535.376 2981
Theoretical Basis for Light-Amplifying Phosphors—F. E. Williams. (*Phys. Rev.*, vol. 98, pp. 547–548; April 15, 1955.) Brief discussion of electroluminescence indicating mechanisms which may be responsible for producing light amplification.

535.376:546.472.21 2982
Decay of Luminescence of Silver-Activated Zinc Sulphide Phosphors following Excitation by Single α Particles and Electrons—D. Smidt. (*Ann. Phys., Lpz.*, vol. 15, pp. 325–336; March 15, 1955.) Measurements on phosphors in powder and in single-crystal form are reported. The decay curve is hyperbolic, as for excitation by light. An empirical formula is derived relating activator concentration and decay time constant. The diffusion of holes and conduction electrons is discussed.

537.226/.227 2983
Dielectric Properties of Lead-Strontium Titanate—S. Nomura and S. Sawada. (*J. phys. Soc. Japan*, vol. 10, pp. 108–111; February, 1955.) Experiments are reported indicating that lead-strontium titanate is ferroelectric. The Curie temperature decreases linearly with increase of the Sr^{2+} content: no other transition point was observed.

537.226/.227 2984
Dielectric Properties of Titanates containing Sn^{4+} Ions: Part 1—S. Nomura. (*J. phys. Soc. Japan*, vol. 10, pp. 112–119; February, 1955.) Dielectric and thermal properties and lattice constants of the solid solutions of $Pb(TiSn)O_3$ and $Ba(TiSn)O_3$ were investigated, for the purpose of making clear the role of the Y ion in compounds of the perovskite type, XYO_3. The variations with composition of the Curie point are reported. An anomalous hysteresis phenomenon observed in Pb(25 per cent Ti-75 per cent Sn)O_3 suggests that the Ti^{4+} and Sn^{4+} ions respond differently to the external field in the ferroelectric state.

537.226/.227:546.431.824–31 2985
Phase Equilibria in the System BaO-TiO_2—D. E. Rase and R. Roy. (*J. Amer. ceram. Soc.*, vol. 38, pp. 102–113; March, 1955.) Extensive investigations using quenching, strip-furnace and thermal techniques indicate the existence of five intermediate compounds in the system BaO—TiO_2; these are the orthotitanate Ba_2TiO_4, the metatitanate $BaTiO_3$, the dititanate $BaTi_2O_5$, the trititanate $BaTi_3O_7$ and the tetratitanate $BaTi_4O_9$. Properties of these compounds are tabulated. Application of the results to the manufacture of titanate bodies and to the growth of single crystals of $BaTiO_3$ is discussed.

537.226.2 2986
Dielectric Anomaly of Ammonium Sulfate at its Transition Temperature—K. Kamiyoshi and T. Miyamoto. (*Sci. Rep. Res. Inst. Tohoku Univ.*, Ser. A, vol. 7, pp. 91–98; February, 1955.) An anomalous variation of the dielectric constant accompanied by a phase transition in a single crystal of ammonium sulphate was observed at af and rf. A sharp peak appeared in the *a*-axial direction and kinks appeared in *b*- and *c*-axial directions; the transition temperature was −36 degrees C on cooling and −29 degrees C on heating. The dielectric constants at room temperature were 8.0, 7.45 and 6.7 along *a*-, *b*- and *c*-axial directions, respectively. They are independent of frequency between 10 and 10^5 kc. The transition temperature of a pressed polycrystalline powder specimen was about −53 degrees C

537.227 2987
New Class of Ferroelectrics—A. N. Holden, B. T. Matthias, W. J. Merz, and J. P. Remeika. (*Phys. Rev.*, vol. 98, p. 546; April 15, 1955.) Guanidine aluminium sulphate hexahydrate $(CN_3H_6)Al(SO_4)_2.6H_2O$ has been observed to be ferroelectric at temperatures from about 200 degrees C downwards.

537.227./228:537.311.33 2988
Space-Charge Layer near the Surface of a Ferro-electric—W. Känzig. (*Phys. Ref.*, vol. 98, pp. 549–550; April 15, 1955.) Theoretical considerations indicate that space-charge layers and associated strong electric fields near the surface of highly polarizable semiconductors could produce observable piezoelectric or electrostrictive strain. Experimental evidence for the existence of such layers in $BaTiO_3$ is mentioned.

537.227:546.321.85–841 2989
Spontaneous Polarisation of KH_2PO_4 and KD_2PO_4 Crystals versus Temperature—J. Pirenne. (*Physica*, vol. 21, pp. 219–222; March, 1955.)

537.227:546.431.824–31 2990
Etch Patterns and Ferroelectric Domains in $BaTiO_3$ Single Crystals—J. A. Hooton and W. J. Merz. (*Phys. Rev.*, vol. 98, pp. 409–413; April 15, 1955.) Technique for investigating ferroelectric domains in $BaTiO_3$ is based on the observed fact that the positive end of the electric dipole in the material etches much faster than the negative end.

537.228.1 2991
Piezoelectricity of Wood—E. Fukada. (*J. Phys. Soc. Japan*, vol. 10, pp. 149–154; February, 1955.) The direct and converse piezoelectric effects were studied in maple, spruce and ash. The magnitude of the piezoelectric constants $d_{14}(=-d_{25})$ is of the order of 10^{-9} esu. The apparent piezoelectricity of wood may be explained by a particular arrangement of natural cellulose micelles. The experimental arrangement is described and results are presented in tabular and graphical form.

537.311.31+537.533 2992
Dependence of Electrical Conductivity and Electron Emission on Power Consumption of Metal during Heating by [pulsed] High-Density Current—L. N. Borodovskaya and S. V. Lebedev. (*Zh. eksp. teor. Fiz.*, vol. 28, pp. 96–110; January, 1955.) In heating Ni wires by currents of densities $6\times10^4-5\times10^5 A/cm^2$ effects similar to those observed in W [3528 and 3574 of 1954 (Lebedev and Khaikin)] were found. Discontinuities were found in the resistance/energy-supplied curve; their positions remained independent of variations of the current density in Ni, W, Au, and constantan wires. The emission from Ni at current densities of about $10^5 A/cm^2$ was $1.6\times10^{-4} A/cm^2$, about 50 times that at the melting point.

537.311.33 2993
Forbidden and Permitted Bands in Impure Semi-conductors and in Disordered Alloys—J. des Cloizeaux. (*J. Phys. Radium*, vol. 16, pp. 320–324; April, 1955.) The semiconductor or disordered alloy is represented by a unidimensional crystal made up of cells of two distinct types, distributed at random. In such a distribution domains of impurity of any concentration may occur, consequently the permitted energy bands are much wider than in ordered distributions. Calculations are made for the general case and for some particular distributions. In the general case permitted bands exist outside the limits of bands permitted in either of the separate constituents.

537.311.33 2994
Propagation and Plasma Oscillation in Semiconductors with Magnetic Fields—B. Lax and L. M. Roth. (*Phys. Rev.*, vol. 98, pp. 548–549; April 15, 1955.) Magneto-ionic theory is applied to study semiconductors whose energy surfaces in the Brillouin zone are ellipsoidal or warped spheres possessing cubic symmetry.

537.311.33:[546.28+546.289 2995
Cyclotron Resonance of Electrons and Holes in Silicon and Germanium Crystals—G. Dresselhaus, A. F. Kip, and C. Kittel. (*Phys. Rev.*, vol. 98, pp. 368–384; April 15, 1955.) Measurements are made at temperatures near 4 degrees K in order to obtain relaxation times long enough to permit observation of cyclotron resonance with X- or K- band equipment. An optical method is used to generate free carriers. Anisotropy effects are observed. In both Si and Ge the electron energy surfaces near the band edge are deduced to be prolate spheroids; formulas are also given for the hole energy surfaces.

537.311.33:546.28 2996
Optical Determination of Base Width in Grown *n-p-n* Silicon Crystals—A. Fowler and P. Levesque. (*Jour. Appl. Phys.*, vol. 26, pp. 641–642; May, 1955.) A development of the etching technique described by Billing and Dowd (3332 of 1953).

537.311.33:546.289 2997
Thermal Acceptors in Germanium—R. J. Hodgkinson (*Phil. Mag.*, vol. 46, pp. 410–421; April, 1955.) Results reported earlier (*G.E.C.J.*, vol. 21, pp. 63–70; January, 1954) are examined on the assumption that the thermal acceptors are Cu atoms. A thermodynamic treatment of the solid solubility of Cu in Ge is given in terms of the Principle of Lowest Free Energy. An equation derived, relating the concentration of Cu on the liquidus and solidus to the temperature, is equivalent to one previously derived by Thurmond and Struthers (2420 of 1954) and is shown to be in good agreement with experimental results.

537.311.33:546.289 2998
Properties of Germanium Doped with Nickel—W. W. Tyler, R. Newman, and H. H. Woodbury. (*Phys. Rev.*, vol. 98, pp. 461–465; April 15, 1955.) "The temperature dependence of electrical resistivity in *p*- and *n*-type nickel-doped germanium crystals indicates that nickel introduces two acceptor levels in germanium at 0.22 ± 0.01 ev from the valence band and 0.30 ± 0.02 ev from the conduction band. Ionization energies deduced from infrared photoconductivity studies at 77 degrees K are in agreement with the values obtained from resistivity measurements. *N*-type samples show higher photosensitivity than *p*-type samples and demonstrate quenching effects. The distribution coefficient for nickel in germanium is about 2.3×10^{-6}."

537.311.33:546.289 2999
Measurement and Interpretation of Conductance of P-Type Inversion Layers on Germanium—G. A. deMars, H. Statz, and L. Davis, Jr. (*Phys. Rev.*, vol. 98, pp. 539–540; April 15, 1955.) Measurements similar to those made previously on *n*-type inversion layers [e.g. 166 of 1954 (Brown)] are reported and discussed.

537.311.33:546.289 3000
Structure of Surface States at the Germanium/Germanium-Oxide Interface—H. Statz, L. Davis, Jr., and G. A. deMars. (*Phys. Rev.*, vol. 98, pp. 540–542; April 15, 1955.) The surface states are discussed in relation to the observed variation of conductance on application of a switching voltage.

537.311.33:546.289 3001
Influence of Various Etchants on Germanium: Part 1—Chemical Action of some Agents on Ge—O. Rösner. (*Z. Metallkde*, vol. 46, pp. 225–229; March, 1955.) The action of some liquid and gaseous agents was investigated by microscope and by gravimetric methods. Ge is strongly attacked by water, especially on prolonged boiling. Oxidation occurs in air; the reaction $GeO_2+Ge=2GeO$ is

observed at 900 degrees C. Carbonic acid attacks Ge at temperatures above 700 degrees C. The possibility of recovering Ge from various etching solutions is discussed and some numerical results are presented

537.311.33:546.289 3002
Influence of Various Etchants on Germanium: Part 2—Physical Considerations—G. Zielasek. (*Z. Metallkde*, vol. 46, pp. 229–233; March, 1955.) Measurements of surface potential of etched polycrystalline specimens indicated sudden resistivity changes of some hundreds of ohm-centimeters at grain boundaries; both these and the ordinary resistivity distributions within single crystals are demonstrated by maps of the equipotential lines. Use of a template to simplify determinations of carrier lifetime is described. A mean value of about 4 μs was found for the hole lifetime in polycrystalline n-type material, and values up to 700 μs for single crystals.

537.311.33:546.289 3003
Mass-Spectrometer Investigations of Germanium—G. Köhl. (*Z. Naturf.*, vol. 9a, pp. 913–918; November, 1954.) A method is described capable of indicating the presence in Ge of elements with relative concentrations as low as 10^{-5} to 10^{-6}.

537.311.33:546.289:537.534.9 3004
Effects produced by the Ionic Bombardment of Germanium—W. D. Cussins. (*Proc. Phys. Soc.*, vol. 68, pp. 213–222; April 1, 1955.) Single-crystal and polycrystalline specimens were bombarded with positive ions of energy ranging from 5 to 90 kev; elements of atomic number ranging from 1 to 51 were used. The effect on rectification characteristics and thermoelectric properties was investigated; in all cases maximum effect was produced by bombardment equivalent to about 6 μC/cm^2. No effect was observed for ion energies less than about 20 kev. The results are consistent with the assumption that bombardment produces a p-type layer, whether the original specimen is p-type or n-type. Reference is made to a similar investigation on Si [see e.g. 1337 of 1952 (Ohl)].

537.311.33:546.289:538.63 3005
On the Hall Effect of *P*-type Germanium in the Near Intrinsic Range—Y. Kanai and K. Furusyō. (*J. phys. Soc. Japan*, vol. 10. pp. 165–166; February, 1955.) Experiments were made using high values of magnetic field H to facilitate examination of terms involving powers of H higher than the first. The variation of Hall constant with values of H up to 7 kg is shown graphically for various temperatures up to 85 degrees C. The variation is in the opposite sense to that calculated by Madelung (3579 of 1954).

537.311.33:546.48–31 3006
The Electrical Conductivity of Cadmium Oxide at Low Temperatures—J. A. Bastin and R. W. Wright. (*Proc. Phys. Soc.*, vol. 68, pp. 312–315; April 1, 1955.) Measurements of the conductivity of sintered CdO over the temperature range 1 degree–250 degrees K together with measurements reported by Wright (2200 of 1951) over the range 100 degrees–700 degrees K are compared with the theoretical expression for the conductivity of an ionic crystal derived by Howarth and Sondheimer (381 of 1954). The resistance at zero temperature is discussed in relation to impurity scattering and crystalline boundary resistances.

537.311.33:546.482.31 3007
Electrical Conductivity of Cadmium Selenide—K. Hauffe and H. G. Flint. (*Ann. Phys., Lpz.*, vol. 15, pp. 141–147; January, 1955.) The dependence of the conductivity χ on Cd- and Se-vapor partial pressures p_{Cd} and p_{Se} was investigated experimentally in the temperature range 300–500 degrees C. For $p_{Cd} > 10^{-1}$ Torr, $\chi \propto p_{Cd}^{1/4.5}$, below 10^{-1} Torr χ is practically independent of p_{Cd}. For $p_{Se} > 10^{-2}$ Torr $\chi \propto p_{Se}^{-1/2}$, below 10^{-2} Torr χ is independent of p_{Se}. Additions of Tl_2Se up to 0.1 per cent mol reduce the conductivity. The results are discussed.

537.311.33:546.561-31 3008
Some Semiconductor Properties of Cu_2O—C. Fritzsche. (*Ann. Phys., Lpz.*, vol. 15, pp. 178–181; January. 15, 1955.) Experimental results indicate that the variation of conductivity of Cu_2O caused by heat treatment is more closely related to the CuO-Cu_2O equilibrium conditions than to the impurity concentration curves for Cu_2O. See also 2432 of 1954.

537.311.33:546.681.18 3009
Semiconductor Properties of Gallium Phosphide—O. G. Folberth and F. Oswald. (*Z. Naturf.*, vol. 9a, pp. 1050–1051; December, 1954.) Optical measurements indicate that the absorption edge lies in the visible region. The width of the energy gap is 2.4 ev at absolute zero and the variation with temperature is -5.5×10^{-4} ev/degrees K over the range 100 degrees–500 degrees K

537.311.33:546.682.19 3010
Electrical Properties of InAs: Part 2—O. G. Folberth, O. Madelung, and H. Weiss. (*Z. Naturf.*, vol. 9a, pp. 954–958; November, 1954.) Continuation of work abstracted previously [3268 of 1954 (Folberth *et al.*)]. The width of the energy gap is 0.47 ± 0.02 ev at absolute zero, with a temperature variation of -4.5×10^{-4} ev/degrees K. The electron mobility passes through a maximum value of about 30,000 cm/s per v/cm at room temperature, the corresponding value for the holes being 200 cm/s per v/cm.

537.311.33:546.682.86 3011
Cyclotron and Spin Resonance in Indium Antimonide—G. Dresselhaus, A. F. Kip, C. Kittel, and G. Wagoner. (*Phys. Rev.*, vol. 98, pp. 556–557; April 15, 1955.) Observations at a frequency of 24 kmc are briefly reported.

537.311.33:546.811–17:538.22 3012
Magnetic Properties of the Exciton—A. G. Samoilovich and M. V. Kononova. (*C.R. Acad. Sci. U.R.S.S.*, vol. 101, pp. 55–57; March 1, 1955. In Russian.) A brief theoretical note with particular reference to the magnetic properties of semiconductors. A numerical check of the formula for magnetic susceptibility for the case of grey tin shows fair agreement with experimental results reported by Busch and Mooser (1476 of 1954) over a large temperature range.

537.311.33:62.314.63 3013
The Effect of Discontinuous Space Charge on Rectifier Characteristics—G. G. Wiles. (*Phil. Mag.*, vol. 46, pp. 363–375; April, 1955.) An expression is derived for the local current density in the blocking direction near an impurity center situated in the semi-conductor at an optimum distance from the metal. The effects of these local currents on the average current through the interface is evaluated for the case of a uniform distribution of impurity centers. For semi-conductors with a dielectric constant of 10 a continuous distribution of space charge can be assumed for impurity-center concentrations up to 10^{16}/cm^3, but the error becomes appreciable at 10^{18}/cm^3. The case of a random distribution is treated by a more approximate method; the results are similar to those for a uniform distribution.

537.32 3014
On the Thermoelectric Power of Metals—D. ter. Haar and A. Neaves. (*Proc. roy. Soc. A*, vol. 228, pp. 568–574; March 22, 1955.) A theoretical paper based on a method employed by Makinson (2343 of 1940). An expression is derived for the contribution of the lattice current to the thermoelectric power of metals at temperatures where electron-phonon scattering predominates. In this range the thermoelectric effect will be of opposite sign to that which follows from simple electron theory of metals. The effect discussed cannot explain the known behavior of alkali metals completely.

538.22 3015
Magnetic Anisotropy and Van Vleck's Relation for Antiferromagnetics—K. F. Niessen. (*Philips Res. Rep.*, vol. 10, pp. 131–140; April, 1955.) Account is taken of the two kinds of magnetic spin in deriving formulas for the influence of magnetic anisotropy on the susceptibility of antiferromagnetics and for the relation between the powder susceptibilities at 0 degrees K and at the Curie temperature.

538.22:548.0 3016
Theory of Ionic Ordering, Crystal Distortion, and Magnetic Exchange Due to Covalent Forces in Spinels—J. B. Goodenough and A. L. Loeb. (*Phys. Rev.*, vol. 98, pp. 391–408; April 15, 1955.) "A new magnetic exchange mechanism, "semicovalent exchange," which is consistent with the covalent model, is used to explain the magnetic properties of spinels."

538.221 3017
The ΔE-Effect and Young's Modulus in Nickel-Cobalt Alloys—M. Yamamoto and S. Taniguchi. (*Sci. Rep. Res. Inst. Tohoku Univ.*, Ser. A, vol. 7, pp. 35–49; February, 1955.) Measurements are reported covering the whole range of composition of Ni-Co alloys; a magnetostrictive-vibration method was used. See also 1077 of April (Yamamoto).

538.221 3018
The Absence of Block Walls in Certain Ferromagnetic Materials—P. M. Prache. (*Câbles & Transm.*, vol. 9, pp. 172–173; April, 1955.) Arising out of the work of Néel (3151 of 1947) it is shown that Block walls cannot exist in polycrystalline specimens of ferromagnetic materials when the crystal diameter is less than a critical value. For ordinary soft iron this value is about 20 μ.

538.221 3019
Causes of Permeability Variations of Iron-Silicon Single Crystals on cooling in a Magnetic Field—H. Fahlenbrach. (*Naturwiss.*, vol. 42, pp. 174–175; April, 1955.) The effect on a 35 per cent Si-Fe alloy of cooling in a magnetic field was investigated by observation of domain structure and by measurement of initial magnetization curves, using corner-shaped specimens and a circular magnetic field. Different results are obtained depending on the orientation of the specimen relative to the field. A detailed report is to appear in Technische Mitteilungen Krupp.

538.221 3020
Characteristic Bitter Patterns on Internally Strained Silicon-Iron Crystals—W. Stephan. (*Ann. Phys., Lpz.*, vol. 15, pp. 337–344; March 15, 1955.)

538.221:538.569.4 3021
Interaction between Spin Waves and Conduction Electrons in Ferromagnetic Metals—E. Abrahams. (*Phys. Rev.*, vol. 98, pp. 387–390; April 15, 1955.) Calculations of relaxation time indicate that the effect due to interaction between ferromagnetic spins and conduction-electron currents is much more important than that due to interaction between ferromagnetic spins and conduction-electron spins

538.221:538.569.4 3022
Ferromagnetic Resonance Absorption in $BaFe_{12}O_{19}$, a Highly Anisotropic Crystal—J. Smit and H. G. Beljers. (*Philips Res. Rep*

vol. 10, pp. 113–130; April, 1955.) Measurements at 24 kmc show that resonance conditions are strongly influenced by the anisotropy of the hexagonal crystal and also with non-saturating fields, by the domain structure. Absorption peaks predicted by theory were observed. Values are found for the anisotropy field and for the gyroscopic splitting factor, g, this latter showing the spin-only value. The anisotropy is probably caused by dipole-dipole interaction.

538.221:538.639:546.3-1-72-74-73 3023
Goldhammer Effect in Alloys of the Ternary System Iron-Nickel-Cobalt—N. V. Grum-Grzhimailo. (*Bull. Acad. Sci. U.R.S.S., tech. Sci.*, pp. 137–139; December, 1954. In Russian.) Results are tabulated and presented graphically of an investigation of the dependence of the relative change of resistance under the influence of a longitudinal magnetic field (Goldhammer effect) on the composition of the alloy. A characteristic of the diagram is the discontinuity near the composition $FeNi_3CoNi$. No special effect is exhibited at phase boundaries.

538.221:621.318.134 3024
Magnetic Rotation Phenomena in a Polycrystalline Ferrite: Part 2—D. Park. (*Phys. Rev.*, vol. 98, pp. 438–441; April 15, 1955.) Calculations made previously (2036 of July) are extended to the determination of the complete permeability tensor for a sample with a net uniform magnetization.

538.221:621.318.134 3025
Direct Observation of Domain Rotation in Ferrites—F. Brown and C. L. Gravel. (*Phys. Rev.*, vol. 98, pp. 442–448; April 15, 1955.) An experimental investigation was made using a Ni-ferrite sphere of diameter 5 mm with mutually perpendicular primary and secondary loops surrounding it. The system was adjusted for minimum rf signal with the sphere demagnetized; application of a magnetic field as low as 5 oersted perpendicular to both loops produced a measurable induction signal attributable to domain rotation as distinct from domain-wall motion. Measurements were made over the frequency range 20–800 mc. Dispersion effects are discussed.

539.23 3026
Optical Constants of Thin-Film Materials—G. D. Scott. (*J. opt. Soc. Amer.*, vol. 45, pp. 176–179; March, 1955.) A short survey covering both metal and dielectric films.

546.719 3027
Rhenium Metal—C. T. Sims. (*Mater. & Meth.*, vol. 41, pp. 109–111; March, 1955.) The physical and mechanical properties of Re are briefly discussed and compared with those of W and Mo. Possible applications include tube heater filaments and electrical contacts. The metal is more resistant than W to water vapor.

549.514.51 3028
Variation of the Elastic Constants of Quartz with Pressure up to 1000 Atm—C. Susse. (*J. Phys. Radium*, vol. 16, pp. 348–349; April, 1955.) Resonance-frequency/pressure characteristics of quartz crystals cut at various angles provide an indication of the variation of the elastic constants with pressure. See also 432 of 1953 (Pérez and Johannin).

621.315.613.1 3029
Conductivity induced in Mica by X-Rays—J. F. Fowler and F. T. Farmer. (*Nature, London*, vol. 175, p. 648; April 9, 1955.) Results of experiments indicate that the conductivity induced in mica by X rays is of the same order as that in perspex and amber.

537.226+621.315.6 3030
Dielectric Materials and Applications. [Book Review]—A. R. von Hippel (Ed.). Publishers: John Wiley and Sons, New York, and Chapman and Hall, London, 1955, 438 pp., 140 s. (*Electronic Engng*, vol. 27, p. 324; July, 1955.) Includes the MIT Tables of Dielectric Materials and gives the electrical constants of some 600 materials over a wide range of frequencies and temperatures.

MATHEMATICS

517 3031
On Spheroidal Functions—T. Aoi. (*J. phys. Soc. Japan*, vol. 10, pp. 130–141; February, 1955.) Functions are discussed which satisfy differential equations of the form

$$d/dz\{(1-z^2)(dZ/dz)\}+(\lambda+\kappa^2\gamma^2)Z=0.$$

The analysis is relevant to the problem of scattering of em waves by spheroidal obstacles.

517.621.372.2 3032
Thq Electromagnetic Delay Line. Source of Relations between Bessel Functions and Elliptic Integrals—Prache. (*See* 2831.)

517.54:537.213:621.372 3033
Nets composed of Parts of Circles for the Approximate Solution of Field Problems—L. Tasny-Tschiassny. (*Aust. J. Phys.*, vol. 8, pp. 8–29; March, 1955.) The differential equation describing the current flow in a plane sheet can be solved approximately by a procedure in which the two-dimensional continuum is replaced by a net of straight-line-bounded meshes, leading to an electrical network of conductances. Using the methods of conformal transformation, meshes bounded by curvilinear rectangles can be similarly dealt with. A method is also developed for reducing the number of meshes without impairing the accuracy of the solutions. Two examples using nets of four meshes illustrate the method; the maximum errors are of the order of a few per cent.

MEASUREMENTS AND TEST GEAR

529.786+621.3.018.4(083.74)]:621.373.421.13 3034
[British] Post Office Quartz Oscillators for Use in Time and Frequency Standardisation Abroad—J. S. McClements. (*P.O. elect. Engrs' J.*, vol. 48, pp. 26–28; April, 1955.) The uses and principles of calibration of oscillator clocks at an observatory are discussed, and a description is given of installations carried out in the United States and Canada.

621.317.3 3035
Power Frequency Measurements—H. D. Hawkes. (*Elect. J.*, vol. 154, pp. 1366–1367; April 29, 1955.) The equipment of a standards room is briefly described. A range of measurement of 40–2,500 c/s, 5–750 V and 10 ma – 5A is covered with an accuracy within 0.1 per cent by a single electronic generator, an ac-dc comparator, two transfer instruments and a frequency standard.

621.317.3:621.315.2 3036
Location of Faults in Cables—F. Nüsseler. (*Tech. Mitt. schweiz. Telegr.-TelephVerw.*, vol. 33, pp. 166–168; April 1, 1955. In German and French.) The influence of the shunt conductance of the undamaged conductor on the accuracy of fault location by the Wheatstone-bridge method is discussed.

621.317.3:[621.315.212+621.372.8 3037
Measurement of Weak Reflections in Coaxial-Line and Waveguide Systems—G. W. Epprecht and C. Stäger. (*Tech. Mitt. schweiz. Telegr-TelephVerw.*, vol. 33, pp. 143–155; April 1, 1955. In German.) Various measurement methods are described using commercially available instruments giving readings accurate to within ±0.3 per cent. Arrangements having greater accuracy are discussed. Measurements are reported on 15 different types of coaxial connectors, some of them specially designed to have low reflection coefficient and dispersion. Reflection coefficients down to 2 or 3 per cent are attainable at frequencies up to 4 kmc.

621.317.3:621.318.4 3038
Theory of Helmholtz Coils—P. Goudal. (*Rev. gén. Élect.*, vol. 64, pp. 199–202; April, 1955.) The field of the coils is calculated from the magnetic potential on the axis, which in turn is calculated using a series development of Legendre polynomials.

621.317.3:621.396.62 3039
Measurements on Radio Receivers—P. Dehmelt, E. Frommer, and W. Kronjäger. (*Arch. tech. Messen*, pp. 51–54, 77–80, 97–100; March/May, 1955.) The measurements described apply to both am and fm receivers and cover sensitivity, selectivity, frequency stability, tuning accuracy, quality of reproduction, and unwanted radiation C.C.I.R. definitions and methods are given.

621.317.3.029.64 3040
Measurements on Dielectric and Ferromagnetic Materials at Frequencies around 10 kMc/s—G. Klätte. (*Fernmeldetech. Z.*, vol. 8, pp. 256–261; May, 1955.) Complex permittivities and permeabilities are measured by means of a standing-wave indicator, the specimen being inserted into a rectangular waveguide. Results are presented in tables and graphs.

621.317.328:621.372.413 3041
Resonant-Cavity Field Measurements—S. W. Kitchen and A. D. Schelberg. (*J. appl. Phys.*, vol. 26, pp. 618–621; May, 1955.) Use of a perturbation technique [see e.g. 2265 of 1952 (Maier and Slater)] for measurements of both electric and magnetic field components is described.

621.317.332.029.55/.62 3042
Measurement of Resistance with the Measuring Junction—A. Egger. (*Fernmeldetech. Z.*, vol. 8, pp. 277–281; May, 1955.) For measurements in the frequency range 20–300 mc a device is used comprising three mutually perpendicular coaxial-line sections, one terminated by the unknown resistance, another terminated by a standard resistance, and the third leading to the supply. A rotatable coupling loop is arranged to respond to the magnetic field due to the currents in the resistance-terminated arms. Operation can be made largely automatic; an impedance plotter can be developed without much additional equipment.

621.317.34 3043
Survey of Methods in Use for Measurements on High-Frequency Cables—E. Widl. (*Fernmeldetech. Z.*, vol. 8, pp. 262–265; May. 1955.) Tables give methods of measuring characteristic impedance, internal nonuniformities, propagation coefficient, and cross-talk and transfer impedance; basic circuit diagrams are included.

621.317.361:621.374.4 3044
Frequency Multipliers and Converters for Measurement and Control—J. M. Shaull. (*Tele-Tech & Electronic Ind.*, vol. 14, Section 1, pp. 86–89, 160; April, 1955.) Circuits, mainly using double-triode tubes, are described which enable frequencies in the range 100 kc–100 mc to be compared with an error not greater than one part in 10^{10}. The design ensures freedom from mains hum and eliminates sidebands and phase instability. A tuned cavity unit extends the working range to 1 kmc. See also 2069 of July.

621.317.42:538.569.4 3045
Magnetic-Field Meter based on Magnetic Resonance of Protons—N. I. Leont'ev. (*Zh. eksp. teor. Fiz.*, vol. 28, pp. 77–84; January, 1955.) The instrument described makes use of the resonance absorption due to nuclear magnetic moments of protons of accurately known gyromagnetic ratio. The probe, which contains a 10 per cent solution of ferric chloride, is described in detail and the circuit is explained

with reference to diagrams. Field strengths between 1,000 and 7,000 oersted are covered in three oscillator-frequency ranges between 4.25 and 30 mc. A measurement precision to within 0.006 per cent has been obtained.

621.317.7 3046
Notes on the Protection of Electrical Measurement Apparatus against Explosions—A. Ohlhans. (*Arch. tech. Messen*, No. 231, pp. 25–27; April, 1955.)

621.317.7:621.314.63 3047
Some Applications of the Nonlinear Characteristic of Germanium Crystal Diodes—Koch. (*See* 3108.)

621.317.7.029.64 3048
Ring-Shaped Waveguide Measurement Line with Automatic Visual Indication—H. Ritzl and H. Groll. (*Fernmeldetech. Z.*, vol. 8, pp. 281–286; May, 1955.) Technique developed for measurements at decimeter wavelengths [see e.g. 3198 of 1949 (Meinke)] is adapted to the centimeter band. Commercially produced apparatus is described.

621.317.725.024 3049
An Electronic D.C. Millivoltmeter—A. L. Biermasz and A. J. Michels. (*Phillips tech. Rev.*, vol. 16, pp. 117–122; October, 1954.) An instrument for measuring voltages between 1 mv and 300 v includes a vibrator for converting the direct voltage to be measured into a square-wave voltage which is amplified by an ac amplifier. The vibrator is driven by an electrodynamic system in which the coil is associated with a tube oscillator. Both the oscillator and the amplifier are operated from batteries, so that voltages can be measured between points at high potential.

621.317.729:537.291 3050
The Determination of Electron Trajectories in the Presence of Space Charge—D. L. Hollway. (*Aust. J. Phys.*, vol. 8, pp. 74–89; March, 1955.) Methods are developed for simulating clouds of distributed charge by discrete current sources in an electrolyte tank. The field patterns of charge regions of simple geometrical shapes are compared with those of sources and rules are deduced giving the dimensions and arrangement of a source array in any particular case. The method is applied to a plane diode, an axially symmetric electron beam and a general asymmetric beam, and the experimental results are compared with analytical solutions.

621.317.733:621.314.7 3051
A Bridge for Measuring Audio-Frequency Transistor Parameters—B. F. C. Cooper. (Proc. IRE, vol. 43, pp. 796–805; July, 1955.) The bridge is designed to measure the usual impedance parameters for point-contact transistors; for junction transistors the parameters measured represent a compromise between the impedance parameters and the *h* parameters derived when input current and output voltage are treated as the independent variables. The frequency of operation is 1 kc. The grounded-base connection is used for point-contact transistors and the grounded-base or grounded-emitter connection for the junction types.

621.317.75 3052
Inexpensive Wave Analyser—M. G. Scroggie. (*Wireless World*, vol. 61, pp. 360–365; August, 1955.) Analysis of the distortion products of an equipment is performed by means of a synchrodyne circuit enabling a simple low-pass filter to be used in place of the usual band-pass if system.

621.317.755.084:621.385.012.3 3053
The Characteristic-Curve Tracer, a Universal Valve Tester—C. Berthold and H. Berthold. (*NachrTech*, vol. 5, pp. 116–120, 177–179; March/April, 1955.) A cro valve tester of East German manufacture is described, intended for testing low-power tubes such as receiver types. Provision is also made for testing crystal diodes, rectifiers, gas triodes and glow lamps. The cro screen area used is 5×6 cm. Some characteristic-curve traces obtained are shown and briefly discussed.

621.397.6.001.4:535.623 3054
Color-Video Envelope-Delay Measurement—Kennedy and French. (*See* 3097.)

621.397.62.001.4 3055
Methods for Measurement of Selectivity and Delay Characteristics of Television Receivers—Griese. (*See* 3102.)

OTHER APPLICATIONS OF RADIO AND ELECTRONICS

531.717.1:621.317.39:534.232–8 3056
Thickness Measurement by Ultrasonic Resonance—E. G. Cook and H. E. VanValkenburg. (*J. acoust. Soc. Amer.*, vol. 27, pp. 564–569; May, 1955.) A mathematical analysis is presented which is applicable generally for any combinations of test specimen, coupling material and driving crystal.

621.317.39:621.376.3 3057
A Linear Capacitance-Change Circuit—Attree. (*See* 2893.)

621.365.54 3058
Power Considerations in Induction Heating—D. W. Brown. (*Electronic Engng.*, vol. 27, pp. 300–303; July, 1955.)

621.384.6 3059
Strong Focusing in [particle] Accelerators—W. Dällenbach. (*Z. Naturf.*, vol. 9a, pp. 1005–1012; December, 1954.) Stability, periodicity and maximum elongation of betatron oscillations with strong focusing are discussed. Unstable oscillations are considered; these may become significant as semistable oscillations in linear and spiral accelerators. A method of treating path deviations in synchrotrons is described. An expression more general than that of Courant *et al.* (1454 of 1953) is derived for the path expansion determining the synchrotron oscillations.

621.384.612 3060
Inelastic Diffusion of Accelerated Particles in a Synchrotron—J. Seiden and F. Lurçat. (*C. R. Acad. Sci., Paris*, vol. 240, pp. 2067–2069; May 23, 1955.) Inelastic collisons give rise to (*a*) changes in particle trajectories and (*b*) loss of energy by the particles. The mechanism of (*b*), which results in synchrotron-type oscillations, is analyzed. The theory is illustrated by investigating conditions for the Brookhaven cosmotron [821 of 1954 (Blewett)]; losses of protons due to inelastic diffusion are shown to be small.

621.384.622:681.142 3061
A Computer for solving some Problems in connection with Travelling-Wave Particle Accelerators—M. C. Crowley-Milling. (*Metrop. Vick. Gaz.*, vol. 26, pp. 127–131; April, 1955.) A mechanical system is described comprising a motor generator which, in conjunction with an amplifier and feedback system, is arranged to have an angular velocity proportional to the translational velocity of the particles.

621.385.833 3062
Reflection Electron Microscopy: Grazing Illumination, High-Angle Observation—C. Fert, B. Marty, and R. Saporte. (*C. R. Acad. Sci., Paris*, vol. 240, pp. 1975–1978; May 16, 1955.) An arrangement for observation at an angle of about 25 degrees is discussed.

621.387.424 3063
Some Characteristics of Chlorine-Quenched Geiger-Müeller Counters—A. L. Ward and A. D. Krumbein. (*Rev. Sci. Instrum.*, vol. 26, pp. 341–351; April, 1955.) Report of a comprehensive study.

621.387.424 3064
Mechanism of the Termination of the Geiger Plateau Region—H. L. Wiser and A. D. Krumbein. (*Phys. Rev.*, vol. 98, pp. 303–310; April 15, 1955.)

621.387.424 3065
Measurement of Recovery Time of Geiger-Müller Counters at the Geiger Threshold—D. Blanc. (*Nuovo Cim.*, vol. 1, pp. 504–506; March 1, 1955. In French.)

621.389:539.155.082.7 3066
Electrical Mass-Filter—W. Paul and M. Raether. (*Z. Phys.*, vol. 140, pp. 262–273; March 21, 1955.) The motion of ions in this spectrometer is in the direction of the axis in a hf electric field applied between two pairs of parallel rods symmetrically placed about the axis. A dc potential is also applied to the rods. Alternating voltages with amplitudes of the order of 1,000 v are used; a frequency range between 1.5 and 12 mc covers ion masses between 250 and 4 at optimum resolution.

621.389:539.155.082.7 3067
Transit-Time Mass Spectrometers—R. Hofmann and W. Walcher. (*Z. Phys.*, vol. 141, pp. 237–245; April 21, 1955.) A system is described in which phase focusing is reduced, with consequent reduction of bunching; this leads to a diminution of field disturbances due to space charges, and hence to improved isotope resolution.

786/789:621.37/.38 3068
Electronic Music Synthesizer—H. F. Olson and H. Belar. (*J. acoust. Soc. Amer.*, vol. 27, pp. 595–612; May, 1955.) Description of an instrument for synthesizing all types of musical sounds from a coded paper record. Use of the arrangement for producing disk records is illustrated.

PROPAGATION OF WAVES

621.396.11:551.510.535 3069
Ionospheric Self-Interaction of Radio Waves—F. H. Hibberd. (*J. atmos. terr. Phys.*, vol. 6, pp. 268–279; May, 1955.) Theory suggests that powerful modulated continuous waves reflected by the E layer should exhibit a measurable degree of self demodulation. The effect is directly proportional to the power radiated and increases with decreasing frequency in the mf and lf bands. It should be possible to deduce the electron collision frequency in the layer. Effects near the gyrofrequency are not considered.

621.396.11:551.510.535 3070
Ionospheric Self-Interaction of Radio Waves at Vertical Incidence—G. J. Aitchison and G. L. Goodwin. (*Nuovo Cim.*, vol. 1, pp. 722–725; April 1, 1955. In English.) Night-time transmissions were made from the University of Adelaide using a carrier frequency of 1.55 mc, which is close to the local gyrofrequency, modulated with af in the range 160 c/s–4 kc. The ground wave and the reflected sky wave were received at a station 5.6 km to the south. Percentage modulation was determined from measurements of received rf and af levels. Errors due to selective fading were eliminated. Similar tests were made on transmissions from broadcasting station 5CL Adelaide, 730 kc. The results show that for the 1.55-mc carrier the modulation depths of both E-reflected and F-reflected waves were significantly less than that of the ground wave, whereas there was no reduction of modulation depth for the 730-kc carrier, this frequency being remote from the gyrofrequency. A tentative explanation is advanced in terms of differential absorption of the wave components.

621.396.11:551.150.535 3071
Experiments on the Interaction of Radio Waves in the Ionosphere—M. Cutolo. (*Nuovo Cim.*, vol. 1, pp. 726–732; April 1, 1955.) De-

tailed reply to the points raised by Boella (245 of January).

621.396.11:551.510.535 3072
Measurement of the Nondeviative Absorption of Radio Waves in the Ionosphere—P. Lejay, G. Pillet, and R. Chezlemas. (*C. R. Acad. Sci., Paris.* vol. 240, pp. 1745–1748; May 2, 1955.) Hourly records of the amplitude of 1×F and 2×F echoes of 3.4-mc signals obtained at Domont are discussed; these exhibit both large fluctuations and slow variations at intervals of a few minutes. Statistical analysis based on a straightforward absorption formula indicates that these latter are due to variations of absorption as distinct from ionospheric focusing effects. Deduced hourly median values of absorption for December, 1954 and January, 1955 are shown; if a variation with zenith angle according to a $\cos^n$ law is assumed, the most likely value of n is about 0.3.

621.396.11:551.510.535 3073
Measurements of Limiting Polarization of Radio Waves reflected from the F Layer—B. Landmark. (*J. atmos. terr. Phys.*, vol. 6, pp. 284–286; May, 1955.) Measurements made at Kjeller, in Southern Norway, during May, 1954, on F-layer echoes at near-critical frequency, do not confirm a previous suggestion that such echoes are linearly polarized.

621.396.11.029.53/.55:551.510.535 3074
Experimental Results of Oblique-Incidence Pulse Transmissions via the Ionosphere—F. Delobeau, R. Eyfrig, and K. Rawer. (*Ann. Télécommun.*, vol. 10, pp. 55–64; March, 1955. Transmissions between fixed stations in Europe, North America, and West Africa were observed using a technique which determined the propagation time. Between Freiburg and Dakar (4730 km), winter reception on both 11.4 mc and 18.6 mc was by multiple-hop F-layer propagation; mixed E-and F-layer propagation was important on 11.4 mc; in summer, mixed-layer propagation at this frequency was observed only in the evening. Between Florida and Dakar (7,000 km) propagation at 1.95 mc occurs only at night, in winter by multiple-hop E reflections; in spring and summer F reflections are occasionally received. Absorption in the D region prevents day-time propagation. Results are similar for transmission between the Faroes and Freiburg (1,500–1,700 km) on 1.95 mc, but here E_s reflection is important. Observations of F_2-layer propagation over a 1,216-km ground path suggest that the "M 3,000" factor of the C.R.P.L. forecasts is really an "M 2,700" factor and that predicted values for muf are too low.

621.396.11.029.55/.62:551.510.535 3075
A Note on Factors affecting the Interpretation of Observations of Transient Echoes from the Ionosphere—C. A. Shain and F. J. Kerr. (*J. atmos. terr. Phys.*, vol. 6, pp. 280–281; May, 1955.) In the frequency range 10–100 mc the echo rate determined by a receiver is inversely proportional to the square root of the cosmic-noise intensity. A correction is therefore necessary in observations of echoes from meteor-trail ionization to allow for the diurnal variation of cosmic noise. The effect may be used to determine the height at which increased absorption occurs in sudden ionospheric disturbances.

621.396.11.029.63/.64 3076
Reflection Coefficients of Irregular Terrain at 10 cm—E. M. Sherwood and E. L. Ginzton. (Proc. IRE, vol. 43, pp. 877–878; July, 1955.) Report of observations made in 1943, of reflections from homogeneous samples of various types of surface, including salt and fresh water, dry sand and soil, moist sand, dry soil with vegetation, and ice.

621.396.81:551.510.535:523.78 3077
A Note on Radio Field Strength Observations made at Ahmedabad during the Total Solar Eclipse on 30 June 1954—R. G. Rastogi and R. M. Sheriff. (*J. sci. industr., Res.*, vol. 14A, pp. 159–161; April, 1955.) Measurements on 15.07-mc transmissions from London are discussed. Field strength is shown plotted against time of day for the eclipse day and for preceding and following control days. The most probable mode of propagation was the two-hop mode via the F_2 layer. An observed increase of signal strength during the eclipse period is probably due to decreased absorption in the lower layers of the ionosphere, mainly the F_1 layer.

621.396.812.3 3078
Probability of Fluctuations in Links between Points within the Visible Range—T. Baldi. (*Ricerca sci.*, vol. 25, pp. 808–827; April, 1955.) Analysis is presented for conditions in which a strong ground-reflected ray is to be expected. An expression is derived for the probability of the attenuation of the reflected ray exceeding a given amount relative to the direct ray, assuming random variation of the refractive-index gradient g. A formula established for the probability density of g is used to plot curves for comparison with experimental results.

RECEPTION

621.396.62:621.317.3 3079
Measurements on Radio Receivers—Dehmelt, Frommer and Kronjäger. (*See* 3039.)

621.396.621.54 3080
A High Performance Battery Receiver—(*Mullard tech. Commun.*, vol. 2, pp. 17–27; April, 1955.) Details are given of a 7-tube superheterodyne receiver covering the frequency range 545 kc–24 mc in four bands; it has one rf stage and a push-pull output stage delivering 425 mw for a voltage of 90 v and 1.2 w for 135 v.

621.396.621.54:621.314.7 3081
Multi-stage Transistor Superheterodyne—C. L. Wright. (*Short Wave Mag.*, vol. 13, pp. 69–75; April, 1955.) An all-transistor receiver designed to cover the 160-m and 80-m amateur bands is described in detail. Both point-contact and junction type transistors are used. The circuit comprises rf stage, Clapp local oscillator, mixer, two if stages operating at 465 kc, detector voltage-doubler comprising two diodes, Clapp beat-frequency oscillator, grounded-collector af matching stage, phase inverter and Class-B push-pull output stage. Complete circuit diagrams and tables of recommended components are given. Experiments are also very briefly mentioned on the application of magnetic bias for extending the frequency range of transistors to 30 mc and on the development of a special mixer transistor with two emitters.

621.396.621.54.029.62:621.376.3 3082
Band-II F.M. Tuner Unit—L. Hampson. (*Wireless World*, vol. 61, pp. 368–374; August, 1955.) Details are given of a design having one rf stage, oscillator-mixer, two if stages and ratio detector, suitable for use with a wide range of af amplifiers, including that described in 2245 of August (Ferguson).

621.396.828:621.316.8 3083
Resistors for Radio-Interference Suppression in Otto-Cycle [internal-combustion] Engines—H. Henniger. (*NachrTech.*, vol. 5, pp. 166–170; April, 1955.) The characteristics of various types of resistor are discussed. At present the inorganic solid-body resistor is the only type satisfying the requirements in respect of frequency, dielectric strength, temperature characteristics and absence of oxidation at high temperatures. A 5-10-kΩ, ½-w resistor, of dimensions 3.5×16 mm, is suitable in most applications; it may be incorporated in the spark plug. The discussion also mentions the applications of LCR suppressors and of damped $\lambda/2$ or $\lambda/4$ lines.

STATIONS AND COMMUNICATION SYSTEMS

621.376.5:621.39.001.1 3084
A Comparison between Delta and Pulse Code Modulation—L. H.Zetterberg. (*Ericsson Tech.*, vol. 11, pp. 95–154; 1955.) Analysis is made on the basis of information theory, and with reference to the quality of speech transmission. The delta and pcm systems have about equal information-transmitting capacity for an equal and reasonably large number of distinguishable signal levels. The amplitude distribution of the ideal signal for the delta system implies a signal power about 60 per cent less than for the corresponding pcm signal. The delta-modulation signal exhibits a spectral distribution in which the density decreases with increasing frequency. The two principal types of fault are overloading and granulation. For optimum signal/noise ratio, the delta system needs a much larger bandwidth than pcm for moderate or high quality.

621.376.55:621.396.822.1:621.3.018.78 3085
Low-Frequency Crosstalk in Pulse-Phase Modulation—J. G. Little. (*Wireless Engr.*, vol. 32, pp. 220–223; August, 1955.) Conditions are considered for the passage of pulses through a single distorting network such as a coupling or decoupling circuit. The method of analysis is discussed in which the effect of low-frequency distortion on each component of the spectrum of a modulated pulse train is examined. A preferred method is to consider the waveform of a single pulse and to sum the effects of a series of disturbing pulses on a given disturbed pulse. The results give an indication of the order of low-frequency response necessary for the attainment of a given quality of transmission.

621.395.43:621.376.56 3086
Pulse-Code-Modulation Multiplex Telephone Transmission System—P. Herreng, R. Blondé, and G. Dureau. (*Câbles & Transm.*, vol. 9, pp. 144–160; April, 1955.) Equipment designed by the Société Alsacienne de Constructions Mécaniques uses binary coding effected by a cr tube of special construction; preliminary 32-level quantization of the signal is effected by a method eliminating feedback with consequent advantages in coding speed. The signal transmitted is a five-pulse combination. Decoding is performed by comparing the stored received signal with a complete pulse sequence identical with that generated at the transmitter, using a specially constructed coincidence detector.

621.395.44:621.315.052.63 3087
Guide to Application and Treatment of Channels for Power-Line Carrier—(*Trans. A.I.E.E.*, Part III-A, *Power Apparatus and Systems*, vol. 73, pp. 417–435; June, 1954. Discussion, pp. 435–436.) A committee report presenting data and discussion relevant to the development of adequate and reliable carrier-current channels.

621.396.41:621.396.65 3088
Protection of Service in the TD-2 Radio Relay System by Automatic Channel Switching—I. Welber, H. W. Evans and G. A. Pullis. (*Bell Syst. Tech. Jour.*, vol. 34, pp. 473–510; May, 1955.) One of the six two-way channels is reserved for use as a substitute in case of interruption or severe degradation of transmission in the other channels. The operation and circuits of the protection system are described in detail.

621.396.41:621.396.82 3089
Interchannel Interference in FM and PM Systems under Noise Loading Conditions—W. R. Bennett, H. E. Curtis and S. O. Rice. (*Bell Syst. Tech. Jour.*, vol. 34, pp. 601–636; May, 1955.) Frequency-division systems with

a large number of channels are considered and analysis is given using a band of random noise to represent the multiplex signal. Interchannel interference due to variation of attenuation and phase shift with frequency is estimated from the effect produced by echoes of relatively small amplitude. Curves are presented for computing the interference power.

621.396.66 3090
Operational Measurements on U.S.W. [f.m.] Broadcast Transmitters: Part 3—L Merkl. (*Arch. tech. Messen*, pp. 31–32; February, 1955.) Noise measurements are discussed. Parts 1 and 2: 1789 of June.

621.396.66 3091
Comparative Measurements with Volume-Meter and Peak-Value Meter for Monitoring Broadcast Transmissions—E. A. Pavel, A. Gastell and M. Bidlingmaier. (*Fernmeldetech. Z.*, vol. 8, pp. 205–212; April, 1955.) The comparison shows that for monitoring modulation depth the peak-value meter is more satisfactory. For high accuracy the integration time of the meter should be $\geqslant 10$ ms.

SUBSIDIARY APPARATUS

621.311.6:621.314.63:546.28:535.215 3092
Silicon Solar-Energy Converters—M. B. Prince. (*J. appl. Phys.*, vol. 26, pp. 534–540; May, 1955.) Theory of operation of the Si junction photodiode is given and compared with experimental data Si is shown to be the most efficient semiconductor available for conversion of solar energy. A design is discussed in which the radiation is incident on the *n* layer; the thickness of the *p*-layer is required to be low to give low resistance, but not so low that minority carriers recombine before diffusing to the junction. Resistance at the metal contacts must be kept as low as possible. Conversion efficiencies of 6 per cent have been attained. Possibilities are indicated of improving the efficiency by use of nonreflecting coatings or auxiliary mirrors and lenses.

621.311.62:621.316.722.1 3093
Regulated D.C. Power Supplies at Low Voltages—R. K. Hayward, J. C. Jennings, and R. C. Barker. (*Electronic Engng.*, vol. 27, pp. 304–307; July, 1955.) A tube-stabilized unit with dc output 250 ma at 50 v or 150 ma at 100 v is described, as well as a unit using Ge-junction rectifiers. The limitations of cold-cathode-tube stabilizers are discussed.

TELEVISION AND PHOTOTELEGRAPHY

621.397.26 3094
The London-Isle-of-Wight Television Link, Stage One—T. Kilvington. (*P.O. elect. Engrs' J.*, vol. 48, Part 1, pp. 36–38; April, 1955.) "The initial television service to the Isle of Wight has been provided by direct pick-up of signals from the London transmission on receivers sited near Alton, Hants, and thence by transmission over a 40-mile microwave link to Rowridge, I.o.W., where it is radiated from a B.B.C. transmitter."

621.397.5:535.623 3095
Transmitting Colour Information—(*Wireless World*, vol. 61, pp. 393–396; August, 1595.) The effects on transmitting and receiving techniques of modifications to the American N.T.S.C. system incorporated in the experimental "British N.T.S.C." system are explained. The system envisaged by the B.B.C. has the advantage that the same transmissions will cater both for simple receivers recovering narrow-band signals and for more elaborate receivers recovering wide-band signals and giving high-definition color reproduction. See also *ibid.*, p. 355, for details of the standards used by the B.B.C.

621.397.6 3096
New Design in Closed-Circuit Television—A. V. J. Martin. (*Tele-Tech. & Electronic Ind.*, vol. 14, Section 1, pp. 94–96, 133; April, 1955.) English version of article noted in 1499 of May.

621.397.6.001.4:535.623 3097
Color-Video Envelope-Delay Measurement—R. C. Kennedy and H. French. (*Electronics*, vol. 28, pp. 144–148; June, 1955.) Description of a test set, comprising transmitter and calibrated distant receiver, and technique for dedetermining the phase-shift of the N.T.S.C. color-picture signal.

621.397.611.2 3098
Development and Operation of the Rieseliko [supericonoscope with stabilizing electron spray]—F. Michels. (*Fernmeldetech. Z.*, vol. 8, pp. 269–272; May, 1955.) A tube operating on the principles described e.g. by Cope et al. (2632 of 1952) is discussed. Spurious picture signals are eliminated by generating a space charge of required density and by providing border electrodes. A method is also described for suppressing hum interference produced when the photocathode supplying the electron spray is illuminated by pulsating sources.

621.397.62:535.623 3099
Designing TV Tuners for Color Receivers—F. Schor. (*Tele-Tech & Electronic Ind.*, vol. 14, Section 1, pp. 80–81; 154; April, 1955.) The effects of unevenness of response curve, mismatching and oscillator frequency drift are discussed. If oscillator drift is <60 kc a tuner correctly designed for monochrome reception will give good results for color television, but tuning is more critical.

621.397.62:535.623:535.88 3100
Large-Screen Color-Television Projection—L. L. Evans and R. V. Little, Jr. (*J. Soc. Mot. Pict. Televis. Engrs*, vol. 64, pp 169–173; April, 1955. Discussion, p. 173.) Description of apparatus producing a picture 15 feet $\times$ 20 feet and operating on F.C.C. standards.

621.397.62:535.88 3101
A Design for Scanning and E. H. T. Generators to Operate a Television Projection System from 170-V H. T. Supply—E. F. Wale. (*J. Brit. IRE*, vol. 15, pp. 315–326; June, 1955.) The design of a receiver without a mains transformer is discussed. The most practical method is to combine high-voltage pulses from the line output circuit and from a separate hv generator. Details are given of a timebase unit with two hv rectifiers providing an output of 25 kv over a current range 0–250 μa. A comparison of components used shows that a considerable reduction in the cost of production as against that of a conventional circuit should be realized.

621.397.62.001.4 3102
Methods for Measurement of Selectivity and Delay Characteristics of Television Receivers—H. J. Griese. (*Arch. elekt. Übertragung*, vol. 9, pp. 167–170; April, 1955.) Methods are described for determining group delay and phase characteristics without modifying the receiver under test.

621.397.621.2:535.623:621.385.832 3103
Development of the RCA 21-Inch Metal-Envelope Color Kinescope—H. R. Seelen, H. C. Moodey, D. D. VanOrmer, and A. M. Morrell. (*Elect. Engng, N. Y.*, vol. 74, pp. 330–335; April, 1955.) See 2771 of September.

621.397.8 3104
Television Picture Definition—W. Dillenburger. (*Fernmeldetech. Z.*, vol. 8, pp. 213–221; April, 1955.) A circuit is described for correcting the frequency characteristic of the pick-up tube so as to maintain the picture definition at 100 per cent for video frequencies up to 5 mc, as required for the C.C.I.R. 625-line system. Tests with a supericonoscope and with a superorthicon are reported; the improvement due to the equalizer was noticeable on test transmissions but not on programme transmissions. The effect on signal/noise ratio of using the equalizer was also investigated.

621.397.8:535.623 3105
Flicker in Frame Sequences in Television—P. Billard. (*Rev. d'Optique*, vol. 34, pp. 129–149; March, 1955.) Experiments were made to determine the characteristics of a color-television system combining the greatest possible bandwidth economy with absence of perceptible flicker; the persistence of red, green, and blue phosphors was simulated by an appropriate lamp-and-filter system in conjunction with graded-density film. The critical repetition frequency depends little on the type of scanning sequence used; for the relatively-short-persistence blue it is much lower than for the relatively-long-persistence red and green; for the latter, visible flicker is suppressed at 43 frames /sec at a luminance level of 30 nt. Red and green signals should receive equal treatment, whether with simultaneous or with binary alternating presentation.

TUBES AND THERMIONICS

537.5:538.56 3106
Plasma Ion Oscillations in Electron Beams—K. G. Hernqvist. (*J. appl. Phys.*, vol. 26, pp. 544–548; May, 1955.) "The frequency of the oscillations observed in ion-neutralized electron streams such as that of an ion-trapping gun or of a tetrode has been shown to agree well with the Langmuir-Tonks theory for plasma ion oscillations. The existence of a dipole mode of oscillation in addition to the longitudinal mode has been observed for a plasma column. A mechanism is proposed for the excitation of these self-sustained oscillations by which the secondary electron current from electrodes bounding the plasma is modulated by the vibration of the ions in such a way as to deliver energy to the ac field associated with the ion oscillations. Experimental observations verify this picture as far as the source of energy is concerned."

621.314.63:535.215 3107
"Gate Modulation" of Electromagnetic Radiation—K. Lehovec. (*J. appl. Phys.*, vol. 26, pp. 495–496; May, 1955.) The space-charge region in the vicinity of a semiconductor *p-n* junction acts as a gate for light incident parallel to the plane of the junction, the gate width depending on the value of an applied blocking voltage. The effect is based on the dependence of the semiconductor absorption on the concentration of free carriers. A proposal to use the principle in the construction of an infrared diffraction grating is mentioned.

621.314.63:621.317.7 3108
Some Applications of the Nonlinear Characteristic of Germanium Crystal Diodes—P. Koch. (*Bull. schweiz. elektrotech. Ver.*, vol. 46, pp. 361–372; April 16, 1955.) The theoretically predicted logarithmic characteristic has been confirmed in commercial diodes. Square-law or other desired special characteristics are obtained by combining diodes. Descriptions are given of a ratiometer and of a modulator designed on the basis of these characteristics. Noise voltage is 5–8 times as great as the value calculated from the diode resistance, with loads up to about 150 mv per diode.

621.314.7 3109
The Transistor: Part 5—Properties and Limitations—J. R. Tillmann and F. F. Roberts. (*P. O. elect. Engrs' J.*, vol., 48, Part 1, pp. 43–47; April, 1955.) The properties are explained in terms of the transistor structure. Production techniques for improving frequency range, switching speed, power capacity, reliability and ability to operate at high temperature are discussed. Part 4: 2464 of August (Yemm and Carasso).

621.314.7 3110
A Two-Emitter Transistor with a High Adjustable Alpha—R. F. Rutz. (PROC. IRE, vol. 43, pp. 834–837; July, 1955.) The enhancement of the current amplification of a point-contact transistor on adding a second emitter is attributed to internal positive feedback which varies the hole-transport factor associated with the second emitter as the first-emitter current is varied. The effect of varying the spacing between second emitter and collector is also discussed and experimental results are reported.

621.314.7 3111
The Effects of Junction Shape and Surface Recombination on Transistor Current Gain: Part 2—K. F. Stripp and A. R. Moore. (PROC. IRE, vol. 43, pp. 856–866; July, 1955.) Continuation of work reported by Moore and Pankove (2797 of 1954). Analytical expressions are derived for the collector-to-base current amplification factor, taking account of surface and volume recombination, for grown-junction transistors with rectangular and round cross section and for alloyed-junction types. The expressions become simpler when volume recombination is neglected, which is justifiable in most practical cases. Parameters involved including a geometrical figure of merit, are evaluated for alloyed-junction types, using a three-dimensional electrolytic analog. The highest figure of merit is obtained by combining a flat emitter junction with a collector penetrating not less than a critical distance into the base.

621.314.7:621.317.733 3112
A Bridge for measuring Audio-Frequency Transistor Parameters—Cooper. (*See* 3051.)

621.314.7:621.372.5 3113
Design Considerations of Junction Transistors at Higher Frequencies—R. A. Pucel. PROC. IRE, vol. 43, pp. 878–879; July, 1955.) Theory given previously [583 of February (Statz et al.)] is extended to derive a form of the equivalent T network applicable down to zero frequency.

621.314.7:621.396.621.54 3114
Multi-stage Transistor Superheterodyne—Wright. (*See* 3081.)

621.38.032.7.002.2 3115
Ceramic-to-Metal Sealing: its Development and Use in the American Radio Valve Industry—D. E. P. Jenkins (*Electronic Engng*, vol. 27, pp. 290–294; July, 1955.) A review of literature. 55 references, including patents and special reports.

621.383.2 3116
Behaviour of Vacuum Photocells illuminated by Light Pulses—W. Kluge and S. Weber. (*Z. angew. Phys.*, vol. 7, pp. 126–131; March, 1955.) Ag-Cs_2O-Cs and SbCs-Cs photocells were illuminated by single and repeated light pulses of duration about 17 μs at an intensity up to 4.9×10^7 lux. The former showed no signs of fatigue until the mean cathode current exceeded a value between 1 and 5 $\mu a/cm^2$, the value depending on the particular cathode structure. Recovery could be accelerated by means of infrared illumination. The transparent SbCs-Cs photocells were found to be less suitable in light-pulse applications.

621.383.27 3117
Theory of Operation of the Last Stage of a Photomultiplier—P. Leuba. (*J. Phys. Radium*, vol. 16, pp. 296–303; April, 1955.) Assuming constancy of photocathode sensitivity and of multiplication factor, linearity is achieved in the final stage by making the time constant of the associated circuit large compared with the duration of the input pulse and by ensuring that all electrons emitted by the final dynode reach the collector electrode. To achieve this it is necessary that the final stage is not space-charge limited, that the transit time of electrons across it is small compared with the pulse duration, and that the pulse shape is regular.

621.385:621.396.822 3118
Investigations of Electron Streams—J. Müller. (*Z. angew. Math. Phys.*, vol. 5, pp. 203–232, 409–419; May 15/September 15, 1954.) Phenomena in controlled beams are analysed by means of perturbation theory based on the laws of conservation of energy and charge. Matrix formulation is used. Nyquist's noise formula is derived for a system in thermal equilibrium, with a potential minimum in the beam and large transit angles. Noise formulas are also presented for a system not in thermal equilibrium.

621.385:621.396.822 3119
Cross Correlation between Velocity and Current Fluctuations in Tube Noise—S. V. Yadavalli. (*J. appl. Phys.*, vol. 26, pp. 605–608; May, 1955.) Correlation between the velocity and current fluctuations in an electron stream at the entrance plane is shown to be zero under stated conditions. See also 301 of January.

621.385.029.6 3120
Backward-Wave Oscillator Efficiency—R. W. Grow and D. A. Watkins. (PROC. IRE, vol. 43, pp. 848–856; July, 1955.) "The dependence of power output upon space charge, circuit loss, beam thickness, velocity spread, and circuit mismatches is determined by a combination of theoretical and empirical means. In addition, the effect of circuit mismatches upon the starting current and frequency is discussed."

621.385.029.6 3121
Variation of High-Frequency Admittance of a Multi-segment Magnetron in the Oscillating State—H. Fricke. (*Fernmeldetech. Z.*, vol. 8, pp. 186–192; April, 1955.) The operation of the magnetron is explained in relation to an approximate calculation of the admittance diagram. Discussion of the electron paths is referred to a plane equivalent system in which the bunched electrons interact with the hf field only in the vicinity of the slots. Both capacitive and inductive reactances may occur. As the anode voltage is varied, the resistive and reactive admittance components vary simultaneously, producing variations of both amplitude and frequency of the oscillations. The influence on the admittance of the magnetic field, the oscillation mode, and the number of slots is also indicated. The theoretical results are supported by measurements and by results of other workers.

621.385.029.6:621.3.012 3122
Graphical Determination of Reflex-Klystron Characteristics—J. Bruijsten. (*Phillips Res. Rep.*, vol. 10, pp. 81–96; April, 1955.) A triangular diagram of normalized efficiency as a function of resonator loss conductance, load conductance and small-signal electronic conductance is derived from the variation of normalized efficiency with bunching parameter. Conditions under which the diagram is valid are discussed; it can be used for constructing curves relating the power parameter to the electronic tuning parameter for nonreactive and reactive loads, or alternatively for evaluating the parameters from experimental data.

621.385.029.6:621.396.822 3123
Noise in One-Dimensional Electron Beams H. A. Haus. (*J. appl. Phys.*, vol. 26, pp. 560–571; May, 1955.) Conditions in long-beam microwave tubes are considered; general theory of the noise in such beams is developed based on use of a reference plane other than that of the beam potential minimum and selected so that the assumption of uniform transverse distribution of electron velocity is valid at and beyond this plane. Analogies with network theory are used in the analysis; transformations of the noise standing wave by means of "lossless beam transducers" constituted by the region between the reference plane and the drift space are discussed. Expressions are derived for the minimum obtainable noise figures of a velocity-jump amplifier, a klystron and a traveling-wave tube. It is shown that these noise figures cannot be reduced by using "lossy beam transducers."

621.385.029.65 3124
A Tunable, Low-Voltage Reflex Klystron for Operation in the 50–60 kMc/s Band—E. D. Reed. (*Bell Syst. Tech. Jour.*, vol. 34, pp. 563–599; May, 1955.) A detailed description is given of the Type-M1805 tube, which delivers cw power of 15–30 mw at a beam voltage of 600 v and has a mechanical tuning range >10 kmc. Features specially studied include the high-convergence gun and the development of an efficient passive circuit consisting of cavity and wide-band output coupling system. Grids used at the interaction gap are of tungsten ribbon with a thickness transverse to the beam of 0.0003 inch and a width of 0.003–0.004 inch in the direction of electron flow. The tube is free from electron hysteresis, indicating either that few electrons reach the interaction gap for a third time or that those which do are no longer bunched.

621.385.032.216 3125
Improved "Impregnated Cathode"—R. Levi. (*J. appl. Phys.*, vol. 26, p. 639; May, 1955.) Improvements in the cathode described in *Le Vide*, vol. 9, pp. 284–289; November, 1954, are indicated.

621.385.2+621.385.029.6 3126
Noise at the Potential Minimum in the High-Frequency Diode—D. A. Watkins. (*J. appl. Phys.*, vol. 26, pp. 622–624; May, 1955.) Analysis is presented based on the assumption that the transit angle between cathode and potential minimum is small compared with that between potential minimum and anode. The mean-square convection current is found to be about half full shot noise for a typical case and the mean-square velocity is found to be the same as in the temperature-limited case. Application of this result to an analysis of the minimum obtainable noise figure of klystrons and traveling-wave tubes using velocity-jump noise reduction shows that their noise figure can be reduced without theoretical limit by increasing the current density at the cathode.

MISCELLANEOUS

621.37/39].004.6:623 3127
Maintainability of Services Equipment—(*J. Brit. IRE*, vol. 15, pp. 283–307; June, 1955. Discussion, pp. 307–313;) Part 1 (pp. 307–313.) Part 1 (pp. 283–290)—G. W. A. Dummer. Summarized analysis of faults in electronic equipment reported to the Ministry of Supply during the period 1950–1953, and discussion of design and constructional techniques for improving reliability and ease of maintenance. Part 2 (pp. 290–298)—R. B. Brenchley. Part 3 (pp. 299–300)—G. C. Godfrey. Part 4 (pp. 303–307)—A. J. B. Naish. Outline descriptions of Army, Royal Air Force, and Royal Navy maintenance systems and equipment design and test requirements.

621.38:53 3128
Advances in Electronics and Electron Physics, Vol. VI. [Book Review]—L. Marton (Ed.). Publishers: Academic Press, New York, 1955, 518 pp., $11.80. (PROC. IRE, vol. 43, p. 898; July, 1955.) Surveys are presented of metallic conduction at high frequencies and low temperatures, relaxation processes in ferromagnetism, physical properties of ferrites, space-charge-limited currents, comparison of analogous semiconductors and gaseous electronic devices, the electron microscope, traveling-wave tubes and paramagnetism.

WRH

WRH